THESIS
Vol. 1



This is to certify that the

dissertation entitled

**THE TIMBER MOUNTAIN TUFF,
SOUTHWESTERN NEVADA VOLCANIC FIELD:
Geochemistry, Mineralogy and Petrogenesis**

presented by

James Gordon Mills, Jr.

has been accepted towards fulfillment
of the requirements for

Ph.D. degree in **Geology**

Thomas A. Vogel
Major professor

Date **March 15, 1991**

MSU is an Affirmative Action/Equal Opportunity Institution

O-12771

LIBRARY
Michigan State
University

PLACE IN RETURN BOX to remove this checkout from your record.
TO AVOID FINES return on or before date due.

DATE DUE	DATE DUE	DATE DUE

MSU Is An Affirmative Action/Equal Opportunity Institution

c:\circ\datedue.pm3-p.1

THE TIMBER MOUNTAIN TUFF, SOUTHWESTERN NEVADA VOLCANIC FIELD: GEOCHEMISTRY, MINERALOGY AND PETROGENESIS

Volume I

By

James Gordon Mills, Jr.

A DISSERTATION

Submitted to
Michigan State University
in partial fulfillment of the requirements
for the degree of

DOCTOR OF PHILOSOPHY

Department of Geological Sciences

1991

ABSTRACT

THE TIMBER MOUNTAIN TUFF, SW NEVADA VOLCANIC FIELD: GEOCHEMISTRY, MINERALOGY AND PETROGENESIS

By

James Gordon Mills, Jr.

Ash-flow tuffs of the Rainier Mesa Member (1200 km^3) and Ammonia Tanks Member (900 km^3) were erupted from chemically, mineralogically and thermally heterogeneous magma bodies approximately 11.6 to 11.4 mya. Chemical, mineralogical and thermal gradients in the magmatic systems were determined from analysis of glassy pumice collected from the basal and upper unwelded zones and vitrophyre of each member. It is interpreted that the initial magmatic system was layered. Over time modification by various processes formed a magmatic system which now appears to be zoned from a basal trachyandesite (57 wt% SiO_2) to a roofward high-silica rhyolite (78 wt% SiO_2). The Rainier Mesa magmatic system appears to have tapped a second high-silica rhyolite magma body with relatively higher concentrations of Nb, Th and Rb than the high-silica rhyolite in the main chamber. Gaps in major and trace element concentration gradients which reflect the initial layering within the magmatic system, occur within each member. Variations in temperature and oxygen fugacity determined from Fe-Ti oxides are inferred to represent gradients that were present in each magma body

(755 ^{o}C, -13.09 to 897 ^{o}C, -10.57; Rainier Mesa Member, high-silica rhyolite to trachyandesite respectively and 727 ^{o}C, -13.86 to 903 ^{o}C, -10.96; Ammonia Tanks Member, high-silica rhyolite to trachydacite respectively). Both members were most likely zoned with respect to H_2O and CO_2 as trachydacitic to rhyolitic magmas followed separate degassing paths. The magmas for both members probably resided at mid-crustal levels (4 to 7 kbars) based on Fe-Ti oxide/feldspar and amphibole/quartz geobarometers. The trachyandesites to high-silica rhyolites of each member probably formed from different degrees of partial melting of crustal rock with differentiation by fractional crystallization, crustal assimilation (up to 10% based on Nd isotopes) and minor magma mixing modifying each partial melt. Pure fractional crystallization models cannot be used to generate the more evolved magmatic compositions of the Rainier Mesa Member, but, are permissive for formation of the more evolved magmas of the Ammonia Tanks Member. Based on the variable stratigraphic location of compositionally heterogeneous pumice fragments within an ash-flow sheet, the style of magma chamber evacuation for each member is inferred to be similar to the model proposed by Blake and Ivey (1986) for a body of fluid stratified by density and viscosity gradients.

To Woody and John

ACKNOWLEDGMENTS

I would like to thank my parents for providing continuous moral support and for spurring me on with the never ending question "When are you going to be done?".

Tom Vogel, who has advised, guided and instructed me throughout this study, has my sincerest thanks and gratitude. Tom however, should not be held responsible in any fashion for my ability to choose a good bottle of wine vinegar. My committee members Dave Long, Bill Cambray, Kaz Fujuita and Dave Matty are thanked for the advice, computer programs and candid comments given during the tenure of this project. This thesis is in part dedicated to the memory of John Wilband, a committee member who provided much of the technical support necessary for this study and was always happy to help empty the refrigerator and discuss life. I would like to thank Gene Smith at the University of Nevada, Las Vegas for continued support from the beginning. I cannot thank Tim Flood and Tim Rose enough for their continuing advice and very special friendship. Days and nights with them at the farm and the PB were an integral part of this study. I would also like to thank Tim Rose for all his help while collecting samples at the Nevada Test Site Resort, and, for all the

work and insight he has contributed to this study both knowingly and unknowingly. Ben Schuraytz is also thanked for his friendship and advice - but will I ever get a copy of your thesis? Dave Cook and Erin Lynch are thanked for their continued friendship and companionship, especially during those long nights in the lab. Jane Ballien has contributed more than she will ever know. Nancy Lariviere is especially wonderful still believing in me and for putting up with three years of significant mood changes while finishing up this study.

Rick Warren, Dave Broxton, David Nealey, and Lang Farmer were essential for providing thought provoking discussions and data. This study would not have been possible without the help of Lee Younker who provided much of the logistical, technical and monetary support through the Basic Energy Science Program at both the Nevada Test Site and at the Lawrence Livermore National Laboratory. The Department of Geological Sciences at Michigan State University provided financial support for a portion of this study through a teaching assistantship. Monmouth College is thanked for providing logistical support while finishing up the manuscript.

And finally I wish to thank Walt Vennum, Woody, Tom Anderson, Terry Wright and Rolfe Erikson of Sonoma State University who are ultimately responsible for this whole bloody mess.

TABLE OF CONTENTS

List of Tables ix
List of Figures xi

Introduction 1
Purpose of study 1
Previous work 3
Regional setting 5
The Timber Mountain Tuff 10
Rainier Mesa Member 10
Ammonia Tanks Member 12

Sampling technique 15
Sample type 15
Site selection and sampling technique 21

Geochemistry 25
Introduction 25
Major element oxides 30
Rainier Mesa Member 30
Ammonia Tanks Member 36
Trace elements 42
Rainier Mesa Member 42
Ammonia Tanks Member 49

Petrography and Mineral Chemistry 61
Overview 61
Petrography 61
Phenocryst and glass chemistry 61
Feldspar 64
Petrography 64
Mineral Chemistry 67
Biotite 74
Petrography 74
Mineral Chemistry 75
Quartz 81
Petrography 81
Clinopyroxene 82
Petrography 82
Mineral Chemistry 83
Orthopyroxene 89
Petrography 89
Mineral Chemistry 89

Amphibole 92
Petrography 92
Mineral Chemistry 92
Olivine 98
Petrography 98
Trace Phenocryst Phases 100
Petrography 100
Glass 104
Chemistry 104

Geothermometry and Geobarometry 112
Fe-Ti Oxide Geothermometry 112
Temperature and Oxygen Fugacity Calculations . . 119
Coexisting Feldspars and Fe-Ti Oxides 122
Amphibole and Quartz Geobarometry 125

Discussion 128
Geochemical zonation in Magma Bodies. 128
Background 128
The Timber Mountain Magmatic System 133
Geochemical Heterogeneity of the Timber Mountain Magmatic System 136
Mineralogical Variations 139
Geothermometric Considerations 142
Oxygen Fugacity and Sphene-Ilmenite Stability 146
Geobarometry 149
Petrogenesis 150
Overview 150
Fractional crystallization 151
Rainier Mesa Member 151
Ammonia Tanks Member 166
Magma mixing 175
Partial melting/Assimilation 179
Trachyandesite and trachydacite 179
Rhyolite 187

Magmatic Water Contents 189
Eruption dynamics 192
Summary and Conclusions 197

Appendix 1. Description of sampling locations 206
Appendix 2. Geochemical data for glassy pumice samples; Major and trace elements (XRF and INAA) 208
Appendix 3. Analytical techniques 230
Major and Trace Elements (XRF) 230
Trace Elements (INAA) 231
Phenocryst Compositions 238
Magnetite/Ilmenite analyses 243
Appendix 4. Electron microprobe data for phenocrysts of the Timber Mountain Tuff 250

Bibliography 318

LIST OF TABLES

Table 1. General stratigraphy of the major volcanic units in the Southwestern Nevada Volcanic Field 8

Table 2. Modal petrography of the Timber Mountain Tuff 62

Table 3. Textural relationships of phenocrysts in the Timber Mountain Tuff 63

Table 4. Fe-Ti oxide temperature and oxygen fugacity data for the Timber Mountain Tuff 121

Table 5. Textural condition of magnetite and ilmenite phenocrysts analyzed for geothermometry in the Rainier Mesa Member and Ammonia Tanks Member of the Timber Mountain Tuff 123

Table 6. Rainier Mesa Member: Major-element Multiple Linear Regression Models 153

Table 7. Phenocryst and pumice block compositions used in fractional crystallization modelling for the Rainier Mesa Member of the Timber Mountain Tuff. 154

Table 8. Distribution coefficients used for fractional crystallization modelling in the Rainier Mesa Member of the Timber Mountain Tuff 160

Table 9. Rayleigh fractionation modelling for the Rainier Mesa Member of the Timber Mountain Tuff 164

Table 10. Mineral analyses used in regressions for crystal fractionation models in the Ammonia Tanks Member. From Rose (1988) 167

Table 11. Distribution coefficients used for Rayleigh fractionation modelling of the Ammonia Tanks Member of the Timber Mountain Tuff. From Rose (1988). 169

Table 12. Major element multiple linear regression models for the Ammonia Tanks Member of the Timber Mountain Tuff 171

Table 13. Rayleigh fractionation trace element models and for the Ammonia Tanks Member of the Timber Mountain Tuff. Data from Rose (1988) 172

Table 14. Magma mixing models for the Ammonia Tanks Member of the Timber Mountain Tuff. From Rose (1988) 173

Table A3a. X-ray fluorescence major element concentrations of USGS standards run as unknowns compared to the reported concentrations in Govindaraju (1984) . . . 232

Table A3b. X-ray fluorescence trace element concentrations of USGS standards run as unknowns compared to the reported concentrations in Govindaraju (1984) . . . 234

Table A3c. Analytical errors for INAA trace element analyses based on linear regression of analyzed USGS (BIR-1, G-1, G-2, QLO-1, RGM-1, STM-1 and W-2), Canadian (MRG-1 and SY-2) and Japanese (JG-1a) rock standards . 239

Table A3d. Electron microprobe beam parameters and analyzed oxides for various phenocryst compositions 242

Table A3e. Electron microprobe analyses of mineral standards 244

LIST OF FIGURES

Figure 1. Location map of the Timber Mountain-Oasis Valley caldera complex and associated sampling sites for this study 6

Figure 2. A) Stratigraphic variation in whole pumice composition for the Rainier Mesa Member. B) Stratigraphic variation in whole pumice composition for the Ammonia Tanks Member . 11

Figure 3. Stratigraphic variation in whole pumice composition for the Ammonia Tanks Member, Section 5 22

Figure 4. SiO_2 versus CaO discrimination diagram for the Rainier Mesa Member and Ammonia Tanks Member 26

Figure 5. A) SiO_2 versus Nb discrimination diagram for the Rainier Mesa Member and Ammonia Tanks Member. B) Rb versus Nb discrimination diagram for the Rainier Mesa Member and Ammonia Tanks Member 27

Figure 6. Total Alkali-silica classification diagram for the Timber Mountain Tuff. 28

Figure 7. Major element variation diagrams for the Rainier Mesa Member 31

Figure 8. Trace element variation diagrams for the Rainier Mesa Member 32

Figure 9. Major element variation diagrams for the Ammonia Tanks Member 37

Figure 10. Trace element variation diagrams for the Ammonia Tanks Member 38

Figure 11. A) Rare-earth element plot for the Rainier Mesa Member. All magmatic compositions plotted 43
B) Rare-earth element plots for the various magmatic groups of the Rainier Mesa Member 44

Figure 12. A) Spidergram for the Rainier Mesa Member. All magmatic compositions plotted. 47
B) Spidergrams for the various magmatic groups of the Rainier Mesa Member 48

Figure 13. A) Trace element enrichment diagram comparing the low-Nb, high-silica rhyolite to the trachyandesite of the Rainier Mesa Member. 50
B) Trace element enrichment diagram comparing the high-Nb, high-silica rhyolite to the trachyandesite of the Rainier Mesa Member. 51

Figure 14. A) Rare-earth element plot for the Ammonia Tanks Member. All magmatic compositions plotted 53
B) Rare-earth element plot for the various magmatic groups in the Ammonia Tanks Member. 54

Figure 15. A) Spidergram for the Ammonia Tanks Member. All compositions plotted 55
B) Spidergrams for the various magmatic groups of the Ammonia Tanks Member 56

Figure 16. Trace element enrichment plot comparing the high-silica rhyolite and the trachyandesite of the Ammonia Tanks Member 57

Figure 17. A) Trace element enrichment plot comparing the low-Nb, high-silica rhyolite of the Rainier Mesa Member to the high-silica rhyolite of the Ammonia Tanks Member. . . . 58
B) Trace element enrichment plot comparing the high-Nb, high-silica rhyolite of the Rainier Mesa Member to the high-silica rhyolite of the Ammonia Tanks Member. . . . 59

Figure 18. A) Feldspar compositions based on electron microprobe analyses of grain edges for the Rainier Mesa Member.
B) Feldspar compositions based on electron microprobe analyses of grain centers for the Rainier Mesa Member 68

Figure 19. Feldspar compositions by sample from electron microprobe analyses for the Rainier Mesa Member 69

Figure 20. A) Celsian versus anorthite content in feldspars of the Rainier Mesa Member. B) Celsian versus anorthite content in feldspars of the Ammonia Tanks Member . . . 70

Figure 21. A) Feldspar compositions based on electron microprobe analyses of grain edges for the Ammonia Tanks Member. B) Feldspar compositions based on electron microprobe analyses of grain centers for the Ammonia Tanks Member 72

Figure 22. Feldspar compositions by sample from electron microprobe analyses for the Ammonia Tanks Member 73

Figure 23. Mg# of biotite phenocrysts in the Rainier Mesa Member. Samples arranged by increasing whole pumice SiO_2 content. Microprobe analyses are from the grain edges only 76

Figure 24. TiO_2 in biotite phenocrysts in the Rainier Mesa Member. Samples arranged by increasing whole pumice SiO_2 content. Microprobe analyses are from the grain edges only 78

Figure 25. Mg# of biotite phenocrysts in the Ammonia Tanks Member. Samples arranged by increasing whole pumice SiO_2 content. Microprobe analyses are from the grain edges only 79

Figure 26. TiO_2 in biotite phenocrysts in the Ammonia Tanks Member. Samples arranged by increasing whole pumice SiO_2 content. Microprobe analyses are from the grain edges only 80

Figure 27. A) Plot of clinopyroxene and orthopyroxene compositions on the pyroxene quadilateral diagram for the Rainier Mesa Member. B) Plot of clinopyroxene and orthopyroxene compositions on the pyroxene quadilateral diagram for the Ammonia Tanks Member . . . 84

Figure 28. Mg# of clinopyroxene phenocrysts in the Rainier Mesa Member. Samples arranged by increasing whole pumice SiO_2 content Microprobe analyses are from the grain edges only 86

Figure 29. Mg# of clinopyroxene phenocrysts in the Ammonia Tanks Member. Samples arranged by increasing whole pumice SiO_2 content. Microprobe analyses are from the grain edges only 88

Figure 30. A) Mg# of orthopyroxene phenocrysts in the Rainier Mesa Member. Samples arranged by whole pumice SiO_2 content. Microprobe analyses are from grain edges only. B) TiO_2 in orthopyroxene phenocrysts in the Rainier Mesa Member 90

Figure 31. Mg# of orthopyroxene phenocrysts in the Ammonia Tanks Member. Samples arranged by increasing SiO_2 content of whole pumice. Microprobe analyses are from grain edges only 91

Figure 32. Mg# of hornblende phenocrysts in the Rainier Mesa Member. Samples arranged by increasing whole pumice SiO_2 content. Microprobe analyses are from grain edges only 93

Figure 33. Al_2O_3 in hornblende phenocrysts of the Rainier Mesa Member. Samples arranged by increasing whole pumice SiO_2 content. Microprobe analyses are from grain edges only 95

Figure 34. CaO in hornblende phenocrysts of the Rainier Mesa Member. Samples arranged by increasing whole pumice SiO_2 content. Microprobe analyses are from grain edges only 96

Figure 35. Mg# of hornblende phenocrysts in the Ammonia Tanks Member. Microprobe analyses are from the grain edge only 97

Figure 36. Manganoan fayalite compositions determined from electron microprobe analyses for the Ammonia Tanks Member of the Timber Mountain Tuff. Olivine compositions from other rhyolitic flows and tuffs are plotted for reference 99

Figure 37. Back-scattered electron photomicrographs of manganoan fayalite phenocrysts in the Ammonia Tanks Member 101

Figure 38. Ilmenite grain from sample R23-13 with inclusions of chevkinite (white), zircon (white, square outlines) and apatite (dark elongate inclusions). Scale bar on the bottom right of the photo is 100 microns long. 103

Figure 39. A) Histograms of glassy matrix compositions in pumice fragments determined by electron microprobe analysis for the Rainier Mesa Member: SiO_2 106
B) Al_2O_3 in pumiceous glass, Rainier Mesa Member 107
C) FeO in pumiceous glass, Rainier Mesa Member 108
D) K_2O in pumiceous glass, Rainier Mesa Member 109
E) CaO in pumiceous glass, Rainier Mesa Member 110
F) TiO_2 in pumiceous glass, Rainier Mesa Member 111

Figure 40. A) SiO_2 in pumiceous glass, Ammonia Tanks Member. 113
B) Al_2O_3 in pumiceous glass, Ammonia Tanks Member 114
C) FeO in pumiceous glass, Ammonia Tanks Member 115
D) K_2O in pumiceous glass, Ammonia Tanks Member 116
E) CaO in pumiceous glass, Ammonia Tanks Member 117
F) TiO_2 in pumiceous glass, Ammonia Tanks Member 118

Figure 41. Temperature versus fO_2 diagram derived from Fe-Ti oxide phenocryst data for the Timber Mountain Tuff. Data are from this study and from Lipman (1971) 120

Figure 42 A) Fe-Ti oxide and co-existing feldspar temperature/pressure diagram from Stormer and Whitney (1985).
B) Fe-Ti oxide and co-existing feldspar temperature/pressure data from the Timber Mountain Tuff 126

Figure 43. SiO_2 versus temperature for the Timber Mountain Tuff 143

Figure 44. SiO_2 versus $-fO_2$ for the Timber Mountain Tuff. 144

Figure 45. Rb versus Nb for the Timber Mountain Tuff . 176

Figure 46. Overlay of the spidergrams for the high-silica rhyolites of the Rainier Mesa Member (low-Nb and high-Nb) and the high-silica rhyolite of the Ammonia Tanks Member 178

Figure 47. Enrichment diagram comparing trace element enrichment in the Rainier Mesa Member and Ammonia Tanks Member trachyandesites . . . 180

Figure 48. Nd versus 1/Nd data from Tegtmeyer, et al., (1989) for the Timber Mountain Tuff 182

Figure 49. SiO_2 versus Th, Yb, Zr and Eu for the Paintbrush Tuff and Timber Mountain Tuff. Trachyandesite and trachydacite data only . 183

Figure 50. Yb/Th versus Th for the Paintbrush Tuff and the Timber Mountain Tuff. 185

Figure 51. Zr/Th and Eu/Th versus Th for the Paintbrush Tuff and Timber Mountain Tuff. Trachyandesite and trachydacite data only . 186

Figure 52. H_2O versus CO_2 concentrations for the Ammonia Tanks Member showing the separate degassing paths for the trachydacites and rhyolites using the degassing curves of Newman, et al., (1988). 190

Figure 53. Schematic diagram of evacuation isochrons as modelled by Blake (1981) for a liquid of homogeneous density and viscosity being drained from a single vent 193

Figure 54. Schematic diagram of the evacuation profile for two liquids of contrasting density (q_1,q_2) and viscosity (v_1,v_2) being drained from a single vent (Blake and Ivey, 1986) . 195

Figure A3-1. Mg/Mn partitioning for magnetite and ilmenite phenocrysts in the Rainier Mesa Member 247

Figure A3-2. Mg/Mn partitioning for magnetite and ilmenite phenocrysts in the Ammonia Tanks Member 248

INTRODUCTION

Purpose of study

The presence of chemical and mineralogical gradients in ash-flow tuffs has been recognized and studied for many years (Williams, 1952, in Ross and Smith, 1961; Ratte and Steven, 1964, Lipman, et al., 1966; Lipman, 1967; Smith, 1979; Hildreth, 1981, 1983). The hypothesis that the compositional gradients in an ash-flow tuff represented compositional gradients in the parent magma chamber was an important step in the understanding of high-level silicic systems (cf. Smith, 1979; Hildreth, 1981). Moreover, the study of large volume ash-flow tuffs as opposed to lavas to gain insight into magmatic processes is advantageous because the tuffs provide a volumetrically substantial, essentially instantaneous, quenched sample of the magma body (Smith, 1979; Hildreth, 1981).

Through the analysis of glassy pumice fragments, this study of the Rainier Mesa Member and Ammonia Tanks Member of the Timber Mountain Tuff attempts to answer several questions concerning the magmatic processes that may have been operating in the Timber Mountain magmatic system:

1) What was the range of the chemical and mineralogical compositions of the magma at the time of eruption?

2) Did the magmas reside in a single chamber, or were they brought together from several different chambers either prior to or at the time of eruption?

3) If a single magma chamber existed for each member, were uniform compositional gradients present, or were there discrete compositional layers within the magma chamber?

4) What is the origin of the compositional variation of the magmas: are they due to an unmixing process such as fractional crystallization, or partial melting of compositionally distinct sources, or, did assimilation or variable degrees of partial melting modify the initial magmatic compositions?

5) Can the style of magmatic withdrawal from the chamber be constrained, i.e., was the chamber evacuated from the top down, or was the magma withdrawal mechanism more complex?

This study of the Timber Mountain Tuff is noteworthy in two ways: 1) it is one of the few studies of ash-flow tuffs that derives its data base from glassy pumice fragments instead of whole-rock tuff samples, and 2) it is part of a systematic investigation of the large volume ash-flow sheets located in the Southwestern Nevada Volcanic Field (SWNVF) by the Michigan State University group (Rose, 1988; Flood, et al., 1989a,b; Schuraytz, et al., 1989; Vogel, et al., 1988).

Other studies of ash-flow tuffs and lavas in the SWNVF have relied almost entirely on whole-rock samples (Broxton, et al., 1989; Sawyer, et al., 1989; Warren, et al., 1989; Weiss and Noble, 1989). By combining the data from this study and that of other workers in the SWNVF, we will eventually be able to examine in detail the origin and evolution of the magmatic system which formed the

Timber Mountain-Oasis Valley and Claim Canyon nested caldera complex.

Previous Work

Prior to 1960, only two geologic studies had been completed for the region; Ball (1907) prepared a regional geologic reconnaissance map and Ransome, et al., (1910) produced a detailed geologic map of the Bullfrog Hills. With the onset of underground nuclear testing in the mid 1960's it was apparent that detailed base maps and stratigraphic data were necessary for continuation of the underground testing program (Eckel, 1968). Thus, extensive detailed mapping of the region was carried out from 1960 to 1966 by the U.S. Geological Survey. The end product of this program was the generation of 34 geologic quadrangle maps ranging in scale from 1:24,000 to 1:62,000 (see Byers, et al., 1976a for a map index). Revisions to, and new geologic data for, the Timber Mountain-Oasis Valley caldera complex mapping project were compiled and published by Byers, et al. (1976b) as a 1:48,000 scale geologic map. An accompanying paper on the structure of the caldera complex was done by Christiansen, et al. (1977).

Byers, et al. (1976a), and Carr (1986) have summarized the stratigraphic, geochemical, and structural relationships of volcanic units within the SW Nevada

Volcanic Field. Warren, et al., (1984) present detailed petrographic data on some of the older volcanic units in the field. Detailed structural studies of the region were completed by Christiansen, et al., (1965), Ekren (1968), and Carr (1984).

The geochemical development and secular evolution of volcanic units and their parental magmas within the SW Nevada Volcanic Field are discussed by Lipman, (1965, 1971), Lipman and Friedman (1975), Christiansen, et al. (1977), Rose (1988), Schuraytz (1988), Vogel, et al. (1983, 1988), Broxton, et al. (1985, 1989), Flood (1987, 1989a,b), Schuraytz, et al. (1986, 1989), and Warren, et al. (1988, 1989).

Over the past several years, workers at Michigan State University have focused their studies on the large volume ash-flow sheets erupted from the Black Mountain caldera (Vogel, et al., 1983), the Claim Canyon caldera (Schuraytz, et al., 1986; Flood, 1987, 1989a,b; Schuraytz, 1988), Schuraytz, et al., (1989) and the Timber Mountain-Oasis Valley caldera (Mills and Rose, 1986; Mills, et al., 1987; Mills and Vogel, 1988; Rose, 1988; Vogel et al., 1989; Mills and Rose, 1991). Other workers at the Los Alamos National Laboratory, New Mexico, have been involved in a continuing comprehensive study of all the volcanic units of the southwestern Nevada Volcanic Field

(Byers, 1985; Byers and Moore, 1987; Broxton, et al., 1982, 1989; Warren, et al., 1984, 1989).

Significant findings of these studies include; the documentation of a greater diversity of magma types present as compared to earlier whole-rock tuff studies (Vogel, et al., 1983, 1988; Rose, 1988; Flood, et al., 1989a), magma mixing of two compositionally discrete magma types to form a new, compositionally homogeneous magma (Flood, et al., 1989b), and the presence of a compositional interface between two discrete magma types (quartz latite and rhyolite) present in the same chamber (Flood, et al., 1989a; Schuraytz, et al., 1986, 1989; Schuraytz, 1988).

Regional Setting

The Timber Mountain-Oasis Valley caldera complex, located in the southern Great Basin, was active from approximately 13 Ma to 9.5 Ma ago (Fig. 1)(Byers, et al., 1976a; Christiansen, et al., 1977). Volcanic activity at the Timber Mountain-Oasis Valley Caldera complex was part of a larger igneous event that occurred throughout the Basin and Range Province from Early Eocene to Early Pliocene time (37 Ma to 5 Ma ago)(Eaton, 1984). This episode of igneous activity may have been related to subduction of the Farallon plate and later regional crustal extension (Lipman, et al., 1972; Snyder et al.,

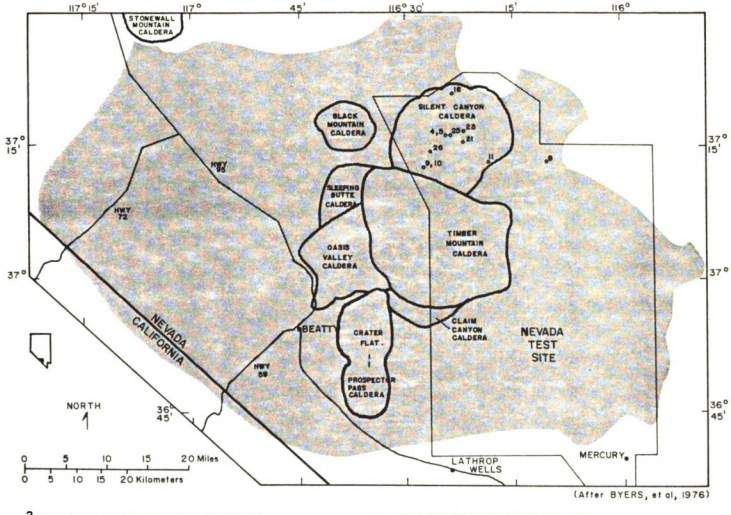


Figure 1. Location map of the Timber Mountain-Oasis Valley caldera complex and associated sampling sites for this study.

1976; Cross and Pilger, 1978; Eaton, 1979, 1984; Zoback, et al., 1981). Quaternary volcanic activity, predominantly basaltic in nature, occurs sporadically throughout the Basin and Range Province and represents the final stage of extension-related igneous activity (Eaton, 1979, 1984).

Several calderas are present in the southwestern Nevada volcanic field (SWNVF). These are, from oldest to youngest; Sleeping Butte (Byers, et al., 1976a), Crater Flat-Prospector Pass (Carr, 1982), Silent Canyon (Noble, et al., 1968), Claim Canyon (Byers, et al., 1976a), Timber Mountain-Oasis Valley (Byers, et al., 1968), Black Mountain (Christiansen and Noble, 1968; Noble and Christiansen, 1968, 1974), and Stonewall Mountain calderas (Weiss and Noble, 1989)(Fig. 1). Eruptions in the SWNVF resulted primarily in the outpouring of small to large volumes (<10 to >1000 km^3) of pyroclastic material which eventually formed a stratigraphic sequence up to several kilometers thick of air-fall and ash-fall tuffs with minor interbedded lavas (Table 1).

Eruptions of the Paintbrush Tuff and Timber Mountain Tuff were responsible for the respective development of the Claim Canyon and Timber Mountain-Oasis Valley calderas (Byers, et al., 1976a; Christiansen, et al., 1977)(Fig. 1). The Paintbrush Tuff has a minimum volume of 2200 km^3 (Scott, et al., 1984) and was erupted periodically over

Table 1. General stratigraphy of the major volcanic units in the Southwestern Nevada Volcanic Field.

Formation[1]	Member	Volume (km^3)	Volcanic Center	Age (Ma)[1]
Alluvium				
Basalts				
Stonewall Flat Tuff	Civet Cat Canyon		Stonewall Mtn.	6.3
	Spearhead		caldera	6.3
Thirsty Canyon Tuff	Gold Flat	20	Black Mtn. caldera	7.5
	Trail Ridge	25		7.5
	Pahute Mesa	50-75		7.8
	Rocket Wash	50-75		7.8
Rhyolite of Shoshone Mountain			Shoshone Mtn.	9.0
Mafic lavas			Moat of Timber Mtn. caldera	9-10
Timber Mountain Tuff	Ammonia Tanks	900	Timber Mtn.-Oasis	11.4
	Rainier Mesa	1200	Valley caldera	11.6
Rhyolite lavas of Fortymile Canyon			Timber Mtn. caldera	11-13
Paintbrush Tuff	Tiva Canyon	1000	Claim Canyon caldera	12.9
	Yucca Mountain	<40	Timber Mtn.-Oasis	13
	Pah Canyon	<20	Valley caldera	13
	Topopah Spring	1200	complex	13.4
Wahmonie and Salyer formations			Wahmonie area	13.5
Crater Flat Tuff	Prow Pass	20	Crater Flat-Prospector	13.9
	Bullfrog	190	Pass caldera complex	13.9
	Tram	170		13.9
Belted Range Tuff	Grouse Canyon	210	Silent Canyon	13.6-14.2
	Tub Spring	60-100	caldera	14
Dacite lavas and breccias			Periphery of Crater Flat	14
Lithic Ridge Tuff		>230	Uncertain	13.9-14.3
Rhyolite of Kawich Valley			Silent Canyon caldera	15
"Older" tuffs			Uncertain	>14.3
Sanidine-rich tuffs			Uncertain	15
Tuff of Yucca Flat			Uncertain	15
Redrock Valley Tuff			Uncertain	16

[1] Stratigraphy from Byers, et al., (1989)

[2] K-Ar dates from Byers, et al. (1976a, 1989); Broxton, et al. (1989); Warren, et al. (1989); Sawyer and Sargent (1989); Vogel, et al. (1989); Weiss and Noble (1989)

0.5 Ma (13.4 mya to 12.9 mya)(Broxton, et al., 1989). Incremental collapse of the caldera is indicated by interbedded breccias of earlier erupted tuffs, and thick deposits of caldera fill (Christiansen, et al., 1977). Lipman, et al., (1966) and Schuraytz, et al., (1986, 1989) have reported detailed lithologic and chemical studies on the compositionally zoned Topopah Spring Member. Analyses of the overlying Pah Canyon, Yucca Mountain, and Tiva Canyon Members have been performed by Warren, et al., (1989) and Flood, et al., (1989a, 1989b).

Approximately 11.6 Ma ago, eruption of the Rainier Mesa Member initiated collapse of the magma chamber roof resulting in formation of the Timber Mountain caldera (Byers, et al., 1976a,b; Broxton, et al., 1989). Further subsidence of the cauldron resulted after eruption of pyroclastic material which formed the Ammonia Tanks Member (Byers, et al., 1976a; Christiansen, et al., 1977; Broxton, et al., 1989). Although initial calculations of K/Ar dates indicated a 0.2 Ma interval between eruption of the Rainier Mesa Member and the Ammonia Tanks Member, re-calculation of these dates and new work by Sawyer (1990, pers. comm.) indicates that the time between eruptions date is virtually indistinguishable with current Ar/Ar dating techniques. Resurgence of the Timber Mountain caldera occurred after eruption of the Ammonia Tanks Member and resulted in 1200 m of uplift forming the

present day Timber Mountain (Christiansen, et al., 1977). Nesting of the calderas, with the exception of the Black Mountain and Stonewall calderas, most likely represents the emplacement and eruption of a series of continuously evolving and periodically replenished magma bodies (Broxton, et al., 1989).

Volcanism waned following eruption of the Rainier Mesa and Ammonia Tanks Members, adding only two small-volume ash-flow tuffs (Fleur de Lis Ranch and tuff of Cutoff Road), a series of rhyolite flows along the caldera rim, and minor basalt flows (Byers, et al., 1976a,b; Christiansen, et al., 1977).

The Timber Mountain Tuff

Rainier Mesa Member

The Rainier Mesa Member of the Timber Mountain Tuff is a compositionally zoned, compound cooling unit (Fig. 2, Table 1). A pink, rhyolitic, tuffaceous base is separated from an overlying dark brown to black trachyandesitic to trachydacitic tuff by a partial cooling break. The more mafic (trachyandesite and trachydacite) whole-rock tuff compositions were originally referred to by Byers, et al. (1976a) as quartz latite for both the Rainier Mesa Member and Ammonia Tanks Member. Only when specific reference is made to the whole-rock tuff work of Byers, et al. (1976a) will the term quartz latite be used.

A

B

Figur

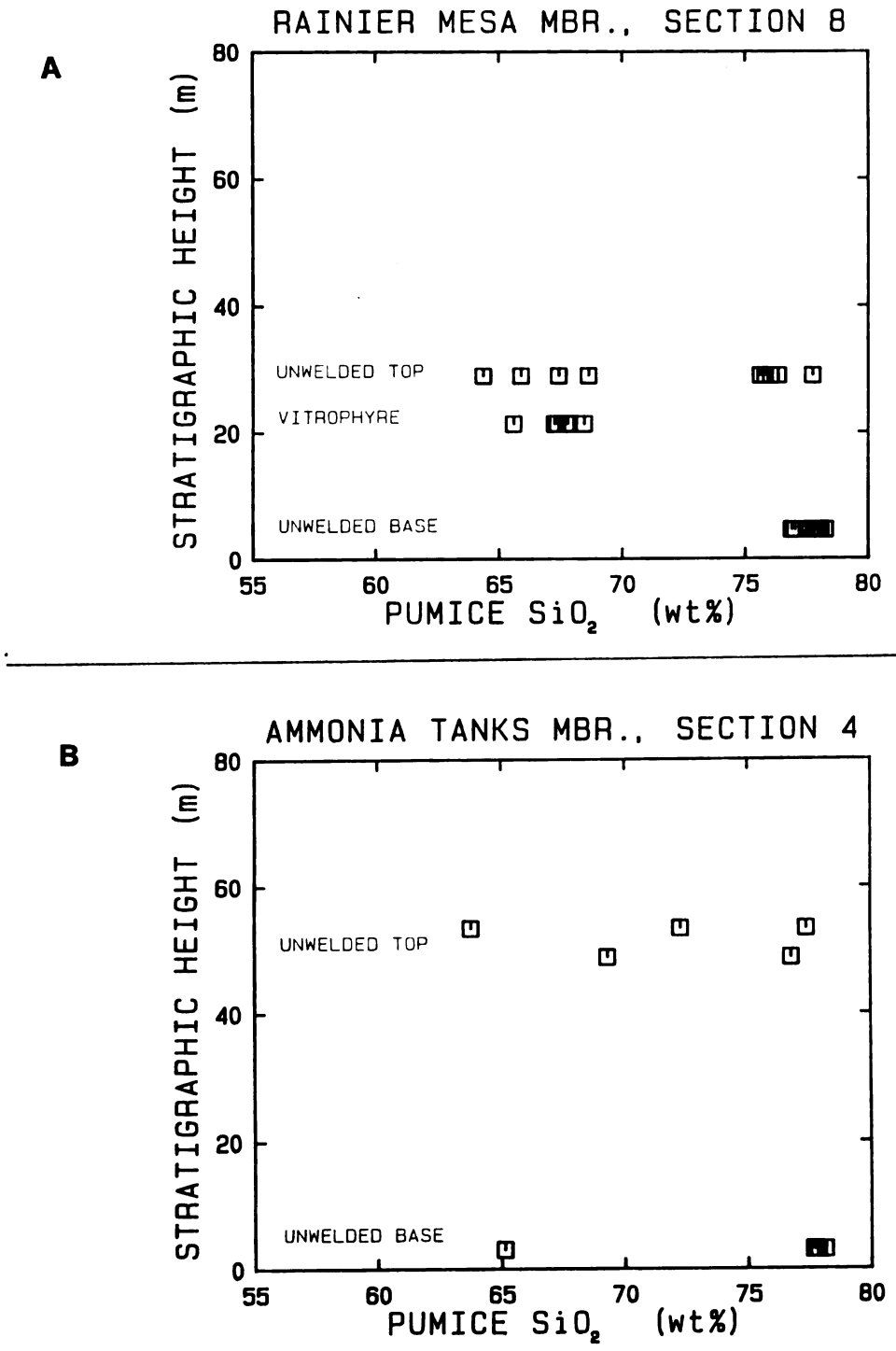


Figure 2. A) Stratigraphic variation in whole pumice composition for the Rainier Mesa Member.
B) Stratigraphic variation in whole pumice composition for the Ammonia Tanks Member.

The outflow sheet of the Rainier Mesa Member typically exhibits all three zones of welding as defined by Smith (1960a,b); 1) zone of no welding, 2) zone of partial welding, and 3) zone of dense welding. Where exposed and not removed by erosion, both a basal and upper zone of no welding are present. These zones of no welding grade rapidly into zones of partial welding which in turn grade into a zone of dense welding where the ash-flow tuff has sufficient thickness. The zone of dense welding commonly forms a black vitrophyre. Fiamme are common in this vitrophyric zone. The basal zone of no welding and lower zone of partial welding are commonly glassy and pumice rich. The upper zone of partial welding is always devitrified and may contain a region of vapor-phase crystallization. The upper zone of no welding is usually glassy and pumice rich. The cooling break noted by Byers, et al. (1976a) is difficult to find in many of the outcrops.

Ammonia Tanks Member

The Ammonia Tanks Member is a compound ash-flow sheet (Fig. 2, Table 1). Byers, et al., (1976a, 1976b) determined that the ash-flow sheet consists of an upper and lower cooling unit. Byers, et al., (1976a) further subdivided the lower and upper units into rhyolitic and quartz latitic subunits.

The areal distribution of cooling units as defined by Byers, et al., (1976a) for the Ammonia Tanks Member within and beyond the Timber Mountain caldera is quite complex (see Byers, et al., 1976a, p. 46-47 for a detailed discussion). The presence of a moderately-faulted, additional cooling unit at the base of the Ammonia Tanks Member on Pahute Mesa has complicated the compositional distinction between the Rainier Mesa Member and the Ammonia Tanks Member. This unit is significant in that it contains some of the most mafic pumice fragments found in all of the collected sections. Noble, et al., (1967) mapped this additional unit as a lower Ammonia Tanks Member. Based on major and trace element chemical analyses performed by Rose (1988), this enigmatic unit is more similar to the Rainier Mesa Member and may represent a previously unrecognized upper cooling unit related to the Rainier Mesa eruptive phase. The compositional similarity of these pumice fragments to both members of the Timber Mountain Tuff may be evidence that this small cooling unit was erupted at a later magmatic evolutionary stage than the main Rainier Mesa Member magmatic phase and thus would represent a transitional magmatic phase between the Rainier Mesa Member and the Ammonia Tanks Member. Further detailed work needs to be performed on this unit.

The Ammonia Tanks Member is highly variable with respect to the presence of the various zones of welding in

any given area. In some areas the basal and upper zones of no welding grade into the zone of dense welding as in the Rainier Mesa Member. In other areas however, the basal zone of no welding may be absent and the tuff will be partially welded at the basal contact with the underlying air-fall tuff. Alternatively, in other areas (such as section 5 (samples A5-XX)), the entire thickness of tuff (up to 35 meters thick) may exhibit only incipient welding. Pumice (and fiamme where densely welded) are ubiquitous throughout the thickness of the Ammonia Tanks Member. The cooling break between the lower and upper units of Byers, et al. (1976a) was difficult to find in most outcrops.

SAMPLING TECHNIQUE

Sample Type

Historically, geochemical and mineralogical studies of ash-flow tuffs have been predominantly based upon whole-rock tuff samples. In many instances, glassy pumice fragments are collected in addition to the whole-rock tuff samples for comparative studies. In a few studies, such as that by Leat, et al. (1984) on calderas of the Kenya Rift Valley, only pumice fragments were used. In these studies relying solely on pumice fragments, sampling technique and sample number must be adequate to document the full range of pumice fragment composition. Some volumetrically large ash-flow tuffs however, such as the Fish Canyon Tuff (>3000 km^3) of the San Juan Volcanic Field, southern Colorado, have surprisingly homogeneous compositions for both whole-rock tuff and pumice fragments (cf. Whitney and Stormer, 1985). Thus a small number of samples in this type of situation may not create a bias in the documentation of the types of magma present in the parent magma body.

Studies of the ash-flow tuffs of the Timber Mountain-Oasis Valley caldera complex by Schuraytz, et al., 1986, 1989; Flood, 1987; Flood, et al., 1989a, 1989b; Rose, 1988; Mills and Rose (1986); Mills, et al. (1987) and Mills and Vogel (1988) have also concentrated on glassy pumice fragments instead of whole-rock tuff with the

exception that their sampling techniques have been designed to ensure thorough sampling and a minimization of sample bias. The motivation for using glassy pumice fragments lies in the very nature of the origin of ash-flow tuffs and is a technique that has been used by several other workers in the past (e.g. Lipman, 1967, 1971; Walker, 1972; Wolff, 1985; Hildreth and Mahood, 1985).

Ash-flow tuffs have four basic components: 1) glassy or devitrified pumice fragments and/or fiamme, 2) a fine grained ashy matrix composed of glass shards, 3) phenocrysts released from the eviscerated and crushed pumice during eruption, and, those still contained within the pumice fragments, and 4) a wide compositional range of xenolithic fragments derived from the vent walls, and, from surface material entrained by the ash-flow during emplacement. Reconstruction of the parental magma chemistry, assuming a simple case of a compositionally homogeneous parent magma, can be complicated by phenocryst elutriation during transport and xenolithic contamination (Walker, 1972; Wolff, 1985). As is the case for most large volume ash-flow tuffs however, the parental magma may have up to several discrete compositions which may be coevally erupted (e.g. Lipman, et al., 1966; Lipman, 1967; Hildreth, 1983; Wolff and Storey, 1984, Schuraytz, et al., 1986). Geochemical and mineralogical

reconstruction of the original magmatic compositions based upon whole-rock tuff samples in this case is very difficult, even with detailed, individual glass shard analyses by an electron microprobe. It must be recognized then that chemical and mineralogic analyses of whole-rock tuff samples represent a mixture of the above mentioned components. Individual shard analyses in a whole-rock sample will provide melt compositions, but magma compositions must include phenocryst phases present within that particular system, a problem we feel best solved by examining pumice fragments.

In an attempt to circumvent some of the problems outlined above, this study concentrates on the glassy pumice fragments found in the unwelded to partially welded zones and fiamme located in the vitrophyres of the individual members of the Timber Mountain Tuff. These pumice fragments most nearly represent the original pre-eruptive magmatic geochemical and mineralogical compositions (cf. Wolff, 1985). Secondary alteration of the glassy pumice fragments does occur as groundwater passes through the porous unwelded to partially welded zones in the ash-flow tuff. The alteration appears to most directly affect the concentration of the alkalis and ferrous iron (Aramaki and Lipman, 1965; Lipman, 1965; Noble, 1965, 1967). This effect appears to be minor in the Timber Mountain Tuff as documented by the small amount

of scatter on geochemical variation diagrams. Phenocrysts within the pumice fragments do not appear to be altered in any fashion.

Pumice fragments of a commingled nature exist within both members of the Timber Mountain Tuff. The term commingling will be used in this study as defined by Bacon (1986), "...(compositionally) banded or inclusion-bearing magmas...". Commingling may occur by several methods which include but are not limited to; commingling from the injection of new magma into the chamber, commingling deep within the chamber as the magma(s) are brought to the vent during eruption, or, commingling directly within the vent as the different magma types are forced through the conduit. Pumice fragments that originate by commingling are often recognized by their distinct color and textural banding. Of a more subtle complexity are pumice fragments that represent compositionally mixed magmas as defined by Bacon (1986), "...(compositionally) homogeneous hybrid magmas...". In this case, two or more magma types have been so thoroughly mixed in the chamber that a new, chemically homogeneous magma is created. Pumice fragments formed by mixing were identified in this study by the presence of disequilibrium phenocrysts. Magma mixing results in bimodal to polymodal distributions of phenocryst compositions in a particular sample. If enough time elapses after mixing however, the phenocryst

populations will reequilibrate to the new physical and chemical conditions and a compositionally and mineralogically distinct magma will be formed which will lack polymodal phenocryst compositions. An excellent example of this process has been shown to have occurred in the Pah Canyon Member of the Paintbrush Tuff (Flood, 1987; Flood et al., 1989b). Complications arising from commingling of magma types during eruption are avoided by omitting samples with macroscopic to microscopic banding (based on color, texture, and mineralogy)(cf. Williams, 1942; Bacon, 1983) and those containing disequilibrium phenocryst assemblages identified on the basis of optical and electron microprobe analyses.

The study of phenocrysts in whole-rock or bulk samples of ash-flow tuffs however can be encumbered by several factors: 1) magma fragmentation processes which cause preferential fractionation of crystals from pumice fragments, and, can enrich bulk samples of the ignimbrite in phenocrysts (Wolff, 1985), 2) atmospheric winnowing of fine ash during transport of the ash-flow which again results in the enhancement of phenocrysts within the deposit (Hay, 1959; Lipman, 1967; Walker, 1972; Sparks and Walker, 1977), 3) inclusion of xenocrysts and xenoliths of country rock abraded from vent walls, and, incorporation of surface material during passage of the ash-flow (Walker, 1972), and 4) the combining of

phenocryst phases during transport of the ash-flow from coevally erupted, chemically discrete magma types.

In addition to problems with whole-rock samples, chemical and mineralogic analyses of pumice fragments within pyroclastic flow deposits must also be performed with caution. As shown by Wolff (1985), consideration of sample size is critical to minimizing the effects of magma fragmentation (preferential loss of phenocrysts in pumice fragments during eruption and transport) and phenocryst control of bulk pumice fragment chemistry due to high crystal/glass ratios. For mineralogic analyses pumice fragments should be used if possible when trying to reconstruct original magmatic phenocryst assemblages as whole rock samples may suffer one or more of the many effects noted above (Lipman, 1967; Sparks and Walker, 1977; Wolff, 1985). Thus attempts to correlate whole-rock tuff samples with original magmatic geochemical and/or mineralogic compositions may lead to erroneous results if caution is not used. In many ash-flow tuffs however, the collection of pumice fragments may be impossible due to the paucity and/or devitrification of the pumice fragments within the tuff. In both members of the Timber Mountain Tuff however, glassy pumice fragments were ubiquitous. Every attempt was made during this study to select large enough samples of pumice fragments so as to minimize size bias. Collection of glassy pumice

fragments from only the unwelded basal zone, vitrophyric zone and unwelded top of the ash-flow sheet would initially seem to be a potential source of sample bias. However, as shown by Schuraytz, et al., (1989), as long as the upper, poorly to non-welded zone of the ash-flow sheet is collected, the full range of pumice compositions present within the interior of the sheet will most likely be represented at the top of the sheet. This has also been verified by data collected by Rose (1988) for the Ammonia Tanks Member. Section #5 of Rose (1988) was collected in a 35 meter thick, completely unwelded section of tuff from base to top in approximately 3 meter intervals. Pumice fragments collected at the top of this section were representative of all compositions present below this region (Fig. 3).

Site Selection and Sampling Technique

Potential collecting localities were identified from USGS geologic topographic maps (see Byers et al., 1976a for a map index). The selection of outcrops to be sampled was based on stratigraphic control of the underlying and overlying units, degree of exposure, absence of hydrothermal alteration, and the presence of an unwelded base and/or top at the exposed section. Partially exposed or eroded units (where only unwelded bases or tops were present) were collected only when nearby exposures that

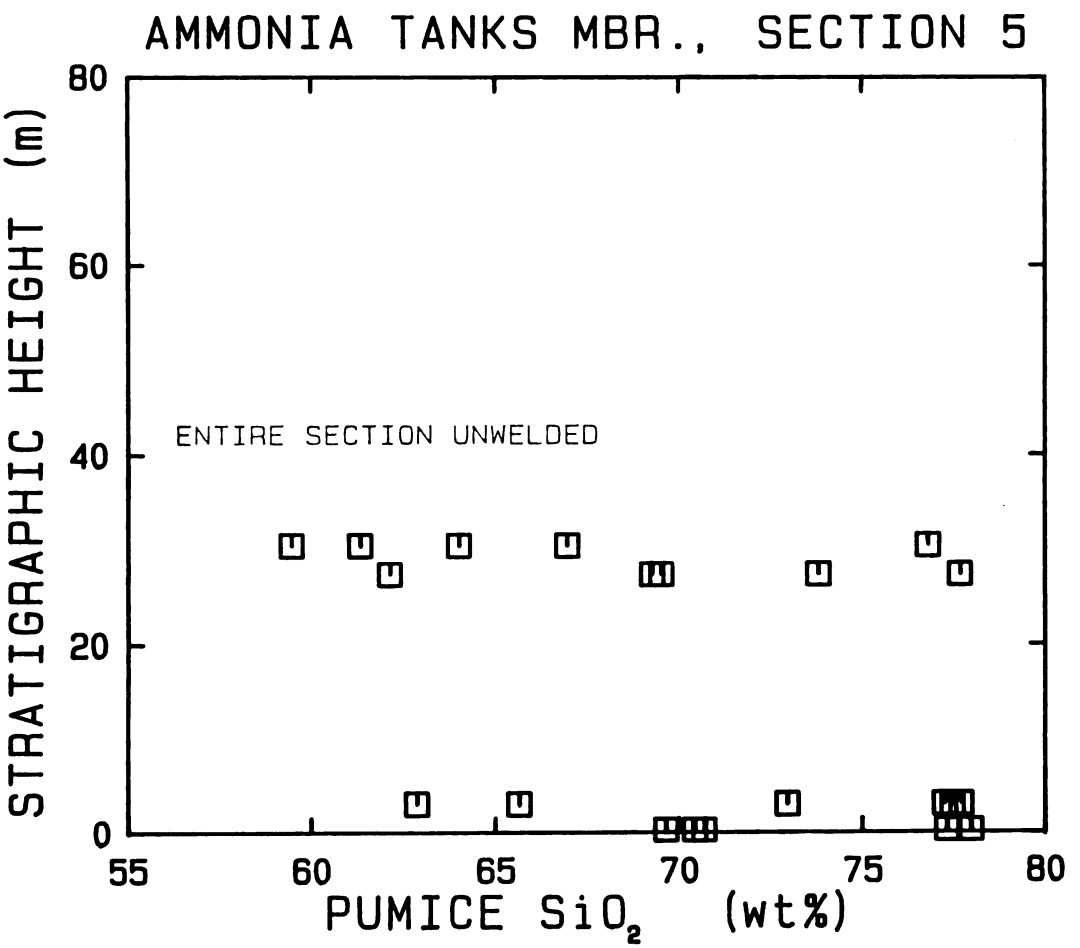


Figure 3. Stratigraphic variation in whole pumice composition for the Ammonia Tanks Member, Section 5.

provided the missing top or bottom of the section could be found. Sampling locations of chemically analyzed pumice fragments are shown in Figure 1. Exact locations of the sampling sites are described in Appendix 1.

Once a site was selected for sampling, pumice fragments were collected over an area of 10 m^2 (1 meter high by 10 meters wide) approximately every 1.5 m up section in the unwelded to partially welded zones. Glassy pumice fragments were selected based on differences in color, texture, phenocryst assemblage, and size. In a typical 10 m^2 area, 20 to 30 pumice fragments were usually collected. Fiamme from vitrophyric zones were collected from the base to the top of the vitrophyre and along a horizontal distance of 5 m to 10 m. In all, over 1400 pumice fragments were collected for potential analysis. Once the pumice fragments were returned to the laboratory, further visual and mineralogic discrimination amongst pumice types was done to select a final suite of pumice fragments for analysis. Selection of the final suite of pumice fragments was, as in the field, based on color, texture, phenocryst assemblage and size.

An initial attempt was made to sample sections from; 1) caldera fill and outflow facies, 2) sections representing proximal to distal outflow facies, and 3) sections circumscribing the Timber Mountain caldera. This procedure proved futile for several reasons; first,

outflow sheets outcropping in the southwestern to western areas of the Timber Mountain caldera are mildly to pervasively hydrothermally altered. This alteration is part of the Bullfrog Hills alteration and mineralization event (Ransome, et al., 1910; Cornwall and Kleinhampl, 1964). Second, the caldera fill of the Rainier Mesa Member is completely buried by the younger Ammonia Tanks Member and is only exposed in small amounts of drill core from USGS drill hole UE18r located in the northern portion of the caldera (see Byers, et al., 1976b for the drill hole location). Third, complete stratigraphic sections of Ammonia Tanks Member caldera fill facies are rarely present due to structural disagregation during caldera resurgence and complete devitrification of the Ammonia Tanks Member. These two factors made pumice identification and removal extremely difficult on the resurgent dome. Finally, poor exposure and incomplete sections in the east-southeast and southern outflow regions surrounding the caldera did not allow for satisfactory pumice fragment collection. Thus, the majority of sampled sections are located to the north and northeast of the caldera (Fig. 1).

GEOCHEMISTRY

Introduction

The Rainier Mesa Member and the Ammonia Tanks Member can usually be distinguished from one another on the basis of selected trace elements and the presence or absence of sphene. Major-element geochemical discrimination between the Rainier Mesa Member and Ammonia Tanks Member however is difficult. The two members are generally distinguishable only on the basis of CaO vs. SiO_2 for compositions more mafic than 75 wt% SiO_2 (Fig. 4). Trace element concentrations for the two members however, are distinctive enough that on some inter-element variation diagrams, for example Nb vs. SiO_2 (Fig. 5a) and Nb vs. Rb (Fig. 5b), the two units can be separately identified in most instances. There is however, some problem with data overlap (Figs. 5a,b). Previous workers relied primarily on the presence or absence of sphene to petrographically discriminate between the two ash-flow tuffs. The Rainier Mesa Member is devoid of sphene while the Ammonia Tanks Member contains a significant percentage of sphene (10-20 grains per standard-size thin section, Byers, et al., 1976a).

The Total Alkali-Silica (TAS) classification system of Le Bas, et al., (1986) is used in this study to classify the pumice sample compositions (Fig. 6). From the TAS diagram it can be observed that the pumice

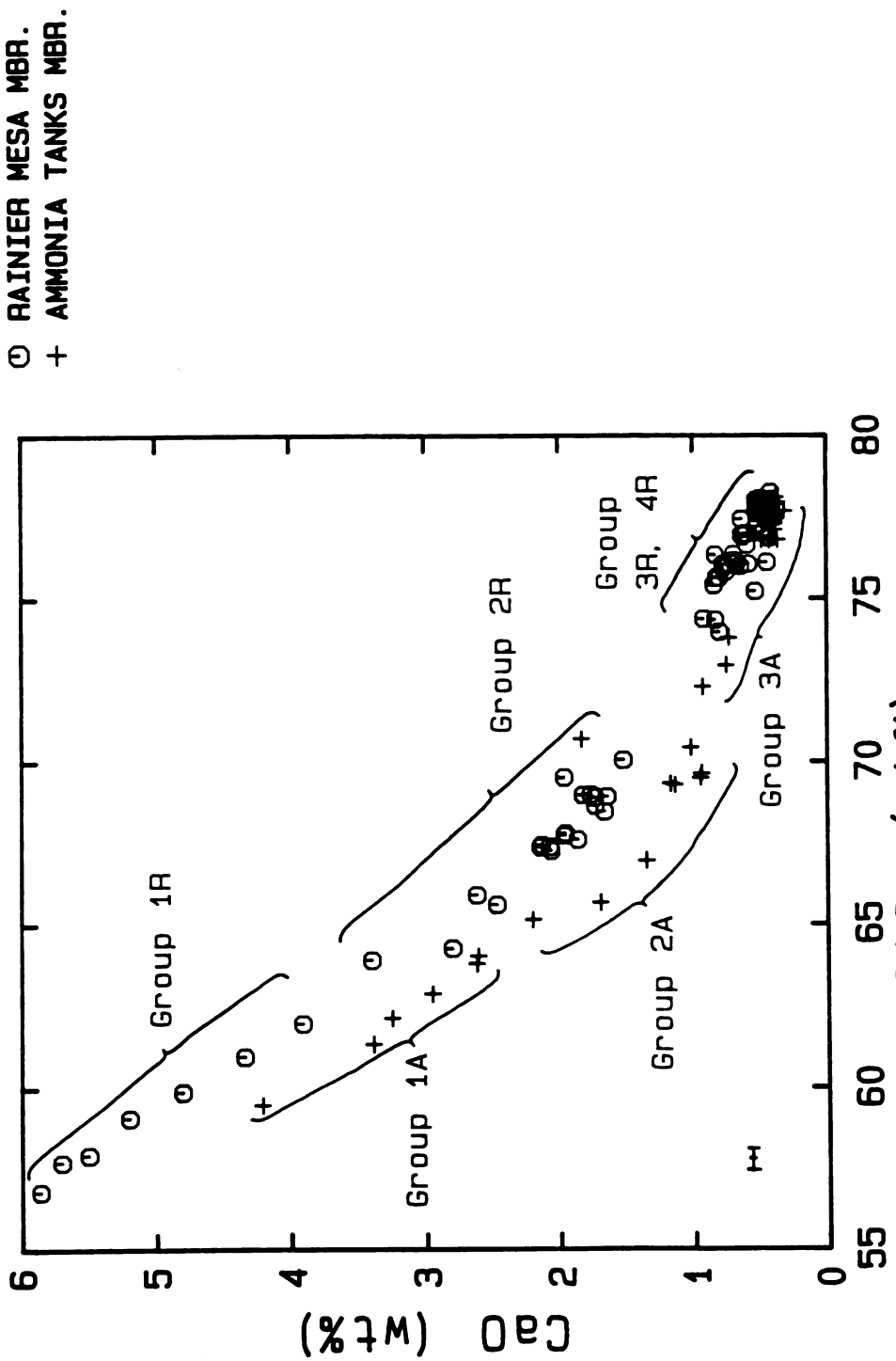


Figure 4. SiO_2 versus CaO discrimination diagram for the Rainier Mesa Member and Ammonia Tanks Member.

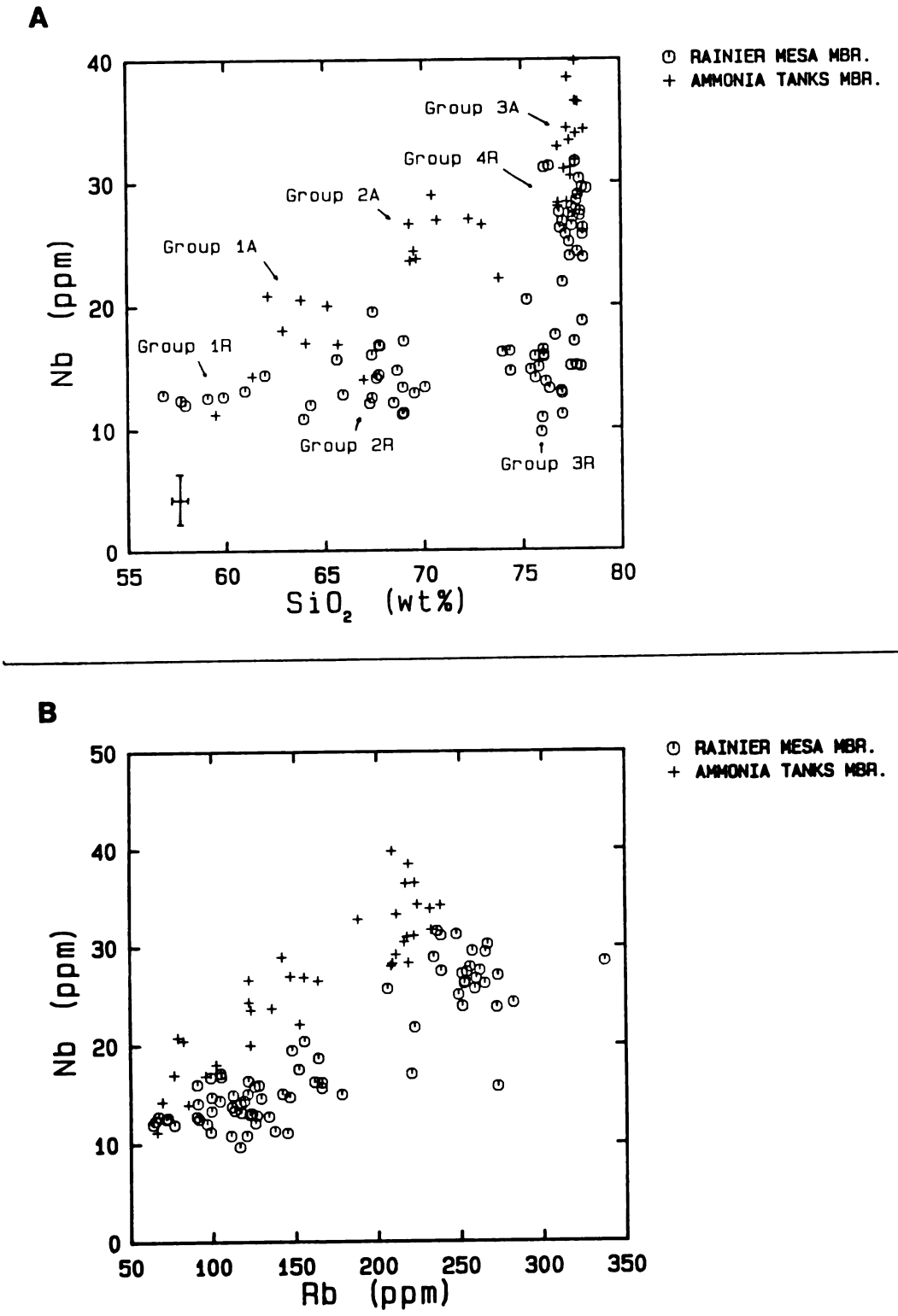


Figure 5. A) SiO_2 versus Nb discrimination diagram for the Rainier Mesa Member and Ammonia Tanks Member.
B) Rb versus Nb discrimination diagram for the Rainier Mesa Member and Ammonia Tanks Member.

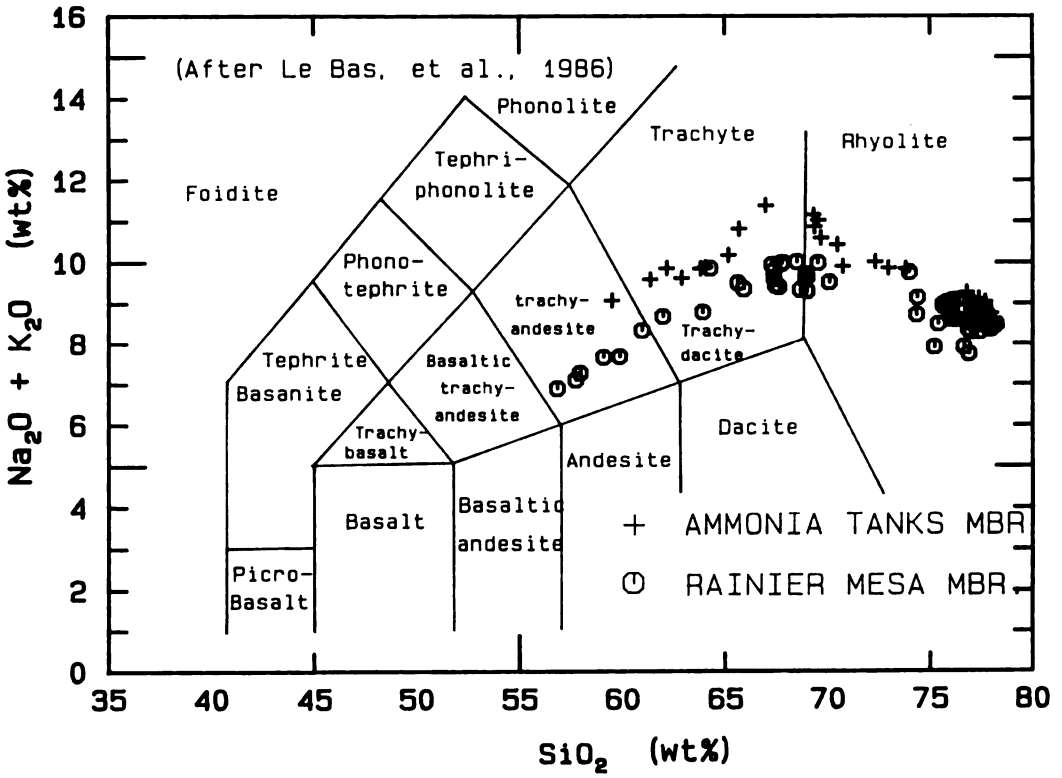


Figure 6. Total Alkali-silica classification diagram for the Timber Mountain Tuff.

fragment compositions in each member of the Timber Mountain Tuff range from trachyandesite to rhyolite. In this study, all pumice fragment compositions which have SiO_2 concentrations greater than 74 wt% SiO_2 will be classified as high-silica rhyolites. Some alkali mobilization may have occurred within the whole-rock tuffs as the tuffs cooled after emplacement, and, from secondary hydration of the whole-rock tuff due to interaction with groundwater (Aramaki and Lipman, 1965; Lipman, 1965; Noble, 1967). The chemical classification systems which rely on total alkalis versus silica should thus be used with some caution (eg. Le Bas, et al., 1986; Irvine and Barager, 1971). Analyses of the alkali elements in this study however do not indicate significant alkali mobilization based on low scatter of the data in the geochemical variation diagrams.

Analytical techniques used to determine major and trace element concentrations in pumice fragments and phenocrysts are described in Appendix 3. USGS, Canadian and Japanese whole-rock standards used to calibrate the analyses are presented in Tables A3a, A3b and A3c. Mineral standard analyses and microprobe beam parameters used for calibration of phenocryst analyses on the electron microprobe are presented in Tables A3d and A3e respectively.

Major Element Oxides

Rainier Mesa Member

Major element analyses were performed on 104 pumice fragments collected from seven stratigraphic sections of the Rainier Mesa Member (sections 8, 11, 18, 21, 23, 25 and 26; Appendix 1)(Fig. 1). Raw major and trace element data for the Rainier Mesa Member is presented in Appendix 2. Harker variation diagrams for the Rainier Mesa Member are presented in Figure 7. SiO_2 was chosen as the abscissa for these plots as it has the largest degree of variation of the major element oxides. MgO was not used because it commonly falls below XRF detection limits for the high-silica rhyolite samples. All major elements, except Al_2O_3, Na_2O and K_2O, consistently decrease in concentration with respect to increasing SiO_2 concentrations from trachyandesite to high-silica rhyolite in the Rainier Mesa Member. Trends of Al_2O_3, Na_2O and K_2O exhibit sharp inflections at approximately 65 wt% SiO_2; this may reflect the removal of various phenocryst phases.

Silica concentrations for the Rainier Mesa Member tend to cluster into groups. The clustering of data can be observed on major element plots, but is more pronounced on trace element versus silica plots (Fig. 8). Three groups can be identified from the major element variation

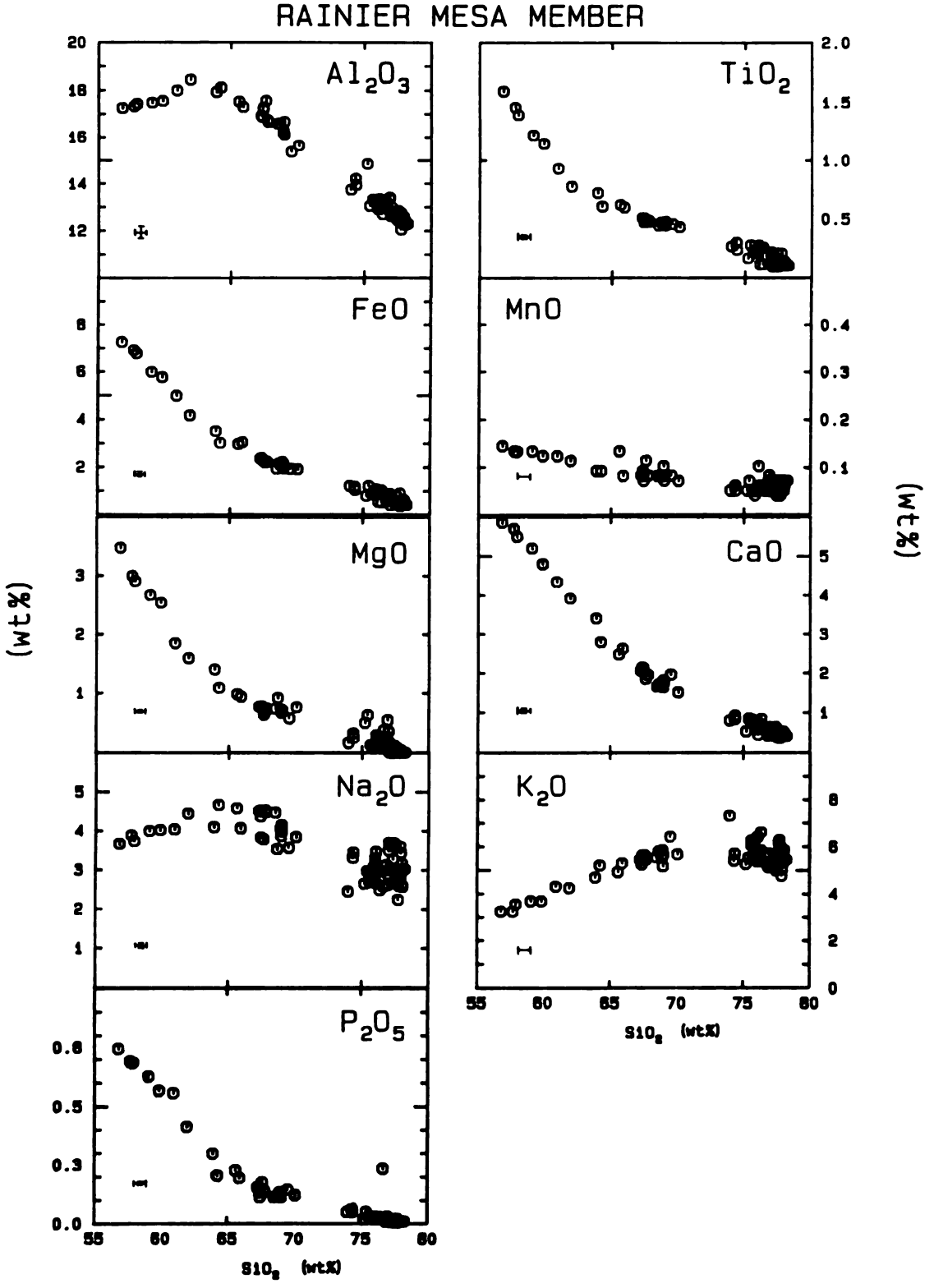


Figure 7. Major element variation diagrams for the Rainier Mesa Member.

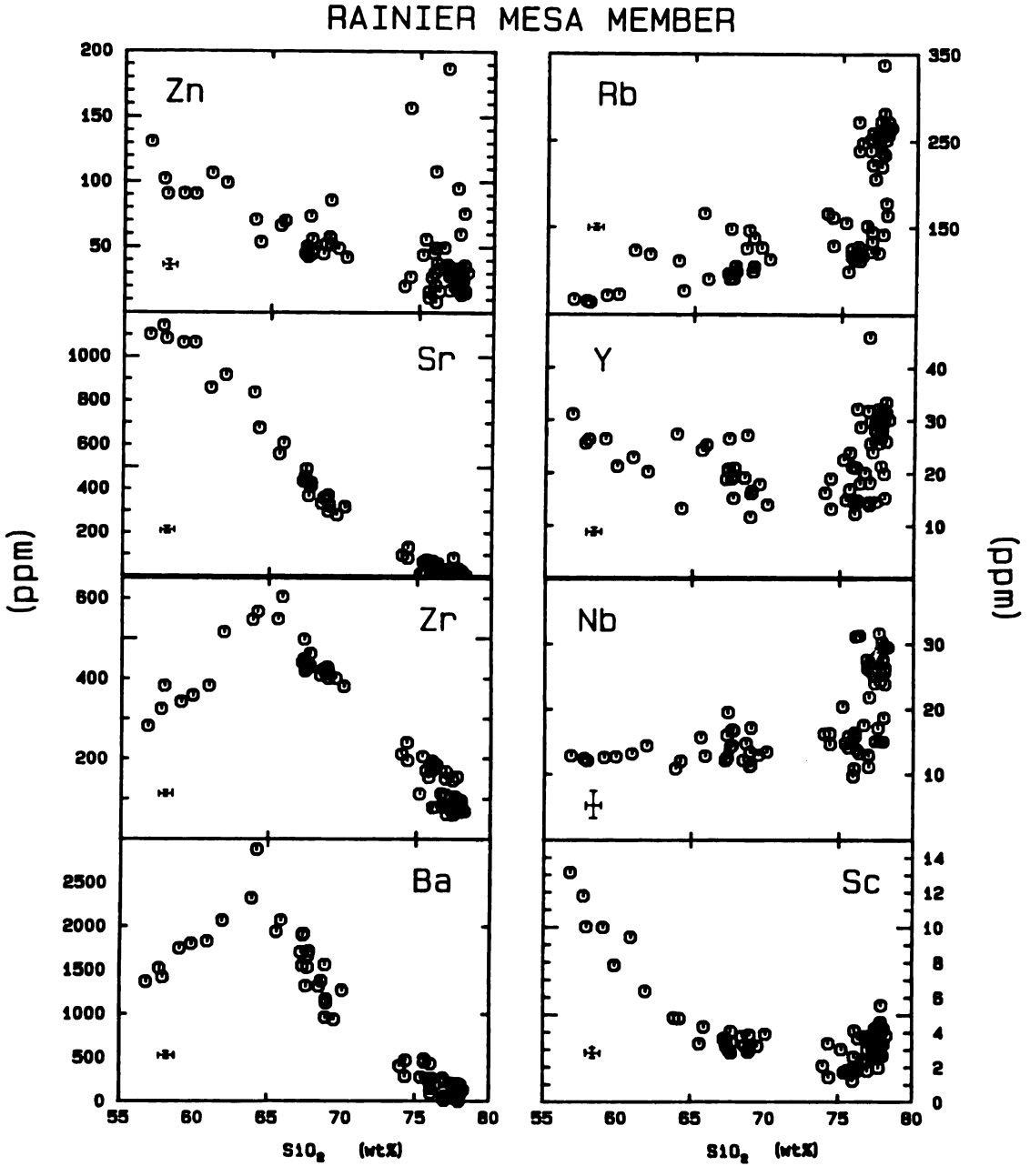


Figure 8. Trace element variation diagrams for the Rainier Mesa Member.

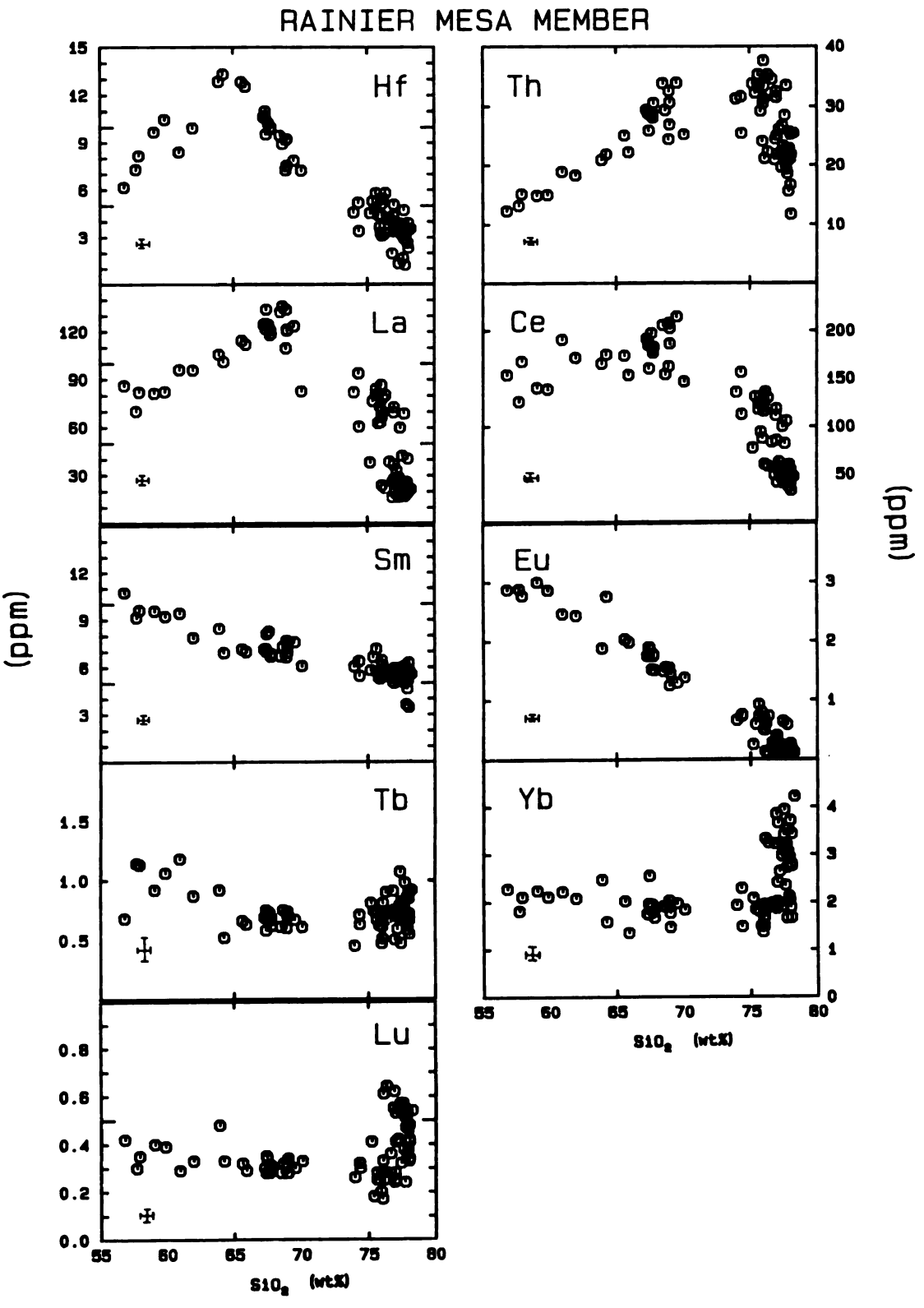


Figure 8. Continued.

diagrams based on silica gaps or zones of low data frequency; 1) trachyandesite to trachydacite (group 1R)(57 wt% to 61 wt% SiO_2), 2) trachydacite to rhyolite (group 2R)(63 wt% to 70 wt% SiO_2) and 3) rhyolite to high-silica rhyolite (group 3R, 4R)(74 wt% to 78 wt% SiO_2)(Figs. 4 and 5a). The silica gap within the trachydacite is not a true gap but a region of low data frequency. The silica gap within the rhyolite however is more pronounced and spans a range of 4 wt% SiO_2.

Synthesis of whole-rock tuff chemistry and petrographic analyses on the Rainier Mesa Member by Byers, et al. (1976a) documented the normal zonation of whole-rock silica concentrations from 78 wt% SiO_2 at the base to 69 wt% SiO_2 at the top. Corresponding changes in the modes of quartz, feldspar, biotite, pyroxene, and amphibole led Byers, et al., (1976a) to propose that the pre-eruptive magma body was zoned from quartz latite in the lower portions of the chamber to high-silica rhyolite at the cupola. This hypothesis is supported by more recent work on both the Paintbrush Tuff and Timber Mountain Tuff by Broxton, et al., (1985, 1989) and Warren, et al., (1989).

A significantly greater compositional range for the Rainier Mesa Member is documented from analyses of the glassy pumice fragments. This range in SiO_2 concentration (57-78 wt% SiO_2) for the Rainier Mesa Member is the

largest thus far documented for an ash-flow tuff (Mills and Rose, 1986; Mills, et al., 1987).

Pumice fragment compositions do not change systematically from high-silica rhyolite to trachyandesite with increasing stratigraphic height. The unwelded to partially welded base of the Rainier Mesa Tuff is composed of a geochemically bimodal population (based on Rb and Nb concentrations) of quartz, feldspar and biotite bearing high-silica rhyolite pumice fragments. The range of pumice fragment compositions becomes larger with increasing stratigraphic height. Hornblende, pyroxene, and feldspar-rich mafic pumice fragments become volumetrically more significant upsection (Fig. 2). All pumice fragment compositions found within the sheet are represented within the upper few meters of the top Rainier Mesa Member. This feature has been noted in several other ash-flow deposits; the Mount Mazama pyroclastic flows (McBirney, 1968; Noble, et al., 1969; Druitt and Bacon, 1986), ash-flow sheets from the Aso caldera, Japan (Lipman, 1967), the Topopah Spring Member of the Paintbrush Tuff, Nevada (Lipman et al., 1966; Schuraytz et al., 1986), the Tiva Canyon Member of the Paintbrush Tuff (Flood, et al., 1989a, 1989b), pyroclastic deposits derived from the Las Canadas caldera on Tenerife Island (Canary Islands)(Wolff and Storey, 1984) and in the 1912 ash-flow of the Valley of Ten Thousand Smokes, Alaska

(Hildreth, 1983). The origin of the compositionally heterogeneous pumice-fragment population is most likely a result of eruption dynamics and will be discussed in more detail in a later section.

Ammonia Tanks Member

Major element analyses were done on 35 pumice fragments collected from two stratigraphic sections of the Ammonia Tanks Member (sections 4 and 5; Appendix 1)(Fig. 1). Raw major and trace element data for the Ammonia Tanks Member is presented in Appendix 2. Geochemical variation diagrams are presented in Figures 9 and 10.

All major elements with the exception of Al_2O_3 and K_2O, consistently decrease in abundance with respect to increasing silica from the trachyandesite to the high-silica rhyolite. Trends of the major elements, with the exception of TiO_2, Na_2O and MnO, are characterized by inflections at approximately 65-68 wt% SiO_2 with respect to increasing silica that may reflect the removal of various phenocryst phases (Fig. 9).

The Ammonia Tanks Member has almost as large a range in pumice fragment major element composition (59-78 wt% SiO_2) as does the Rainier Mesa Member. As in the Rainier Mesa Member, the major element oxide data exhibit little scatter with the exception of the Na_2O and K_2O which is

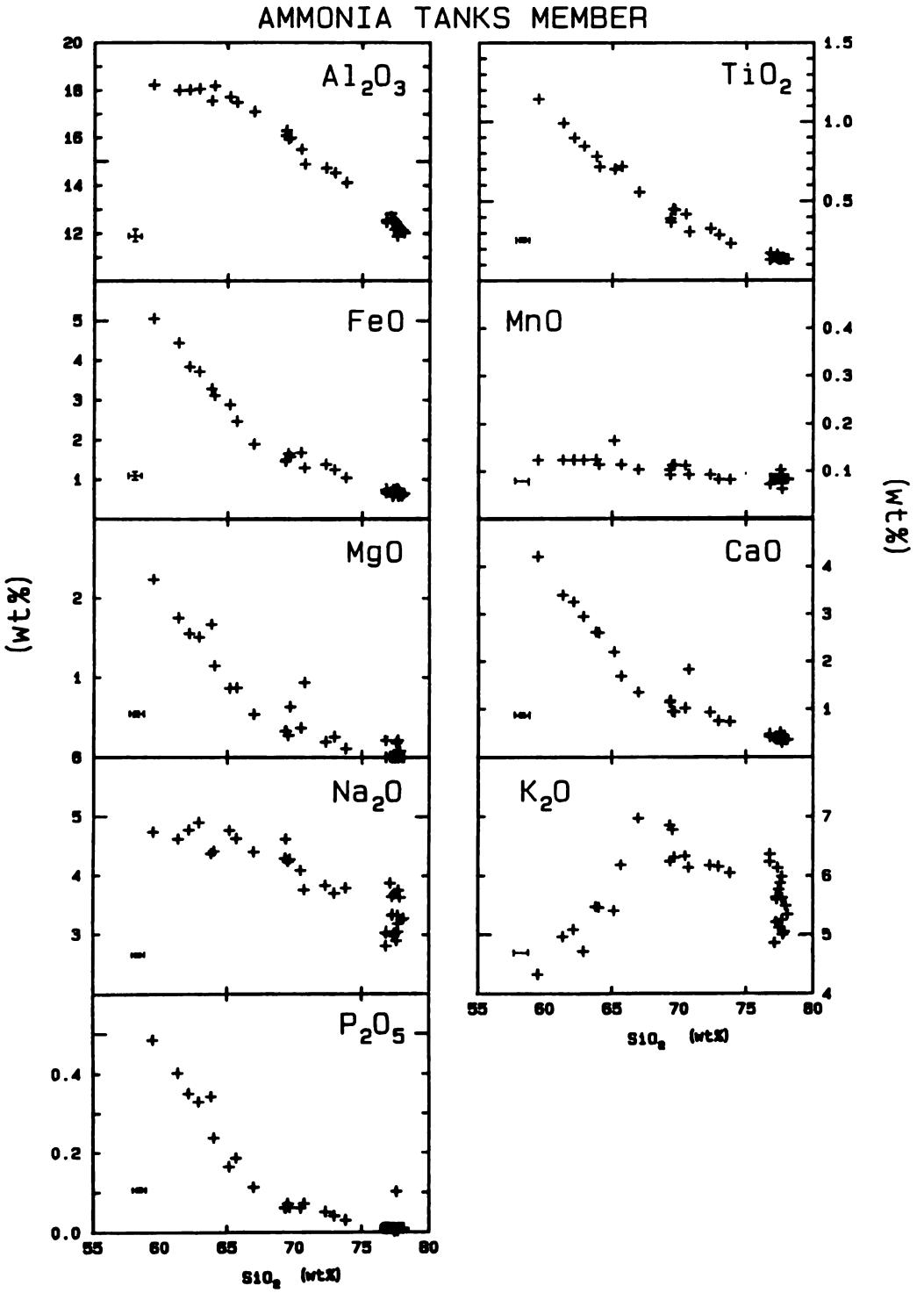


Figure 9. Major element variation diagrams for the Ammonia Tanks Member.

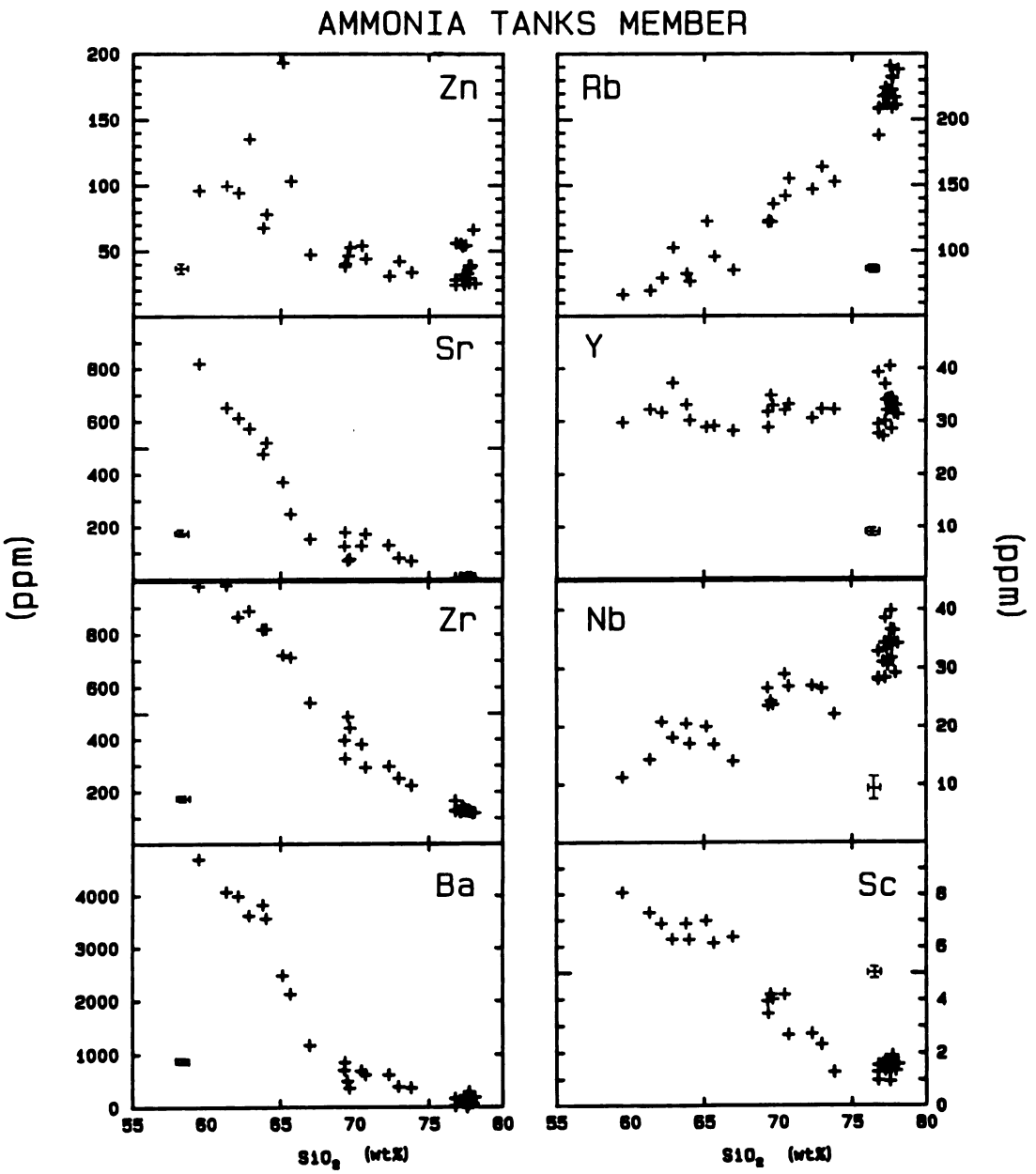


Figure 10. Trace element variation diagrams for the Ammonia Tanks Member.

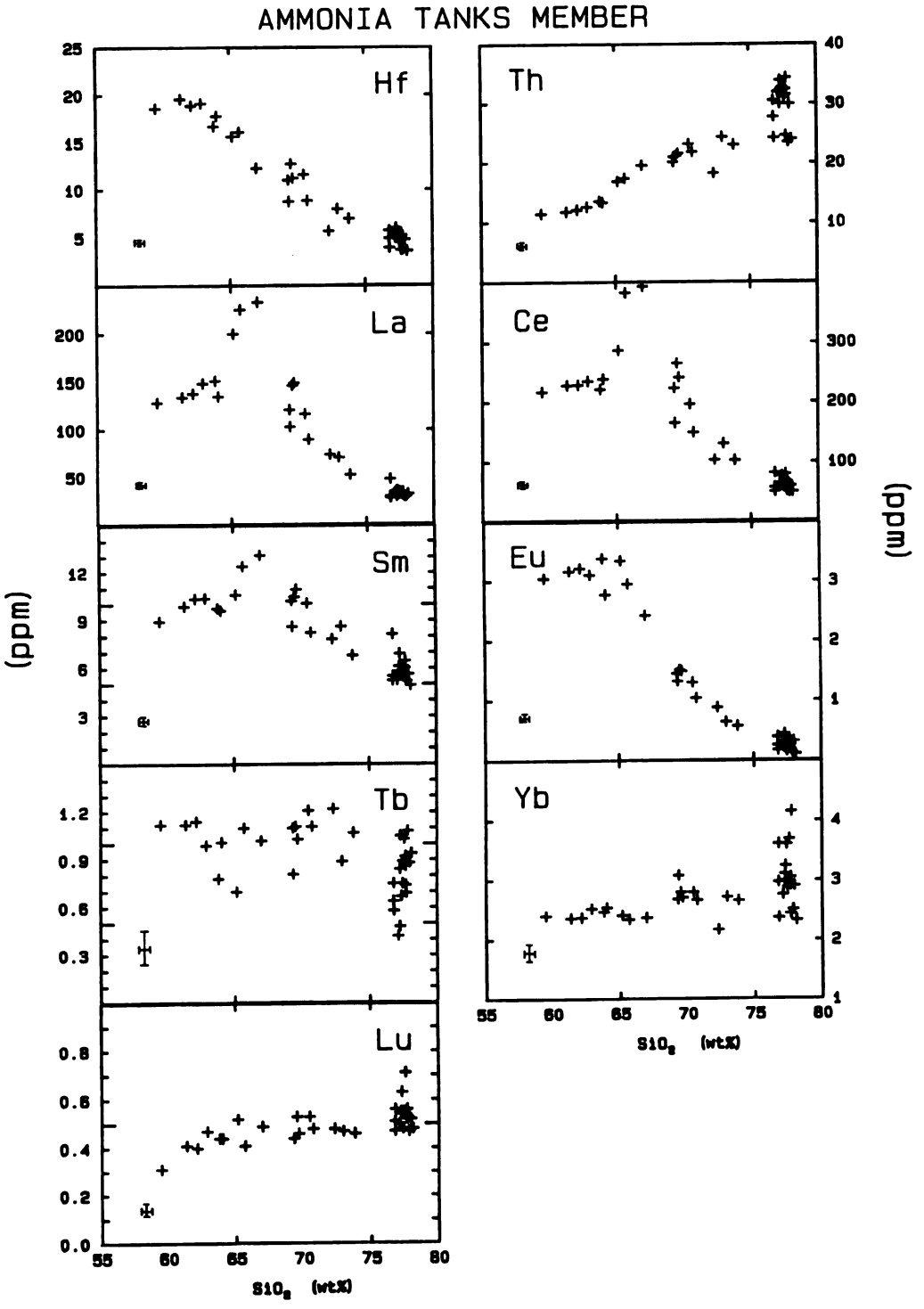


Figure 10. Continued.

most likely due to minor secondary hydration of the glassy pumice fragments.

Early studies based on whole-rock tuff geochemical analyses led Byers, et al., (1968, 1976a) to infer that the lower unit of Ammonia Tanks Member was reversely zoned with respect to silica concentration. Whole-rock tuff silica concentrations range from 68 wt% SiO_2 at the base to 78 wt% SiO_2 at the top. Whole-rock analyses of tuffs from the upper portion of the upper cooling unit were not reported, but this unit was also inferred to be reversely zoned based on the presence of a quartz latitic base (66 wt% SiO_2) (Byers, et al., 1976a).

Recent work using glassy pumice fragments on the compound cooling unit of the Ammonia Tanks Member by Mills and Rose (1986) and Rose (1988) has shown that high-silica rhyolite pumice fragments form the bulk of the pumice fragment population at the base of the lower unit and decrease rapidly (usually within one meter of the base) in abundance towards the top of the upper unit. The base of the upper unit does not have high-silica rhyolite pumice-rich zone. All pumice fragment compositions found in the lower portion of the sheet can be found at the very top of the compound cooling unit (Figs. 2 and 3). It is questionable whether the Ammonia Tanks Member can be labeled as either a normal or reversely zoned tuff for two reasons; 1) the high-silica rhyolite pumice-rich zone at

the base is not always present and 2) depending on the type and number of pumice fragments present within the whole-rock tuff at any given location, the overall composition of the whole-rock tuff sample will be highly variable.

Two of the three stratigraphic sections chosen for sampling contained compositionally heterogeneous pumice fragment populations from the base to the top of the ash-flow sheet (Mills and Rose, 1986; Mills, et al., 1987; Rose, 1988). The silica content of the pumice fragments in the basal portions of the sections located along the southern margin of Pahute Mesa range from 69.6 wt% to 78 wt% SiO_2 whereas at the top of the sections, the range increases from 59.4 wt% to 77.7 wt% SiO_2 (samples from the analytical groups A4-XX and A5-XX). A third section along the northern cauldron margin a few kilometers to the southwest of the other two sections, has a distinct 1.5 meter thick base consisting entirely of quartz, feldspar, and biotite-bearing rhyolitic pumice fragments. Preliminary chemical analyses on these pumice fragments indicate that they are high-silica rhyolite (Mills, unpub. data). Above this rhyolitic base, the pumice fragments rapidly become heterogeneous in composition over a 5 cm to 10 cm interval in a fashion similar to the two sections to the northeast.

Compositionally banded pumice are common in all observed sections of the Ammonia Tanks Member. Commingling of rhyolitic and trachydacitic to trachyandesitic magmas appears to have been common throughout the eruption of the Ammonia Tanks ash-flow tuff.

Trace Elements

Concentrations of Cr, Ni, Cu, Zn, Rb, Sr, Y, Zr, Nb, Ba, Sc, Hf, Th, and the rare-earth elements La, Ce, Sm, Eu, Tb, Yb and Lu were determined for the pumice fragments. These data are listed in Appendix 2.

For the Rainier Mesa Member and the Ammonia Tanks Member, the transitional metals Cr, Ni and Cu were consistently below detection limits except in a few of the more mafic pumice samples.

Rainier Mesa Member

For the Rainier Mesa Member, the trace elements are characterized by large ranges in concentration between the trachyandesite and high-silica rhyolite (Fig. 8). Scatter in the data is generally low with the exception of Zn and Y. In the Rainier Mesa Member, only Rb has a consistent increase in concentration with increasing SiO_2 concentration. All other elements either decrease

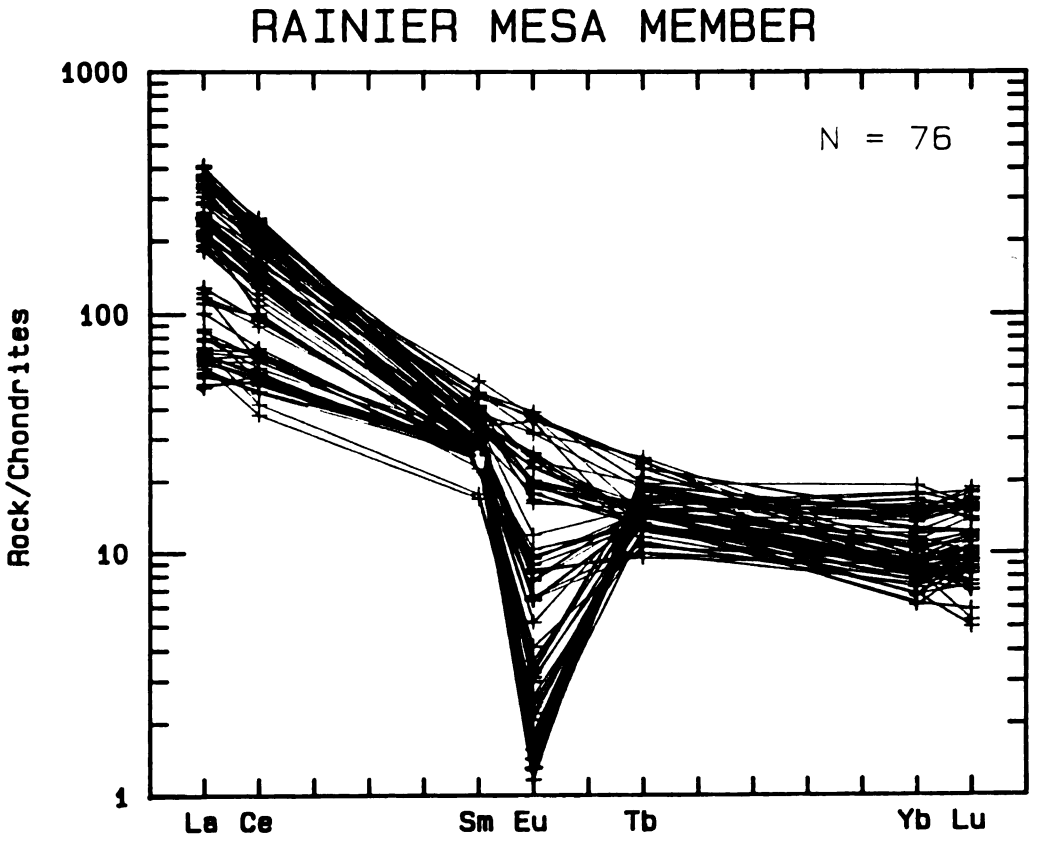


Figure 11a. Rare-earth element plot for the Rainier Mesa Member. All magmatic compositions plotted.

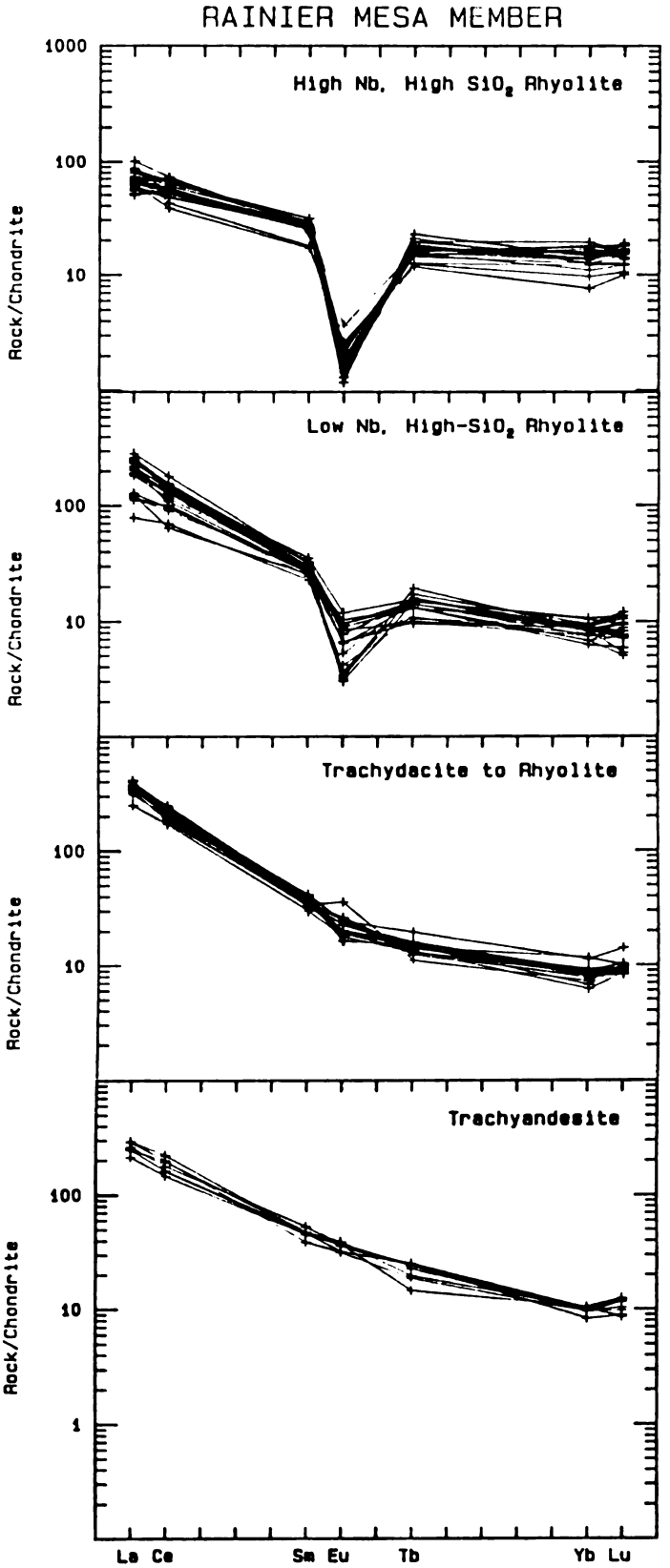


Figure 11b. Rare-earth element plots for the various magmatic groups of the Rainier Mesa Member.

consistently in concentration or have inflections in their trends with increasing SiO_2 concentration (Fig. 8).

On several trace element plots (Rb, Sc, Y, Nb, Th and La), the high-silica rhyolite data can divided into two separate components (group 3R, 4R; Fig. 5a). For this study, the designation low-Nb, high-silica rhyolite and high-Nb, high-silica rhyolite will be used to identify the respective rhyolitic components. Nb was chosen because of the low scatter in the data and the good separation of the two high-silica rhyolite components. Rb may also be used to discriminate the two rhyolitic components. Thus, the Rainier Mesa Member contains a total of four magmatic groups based upon major-element and trace-element chemistry; trachyandesite to trachydacite (group 1R), trachydacite to rhyolite (group 2R), low-Nb high-silica rhyolite (group 3R) and high-Nb high-silica rhyolite (group 4R)(Figs. 4 and 5a).

Chondrite normalized rare-earth element plots for the Rainier Mesa Member are shown in Figures 11a and 11b. Chondrite normalization factors are from Haskins, et al., (1968).

Rare-earth element data for the Rainier Mesa Member can be separated into distinct compositional groups, within which, samples exhibit similar trends on the chondrite normalized REE plots. These groups are distinguished from one another by significant changes in

concentration of the REE's as magmatic evolution increases (increasing SiO_2 concentration). The compositional groups are closely associated with the compositional groups defined by pumice fragment SiO_2 concentration, as should be expected. REE compositional group boundaries typically occur where significant gaps of up to 4 wt% SiO_2 occur, or, where apparent gaps occur due to low data point frequency. Figure 11b shows the apparent systematic change from the light rare-earth element (LREE) enriched trachyandesite samples to the less LREE enriched rhyolitic samples. As magmatic evolution increases, the LREE's are depleted and the negative Eu anomaly becomes more prominent. The HREE's remain relatively constant in concentration from the trachyandesite to the low-Nb high-silica rhyolite. Comparison of the high-silica rhyolites however, reveals the depletion in LREE concentration, the deeper negative Eu anomaly, and the **enriched** HREE concentration of the high-Nb high-silica rhyolite as compared to the low-Nb high-silica rhyolite.

Trace element concentrations normalized to chondritic meteorite abundances for the Rainier Mesa are presented as spidergrams in Figures 12a and 12b (after Thompson, et al., 1984). The elements Rb, Th, K and Nb behave incompatibly by increasing in concentration with increasing magmatic differentiation while the rest of the elements behave compatibly and either decrease in

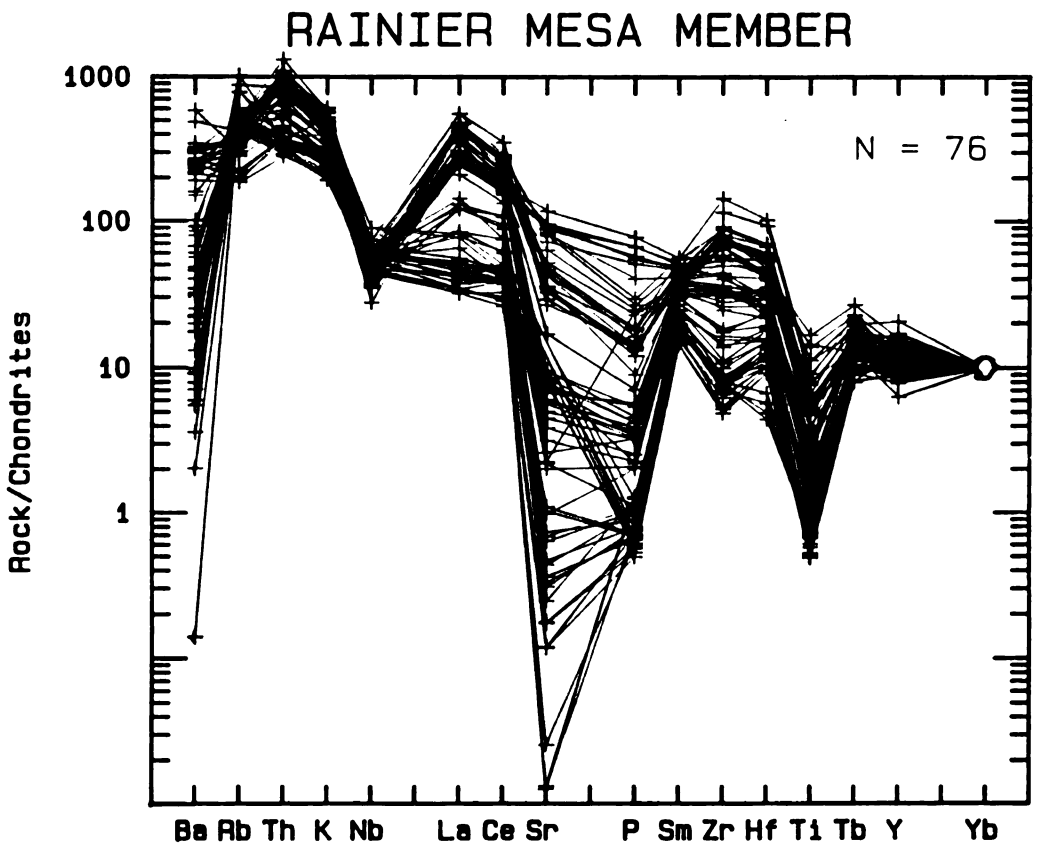


Figure 12a. Spidergram for the Rainier Mesa Member. All magmatic compositions plotted.

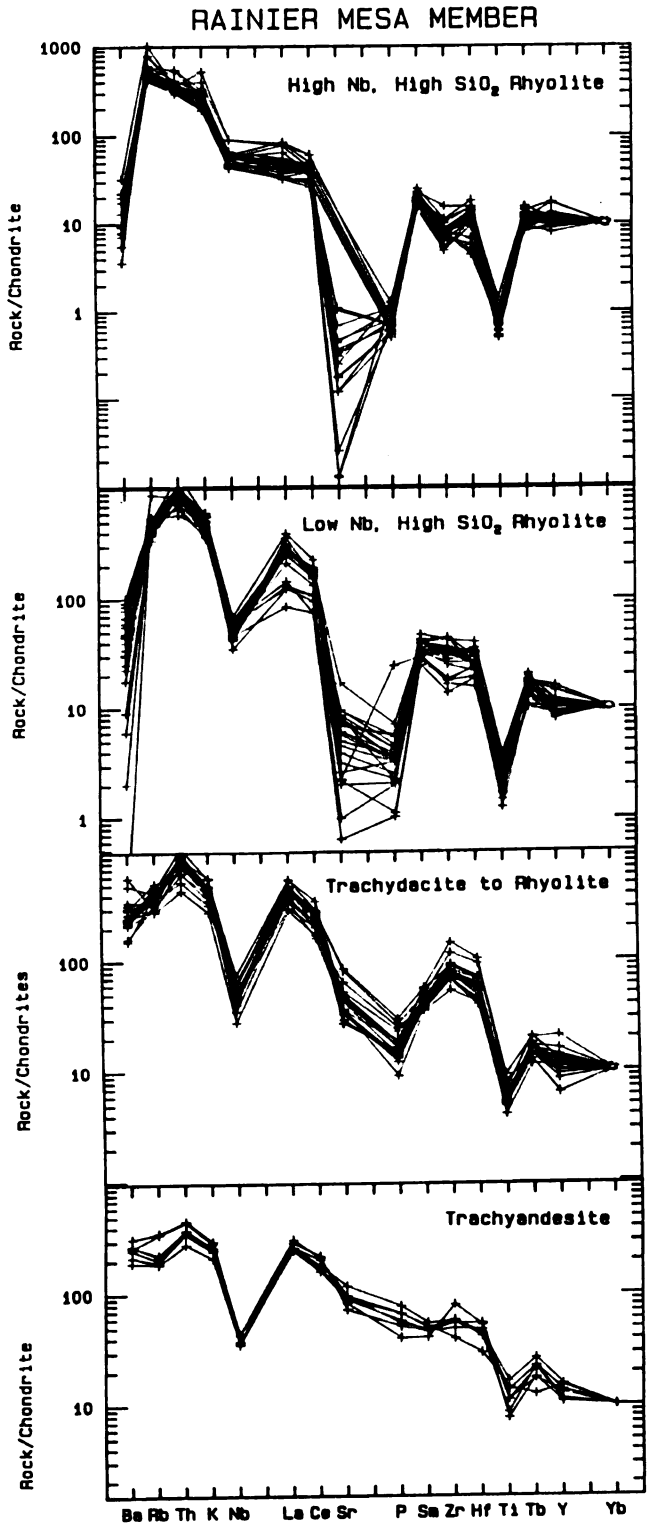


Figure 12b. Spidergrams for the various magmatic groups of the Rainier Mesa Member.

concentration with increasing magmatic differentiation, or, maintain a constant concentration (Fig. 12b). These enrichments or depletions in concentrations are also shown on trace-element enrichment diagrams and are presented in Figures 13a and 13b. This type of diagram, initially used by Hildreth (1981) to look at trace element concentrations in the Bishop Tuff, is used to show whether a particular element is enriched or depleted towards the magma chamber roof. Calculation of trace element enrichment or depletion for the Rainier Mesa Member was determined by using the trace element concentrations in the most mafic and most felsic pumice fragment samples. The concentration of the most felsic sample (low-Nb high-silica rhyolite sample R18-18, 77.96 wt% SiO_2, or, high-Nb high-silica rhyolite sample R8-7 78.05 wt% SiO_2) was divided by that of the most mafic sample (trachyandesite sample R21-13, 56.80 wt% SiO_2)(Figs. 13a,b). For both enrichment diagrams, Rb, Th, K and Nb are moderately to significantly enriched in the high-silica rhyolites (for both the high-Nb and low-Nb high-silica rhyolites), all other elements are depleted (Figs. 13a,b).

Ammonia Tanks Member

In the Ammonia Tanks Member, Rb, Nb, Th, Yb and Lu increase in concentration and Zn, Sr, Zr, Ba, Sc, Hf, La and Eu consistently decrease in concentration with

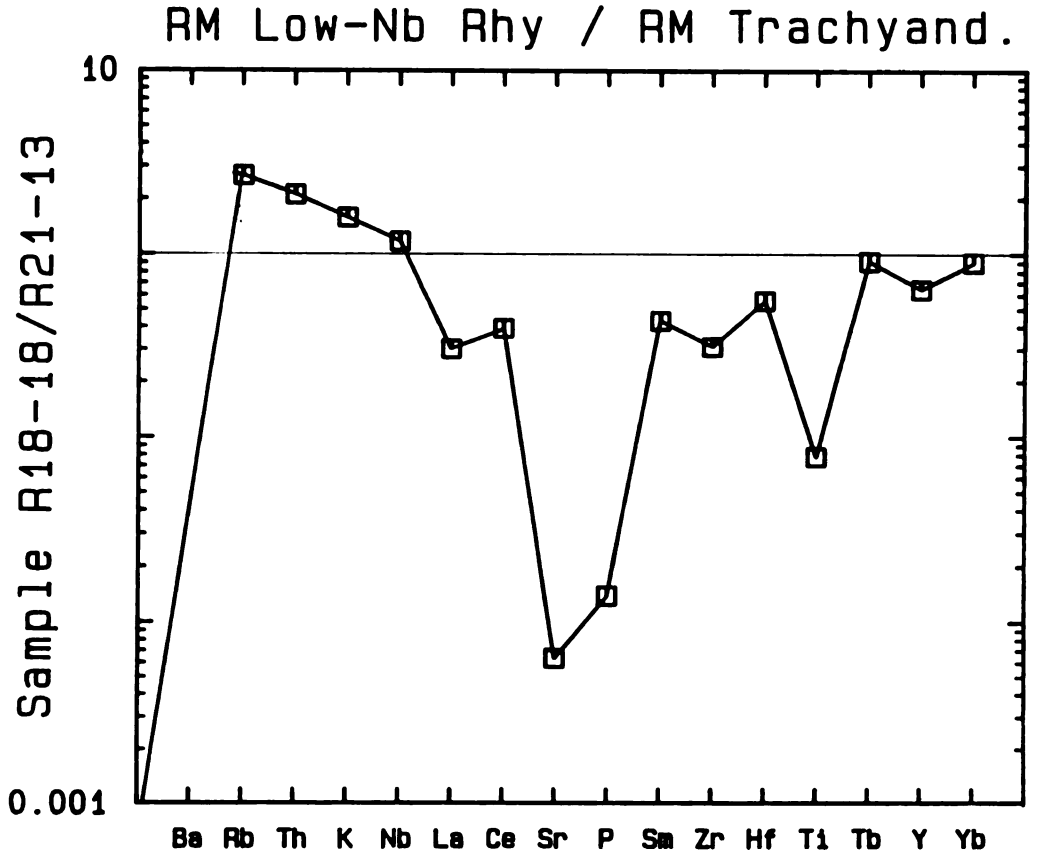


Figure 13a. Trace element enrichment diagram comparing the low-Nb, high-silica rhyolite to the trachyandesite of the Rainier Mesa Member.

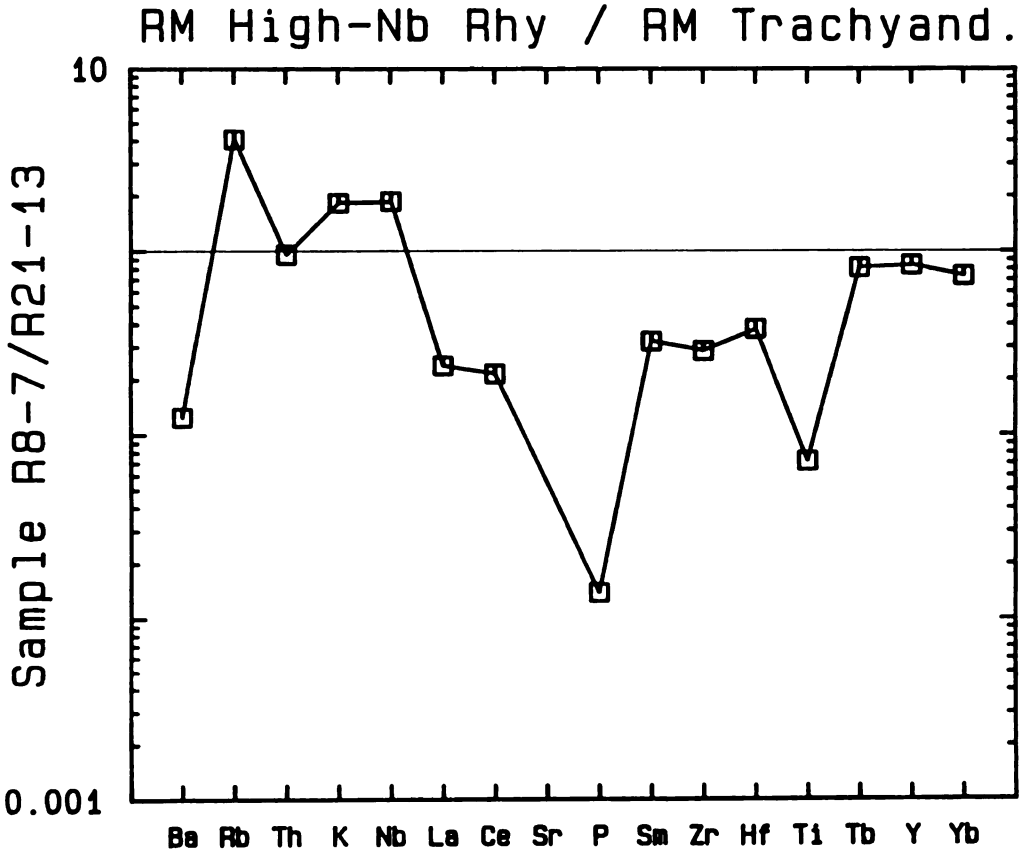


Figure 13b. Trace element enrichment diagram comparing the high-Nb, high-silica rhyolite to the trachyandesite of the Rainier Mesa Member.

increasing SiO_2 concentration (Fig. 10). Y, Ce, Sm and Tb however, exhibit inflections in the data trends.

Chondrite normalized rare-earth element plots for the Ammonia Tanks Member are shown in Figures 14a and 14b. Rare-earth element plots for the Ammonia Tanks Member reveal the systematic change of REE concentrations in the LREE enriched trachyandesite to the less LREE enriched high-silica rhyolite (Fig. 14b). As magmatic evolution increases (increasing SiO_2 content), the Eu anomaly deepens which most likely reflects the fractionation of plagioclase (cf. Cox, et al., 1979). The HREE concentration in the Ammonia Tanks Member remains relatively constant with magmatic evolution.

Trace element concentrations normalized to chondritic meteorite abundances for the Ammonia Tanks Member are presented as spidergrams (after Thompson, et al., 1984) in Figure 15a and 15b. The elements Rb, Th and Nb behave incompatibly by increasing in concentration with increasing magmatic differentiation while the rest of the elements behave compatibly and either decrease in concentration with increasing magmatic differentiation, or, maintain a constant concentration (Fig. 15b). These enrichments or depletions in concentrations are also shown on trace-element enrichment diagrams and are presented in Figure 16. The concentration of the most felsic sample (high-silica rhyolite sample A5-3, 77.96 wt% SiO_2) was

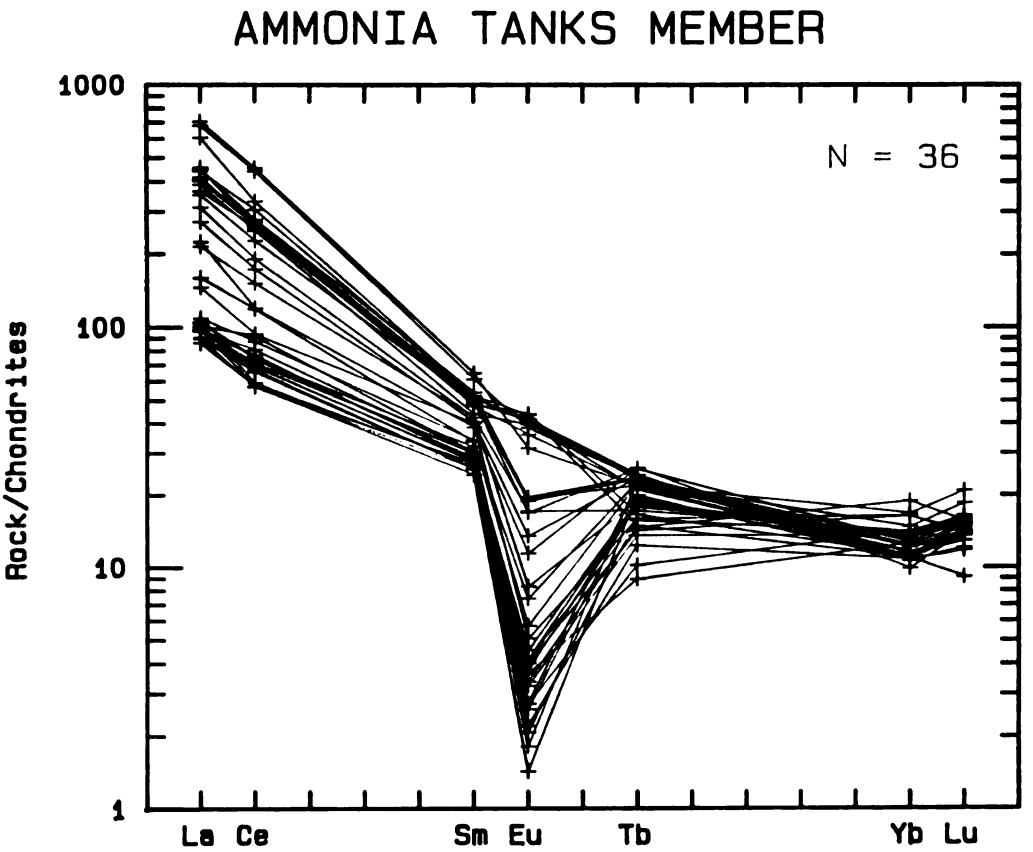


Figure 14a. Rare-earth element plot for the Ammonia Tanks Member. All magmatic compositions plotted.

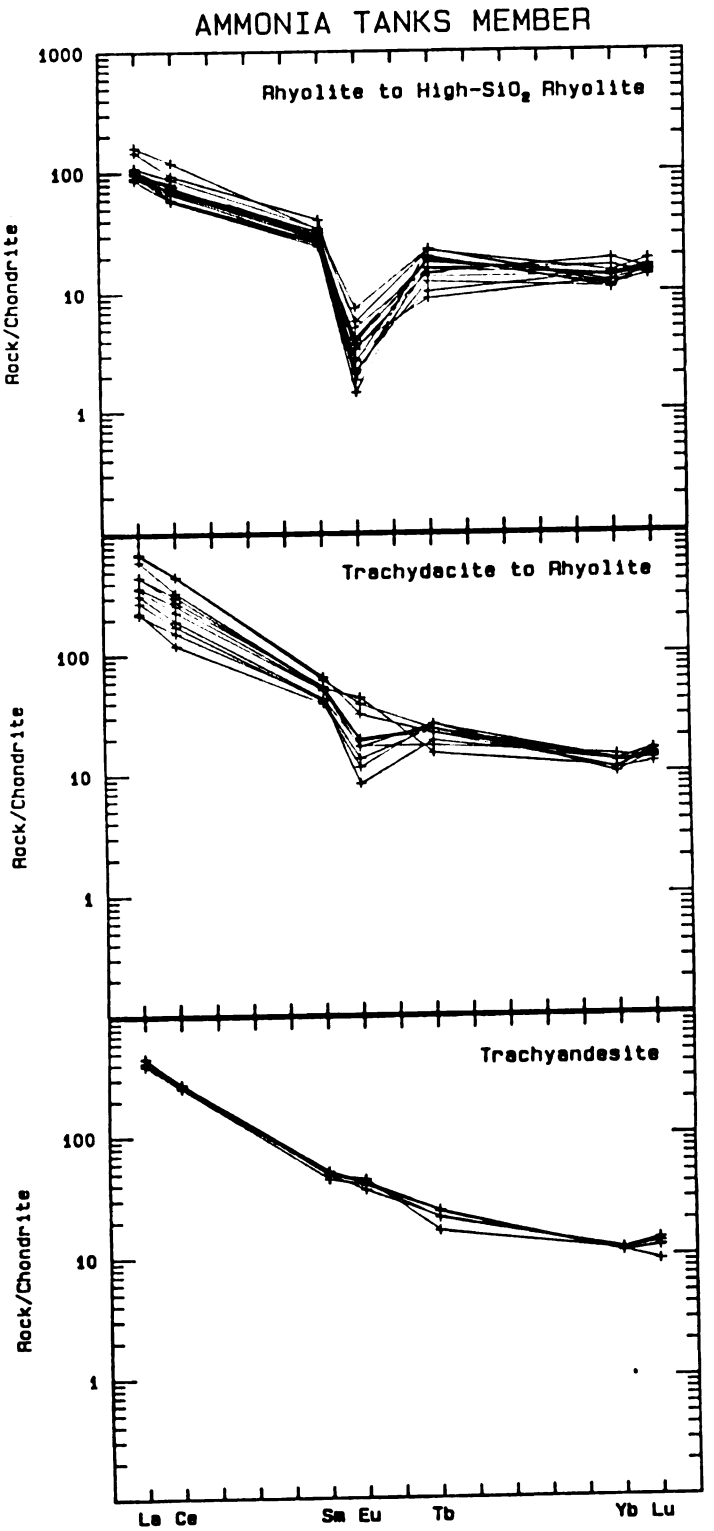


Figure 14b. Rare-earth element plot for the various magmatic groups in the Ammonia Tanks Member.

Fig

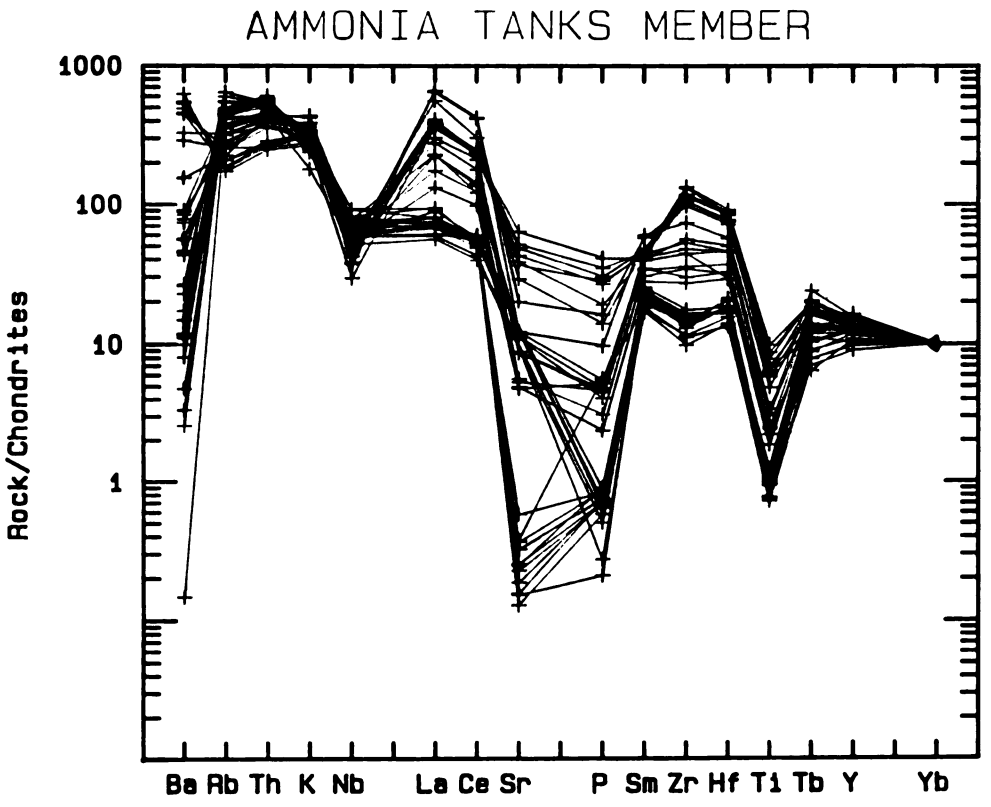


Figure 15a. Spidergram for the Ammonia Tanks Member. All compositions plotted.

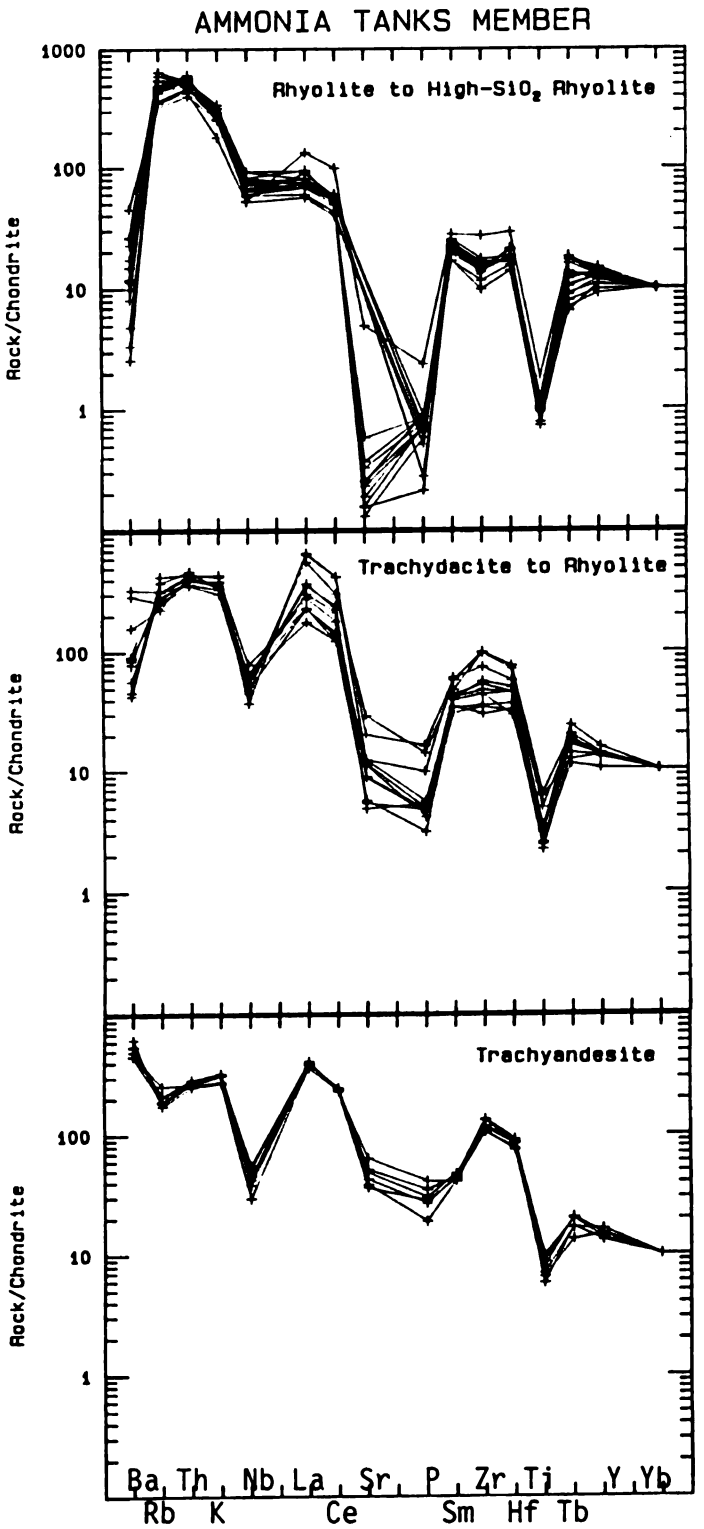


Figure 15b. Spidergrams for the various magmatic groups of the Ammonia Tanks Member.

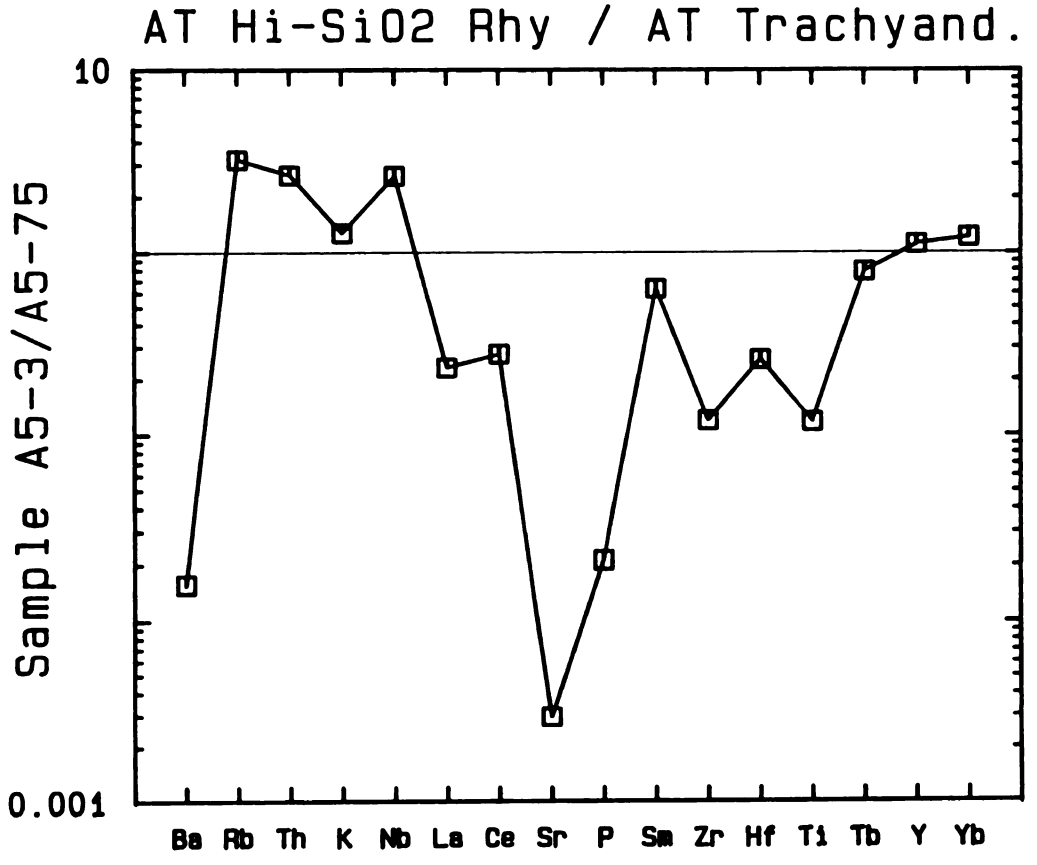


Figure 16. Trace element enrichment plot comparing the high-silica rhyolite and the trachyandesite of the Ammonia Tanks Member.

Fig

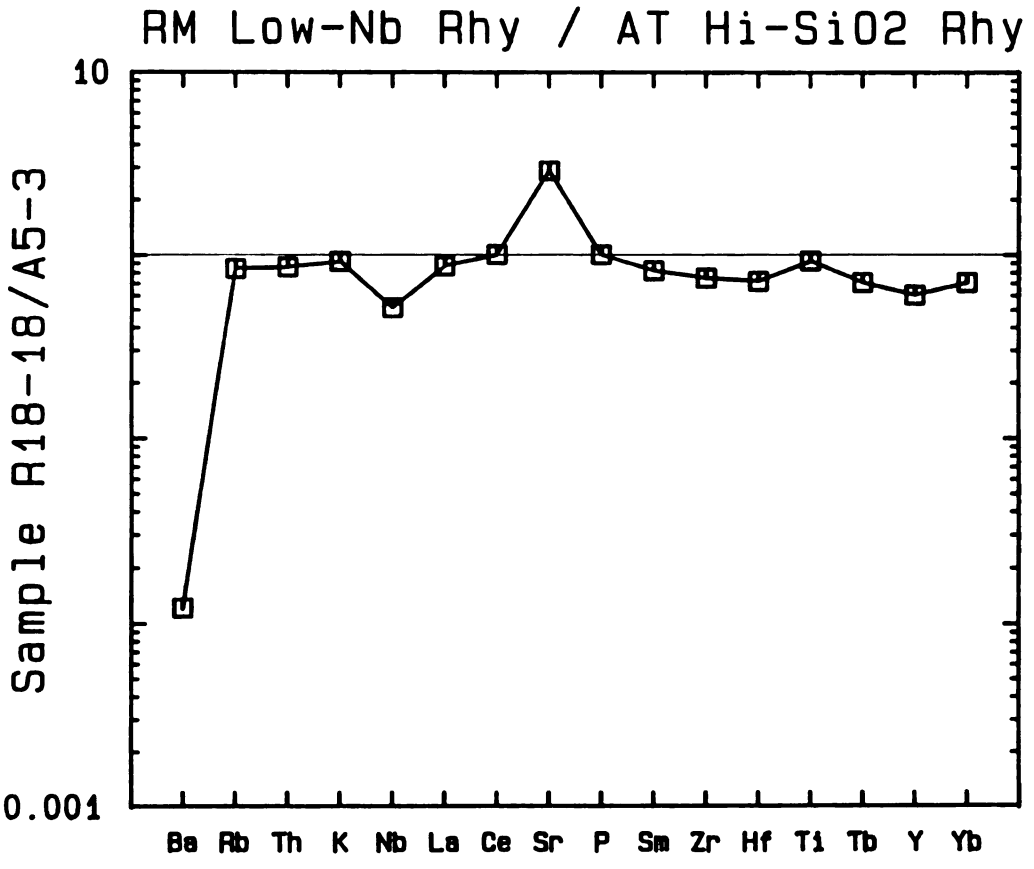


Figure 17a. Trace element enrichment plot comparing the low-Nb, high-silica rhyolite of the Rainier Mesa Member to the high-silica rhyolite of the Ammonia Tanks Member.

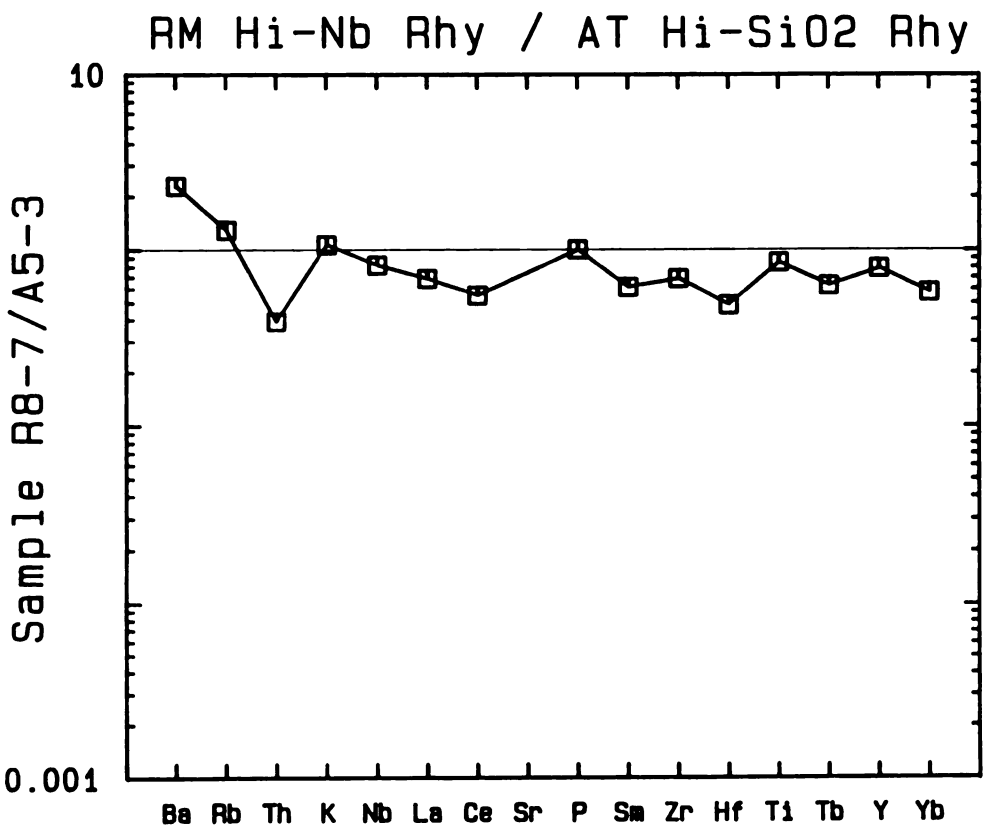


Figure 17b. Trace element enrichment plot comparing the high-Nb, high-silica rhyolite of the Rainier Mesa Member to the high-silica rhyolite of the Ammonia Tanks Member.

divided by that of the most mafic sample (trachyandesite sample A5-75, 59.45 wt% SiO_2). From the enrichment diagram, Rb, Th, K, Nb, Y and Yb are moderately to significantly enriched in the high-silica rhyolite, all other elements are depleted (Fig. 16). Elemental behavior in the high-silica rhyolite of the Ammonia Tanks Member mimics the low-Nb, high-silica rhyolite Rainier Mesa Member with the exception of Ba, Nb and Sr (Figs. 17a,b). Ba and Nb are depleted in the Ammonia Tanks Member while Sr is enriched relative to the Rainier Mesa Member (Fig. 17a).

PETROGRAPHY AND MINERAL CHEMISTRY

Overview

Petrography

Twenty-five thin sections from the Rainier Mesa Member and nineteen thin sections from the Ammonia Tanks Member were examined petrographically. Of the examined thin sections, modes of seventeen of the Rainier Mesa thin sections and eleven of the Ammonia Tanks thin sections were determined. The modes of thin sections that were either too small or too badly plucked during grinding were not determined. Modal data for the Rainier Mesa and Ammonia Tanks Members are given in Table 2. Only one thin section per pumice sample was examined with the total number of point counts ranging from 500 to 1000 per section. Caution should be exercised when interpreting the modal data due to the small number of thin sections analyzed, the low number of counted points and the vesicular nature of the pumice fragments which lowers absolute phenocryst abundances per thin section. Textural data relating to resorption of phenocrysts for the Rainier Mesa and Ammonia Tanks Members is presented in Table 3.

Phenocryst and Glass Chemistry

To reconstruct the mineralogic assemblages of the magma types present in the Timber Mountain system, pumice fragments were selected for electron microprobe analysis

TABLE 2. Modal petrography of the Timber Mountain Tuff.

SAMPLE	WT% SiO_2	PLG	SAN	QTZ	BIO	HRN	CPX	MT/ IL	DRE[1] TOTAL	APA	POINT COUNTS
Rainier Mesa Member											
R23-27	57	10.3	-	-	3.0	6.4	-	1.7	21.4	-	1000
R23-17	59	18.4	-	-	2.2	6.7	-	2.4	29.7	-	1000
R23-24	60	15.6	-	-	1.7	5.0	0.1	0.9	23.3	0.9	1000
R11-9	61										
R8-45	66	15.9*	-	-	0.8	tr	0.4	0.8	17.9	0.4	1000
R8-23	67										
R8-25	67	28.0*	-	-	2.8	-	0.7	0.8	32.3	-	1000
R8-39	67	13.9*	-	-	2.1	-	0.1	0.6	16.7	-	1000
R8-24-1	68	20.7*	-	-	3.0	-	0.1	0.5	24.6	-	1000
R8-26	68										
R11-2	68	11.5	13.1	-	1.5	-	0.3	0.3	26.7	-	1000
R25-21-1	68	7.8	1.9	-	1.7	-	0.4	0.8	12.6	-	1000
R8-44	69	7.1	0.8	-	1.6	-	tr	0.1	9.6	-	1000
R23-4	69										
R23-13	70	7.4	5.8	1.0	2.0	tr	0.5	0.7	17.5	-	1000
R11-3	75										
R18-2	75	2.4	0.1	2.3	0.1	-	-	tr	4.9	-	1000
R11-7	76	0.4	5.5	3.7	tr	tr	-	0.3	9.9	-	1000
R23-22	76										
R21-44	76	2.6	2.8	1.3	0.4	-	tr	0.3	7.4	-	1000
R18-3	77	4.8	4.8	1.7	0.2	-	-	tr	11.5	-	1000
R18-8	77										
R18-16	77	0.6	6.8	6.2	0.3	-	-	0.2	14.1	-	1000
R21-40	78	1.8*		tr	tr	-	-	0.2	2.0	-	1000
R18-1	78										
Ammonia Tanks Member											
A5-75	59	21.54	0	-	2.66	-	1.20	1.20	26.60	-	1000
A5-69	61	22.31*	-	-	2.50	-	0.19	0.19	24.81	-	1000
A5-63	62	19.29*	-	-	2.50	-	0.71	1.07	23.57	-	514
A5-31	63										
A5-72	64	11.26	.3	-	2.30	-	-	0.33	15.19	-	500
A5-30	65	14.83	4.65	-	2.33	-	0.29	tr	22.10	-	502
A5-71	67	12.50	10.47	-	0.58	-	-	0.87	24.42	-	503
A21-1	69										
A5-58	69	6.25	7.03	-	0.26	-	0.26	tr	13.80	-	501
A5-9	70	7.58	1.69	-	0.28	-	-	tr	9.55	-	500
A4-70	70										
A5-35	73	4.83	3.75	-	0.27	-	-	tr	8.85	-	500
A5-68	74	1.47	6.99	-	tr	-	-	tr	8.46	-	458
A21-5	75										
A5-29	77	2.79	1.40	1.12	-	-	-	tr	5.31	-	500
A5-79	77										
A5-3	78										
A21-18	78										
A5-56	78										

*All feldspar counted as plagioclase 1 = DRE = Dense rock equivalent

TABLE 3. Textural relationships of phenocrysts in the Timber Mountain Tuff.

SAMPLE	WT% SiO_2	PLG	SAN	QTZ	BIO	HRN	CPX	MT/ IL	DRE[1] TOTAL
Rainier Mesa Member									
R23-27	57	○			○	◑		○	21.4
R23-17	59	◑			◑	○		○	29.7
R23-24	60	●			◑	○	○	○	23.3
R11-9	61	●	●		○	○	○	○	
R8-45	66	●	●		◑	○	○	○	17.9
R8-23	67	●	●		◑		○	○	
R8-25	67	●	●		◑		○	○	32.3
R8-39	67	●	●		◑		○	○	16.7
R8-24-1	68	◑	●		◑		○	○	24.6
R8-26	68	◑	●		◑		○	○	
R11-2	68	○	◑		◑		○	○	26.7
R25-21-2	68	◑	○		○		○	○	12.6
R8-44	69	○	●		○		○	○	9.6
R23-4	69	●	◑		○		○	○	
R23-13	70	◑	◑	◑	◑	○	○	○	17.5
R11-3	75	◑	○	○	○			○	
R18-2	75	○	○	◑	○			○	4.9
R11-7	76	○	◑	◑	○	○		○	9.9
R23-22	76	○	○	◑	○			○	
R21-44	76	○	○	○	○		○	○	7.4
R18-3	77	○	○	○	○			○	11.5
R18-8	77	○	◑		○			○	
R18-16	77	◑	◑	◑	○			○	14.1
R21-40	78	○	○	○	○			○	2.0
R18-1	78	○	○		○			○	
Ammonia Tanks Member									
A5-75	59	●			●	◑	◑	○	26.60
A5-69	61	●			◑		○	○	24.81
A5-63	62	●	●		○		○	○	23.57
A5-31	63	●	◑		○		○	○	
A5-72	64	◑	◑		○		○	○	15.19
A5-30	65	◑	◑		○		○	○	22.10
A5-71	67	◑	◑		○		○	○	24.42
A21-1	69	◑	◑		○		○	○	
A5-58	69	◑	◑		○		○	○	13.80
A5-9	70	◑	○		○		○	○	9.55
A4-70	70	○	○	○	○			○	
A5-35	73	◑	○	○	○		○	○	8.85
A5-68	74	○	○	○	○			○	8.46
A21-5	75	○	○	○	○			○	
A5-29	77	○	○	○	○			○	5.31
A5-79	77	○	○	○	○			○	
A5-3	78	○	○		○			○	
A21-18	78	●	●		○			○	
A5-56	78	○	○	○	○			○	

○ = Fresh ◑ = Sl. resorbed to fresh ● = Strongly resorbed
1 = Dense rock equivalent

such that the full compositional range as delineated by major and trace element analyses was represented. Twelve pumice fragments from the Rainier Mesa Member and thirteen pumice fragments from the Ammonia Tanks Member were selected for analysis with the electron microprobe.

Microprobe analyses of plagioclase, sanidine, biotite, clinopyroxene, orthopyroxene, hornblende, manganoan fayalite and magnetite/ilmenite are presented in Appendix 4. The petrography and chemistry of each of the above phenocryst phases will be discussed in detail below. Several other trace phases such as chevkinite, sphene, apatite, and monazite were observed but not analyzed. These phases are discussed collectively in the section on trace phenocryst phases.

Feldspar

Petrography

Phenocrysts of plagioclase and sanidine are abundant within the Timber Mountain Tuff (Table 2). Plagioclase is present throughout the compositional range of both the Rainier Mesa Member and the Ammonia Tanks Member. Sanidine however, is absent as a phenocryst phase in the trachyandesite of both members. Sanidine first appears in samples with a SiO_2 content of 61 wt% and then remains as a phenocryst phase throughout the magmatic sequence in both members. The feldspars do not exhibit any evidence

of sausseritization or sericitic alteration. Secondary carbonate is more common in the Ammonia Tanks Member and may at times surround the feldspars, and rarely, may fill fractures in the grains.

Modally, feldspars are the most ubiquitous phases in the Timber Mountain Tuff with the highest concentrations occurring in the trachyandesite and trachydacite (up to 28% in the Rainier Mesa Member and 22% in the Ammonia Tanks Member)(Table 2). The absolute concentration of feldspar steadily decreases to approximately 2% in the high-silica rhyolite of each member. The ratio of plagioclase to sanidine is quite variable throughout both members. Typically however, plagioclase dominates in the more mafic pumice compositions while sanidine dominates in the rhyolite and high-silica rhyolite. The variability in the feldspar ratio is due to a combination of difficulty in petrographic identification of untwined plagioclase versus sanidine, and, in the small number of thin sections examined.

Texturally, plagioclase in the Rainier Mesa Member ranges from fine grained (0.25 mm to 1 mm), unzoned, euhedral phenocrysts to zoned, medium grained (1 mm to 4.25 mm), slightly to pervasively resorbed phenocrysts. Zoning is common in the medium grained plagioclase grains and may be normal, oscillatory, or rarely reverse in nature. Apatite and fluid/glass inclusions are common to

abundant in the plagioclase phenocrysts. Sanidine typically occurs as medium grained (1 mm to 4.5 mm), fresh to pervasively resorbed phenocrysts. Carlsbad twins are common in sanidine while inclusions of apatite or other phases are extremely rare.

Resorption of the feldspars (predominantly plagioclase, rarely sanidine) in the Rainier Mesa Member is pervasive in the larger phenocryst size fraction that occurs in pumice fragments with compositions ranging from trachyandesite through trachydacite (Table 3). The smaller size fraction of feldspar in these samples is usually not resorbed. The only exception to this phenomena occurs in the most mafic of all the Rainier Mesa Member pumice fragments, sample R23-27 (57 wt% SiO_2). In this sample, the large feldspar grains are not resorbed. Feldspars present in the rhyolitic samples (>70 wt% SiO_2) are dominantly fresh, medium grained, slightly zoned, and broken. Very few of these feldspars show evidence of resorption.

Texturally, feldspars of the Ammonia Tanks Member differ from those of the Rainier Mesa Member. Plagioclase phenocrysts are typically larger in the Ammonia Tanks Member (1 mm to 4.5mm) with the fine-grained size fraction being noticeably uncommon to absent. Zoning in the plagioclase feldspars in Ammonia Tanks Member may be normal, oscillatory, or rarely reverse in nature. Both

plagioclase and sanidine exhibit more pervasive resorption from the trachyandesite through the trachydacite than do the feldspars in the same compositional range of the Rainier Mesa Member. Plagioclase in the Ammonia Tanks Member occurs more commonly as glomerocrysts than in the Rainier Mesa Member. Biotite, clinopyroxene, and Fe-Ti oxides are commonly found in association in the glomerocrysts. Apatite and fluid/glass inclusions are rare to abundant.

Mineral Chemistry

The plagioclase feldspars in the Timber Mountain Tuff have a large compositional range. Within the Rainier Mesa Member, the plagioclase normative compositions for phenocryst cores are as high as An_{77} whereas phenocryst edge compositions range from An_{52} to An_{13} based on electron microprobe analyses (Figs. 18, 19). Sanidine phenocrysts also exhibit a large range in composition. Edge compositions range from $Or_{65}Cn_{0.2}$ to $Or_{47}Cn_{2.2}$ while core compositions range from $Or_{65}Cn_{0.3}$ to $Or_{55}Cn_{3.4}$ (Figs. 18, 19). In the Rainier Mesa Member, celsian concentrations in sanidine phenocrysts are directly correlated with the anorthite content (Fig. 20a). Celsian concentrations in the Ammonia Tanks Member sanidine

RAINIER MESA MEMBER

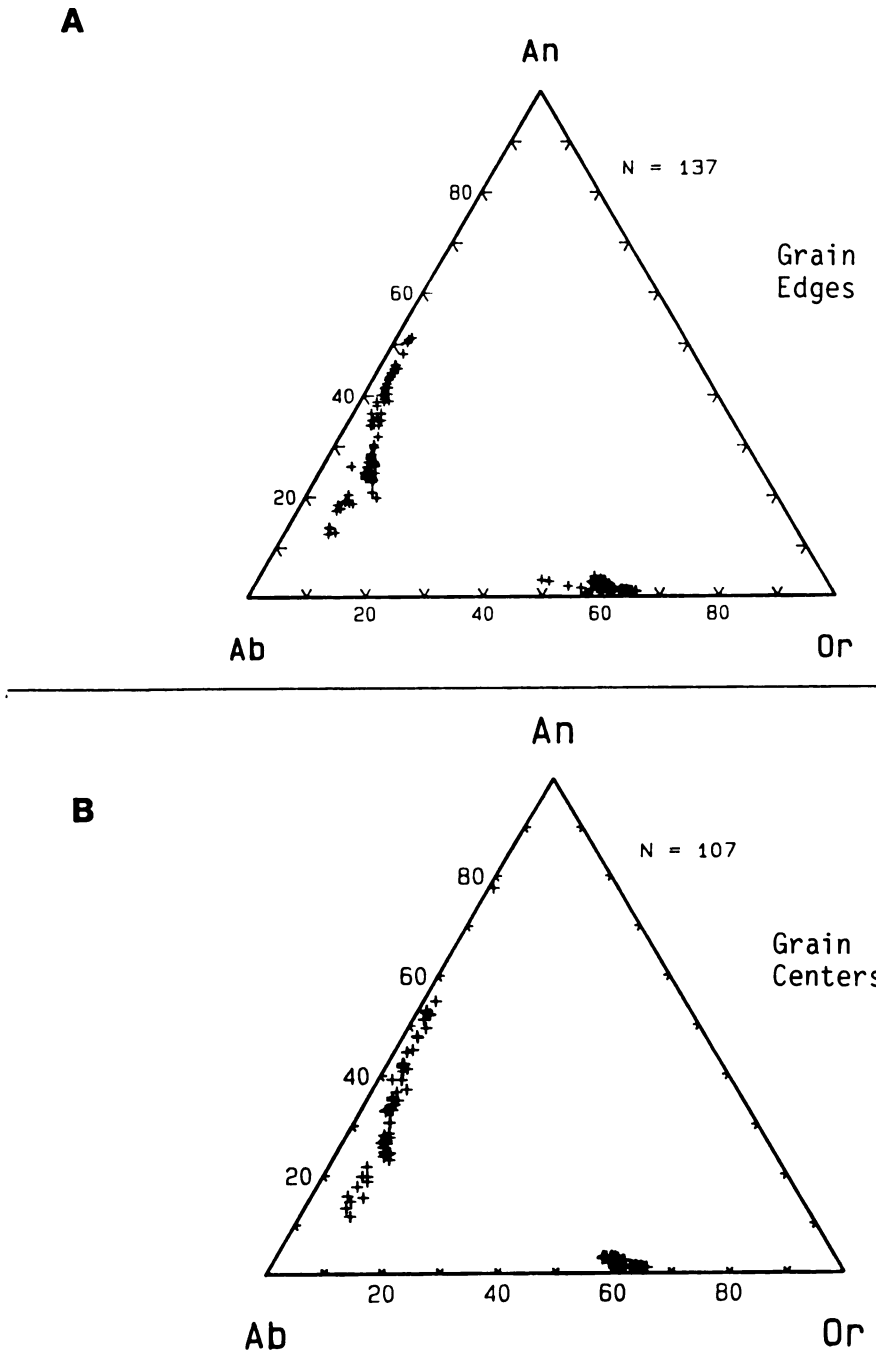


Figure 18. A) Feldspar compositions based on electron microprobe analyses of grain edges for the Rainier Mesa Member.
B) Feldspar compositions based on electron microprobe analyses of grain centers for the Rainier Mesa Member.

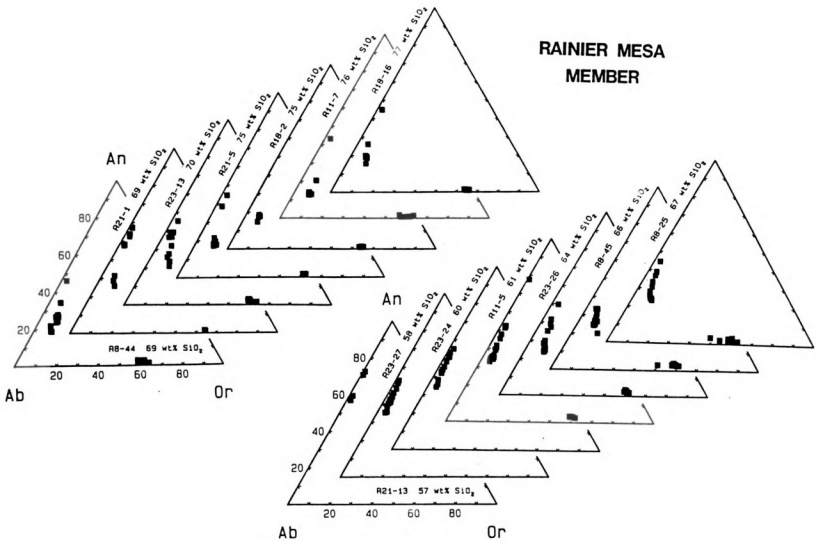
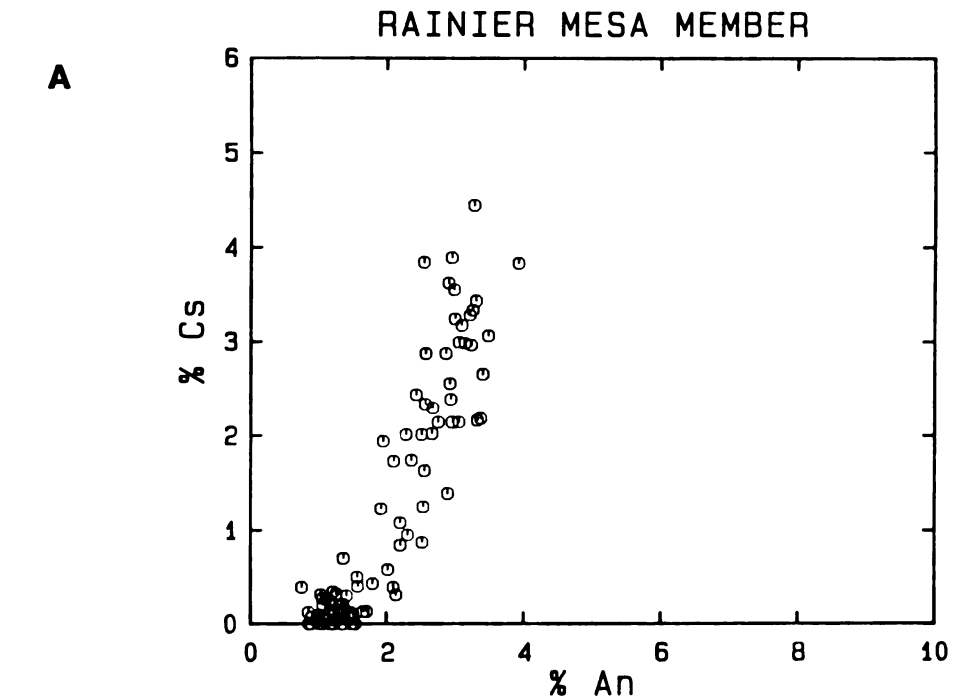


Figure 19. Feldspar compositions by sample from electron microprobe analyses for the Rainier Mesa Member.



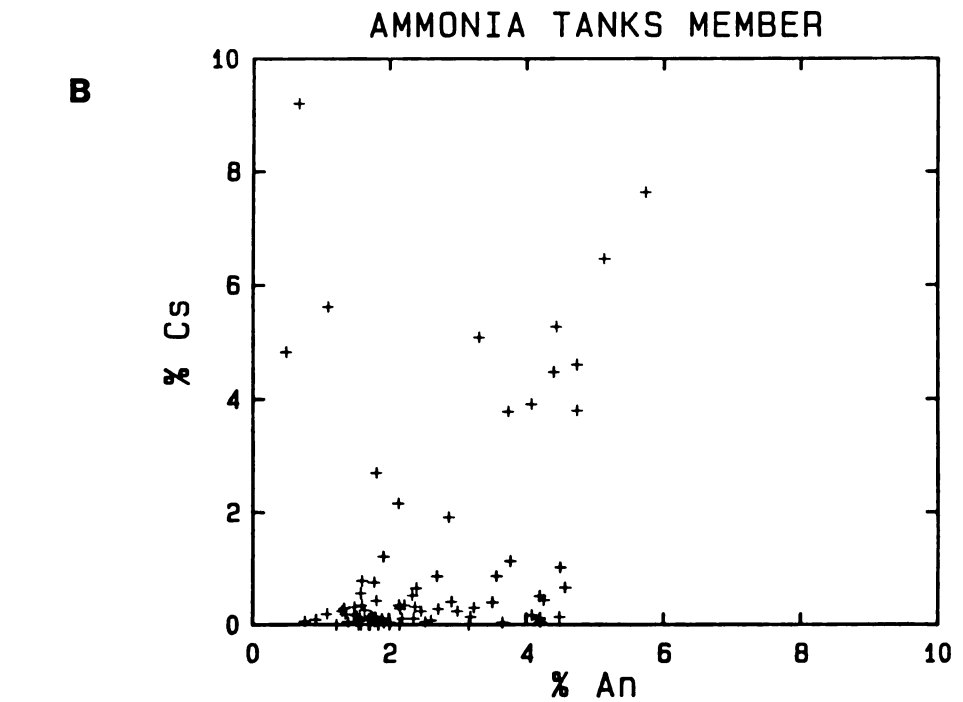


Figure 20. A) Celsian versus anorthite content in feldspars of the Rainier Mesa Member.
B) Celsian versus anorthite content in feldspars of the Ammonia Tanks Member.

phenocrysts however reveal a much poorer correlation with the anorthite content (Fig. 20b).

Plagioclase phenocrysts in the Ammonia Tanks Member exhibit almost exactly the same compositional range as those in the Rainier Mesa Member (Figs. 18, 21). Edge compositions of the plagioclase feldspars range from An_{59} to An_{17} (Figs. 21, 22). Core compositions are as high as An_{52}. A few feldspar grains have rim An values exceeding An_{70}. The An_{70} phenocrysts may represent broken grains with the microprobe analyses taken towards the true core of the grains. The feldspars with albitic compositions of approximately $An_{10}Ab_{65}Or_{25}$ are predominantly groundmass feldspars, some of which are visible in thin section.

Comparison of the sanidine compositions (grain edge analyses only) for the Rainier Mesa Member and Ammonia Tanks Member reveals that a gap of 1% to 2% Or content (Or_{56} to Or_{58}) occurs within each of these two members (Figs. 18, 21). Sanidine compositions for the Rainier Mesa Member range from a few scattered values at Or_{50} to the dominant population at approximately Or_{60} (Fig. 18) while sanidines of the Ammonia Tanks Member range from Or_{43} to Or_{55} (Fig. 21). As in the plagioclase feldspars, a few sanidine phenocrysts in the Ammonia Tanks Member have extreme Or compositions ($>Or_{70}$). The range of core compositions for the sanidine phenocrysts in the Ammonia

AMMONIA TANKS MEMBER

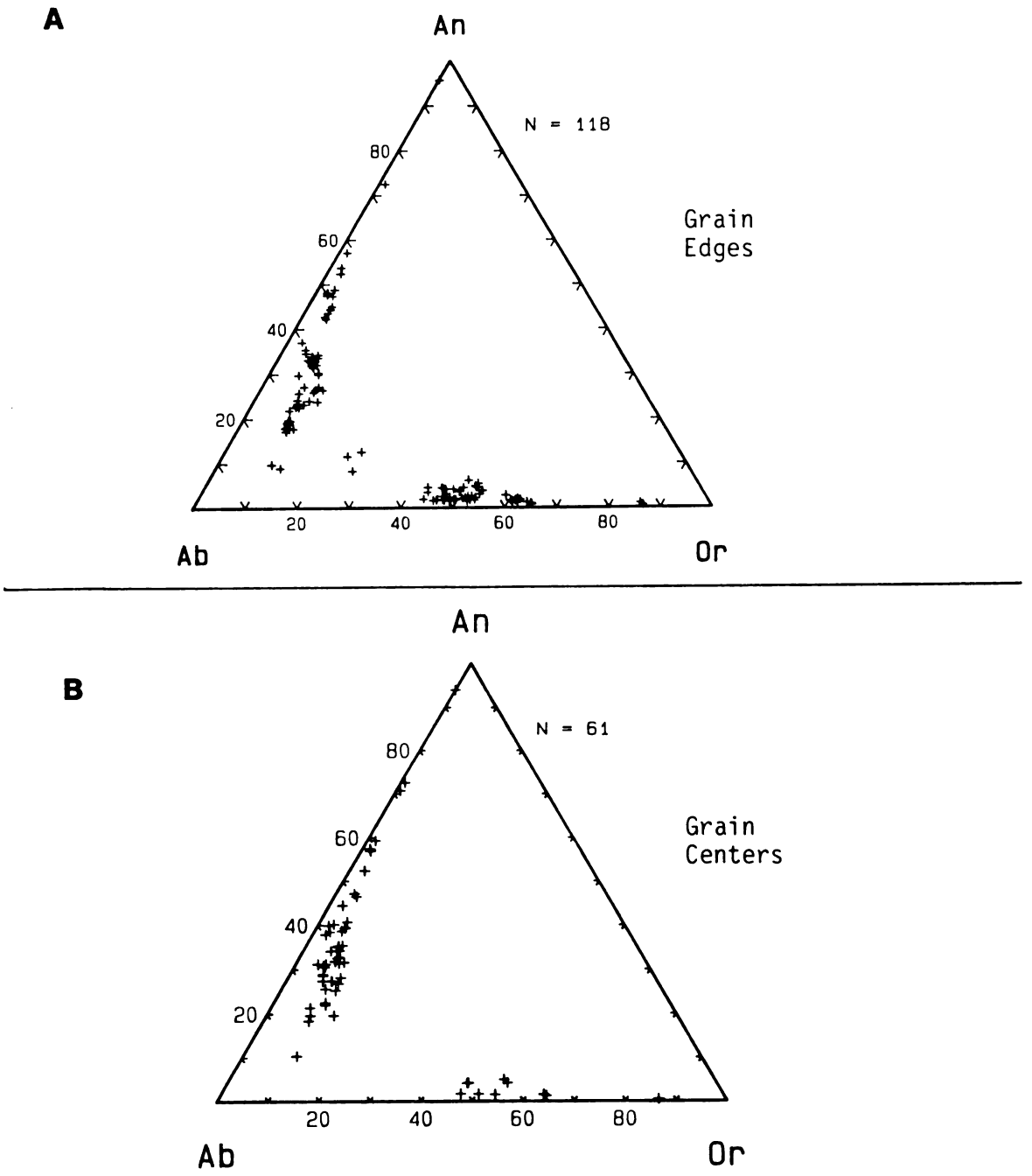


Figure 21. A) Feldspar compositions based on electron microprobe analyses of grain edges for the Ammonia Tanks Member.
B) Feldspar compositions based on electron microprobe analyses of grain centers for the Ammonia Tanks Member.

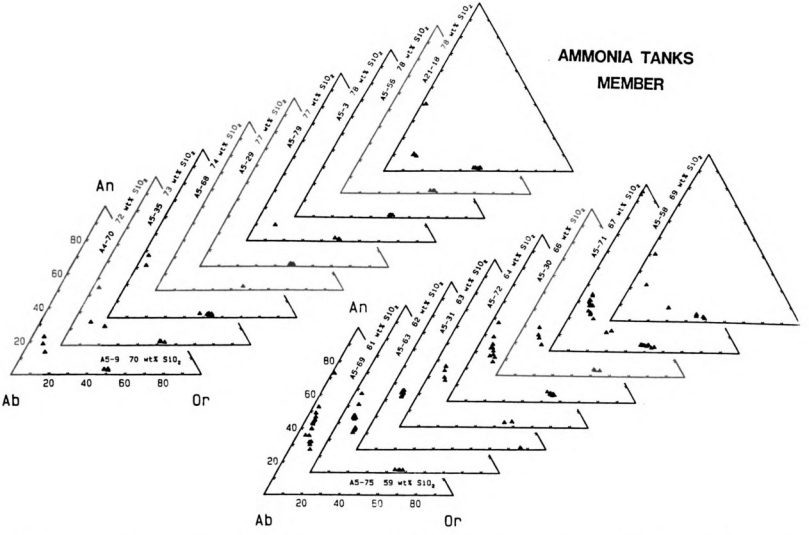


Figure 22. Feldspar compositions by sample from electron microprobe analyses for the Ammonia Tanks Member.

Tanks Member is identical to the edge compositions (Fig. 21).

Biotite

Petrography

Next to the feldspars, biotite is the most ubiquitous mineral phase in the Timber Mountain magmatic system. Biotite occurs as a phenocryst phase throughout the sequence from trachyandesite to the high-silica rhyolite of both the Rainier Mesa Member and Ammonia Tanks Member of the Timber Mountain Tuff (Table 2). In both units, modal concentrations of biotite range from a few tenths of a percent (DRE, dense rock equivalent) in the rhyolitic samples up to 3% in the trachyandesite samples (Table 2).

Petrographically, biotite phenocrysts in both the Rainier Mesa Member and Ammonia Tanks Member are commonly associated with, in decreasing order of abundance, apatite, magnetite, ilmenite, sphene, zircon, chevkinite, and +/- monazite (monazite only occurs in the Rainier Mesa Member and sphene only occurs in the Ammonia Tanks Member). The biotites have a consistent pleochroic scheme of yellow < dark red-brown or green (X < Y,Z).

Resorption of biotite phenocrysts occurs only in samples with compositions ranging from trachyandesite to trachydacite in the Rainier Mesa Member (Table 3). Biotites in the Ammonia Tanks Member are resorbed only in

samples of the trachyandesite (Table 3). In both units, the resorption is only slight to moderate as compared to resorption of the feldspars.

Mineral Chemistry

For most samples, microprobe analyses were concentrated towards the edges of the biotite grains because this region was most likely in equilibrium with the erupted melt. A few grains in each sample were checked for compositional zonation by analyzing the core and edge portions of the grain. Grains analyzed in this fashion were homogeneous in composition.

In the Rainier Mesa Member, the Mg# (MgO/(MgO + FeO_T)) of biotite ranges from a mean of 0.67 in the trachyandesite to 0.64 in the high-silica rhyolite (Fig. 23). The collective range in Mg# however ranges from 0.72 within the trachydacite to 0.60 in the high-silica rhyolite. Intrasample variations of the Mg# can range up to 0.09 units as in the trachydacite sample R8-25 (0.61 to 0.70)(Fig. 23).

The large variation in Mg# and elemental composition of the biotite phenocrysts within any one sample may reflect either the actual compositional range of phenocrysts within that particular melt, compositional zonation within the phenocryst, and\or commingling of discrete magmas with unique phenocryst compositions.

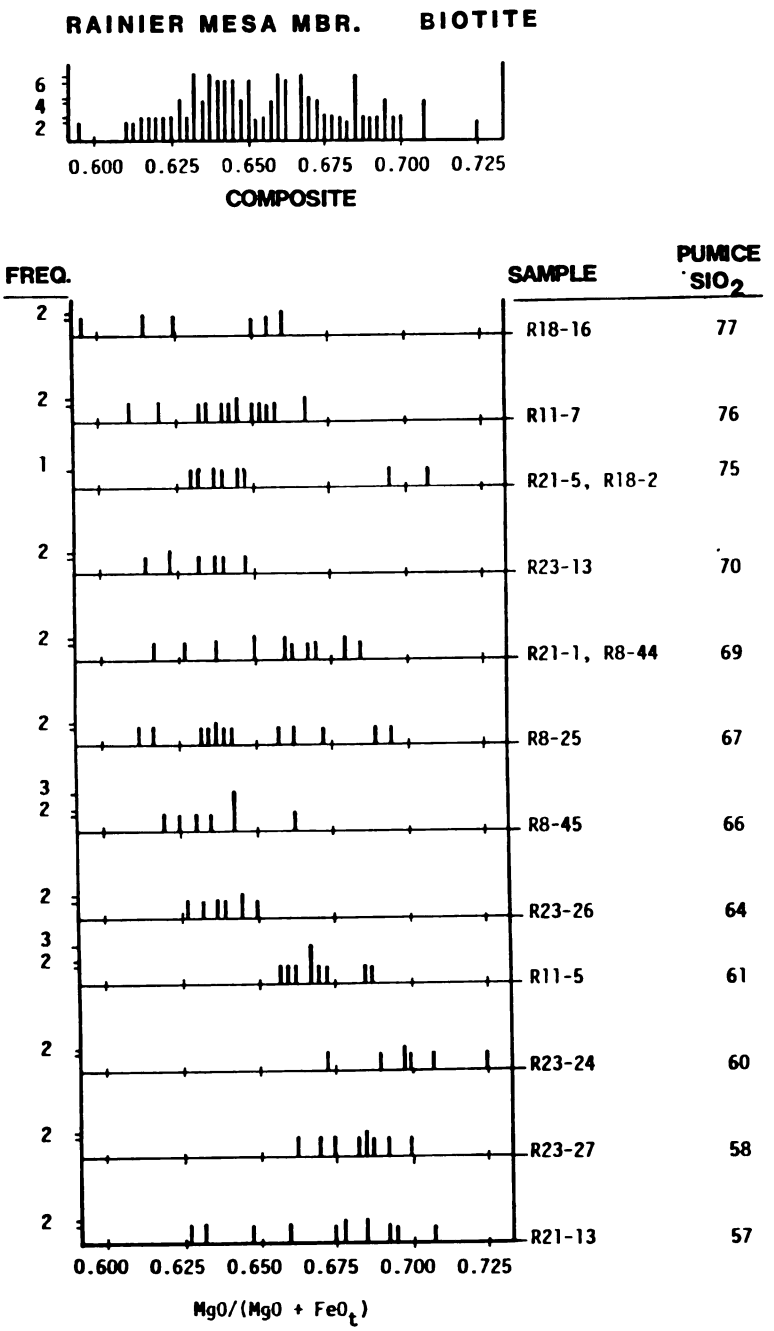


Figure 23. Mg# of biotite phenocrysts in the Rainier Mesa Member. Samples arranged by increasing whole pumice SiO_2 content. Microprobe analyses are from the grain edges only.

Intrasample biotite data for MnO, TiO_2, and to a lesser degree Al_2O_3, exhibit relatively small ranges and are useful as tracer elements in examining geochemical changes over the compositional range of the magmatic system (for demonstrative purposes only TiO_2 is plotted). For example, in Figure 24, the TiO_2 content in biotite in the Rainier Mesa Member exhibits a general change from the most mafic sample (a median value of 5.8 wt% TiO_2) to the most silicic sample (a median value of 4.5 wt% TiO_2). The compositions plotted are those of grain edge analyses only. Analyses of 'core' compositions are not plotted as it is uncertain whether or not the true 'core' of the phenocryst was actually analyzed.

For the Ammonia Tanks Member, the Mg# for biotite ranges from 0.67 in the trachyandesite to 0.80 in the high-silica rhyolite (Fig. 25). TiO_2 ranges from 2.73 wt% to 7.57 wt% in the trachyandesite to high-silica rhyolite respectively (Fig. 26). A histogram plot of the Mg# does not reveal significant population differences (ie. bimodal vs. unimodal)(Fig. 25): TiO_2 however does reveal a possible trimodal distribution with medians occurring at approximately 3.00 wt% TiO_2, 4.75 wt% TiO_2 and 6.95 wt% TiO_2 (Fig. 26). This trimodality is also present in the K_2O and MnO data. FeO exhibits a bimodal distribution.

Within a single sample, large ranges in composition which are unimodal in distribution are interpreted to

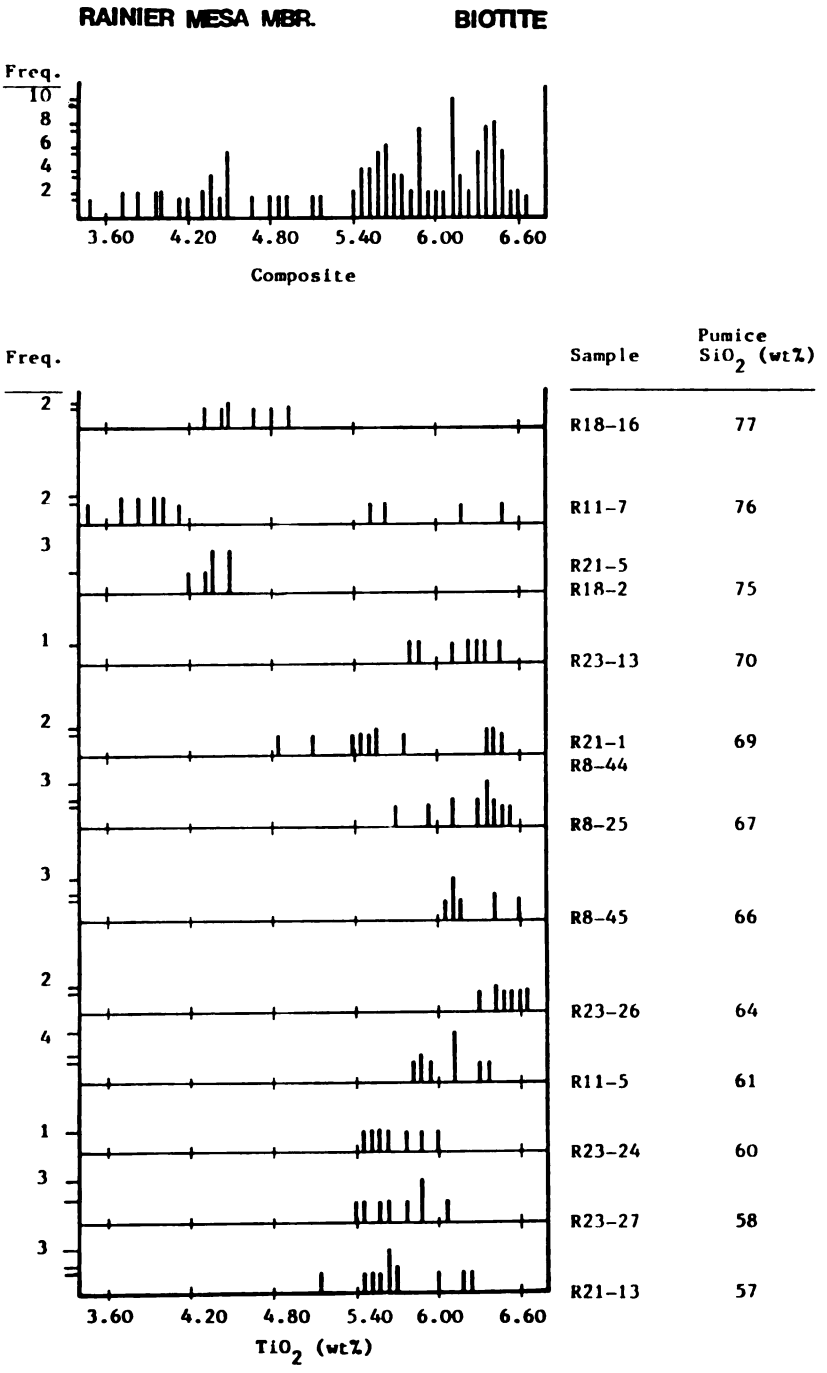


Figure 24. TiO_2 in biotite phenocrysts of the Rainier Mesa Member. Samples arranged by increasing whole pumice SiO_2 content. Microprobe analyses are from the grain edges only.

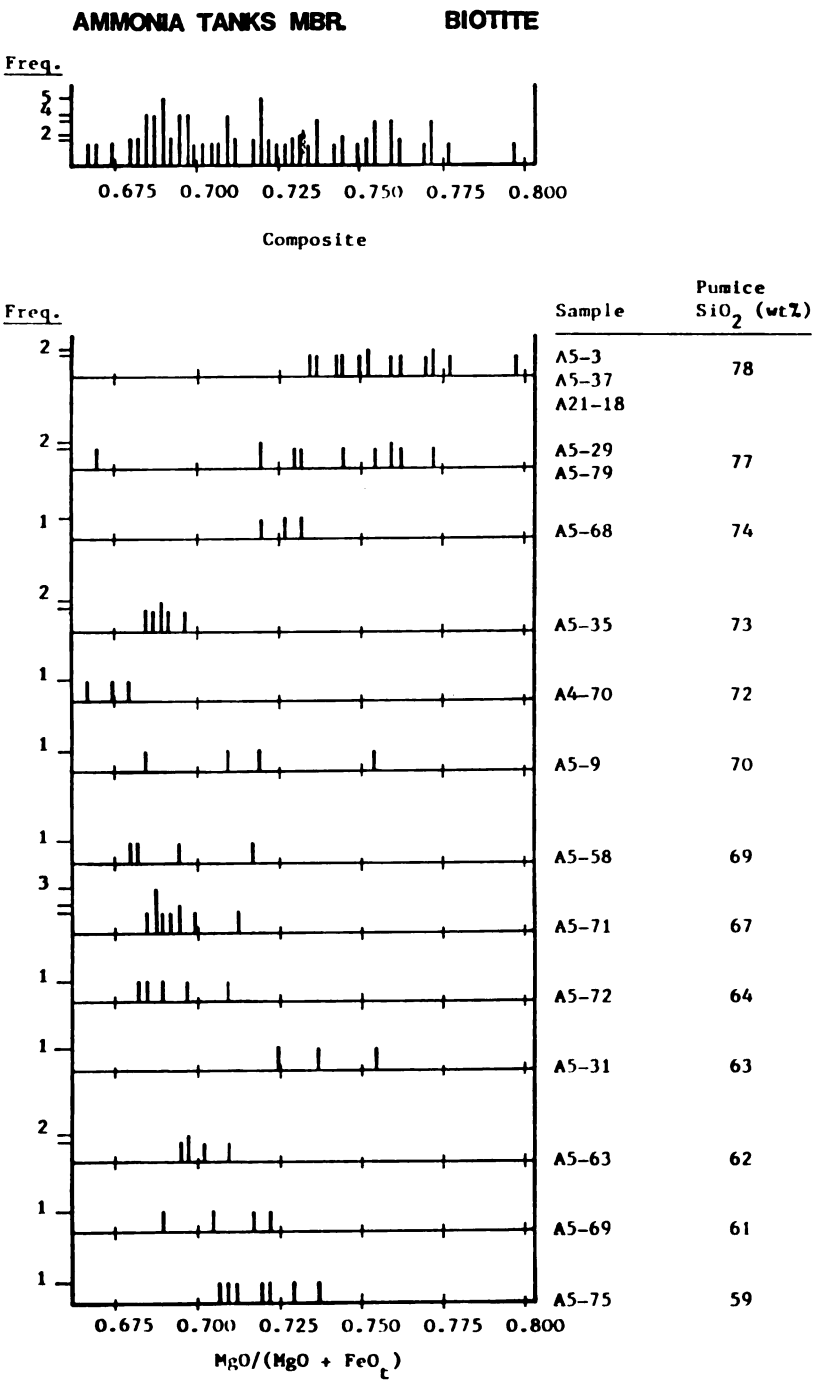


Figure 25. Mg# of biotite phenocrysts in the Ammonia Tanks Member. Samples arranged by increasing whole pumice SiO_2 content. Microprobe analyses are from the grain edges only.

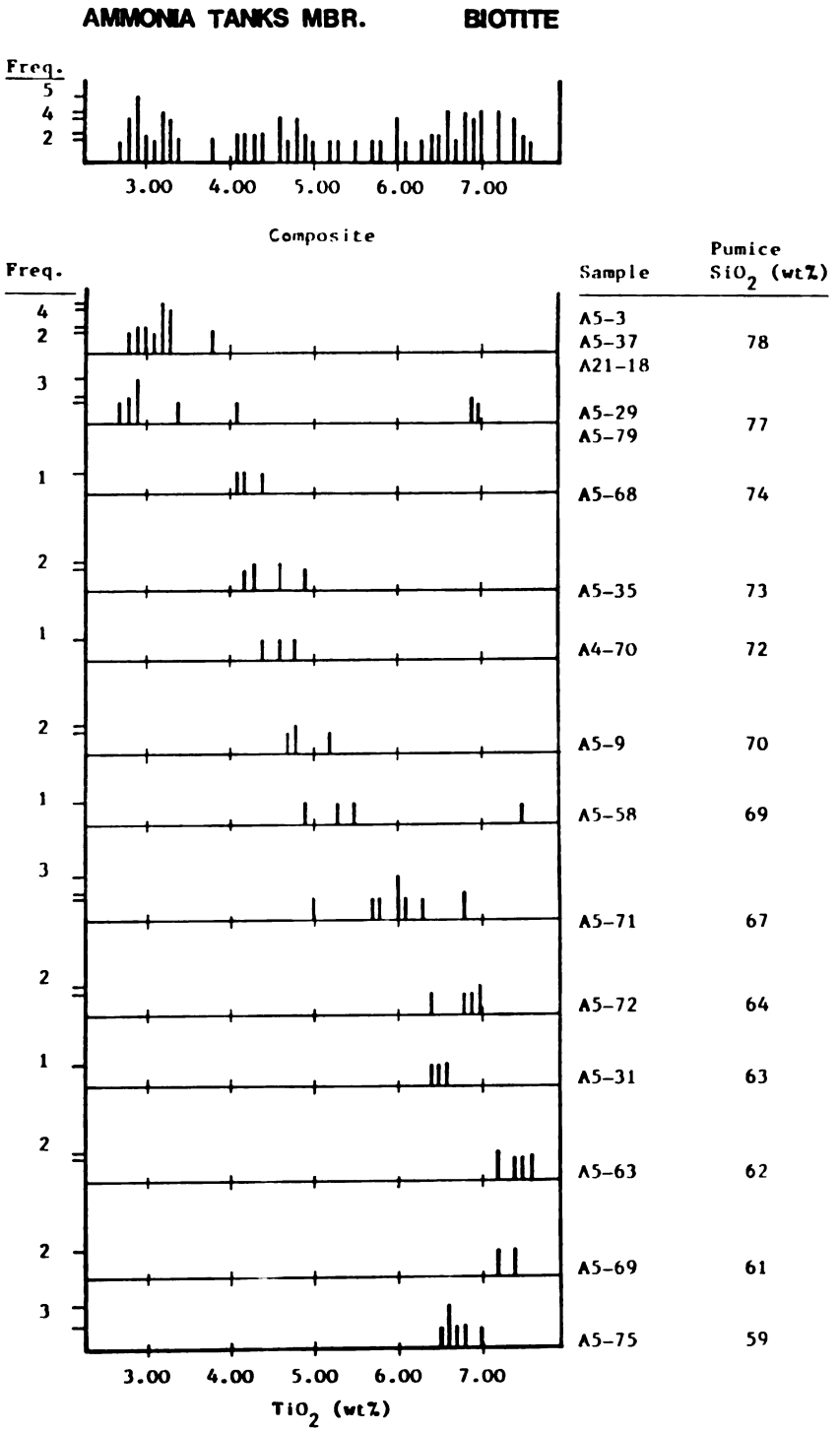


Figure 26. TiO_2 in biotite phenocrysts in the Ammonia Tanks Member. Samples arranged by increasing whole pumice SiO_2 content. Microprobe analyses are from the grain edges only.

represent the actual compositional range among phenocrysts within the sample. Commingling can be identified in a sample in which the compositional variation of a particular element is small, but a bimodal to polymodal distribution of data is present. Two examples of this can be observed in the TiO_2 data for biotite of the Rainier Mesa Member; samples R11-7, R21-1 and R8-44 (Fig. 24). In this example, the variation in TiO_2 for a particular sample is small. Sample R11-7 however contains a distinct bimodal distribution in the TiO_2 concentration which is interpreted to represent commingling of high-silica rhyolite and andesitic magma. Glass matrix analyses for all analyzed elements exhibit a similar bimodal distribution for R11-7; a priori evidence for commingling (Fig. 39a).

Quartz

Petrography

Quartz phenocrysts are present in the rhyolitic portions of both members (70 wt% SiO_2 to 78 wt% SiO_2) of the Timber Mountain Tuff.

In the Rainier Mesa Member, quartz comprises 1% to 6.2% (DRE) of the rock (Table 2). The grains are typically broken and may be slightly to moderately resorbed (Table 3). The grains are inclusion free and range in size from <0.5mm to 2mm.

In the Ammonia Tanks Member, the quartz grains are present in concentrations up to 1% (DRE) and are typically broken (Table 2). In contrast to quartz of the Rainier Mesa Member, the quartz phenocrysts are not resorbed (Table 3). Glass inclusions are rare to common in quartz phenocrysts from both members of the Timber Mountain Tuff.

Clinopyroxene

Petrography

Clinopyroxene phenocrysts are common in samples of trachyandesite through rhyolite in both the Rainier Mesa and Ammonia Tanks Members (Table 2). In the Rainier Mesa Member, clinopyroxene does not appear as a phenocryst phase in low SiO_2 samples until a whole-pumice SiO_2 composition of 61 wt% is reached. In the more mafic samples, hornblende and biotite are the dominant ferromagnesian phases. In both members, clinopyroxene ceases to be a phase as quartz phenocrysts appear.

Petrographically, clinopyroxene grains are euhedral to subhedral and range in size from <1.0mm to 2.0 mm. Color of the clinopyroxene is clear to slightly pale green. In each member, several clinopyroxene grains were noted to contain irregularly shaped orthopyroxene cores. In these same samples, clinopyroxene grains may also have optically discontinuous, irregularly shaped cores of

clinopyroxene in addition to orthopyroxene cores which may reflect the presence of relict grains.

Modally, clinopyroxene only occurs in concentrations of a few tenths of a percent except in trachyandesite of the Ammonia Tanks Member where it reaches a total concentration of 1.2% (DRE)(Table 2). Inclusions in the clinopyroxene grains include apatite, magnetite, ilmenite, zircon, and chevkinite.

Mineral Chemistry

Mole fractions of Wo-En-Fs were calculated for the clinopyroxene and orthopyroxene phenocrysts using the program "CATIONS" (Wilband, unpublished program). These data are plotted on the pyroxene quadrilateral in Figures 27a and 27b. Compositionally, the dominant group of clinopyroxene phenocrysts, based on edge analyses, ranges from $Wo_{49}En_{43}Fs_{8}$ to $Wo_{37}En_{47}Fs_{16}$. Two grain-center analyses have significantly lower Wo mole fractions of $Wo_{27}En_{53}Fs_{20}$ and $Wo_{31}En_{49}Fs_{20}$. The respective edge compositions of these two grains are $Wo_{44}En_{43}Fs_{13}$ and $Wo_{37}En_{48}Fs_{16}$ (samples R23-26 and R21-1). Compositional zoning was common in clinopyroxenes of the Rainier Mesa Member with a usual Wo mole fraction range of +/- Wo_2, with a few grains having a range of up to +/- Wo_5. Zoning with respect to MgO and FeO from the grain center to the grain edge did not show any consistent pattern. In some

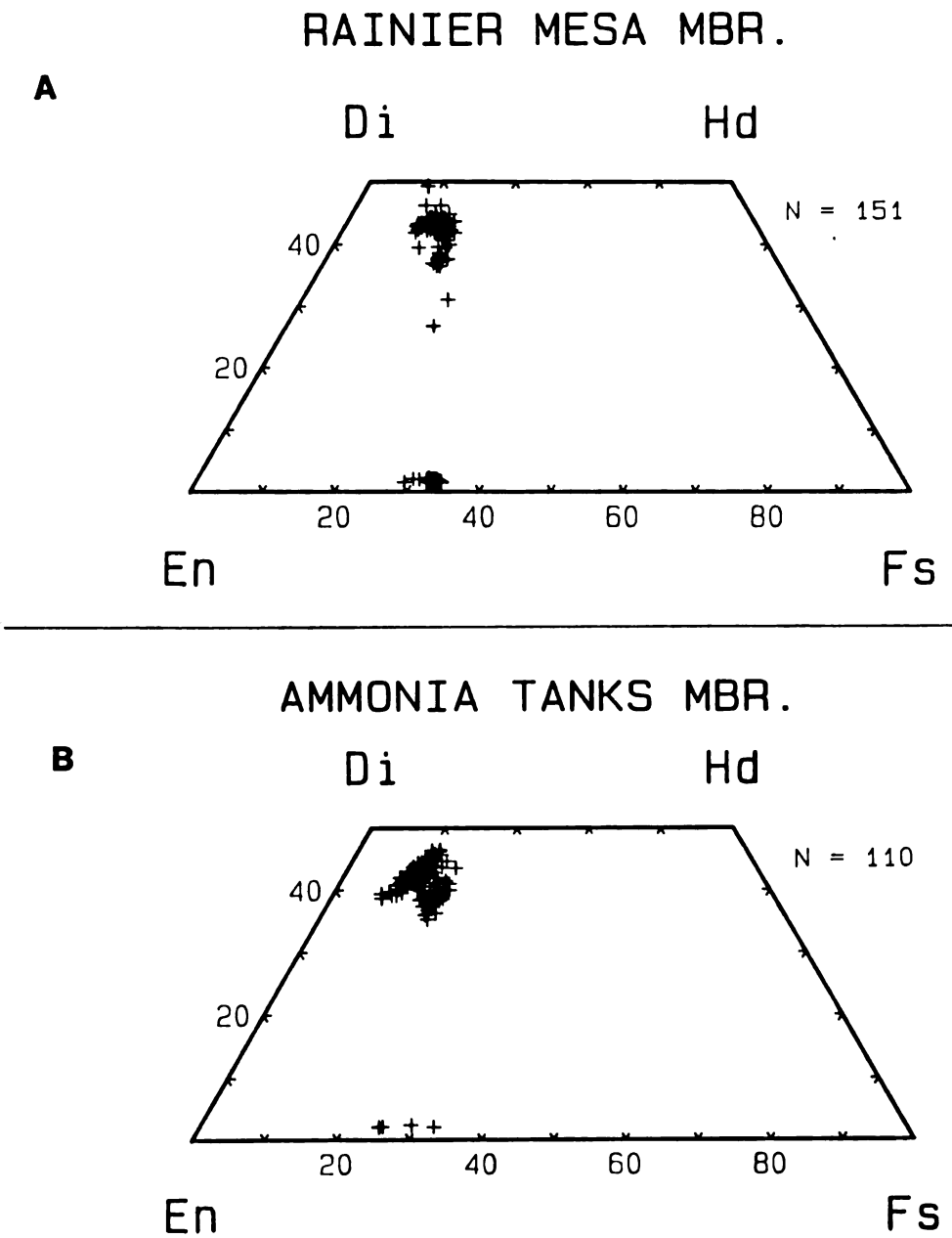


Figure 27. A) Plot of clinopyroxene and orthopyroxene compositions on the pyroxene quadilateral diagram for the Rainier Mesa Member.
B) Plot of clinopyroxene and orthopyroxene compositions on the pyroxene quadilateral diagram for the Ammonia Tanks Member.

grains FeO was enriched towards the edge of the grain and in others MgO was enriched edgeward. Normally, a FeO enrichment edgeward would be expected for grains growing in a melt compositionally evolving toward a more silicic composition. This discrepancy can be explained due the random orientation of the broken grains as a result of sample preparation. Edge analyses may actually have been taken towards the true grain center. Analyses of hand picked phenocrysts and analyses of phenocrysts in thin section however do consistently indicate Fe-rich rims and Mg-rich cores, as should be expected.

The Mg# of clinopyroxene in the Rainier Mesa Member ranges from 0.77 to 0.72. The mean Mg# of clinopyroxene in the most mafic pumice fragment (59 wt% SiO_2) and in the most evolved pumice fragment (75 wt% SiO_2) is 0.76 and 0.74 respectively (Fig. 28).

Compositionally, clinopyroxene in the Ammonia Tanks Member is very similar to clinopyroxene in the Rainier Mesa Member except for a few analyses in the Ammonia Tanks Member which are slightly more enriched in the En component (Fig. 27b). The range in the Wo mole fraction in the Ammonia Tanks Member however, is virtually the same as that in the Rainier Mesa Member. The bimodal distribution of data on the quadrilateral plot most likely represents true phenocryst edge versus center compositions (Fig. 27b). Due to the broken nature of the grains in the

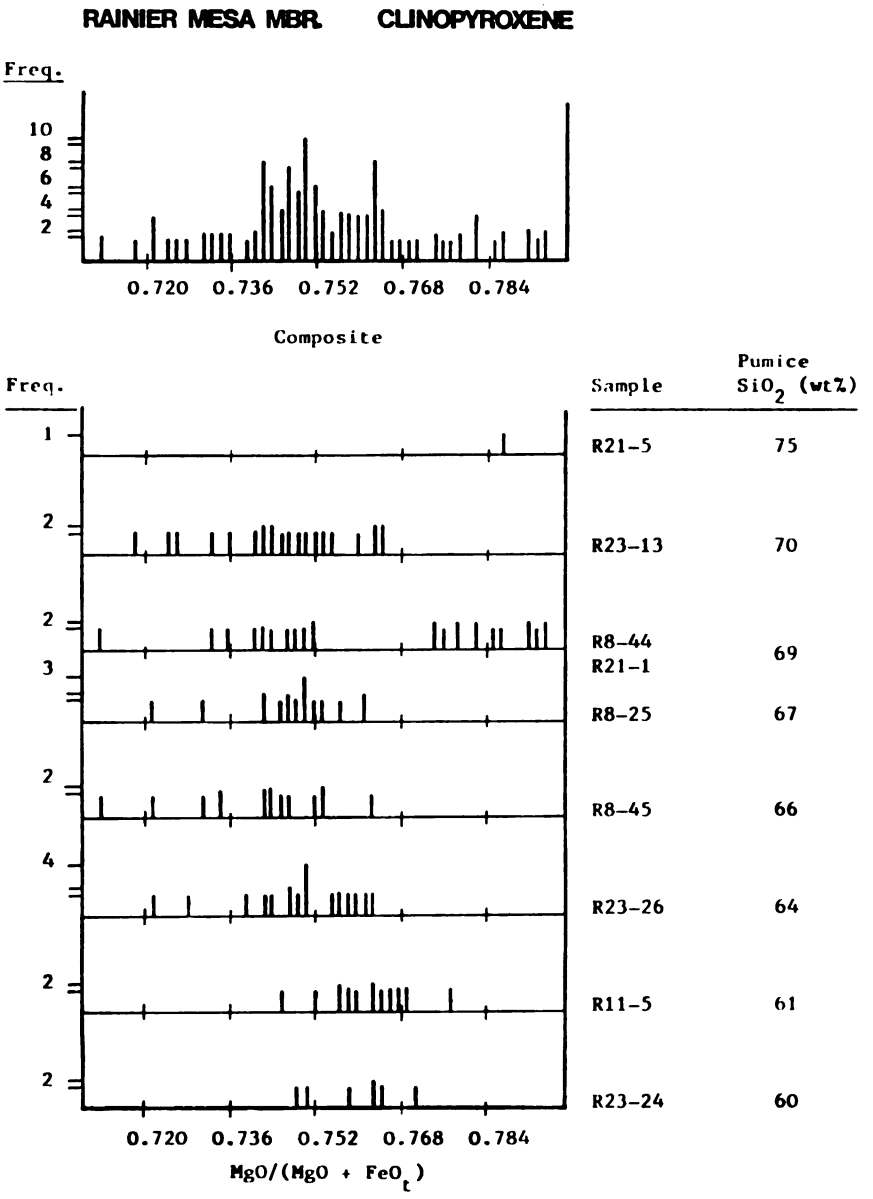


Figure 28. Mg# of clinopyroxene phenocrysts in the Rainier Mesa Member. Samples arranged by increasing whole pumice SiO_2 content. Microprobe analyses are from the grain edges only.

grain mounts as noted for the Rainier Mesa Member samples, the true edge or center of the grain could not be determined during analysis. The implications of the bimodal distribution of the data will be discussed in a later section. Zoning studies on hand picked phenocrysts and thin-section phenocrysts indicate Fe-rich rims and Mg-rich cores (sample A5-35).

The Mg# ranges from 0.72 to 0.82 for all clinopyroxene phenocrysts in the Ammonia Tanks Member. Clinopyroxene grains from the trachyandesite have a mean Mg# of 0.79 while clinopyroxene grains from the rhyolite have a mean Mg# of 0.77 (Fig. 29).

Elemental concentrations of the clinopyroxene phenocrysts in the Ammonia Tanks Member remain nearly constant in pumice fragments ranging from 59 wt% to 63 wt% SiO_2. At approximately 67 wt% SiO_2, the clinopyroxene composition changes gradually towards the evolved composition of the clinopyroxene grains in the rhyolitic pumice fragments. This is consistent with a change toward more evolved biotite and glass compositions in the Ammonia Tanks Member at approximately 64 wt% SiO_2. Similarly, the Rainier Mesa Member exhibits a gradual change in clinopyroxene composition at 64 wt% SiO_2, while biotite and glass compositional data for the Rainier Mesa Member exhibit an inflection at approximately 61 wt% SiO_2.

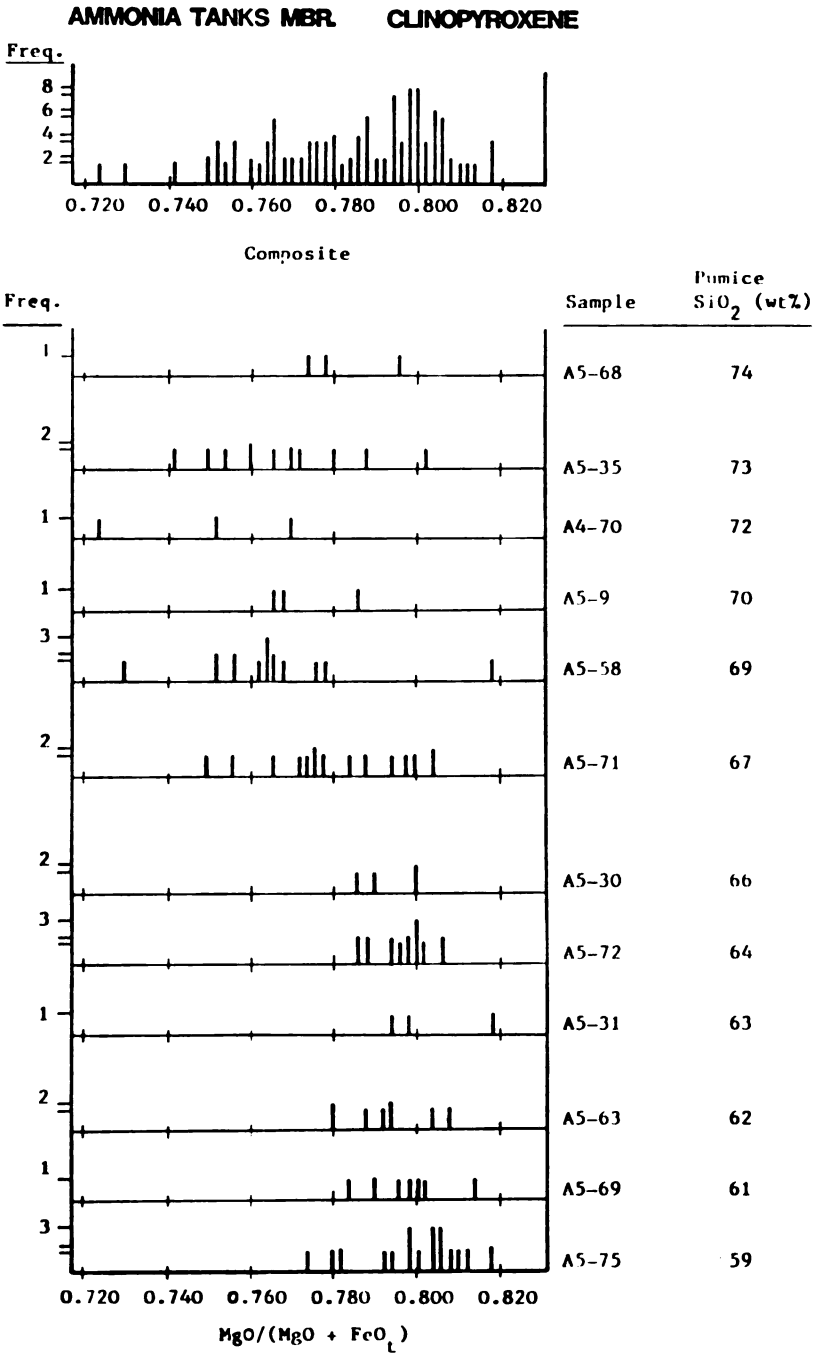


Figure 29. Mg# of clinopyroxene phenocrysts in the Ammonia Tanks Member. Samples arranged by increasing whole pumice SiO_2 content. Microprobe analyses are from the grain edges only.

Orthopyroxene

Petrography

As noted in the section on clinopyroxene, orthopyroxene occurs in both members of the Timber Mountain Tuff, but, only as irregularly shaped cores within the clinopyroxene phenocrysts.

Mineral Chemistry

In the Rainier Mesa Member, the Wo-En-Fs mole fractions have a limited range; $Wo_2En_{70}Fs_{29}$ to $Wo_2En_{65}Fs_{34}$ (Fig. 27a).

The absolute range in Mg# for orthopyroxene in the Rainier Mesa Member is 0.66 to 0.71. The mean Mg# for orthopyroxene in the most mafic pumice fragment is 0.67 while the Mg# for orthopyroxene in the most felsic pumice fragment is also 0.67 (Fig. 30a). While the Mg# exhibits a very small range for the Rainier Mesa Member, the orthopyroxene TiO_2 concentrations decrease systematically from approximately 0.13 wt% in the trachydacite to 0.07 wt% in the high-silica rhyolite (Fig. 30b).

In the Ammonia Tanks Member, orthopyroxene is rare and only four analyses were performed on the three grains found in one sample (A5-58, 69 wt% SiO_2). The Wo-En-Fs mole fraction range for these analyses is $Wo_2En_{73}Fs_{25}$ to $Wo_2En_{66}Fs_{32}$ (Fig. 27b). The absolute range in Mg# is from 0.74 to 0.70 (Fig. 31).

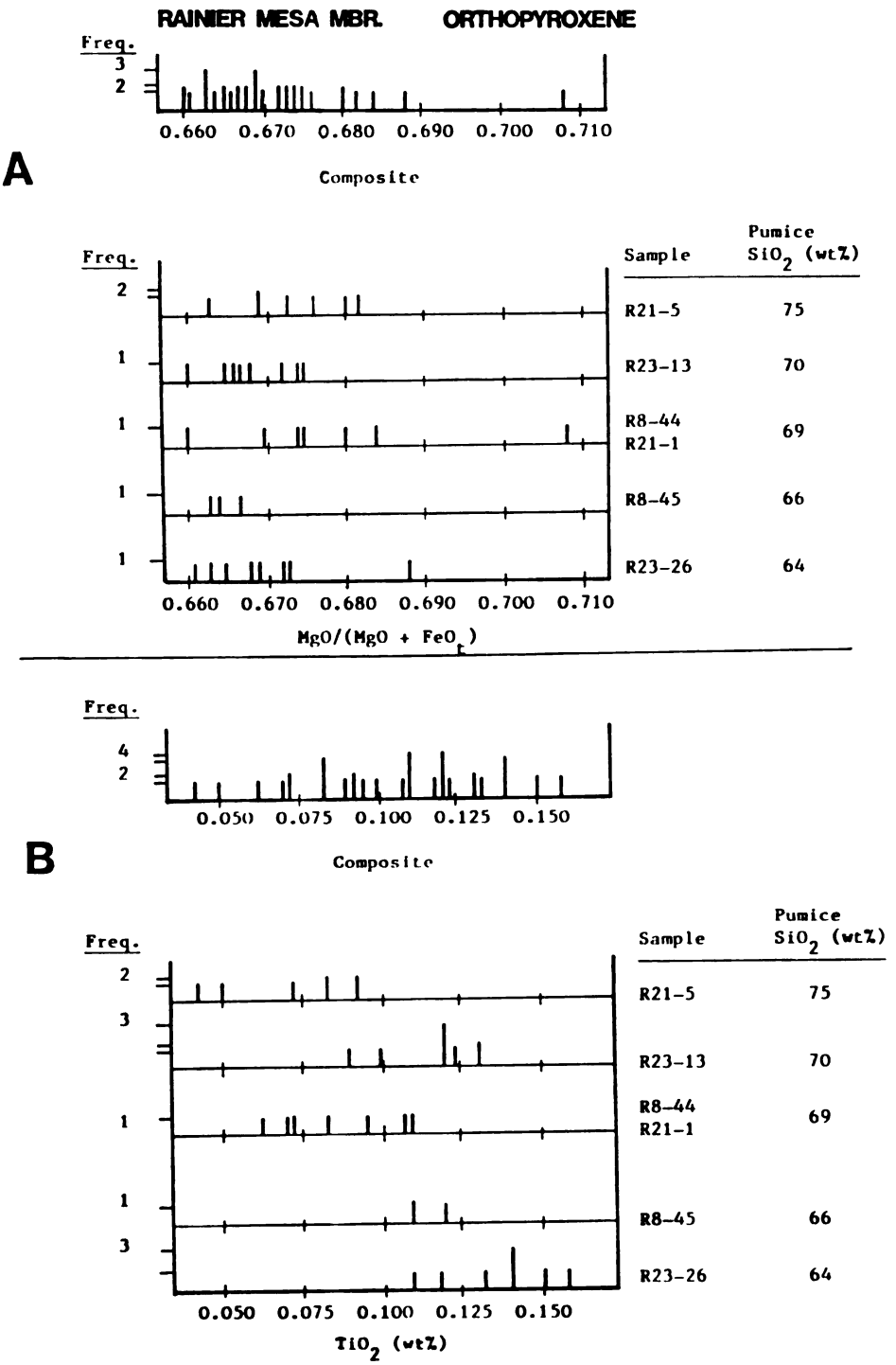


Figure 30. A) Mg# of orthopyroxene phenocrysts in the Rainier Mesa Member. Samples arranged by whole pumice SiO_2 content. Microprobe analyses are from grain edges only.
B) TiO_2 in orthopyroxene phenocyrsts in the Rainier Mesa Member.

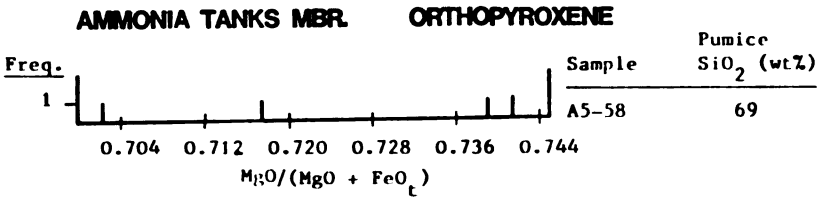


Figure 31. Mg# of orthopyroxene phenocrysts in the Ammonia Tanks Member. Samples arranged by increasing SiO_2 content of whole pumice. Microprobe analyses are from grain edges only.

Amphibole

Petrography

Hornblende is common in the Rainier Mesa Member as a phenocryst phase and occurs sporadically from the trachyandesite to the rhyolite. Hornblende is absent in samples with a SiO_2 content equal to or greater than 67 wt% and is present only in minute quantities in pumice samples of 61 wt% to 66 wt% SiO_2. A small cluster of euhedral hornblende was also identified in the rhyolitic sample R23-13 (70.03 wt% SiO_2).

The pleochroic scheme for hornblende in the Rainier Mesa Member is consistently light green < orange to green-brown (X < Y,Z). Generally the hornblendes are euhedral to subhedral. Only in the most mafic samples of each member do the hornblende phenocrysts exhibit minor embayment of grain boundaries. It is unclear whether or not these grains were resorbed.

Mineral Chemistry

In the Rainier Mesa Member, the Mg# of hornblende phenocrysts have an absolute range of 0.71 to 0.63. In the most mafic pumice fragment, the mean Mg# is 0.68 while in the most felsic pumice fragment the mean Mg# is 0.66 (Fig. 32). The intrasample variation in Mg# is quite large and may be due to secondary iron gain and/or loss from post-emplacement processes such as volatile migration

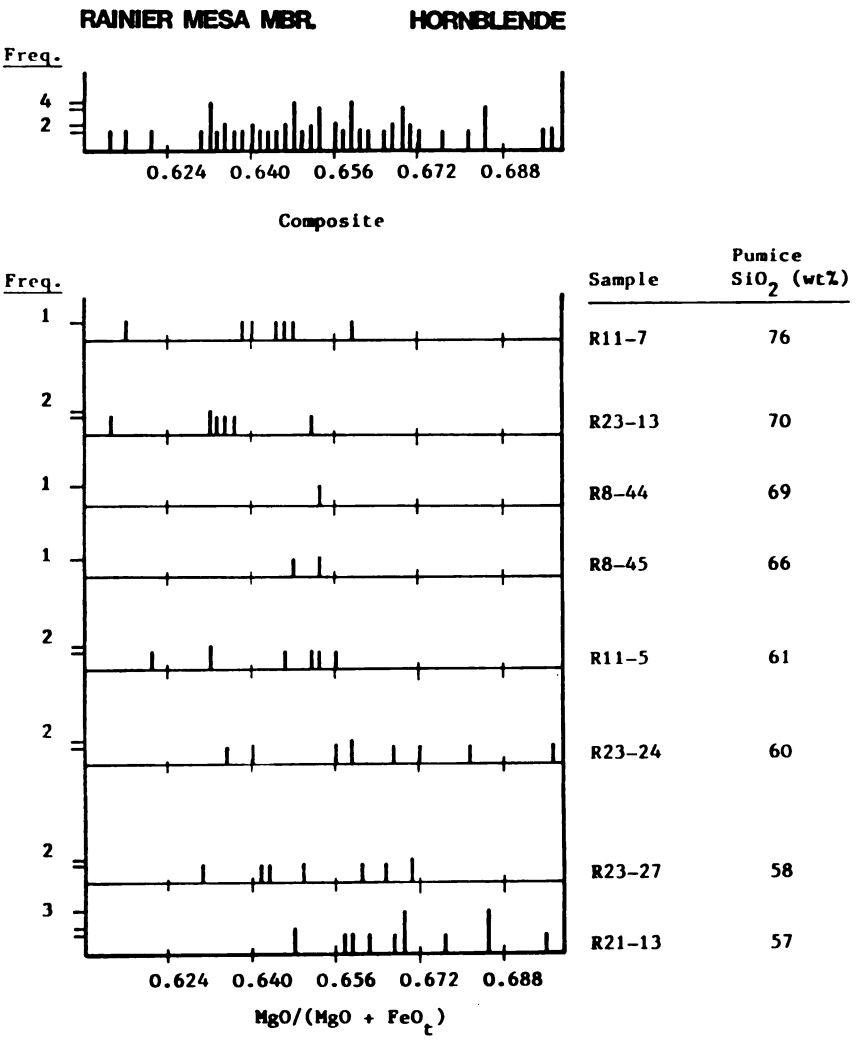


Figure 32. Mg# of hornblende phenocrysts in the Rainier Mesa Member. Samples arranged by increasing whole pumice SiO_2 content. Microprobe analyses are from grain edges only.

during cooling of the sheet, or, meteoric water flow. Al_2O_3 reflects the gradual compositional change of the hornblende phenocrysts with increasing SiO_2 content of the pumice samples (Fig. 33). CaO concentration for hornblende is consistent throughout the range of pumice fragment compositions with a mean value of 11.26 wt% CaO. The CaO concentration for hornblende of sample R21-13, the most mafic pumice fragment at 57 wt% SiO_2, is distinctly different than hornblende in the other pumice samples (Fig. 34). The mean value of CaO in R21-13 is 9.83 wt%. Other elemental concentrations for R21-13 do not exhibit such large variations.

Only two grains of hornblende were identified in the Ammonia Tanks Member and are associated with the most mafic pumice fragment (A5-75, 59 wt% SiO_2). The two hornblende grains are roughly similar in composition to hornblende of the Rainier Mesa Member. Hornblende in the Ammonia Tanks Member has a slightly higher concentration of CaO, K_2O, and MgO, and, a slightly lower FeO concentration than hornblende of the Rainier Mesa Member. The Mg# of the two grains is approximately 0.70 which is slightly above the mean of the most primitive sample for the Rainier Mesa Member (Mg# = 0.68)(Fig. 35).

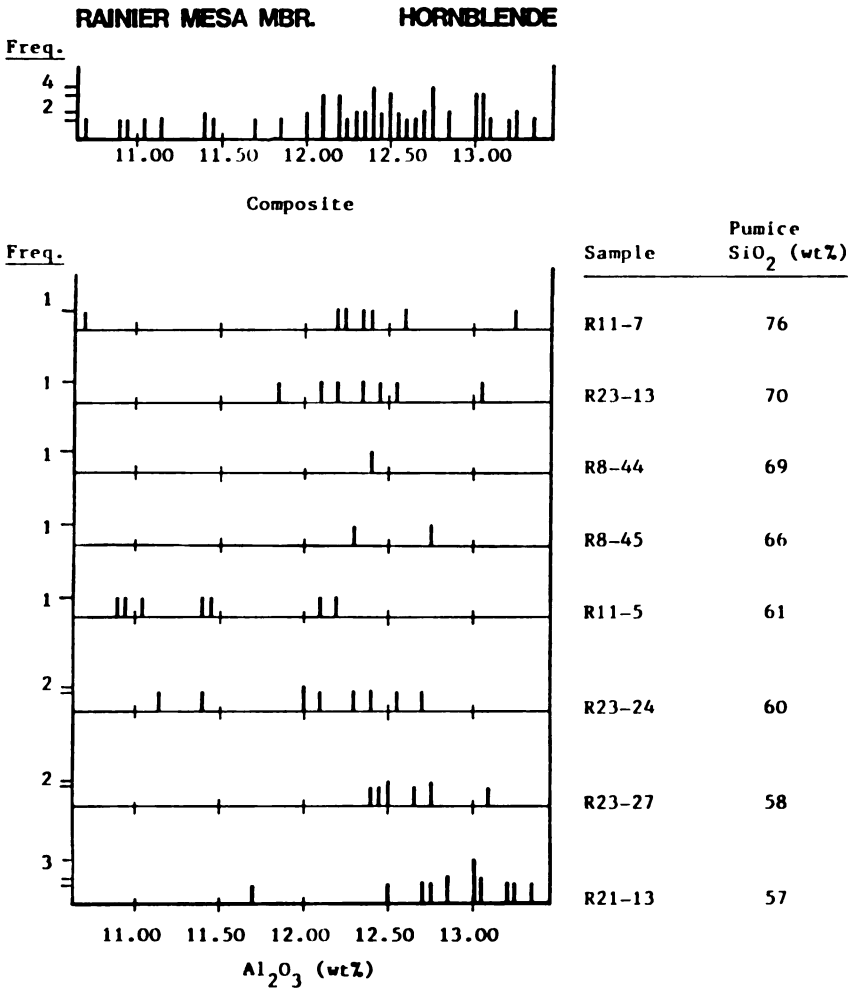


Figure 33. Al_2O_3 in hornblende phenocrysts of the Rainier Mesa Member. Samples arranged by increasing whole pumice SiO_2 content. Microprobe analyses from grain edges only.

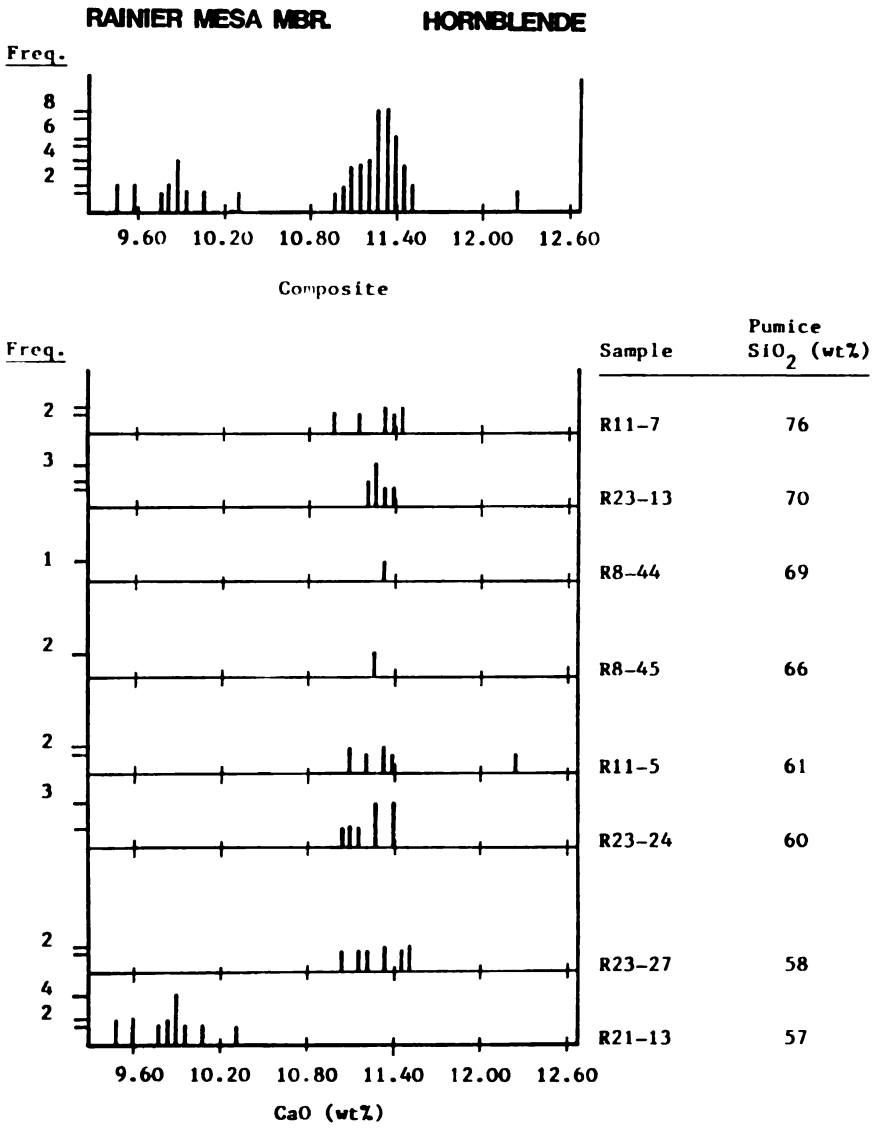


Figure 34. CaO in hornblende phenocrysts of the Rainier Mesa Member. Samples arranged by increasing whole pumice SiO_2 content. Microprobe analyses are from grain edges only.

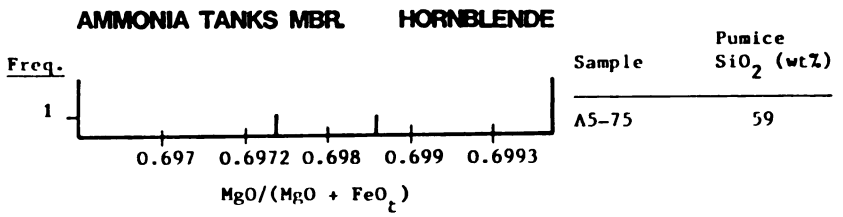


Figure 35. Mg# of hornblende phenocrysts in the Ammonia Tanks Member. Microprobe analyses are from the grain edge only.

Olivine

Olivine does not occur as forsteritic phenocrysts within the Timber Mountain Tuff with the exception of one grain, but instead occurs in the high-silica rhyolites as a Mn-rich fayalite. From the classification scheme of Mossman and Pawson (1976) the olivine phenocrysts range in composition from iron knebelite to knebelite of the fayalite-tephroite solid-solution series (tephroite index: Te_{28}-Te_{37}). Current naming of olivine species is trending away from species specific names and is moving towards chemical modifiers. Thus in this paper, knebelite and iron knebelite will be referred to as manganoan fayalite or Mn-rich fayalite (Fig. 36). A single olivine grain having a forsterite composition of Fo_{57} was identified in sample A5-68 (74 wt% SiO_2) of the Ammonia Tanks Member. This grain may be xenocrystic in origin.

Manganese-rich fayalites have not been documented in volcanic rocks prior to this occurrence and are more commonly associated with Mn-rich metasomatized sedimentary rocks such as those at the Bluebell Mine, British Columbia (Mossman and Pawson, 1976; Mills and Rose, 1991).

Petrography

The Mn-rich fayalites from this study were first identified via electron microprobe analysis on grain mounts made from crushed pumice fragments. Re-examination

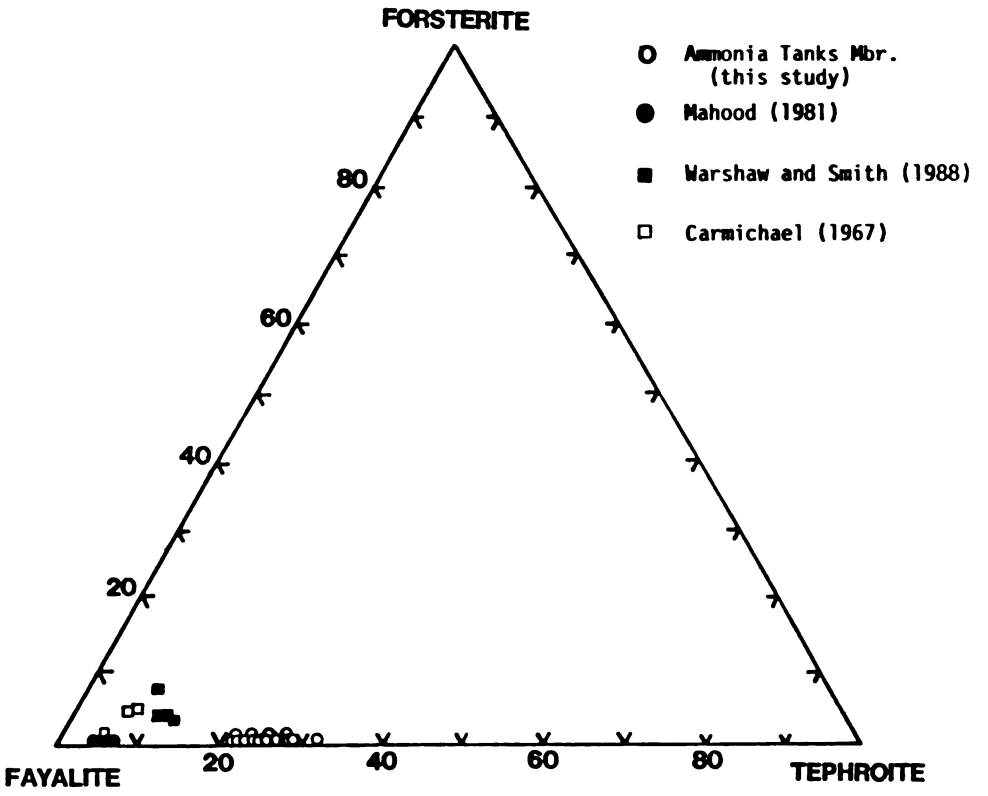


Figure 36. Manganoan fayalite compositions determined from electron microprobe analyses for the Ammonia Tanks Member of the Timber Mountain Tuff. Olivine compositions from other rhyolitic flows and tuffs are plotted for reference.

of thin sections made from the olivine-bearing pumice fragments revealed several potential grains. Most of the Mn-rich fayalite grains are 0.1-0.2 mm in length, are highly birefringent, and are acicular in habit. No optical data could be obtained due to the small size of the grains. Backscattered electron images of the Mn-rich fayalite grains were photographed using the electron microprobe and are presented in Figure 37. High-magnification images of the Mn-rich fayalite phenocrysts did not reveal any fine-scale structure.

Trace Phenocryst Phases

Petrography

Several trace phenocryst phases are present in the Timber Mountain Tuff. Apatite, chevkinite, perrierite, and zircon are common to both the Rainier Mesa and Ammonia Tanks Members. Monazite and sphene occur in the Rainier Mesa Member and the Ammonia Tanks Member respectively.

Apatite is ubiquitous throughout both members and commonly occurs as euhedral, acicular poikiocrysts in plagioclase, biotite, hornblende, clinopyroxene, and magnetite. Apatite can usually be identified within the glassy matrix of most pumice fragments.

The pseudomorphs, chevkinite and perrierite ($(Ce_4Fe_2Ti_3(Si_2O_7)_2O_8$ and $(Ca,Ce,Th)_4(Mg,Fe)_2(Ti,Fe)_3Si_4O_{22}$ respectively (Phillips and Griffen, 1981)), are relatively

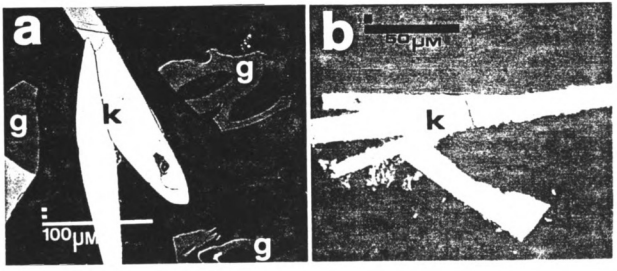


Figure 37. Back-scattered electron photomicrographs of manganoan fayalite phenocrysts in the Ammonia Tanks Member.

common in both members of the Timber Mountain Tuff. Chevkinite and perrierite are most commonly found as inclusions in magnetite and ilmenite and less commonly in clinopyroxene and biotite grains. They may be associated with other inclusions of apatite, zircon, and +/- sphene. In thin section, the grains are very difficult to distinguish from zircon. SEM images of magnetite/ilmenite grain mounts however can be used to easily distinguish chevkinite from the other trace phases as the chevkinite grains are typically bright white in color (Fig. 38). The REE bearing phases, such as chevkinite, are significant in that they strongly control the distribution coefficients of the light rare-elements in dacitic to rhyolitic magmas (cf. Michael, 1988).

Zircon is most commonly found within magnetite and ilmenite phenocrysts and less commonly within biotite and clinopyroxene phenocrysts. The zircons are usually euhedral and have second-order birefringence.

Monazite was only identified in a few mafic silicate grain mounts of the Rainier Mesa Member. In thin section, monazite was only positively identified as an inclusion in biotite in sample R8-23 (67 wt% SiO_2) of the Rainier Mesa Member. Grains of monazite were associated with magnetite and ilmenite phenocrysts in the microprobe mounts. Warren, et al., (1989) however, have indicated that monazite may be more common in the Rainier Mesa Member

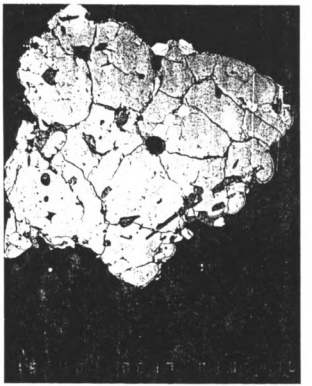


Figure 38. Ilmenite grain from sample R23-13 with inclusions of chevkinite (white), zircon (white, square outlines) and apatite (dark elongate inclusions). Scale bar on the bottom right of the photo is 100 microns long.

than was found in this study. The Ammonia Tanks Member is monazite free. Sphene is abundant in the Ammonia Tanks Member and sparse in the Rainier Mesa Member. Therefore, it has been used as an indicator mineral by several workers for petrographically distinguishing samples of the Ammonia Tanks and Rainier Mesa Members collected during drilling (cf. Byers, et al., 1976a). Phenocrysts of sphene are readily identifiable in thin section by their high relief, light brown color, and characteristic wedge shape. These phenocrysts are usually found associated with the mafic silicate phenocrysts such as biotite and clinopyroxene. SEM imaging also shows sphene as a common inclusion in magnetite and ilmenite phenocrysts in trachydacitic to rhyolitic pumice fragments. The presence of abundant sphene and paucity of ilmenite in the Ammonia Tanks Member as opposed to the reverse in the Rainier Mesa Member, may be a function of magmatic oxygen fugacity and silica activity which will be discussed in a later section.

Glass

Chemistry

Compositional data for the matrix glasses (determined by electron microprobe) of the pumice fragments in the Timber Mountain Tuff reveals distinct differences between glasses of the Rainier Mesa Member and Ammonia Tanks

Member. As should be expected, glass compositions for both members become more felsic in a systematic fashion from the trachyandesite to the high-silica rhyolite. Distinction between pumice fragments of Rainier Mesa Member or Ammonia Tanks Member can be made in most cases using the glass compositions for the trachyandesite to rhyolite samples. The overall glass compositions in the Ammonia Tanks Member are typically more mafic than those of the Rainier Mesa Member. The high-silica rhyolite of both members of the Timber Mountain Tuff are difficult to distinguish based on major-element glass chemistry; this includes distinction between the high-Nb and low-Nb high-silica rhyolites of the Rainier Mesa Member.

Histograms of SiO_2, Al_2O_3, FeO, K_2O, CaO, and TiO_2 from glass analyses of the Rainier Mesa Member are distinctly polymodal (Fig. 39a-f). Silica concentrations of glasses in pumice fragments associated with the Rainier Mesa Member have an absolute range of 68.11 wt% SiO_2 to 78.15 wt% SiO_2. The most mafic compositions of glass do not however occur in the most mafic pumice fragment. Glass compositions in the 68 wt% to 69 wt% SiO_2 range occur in several pumice fragments having bulk SiO_2 values ranging from 61 wt% to 76 wt% SiO_2 (Fig. 39a). This is also consistent for other elemental components such as FeO, Al_2O_3, TiO_2, and BaO.

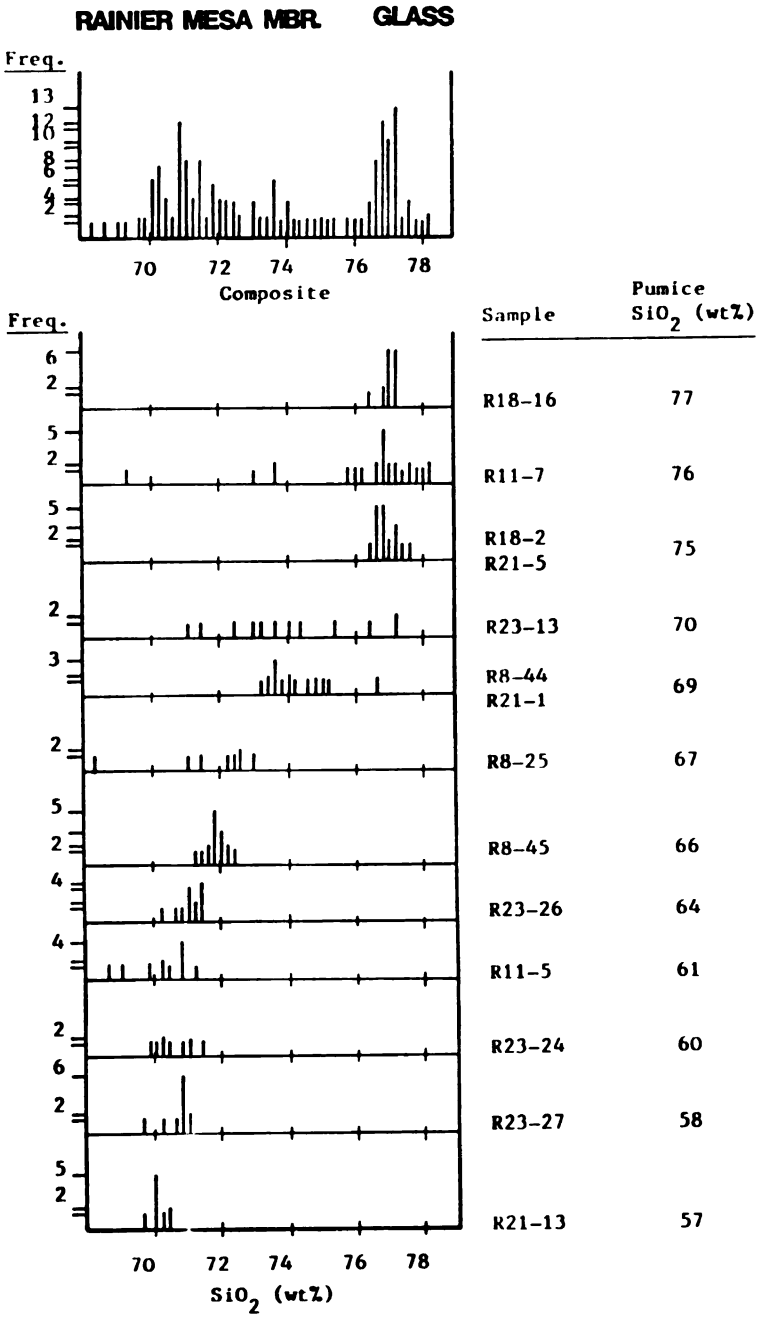


Figure 39a. Histograms of glassy matrix compositions in pumice fragments determined by electron microprobe analysis for the Rainier Mesa Member. SiO_2.

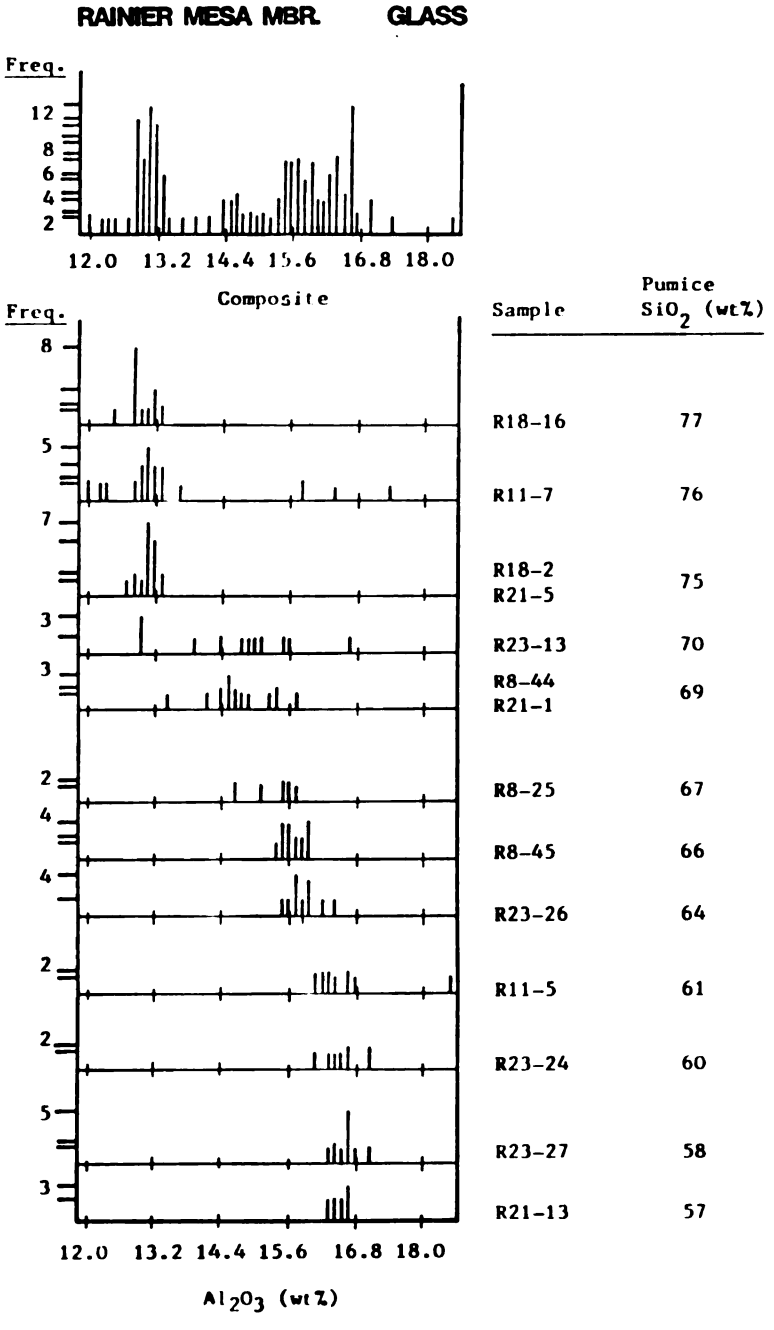


Figure 39b. Al_2O_3 in pumiceous glass, Rainier Mesa Member.

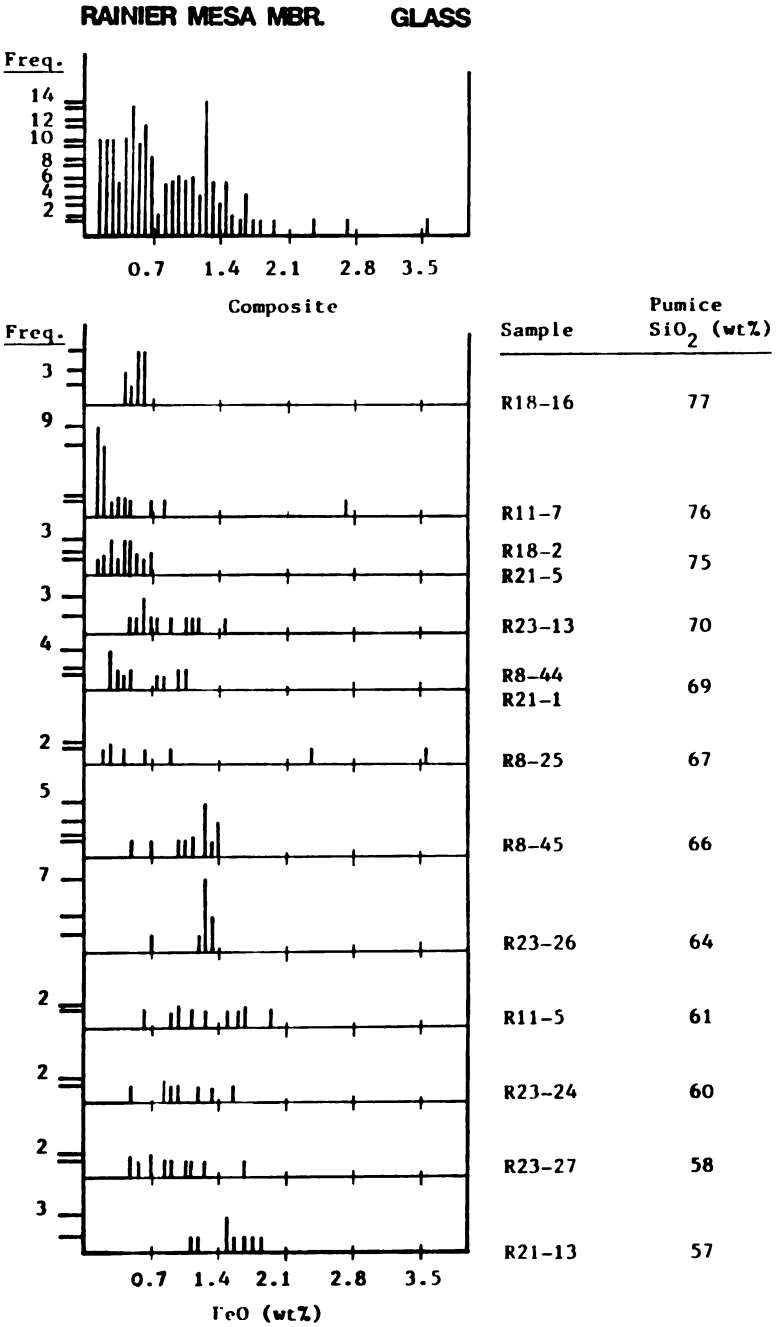


Figure 39c. FeO in pumiceous glass, Rainier Mesa Member.

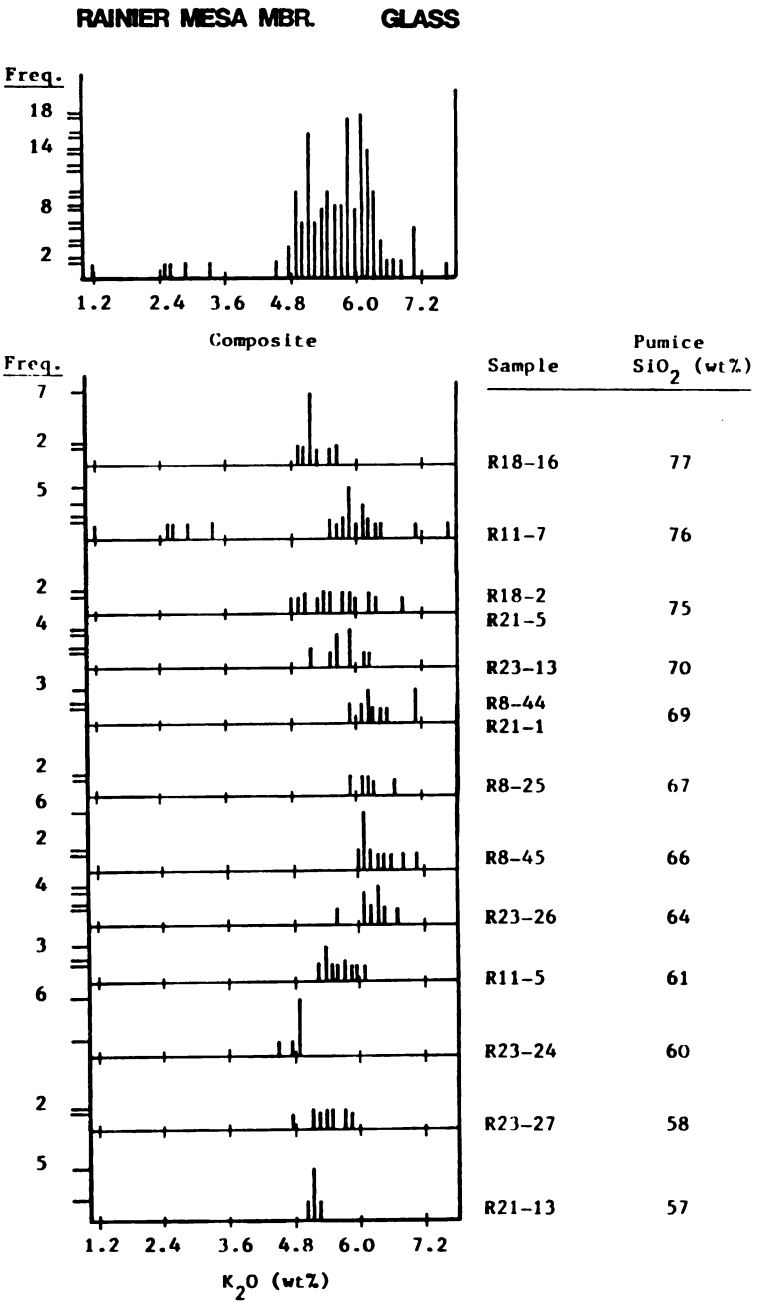


Figure 39d. K_2O in pumiceous glass, Rainier Mesa Member.

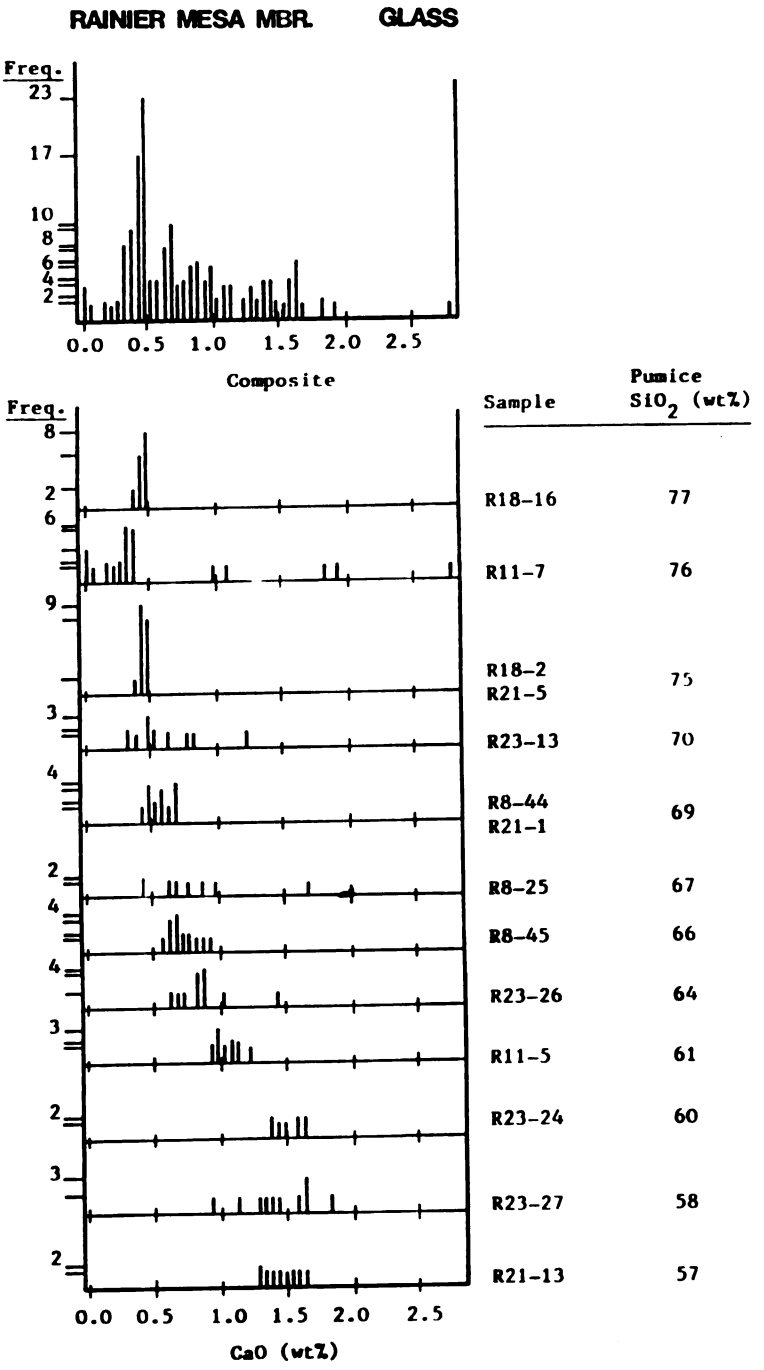


Figure 39e. CaO in pumiceous glass, Rainier Mesa Member.

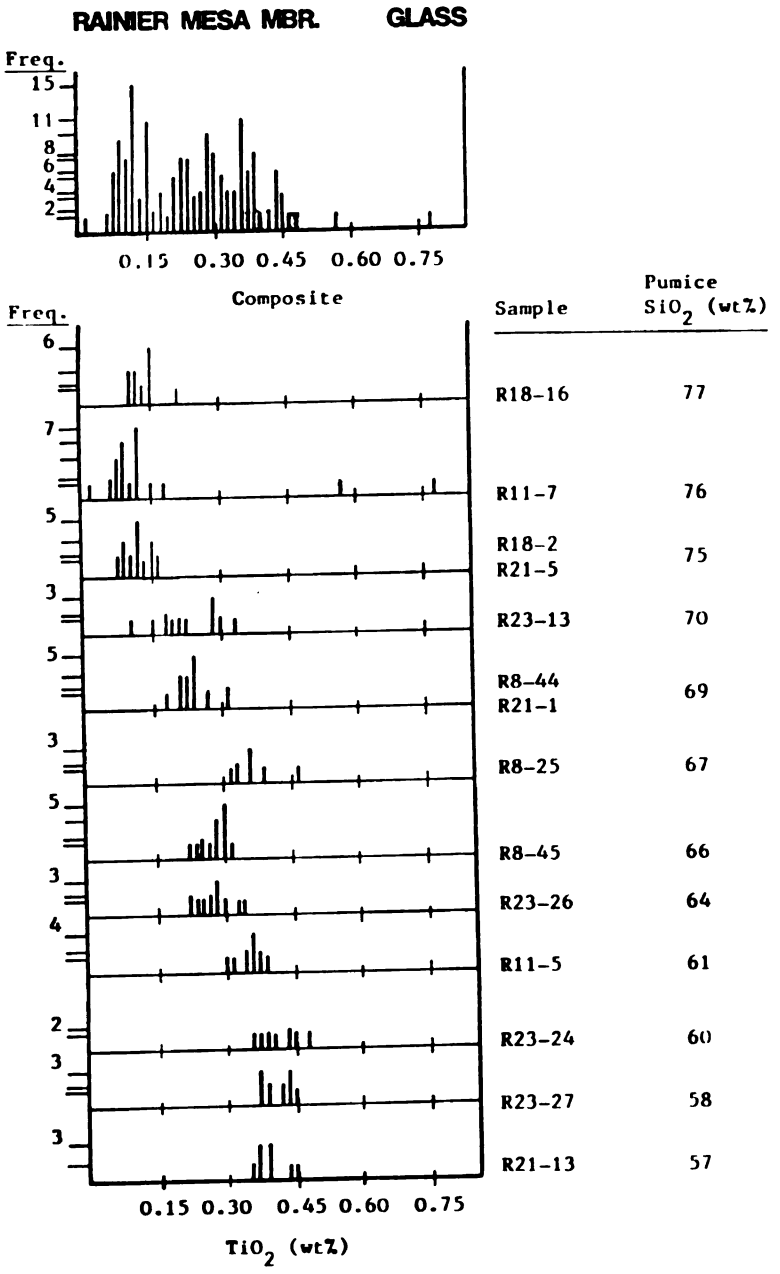


Figure 39f. TiO_2 in pumiceous glass, Rainier Mesa Member.

Conversely, concentrations of SiO_2, Al_2O_3, FeO, K_2O, CaO and TiO_2 in the glass matrix of pumice fragments from the Ammonia Tanks Member, vary systematically from the lower to higher whole-pumice silica contents (Fig. 40a-f). The composition of glasses from trachyandesite to the trachydacite at 64 wt% SiO_2 do not change significantly. Glass compositions for the high-silica rhyolites are constant from whole pumice silica values of 72 wt% SiO_2 to 78 wt% SiO_2. Between 64 wt% SiO_2 and 72 wt% SiO_2 the glass compositions vary in a systematic fashion. Within this interval, the various major element oxides either increase or decrease in concentration as the whole-pumice SiO_2 increases. In samples R8-25 (67 wt% SiO_2) and R11-5 (61 wt% SiO_2) the presence of anomalous glass compositions (68 wt% and 69 wt% SiO_2 respectively) may represent a more mafic component not recognized in the bulk pumice fragment chemical analyses (Appendix 3).

Geothermometry and Geobarometry

Fe-Ti Oxide Geothermometry

As compositional and mineralogical gradients in ash-flow sheets are generally acknowledged to represent pre-eruptive gradients in the parental magma chamber, systematic variations in calculated temperatures from Fe-Ti oxide phenocrysts collected from ash-flow sheets may also be interpreted to represent pre-eruptive magmatic

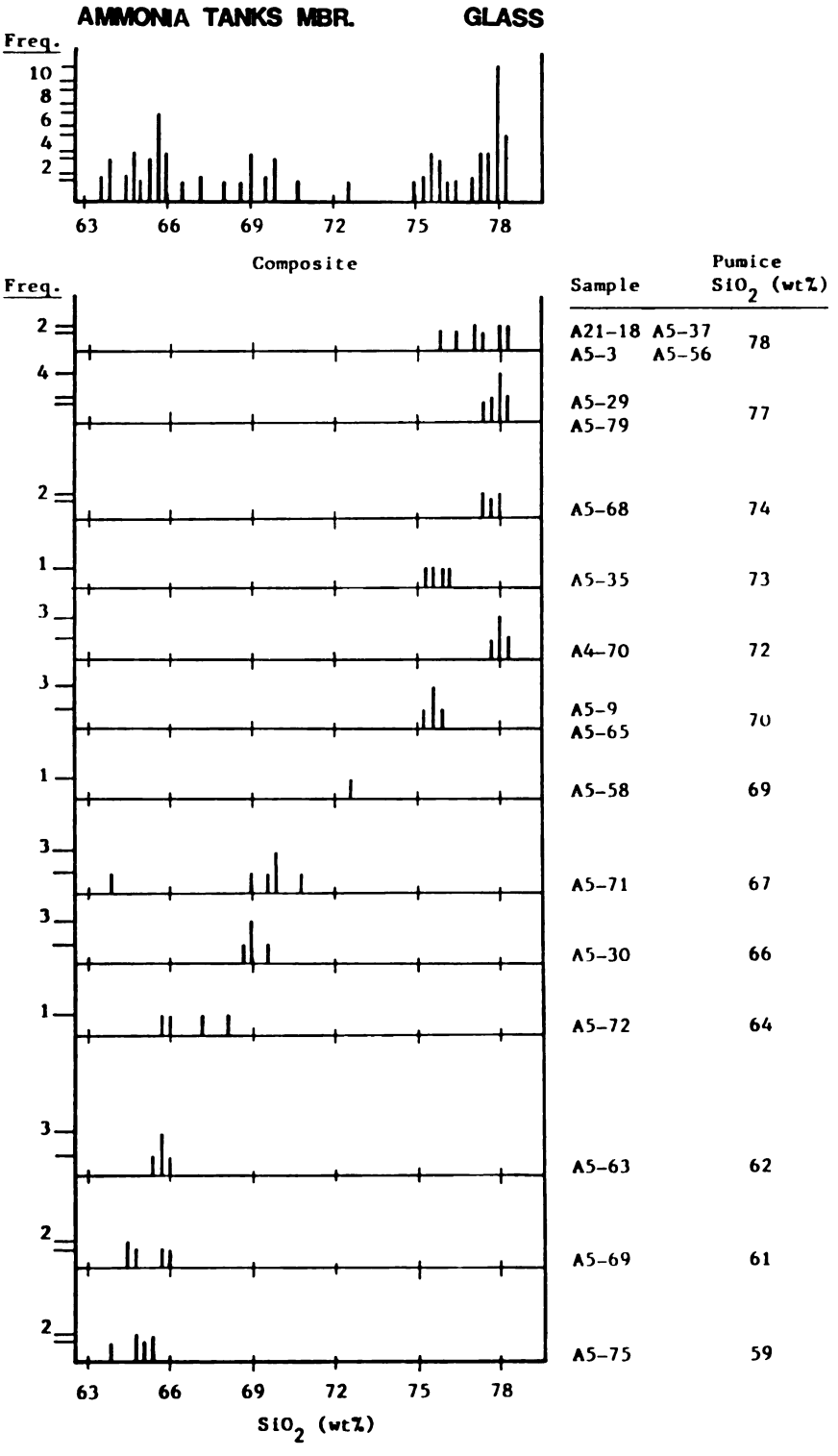


Figure 40a. SiO_2 in pumiceous glass, Ammonia Tanks Member.

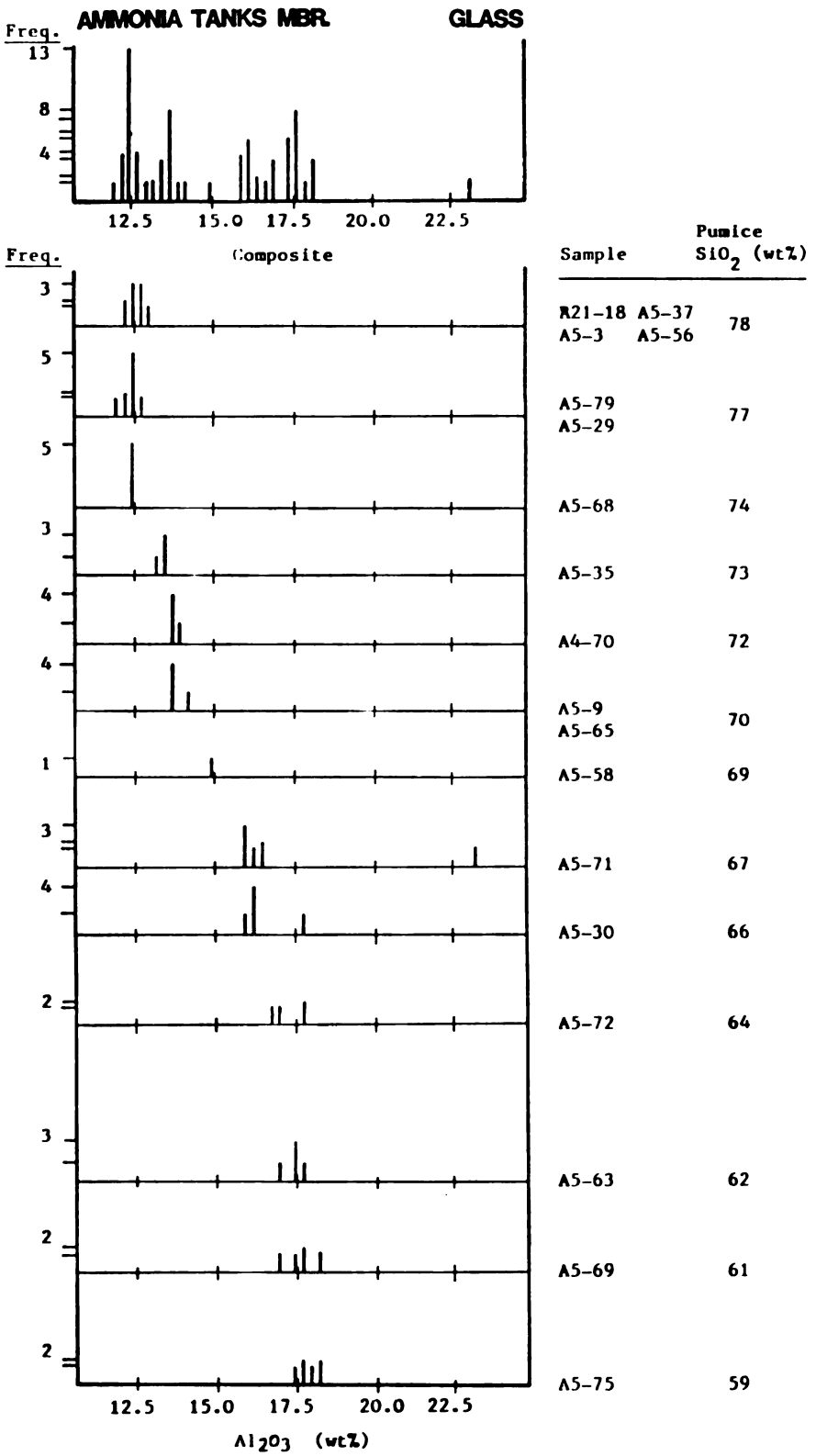


Figure 40b. Al_2O_3 in pumiceous glass, Ammonia Tanks Member.

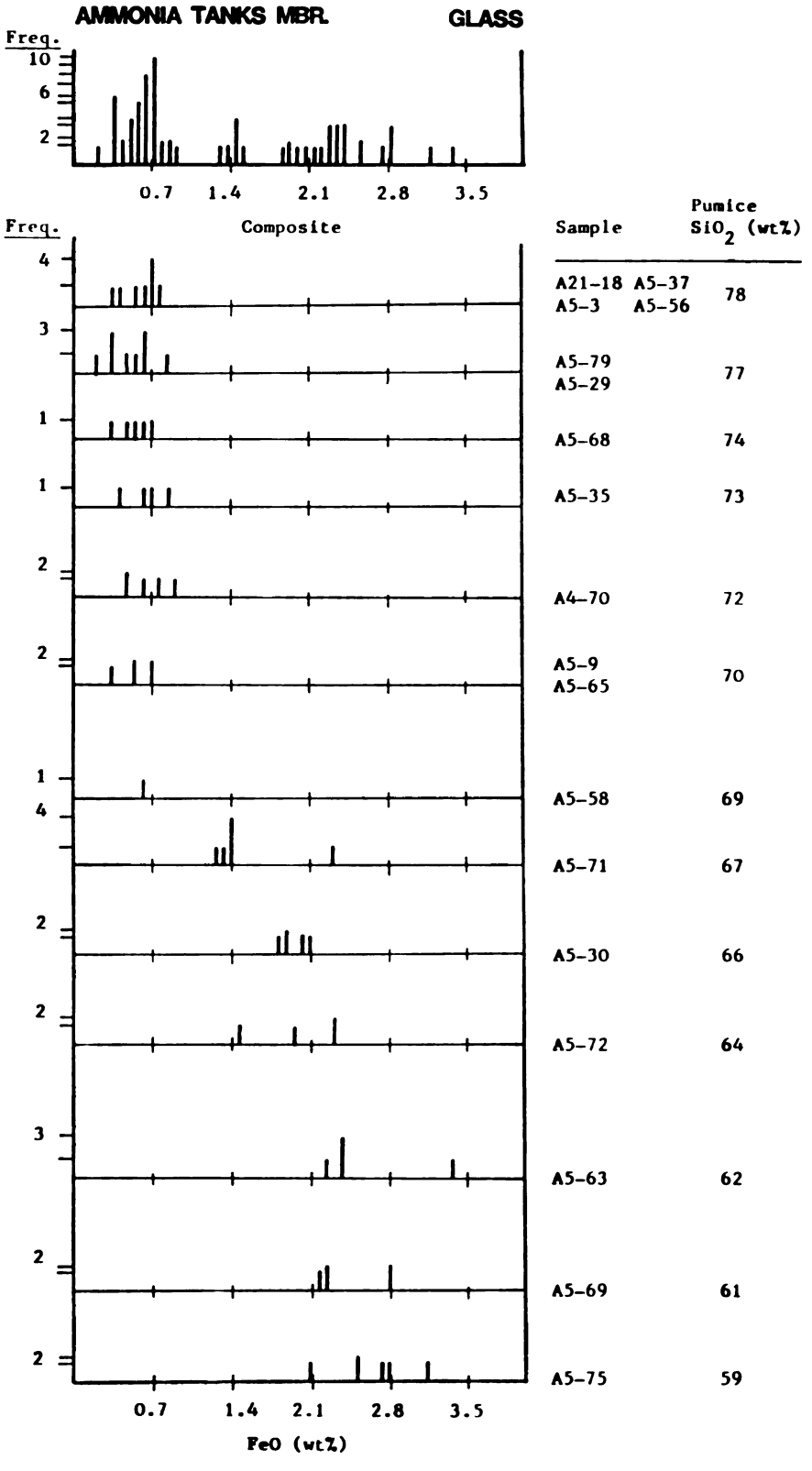


Figure 40c. FeO in pumiceous glass, Ammonia Tanks Member.

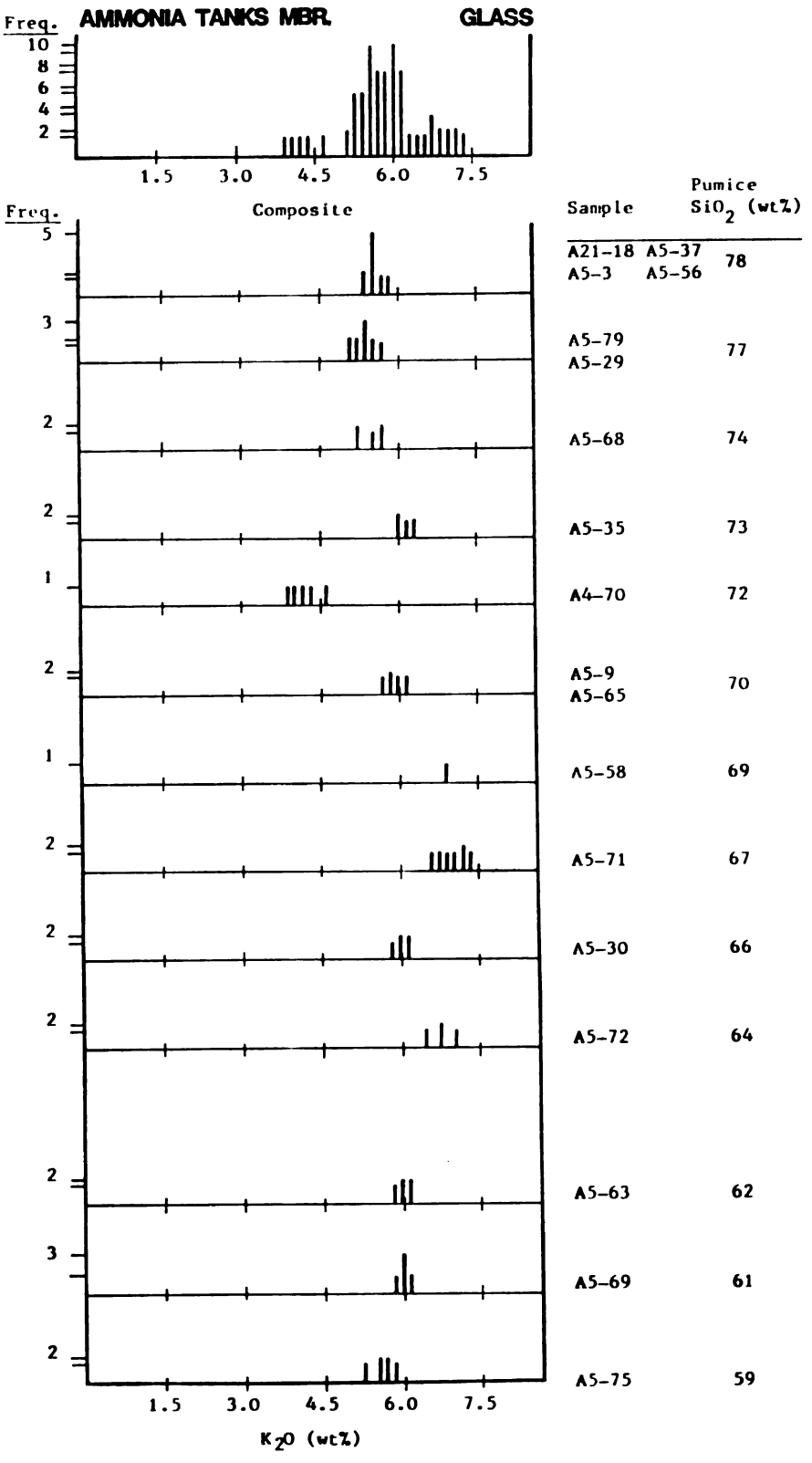


Figure 40d. K_2O in pumiceous glass, Ammonia Tanks Member.

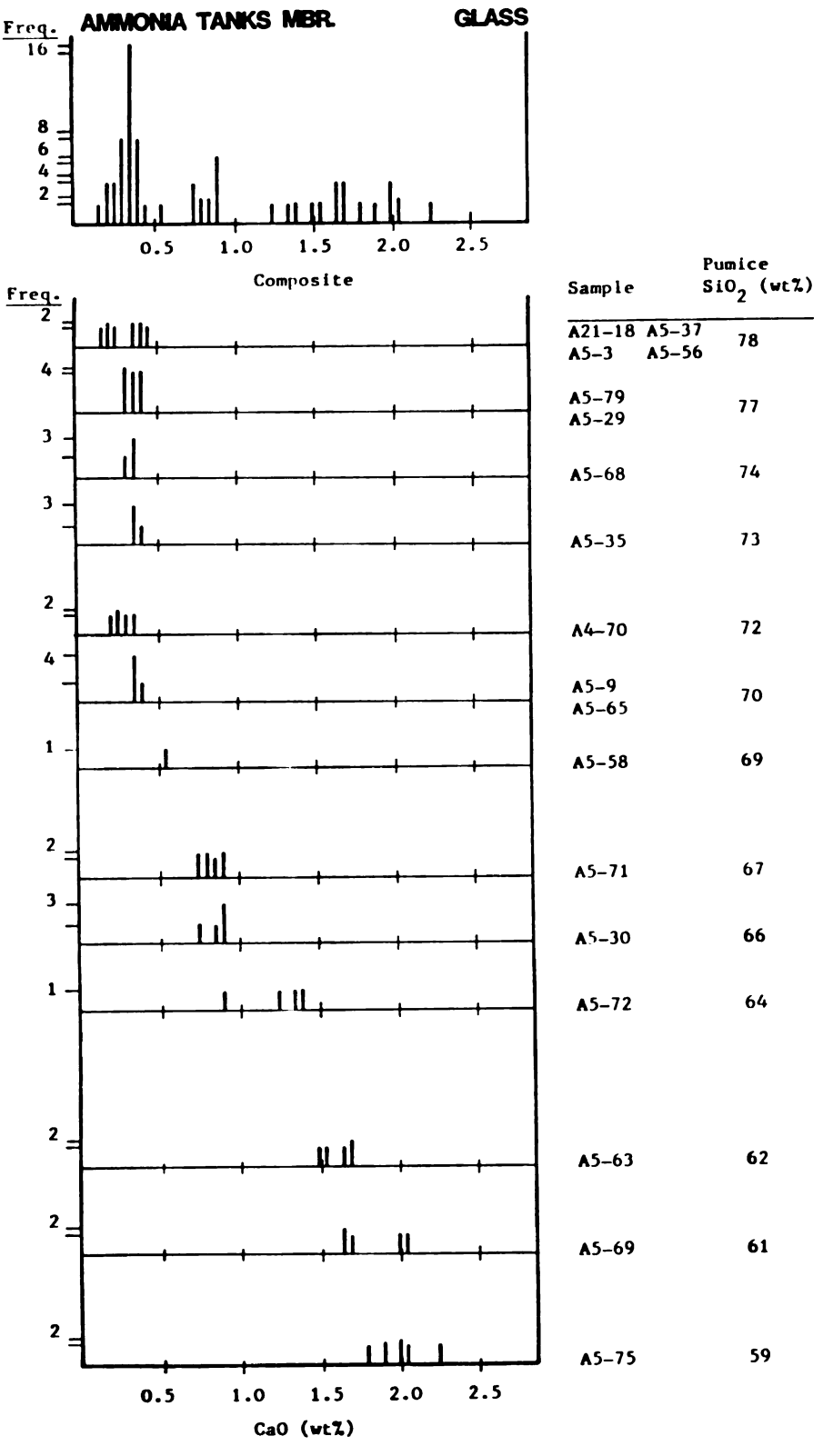


Figure 40e. CaO in pumiceous glass, Ammonia Tanks Member.

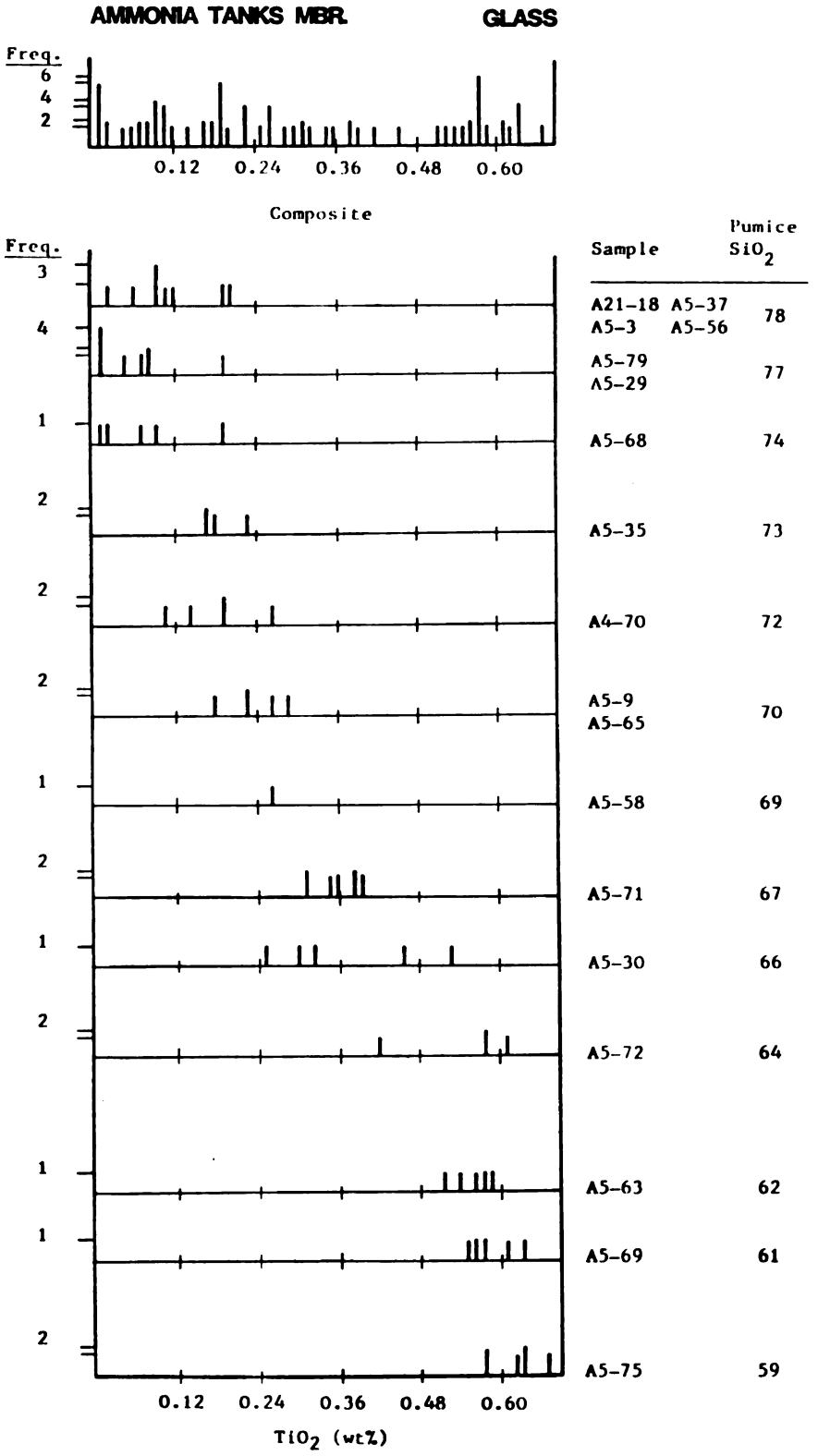


Figure 40f. TiO_2 in pumiceous glass, Ammonia Tanks Member.

temperatures (Buddington and Lindsley, 1964; Lipman, 1971; Smith, 1979; Hildreth, 1981).

Temperature and Oxygen Fugacity Calculations

Recalculation of ulvospinel and hematite compositions using the technique of Andersen and Lindsley (1988) for data presented by Lipman (1971) for the Rainier Mesa Member range from 766 ^{o}C, -12.15 log fO_2 for rhyolitic samples (77 wt% SiO_2) to 838 ^{o}C, -10.88 log fO_2 for samples of trachydacite (66 wt% SiO_2). Estimates for the Ammonia Tanks Member range from 763 ^{o}C, -12.15 fO_2 in the high-silica rhyolite to 872 ^{o}C, -10.63 log fO_2 in the trachydacite.

New temperature and oxygen fugacity calculations from this study exhibit a significantly larger range in values than those of Lipman (1971)(Fig. 41)(Table 4). The Rainier Mesa Member varies from 755 ^{o}C, -13.09 log fO_2 for the high-silica rhyolite to 897 ^{o}C, -10.57 log fO_2 for the trachyandesite. The Ammonia Tanks Member exhibits a similar range in temperature and oxygen fugacity (Table 4). Minimum temperature and oxygen fugacity data in the Ammonia Tanks Member occur in the high-silica rhyolite at 727 ^{o}C, -13.86 log fO_2 while the maximum temperature and oxygen fugacity occur in the trachyandesite at 903 ^{o}C, -10.96 log fO_2. All calculated values for the Timber Mountain Tuff lie within the boundary curves for the

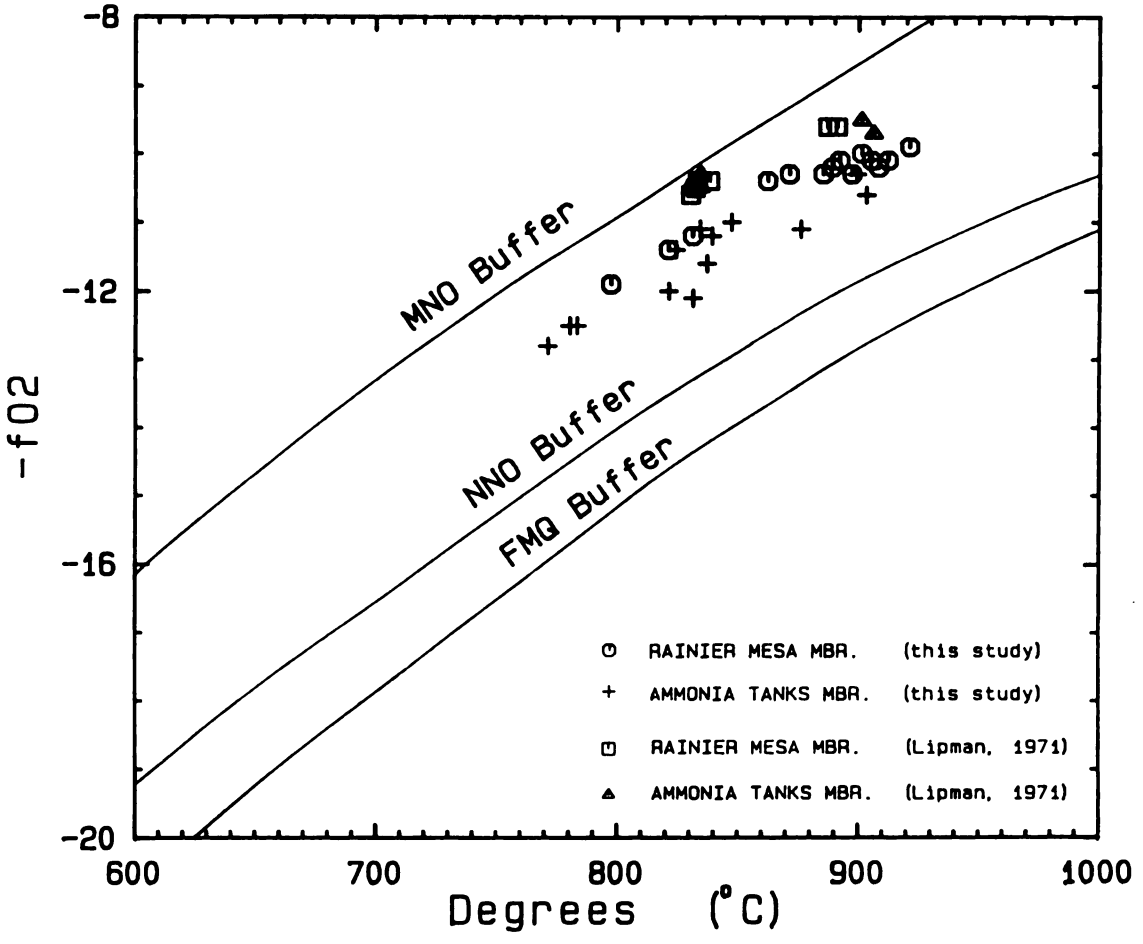


Figure 41. Temperature versus fO_2 diagram derived from Fe-Ti oxide phenocryst data for the Timber Mountain Tuff. Data are from this study and from Lipman (1971).

Table 4. Fe-Ti oxide temperature and oxygen fugacity data for the Timber Mountain Tuff.

Sample #	SiO_2[1] (wt%)	Temp[2] (°C)	fO_2
RAINIER MESA MEMBER			
LIP17	78	826	-10.47
LIP14	77	815	-10.59
LIP15	77	812	-10.67
LIP16	77	815	-10.55
R18-16	77	796	-12.25
R11-7	76	755	-13.09
R18-2	75	773	-12.86
R21-5	75	819	-11.56
R23-13	70	863	-11.31
LIP18	69	875	-9.81
R8-44	69	855	-11.18
R21-1	69	855	-11.15
LIP19	68	880	-9.73
R8-25	67	869	-10.94
R8-45	66	864	-10.97
R23-26	64	882	-10.82
R11-5	61	873	-10.83
R23-24	60	887	-10.84
R23-27	58	890	-10.74
R21-13	57	897	-10.57
AMMONIA TANKS MEMBER			
LIP20	77	806	-10.06
LIP21	77	801	-10.52
LIP22	77	801	-10.60
LIP23	77	809	-10.57
A4-70	72	818	-11.91
A5-3	78	727	-13.86
A5-9	70	806	-12.16
A5-29	77	744	-13.51
LIP24	68	895	-9.89
LIP25	66	887	-9.75
A5-30	66	880	-11.01
A5-35a	73	797	-12.21
A5-35b	73	787	-12.43
A5-37	78	739	-13.59
A5-58	69	812	-12.48
A5-68	74	774	-13.09
A5-71	67	860	-11.69
A5-72	64	903	-10.96

[1]Whole-pumice silica concentration
[2]Andersen and Lindsley, 1988

nickel-nickel oxide (NNO) and the magnetite-nickel oxide (MNO) buffers of Buddington and Lindsley (1964)(Fig. 41). The textural condition of the magnetite and ilmenite phenocrysts used in this study is presented in Table 5.

Coexisting Feldspars and Fe-Ti Oxides

The coexistence of plagioclase, sanidine, and Fe-Ti oxides in many of the pumice fragments of the Timber Mountain Tuff is conducive to the use of two-feldspar, Fe-Ti oxide geothermometry/geobarometry. Two-feldspar geothermometers and geobarometers have been in existence since original studies by Barth (1934). Continual refinements to the models have led to more accurate temperature and pressure estimates for the feldspar assemblages (Barth, 1951; Perchuck and Ryabchikov, 1968; Stormer, 1975; Brown and Parsons, 1981). Many workers have applied these models to igneous and high-grade metamorphic rocks (cf. Whitney and Stormer, 1976, 1977, 1985; Bohlen and Essene, 1977; Hildreth, 1979, 1981; Czamanske, et al., 1981; Green and Usdansky, 1986; Grunder and Boden, 1987).

For the Timber Mountain Tuff, temperatures were calculated for coexisting feldspars using the program "MTHERM3.BAS" (Fuhrman and Lindsley, 1988). Plagioclase-sanidine pairs were selected such that the compositional range within a given sample was represented. Only

Table 5. Textural condition of magnetite and ilmenite phenocrysts analyzed for geothermometry in the Rainier Mesa Member and Ammonia Tanks Member of the Timber Mountain Tuff.

Sample Number	Whole Pumice SiO_2 Content[1]	Magnetite[2]	Ilmenite
R21-13	57 wt%	Fr	Fr
R23-27	58 wt%	Sl. Ex	Fr
R23-24	60 wt%	Fr	Fr
R11-5	61 wt%	Sl. Ex	Fr
R23-26	64 wt%	Sl. Ex	Fr
R8-45	66 wt%	Fr	Fr
R8-25	67 wt%	Ex	Ex
R8-44	69 wt%	Fr	Fr
R21-1	69 wt%	Ex	Fr
R23-13	70 wt%	Sl. Ex	Fr
R18-2	75 wt%	Fr	Fr
R21-5	75 wt%	Ex	Fr
R11-7	76 wt%	Fr	Fr
R18-16	77 wt%	Sl. Ex	Fr
A5-72	64 wt%	Ex	Fr
A5-30	66 wt%	Ex	Fr
A5-71	67 wt%	Ex	Fr
A5-58	69 wt%	Ex	Fr
A5-9	70 wt%	Sl. Ex	Fr
A4-70	72 wt%	Ex	Fr
A5-35	73 wt%	Fr	Fr
A5-68	74 wt%	Fr	Fr
A5-29	77 wt%	Fr	Fr
A5-79	77 wt%	Ex	Fr
A5-3	78 wt%	Fr	Fr
A5-37	78 wt%	Fr	Fr

[1] Calculated 100% anhydrous
[2] Fr = Fresh Sl. Ex = Slightly exsolved Ex = Exsolved

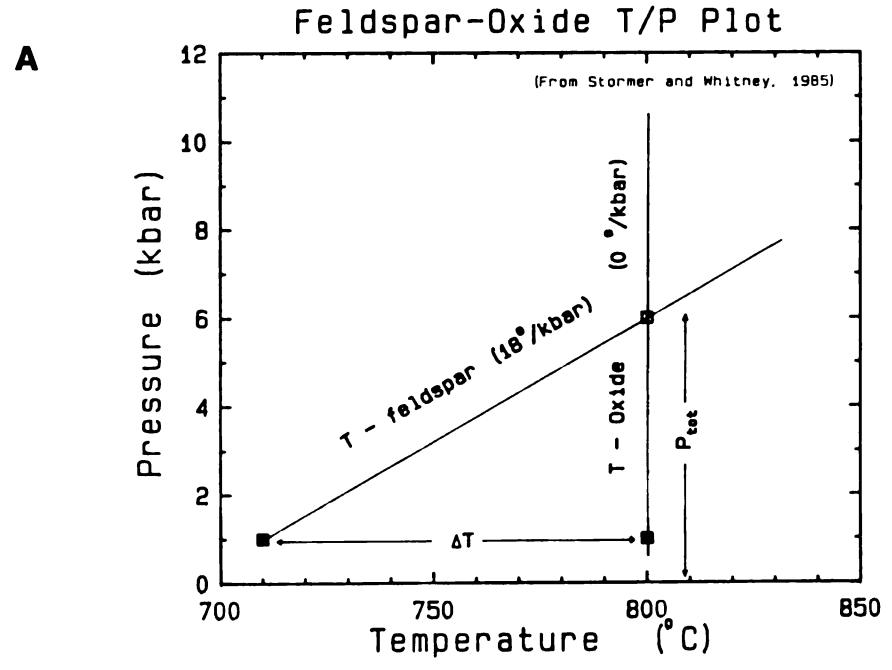
phenocryst edge compositions from whole-phenocryst grain mounts and from thin section were used in the calculations. Temperatures were calculated using the mole fraction of albite, anorthite, kspar, and celsian in the plagioclase and sanidine phenocrysts at various pressures. Within the program, these mole fractions were run through an iterative process in which one composition was held constant while the other compositions were varied in increasing increments of 0.5% until a total change of 2.0% was reached. As soon as a best fit composition was reached, the program printed out the calculated temperature. If a best fit was not achieved once the 2.0% increment was reached, the calculated temperature was printed with a warning. For this study, only the temperatures which fell within the acceptable limits of the model were used. All phenocryst pairs selected were run through the program at various pressures. In some cases, a best fit could be obtained through a range of pressures, but the calculations with the lowest error were usually achieved at 1 kbar.

Stormer and Whitney (1985) developed a method using the temperatures calculated from both Fe-Ti oxides and coexisting plagioclase and alkali feldspars to derive the pressure at which the feldspars and Fe-Ti oxides were most likely in equilibrium. Based on the work of Rumble (1969; in Stormer and Whitney, 1985) the Fe-Ti oxide

geothermometer is independent of temperature up to 10 kbars. The feldspar geothermometer on the other hand, is strongly dependant on pressure. For every 1 kbar increase in pressure the temperature increases by 18 ^{o}C (Brown and Parsons, 1981; Stormer, 1975). The results of this technique as applied to temperatures calculated for the Timber Mountain Tuff are plotted in Figure 42. Error bars based on the variation in calculated pressure between different phenocryst pairs in a given sample are shown. Data points in which only one pair of feldspars was available are assumed to have a minimum error of +/- 1 kbar. It should be noted that the concordance of the temperature data between the two methods (two-feldspar and Fe-Ti oxides) is poor at best. Thus, this technique can only be used for speculative purposes with regard to geobarometry and geothermometry.

Amphibole-Quartz geobarometry

Using the method of Hammarstrom and Zen (1986), the total aluminum content of hornblende in equilibrium with quartz, from sample R23-13 (70 wt% SiO_2) was used to estimate the pressure of hornblende crystallization. Although the possibility exists that trachyandesitic hornblende was commingled with the rhyolite, the euhedral form and lack of colored glass surrounding the hornblende grains which would be present if two chemically discrete



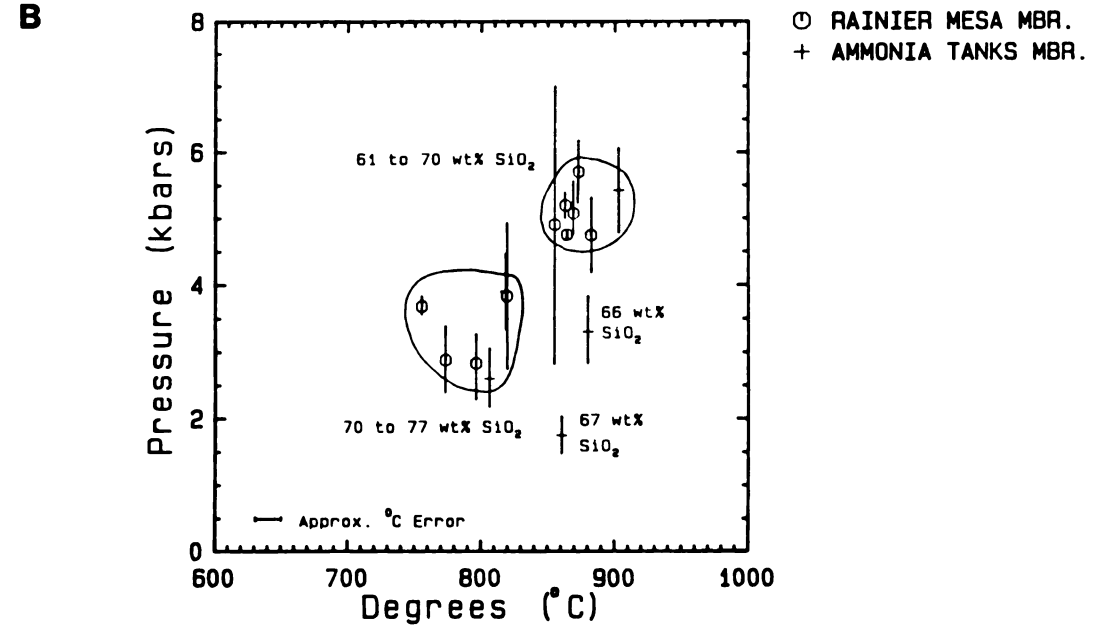


Figure 42. A) Fe-Ti oxide and co-existing feldspar temperature/ pressure diagram from Stormer and Whitney (1985).
B) Fe-Ti oxide and co-existing feldspar temperature/ pressure data from the Timber Mountain Tuff.

magmas were commingled, may indicate that these grains are a primary phase within the rhyolite.

Six hornblende grains were analyzed from sample R23-13. One of these grains was analyzed along the edge and within the core (Appendix 3). The calculated pressures of formation range from 4.8 kb to 3.9 kb. The average value is 4.2 kb with a standard deviation of 0.28 kb. Pressure estimates calculated from the analyzed grain both near the edge and in the core vary by 0.2 kb (edge = 4.0 kb, core = 4.2 kb).

DISCUSSION

Geochemical Zonation in Magma Bodies

Many explanations have been offered for the origin of the compositional heterogeneity of magma bodies; elemental diffusion, convective differentiation, crystal fractionation and magma mixing to name but a few. A brief discussion on the application of these processes to ash-flow tuff magmatic systems by various workers is presented below.

Background

It has long been recognized that many ash-flow sheets are compositionally zoned, i.e. systematic variations occur in chemistry, mineralogy, and inferred pre-eruptive thermal gradients from the stratigraphic base to the top of ash-flow sheets (cf. Ratte and Steven, 1967; Lipman, et al., 1966; Lipman, 1967; Byers, et al., 1976a; Smith, 1979; Hildreth, 1981, 1983). It has been suggested that all large eruptions of a non-basaltic nature tap thermally and compositionally zoned magma chambers (Hildreth, 1981) and that all pyroclastic flows with a volume greater than 1 km^3 are compositionally zoned (Fisher and Schmincke, 1984, p. 26). Geochemical and thermal data for the Fish Canyon Tuff of southwestern Colorado and two members of the Paintbrush Tuff of southwestern Nevada do seem to contradict the above hypotheses. The Fish Canyon Tuff,

the Pah Canyon Member (40 km^3) and the Yucca Mountain Member (20 km^3) of the Paintbrush Tuff are chemically and mineralogically homogeneous (Lipman, 1975; Byers, et al., 1976a; Flood, et al., 1989; Stormer and Whitney, 1985). Recent lead isotope data for the Fish Canyon Tuff also indicates that it is homogeneous in composition (Matty, 1990, personal communication).

Along with the recognition of compositional zonation in ash-flow sheets came the implication that this zonation reflected pre-eruptive gradients within the parent magma chamber (Williams, 1942; Katsui, 1963; Lipman, et al., 1966; Smith, 1979; Hildreth, 1981). It was argued that as an eruption occurred and the chamber was tapped, simple vertical drawdown of the magma occurred. Such studies include those of the Bishop Tuff (Hildreth, 1981), the Sierra La Primavera silicic center (Mahood, 1981), the Crater Lake pyroclastic flows (Bacon, 1983; Bacon and Druitt, 1988), pyroclastic flows on Tenerife Island (Wolff and Storey, 1984), and the Fish Canyon Tuff (Stormer and Whitney, 1985).

Based on these and other pyroclastic flow studies (cf. Lipman, et al., 1966; Hildreth, 1983) it was interpreted that a parental magma body contained systematic variations in chemistry, mineralogy, temperature, and pressure from the cool, silicic cupola to the hotter, more mafic region deeper within the chamber.

Today, this model of magma chamber zonation is widely accepted and is strongly supported by both experimental and petrologic work (Lipman, 1967; Smith, 1979; McBirney, 1980; Hildreth, 1981; Wolff and Storey, 1984; Baker and McBirney, 1985; Bacon and Druitt, 1988). The model for vertical drawdown of the magma chamber during eruption however, has been extensively modified over the past few years, and will be discussed more fully in the section on eruption dynamics.

Recognition that the compositional variation in an ash-flow tuff represents compositional gradients in the parent magma chamber was an important step in understanding high-level silicic systems (Smith, 1979; Hildreth, 1981). Crystal fractionation, crustal anatexis, magma mixing, and volatile transfer were for many years the mainstay processes by which it was thought differentiation of magma bodies occurred (cf. Bowen, 1928; Lipman, 1967; Smith, 1979). A landmark study of magmatic differentiation presented by Hildreth (1981) used many of the ideas of earlier workers and incorporated them within the framework of thermogravitational diffusion. Thermogravitational diffusion can be separated into two processes; these are double-diffusive convection and Soret diffusion. Double-diffusive convection and Soret diffusion rely on thermal and/or density gradients within the magma chamber to initiate convection, and it has been

argued that they provide a strong impetus for magma differentiation. Hildreth (1979, 1981) proposed that enrichment/depletion trends for major and trace elements roofward in the Long Valley magmatic system were formed by Soret diffusion and volatile complexing coupled with convective circulation. Hildreth (1981) also concluded that crystal-liquid fractionation could not have generated the observed trends. Michael (1983a,b) reanalyzed Hildreth's data, and Cameron (1983) presented new data that was interpreted to show that crystal-liquid fractionation could not be dismissed as a viable evolutionary mechanism for the Long Valley magmatic system based on trace element partitioning between glass and phenocryst phases present in the Bishop Tuff. Thus geochemical or petrologic evidence for the occurrence of Soret diffusion in magma bodies still remains to be found.

Experimental work by Huppert and Sparks (1984); Huppert, et al., (1984); Sparks, et al., (1984); McBirney, et al., (1985); Baker and McBirney, (1985); and Nilson, et al., (1985) have shown that spontaneous double-diffusive convection could occur in fluids which contained initial temperature and/or compositional gradients. With time, double-diffusive convection would form thermally and compositionally stable horizontal layers in a fluid. Baker and McBirney (1985) argued that boundary layer transport along the magma chamber walls coupled with

crystal-liquid fractionation in the main magma body was the dominant mechanism responsible for differentiation and zonation of most magma bodies; not double-diffusive convection as proposed by other workers (cf. Hildreth, 1979, 1981; Mahood, 1981). Recent mathematical modelling of double-diffusive convection which simulates real magmatic conditions (Spera, et al., 1986) has been interpreted to show that steady-state layering formed by double-diffusive convection never occurs within the magma chamber. However, this mechanism was later proposed by Fridrich and Mahood (1987) to account for the compositional variation observed in the Grizzly Peak magmatic system. If double-diffusive convection is not a viable mechanism for creating compositional layering, this implies that chemical and thermal zonations must occur by some other process such as, but not limited to: 1) boundary layer transport (cf. Baker and McBirney, 1985), 2) crystal fractionation (Michael, 1983a), 3) magma mixing (cf. Flood, et al., 1989b), and/or 4) injection into or underplating of the magma body by more mafic (primitive) magma (cf. Whitney, et al., 1988).

Differentiation processes such as crystal fractionation, assimilation, magma mixing, and partial melting are the only processes that can currently be quantitatively evaluated for the Timber Mountain magmatic system with the existing data base.

The Timber Mountain Magmatic System

The compositional variation found in the Timber Mountain Tuff from analyses of glassy pumice fragments and phenocrysts is interpreted to represent the minimum compositional variation present in the parental magmatic system of each member approximately 11 Ma ago (Figs. 7, 9). A few anomalous glass, feldspar, biotite and amphibole analyses may reflect the presence of a more mafic magma composition not currently identified in the pumice samples (Figs. 23, 25 and 35). Warren, et al., (1989) also note the presence of a basaltic component in their whole-rock tuff samples.

Based on the compositional heterogeneity present in each member, the configuration of the parental magmatic system can potentially be modelled in several ways:

1) A single magma chamber in which the entire magma body is continuously zoned from a more mafic base to a more felsic top due to the fractional crystallization of an initially homogeneous parent magma (with some possible assimilation of surrounding country rock).

2) A single magma chamber in which magmas of different compositions are brought together sometime prior to eruption forming a layered sequence. The origin of the various magmas being most likely due to variations in partial melting processes or source rock heterogeneities (+/- fractional crystallization and assimilation within each magma batch).

3) Multiple magma chambers where each discrete magmatic composition resides in a separate chamber. The origin of each magma being any one or combination of processes which can generate a homogeneous to heterogeneous magma body.

4) Some combination of the above models.

For each member of the Timber Mountain Tuff, model number four is the most consistent with the data. The data are more consistent with a model where the various magmatic compositional groups as defined by the geochemical data (groups 1R to 3R and groups 1A to 3A; Figs. 4, 5a), have been generated by either different degrees of partial melting of a source rock or partial

melting of different source rocks. These magmas were brought together at some point in time to form a large volume magma body. The geochemical similarity between the Rainier Mesa Member and the Ammonia Tanks Member probably indicates that the bulk of the dominant volume magma in the Rainier Mesa Member was not erupted and remained to form the kernel for the Ammonia Tanks magmatic system. The presence of discrete layers however is equivocal with the current data but are inferred here to have initially existed. These magmas were probably then modified over time by fractional crystallization, assimilation and magma mixing. For the Rainier Mesa Member, it is also inferred that at least two magma chambers were in existance at the time of eruption; the dominant volume chamber containing geochemical groups 1R to 3R (trachyandesite to low-Nb, high silica rhyolite) and a much smaller chamber containing group 4R (high-Nb, high-silica rhyolite)(Figs. 4, 5a). For the Ammonia Tanks Member, it is unclear whether two separate chambers remained in existance although Th and Yb trace element data suggest that two high-silica rhyolites may have been present.

The discussion that follows attempts to outline how the various geochemical, mineralogical, geothermometric data and petrogenetic modelling are either consistent or inconsistent with models 1 thru 3 given above and the proposed model.

Geochemical Heterogeneity of the Timber Mountain Magmatic Systems

The gradual change in pumice and phenocryst geochemical data for both members of the Timber Mountain Tuff is consistent with the model of a magma chamber zoned from a basal trachyandesite to a roofward high-silica rhyolite. Complicating this model however, is the presence of gaps in the major and trace element data, best seen in variation plots with SiO_2 as one of the variables (Figs. 7, 9). Other elements such as Al_2O_3, MgO, P_2O_5, Sr, Sc, and Hf also have gaps in their range of concentrations (Figs. 7, 8, 9, 10). These gaps correspond to compositional changes between trachyandesitic and trachydacitic components (62 wt% to 64 wt% SiO_2), and, in the rhyolitic components (71 wt% to 74 wt% SiO_2).

Possible origins for these compositional gaps include sampling bias, changing rates of eruption (Spera, et al., 1986), the presence of a compositionally layered magma chamber, or, coeval eruption of unrelated magma bodies. With the current data however, it is equivocal as to whether or not compositional gaps were present in the parent magma chamber. A discussion of each of the possible origins for the clustering of data and presence of compositional gaps is given below.

In light of the detailed sampling performed for this study, it seems unlikely that sample bias was responsible

for the gaps in data. An intriguing, but not surprising observation made by Warren, et al., (1989), based on data from whole-rock tuff samples for the Paintbrush Tuff and Timber Mountain Tuff, indicates that lateral variations in the composition of the tuffs does occur. Warren, et al., (1989) note that the magmatic compositions present in some areas of the outflow sheets may not occur in other areas. Further detailed work with other stratigraphic sections will have to be done to resolve this potential problem.

The origin of compositional gaps in fossil volcanic systems due to the secular variation in eruption rate as discussed by Spera, et al., (1986) is a kinematic problem that volcanologists and igneous petrologists will in most cases be unable to reconstruct. To test this hypothesis, the eruption rate must be known or at least approximated; a problem that is currently difficult to resolve for historic eruptions, let alone 12 Ma old eruptions. However, the presence of compositional gaps in chemical data for ash-flow sheets of the Paintbrush Tuff and Timber Mountain Tuff may signify, as obvious as it seems, that there were fundamental physiochemical properties present in these magmatic systems that consistently allowed for compositional gaps to occur. If it is assumed that each magma chamber was continuously zoned with respect to composition and temperature, the options are: 1) it may have been fortuitous that changing rates of eruption

resulted in compositional gaps between the trachydacitic or quartz latitic magma and upper level rhyolites in each of the ash-flow sheets, 2) it may be a fundamental property of the eruption of a compositionally layered magmatic system, or 3) coeval eruption of multiple magma bodies. If eruption rate variation was responsible for the gaps, then the controlling factor in the rate of eruption would most likely be a function of melt viscosity, density and/or volatile content where a rapid increase or decrease in these parameters would have at least temporarily sped up or slowed down chamber evacuation. This explanation however, is in support of compositional discontinuities; the very argument Spera, et al., (1986) wish to discount. More detailed work needs to be done on this phenomena.

Structural controls such as chamber morphology, lateral compositional variations in the magma body, or, trapdoor subsidence may also lead to differential sampling of the magma chamber upon eruption (cf. Warren, et al., 1989). It would be geologically reasonable to assume that some, if not all, of the above mechanisms were acting to some degree during eruption of the Paintbrush Tuff and Timber Mountain Tuff. The question remains as to the degree of effectiveness of each factor in creating potential compositional gaps. It would still seem somewhat fortuitous however that compositional gaps

continually appear in the major ash-flow sheets of the SWNVF (Schuraytz, et al., 1989; Flood, et al., 1989a) and in other ash-flow tuffs from around the world (see Figure 1, Hildreth, 1981) at roughly the same magmatic compositional interval if some mechanism other than the presence of a layered magma body, or multiple magma bodies, were operating.

In light of the modelling of Spera, et al., (1986), there is no data to support or reject the generation of compositional gaps by eruption kinetics for the Timber Mountain system. In addition, if the experimental work of Blake (1981) and Blake and Ivey (1986) on magma withdrawal is even partially correct, then once again it becomes difficult to explain away the absence of intermediate magma compositions (see eruption dynamics discussion). Based only on the geochemical data then, a layered magmatic system and/or multiple-bodied magmatic system may have existed for the Timber Mountain system, as that of the Topopah Spring Tuff parental magma chamber (Schuraytz, et al., 1986, 1989).

Mineralogical Variations

Mineralogical data in support of magma chamber compositional gaps are again equivocal. Modal phenocryst data for both members of the Timber Mountain tuff reveal a sharp drop in phenocryst modal percentages in pumice

fragments (25% DRE (dense rock equivalent) to 10% DRE) from approximately 67 wt% SiO_2 to 70 wt% whole-pumice SiO_2 respectively (Table 2). This corresponds directly with the geochemical data gap between the trachydacitic and rhyolitic pumice fragment compositions (Figs. 7, 9). Also occurring in both members at approximately 64 wt% SiO_2 is a significant decrease in phenocryst content from approximately 23% DRE to 16% DRE which again corresponds to a minor geochemical gap (Table 2; Figs. 7, 9).

Histograms of phenocryst compositions for both members of the Timber Mountain Tuff do not however reveal distinct bimodal or polymodal distributions in composition like those observed in the Topopah Spring Member of the Paintbrush Tuff (Schuraytz, et al., 1986, 1989). The bimodal distribution in biotite compositions in the Topopah Spring Tuff was used by these workers as one line of evidence to infer the presence of a compositional interface between quartz latitic and rhyolitic magmas in the Paintbrush Tuff magmatic system.

Examination of stacked histograms of the Mg# or selected elements (those which have minimal scatter) versus increasing magmatic evolution for both members of the Timber Mountain Tuff reveals curvilinear trends in the data from the most mafic pumice fragment to most evolved pumice fragment (cf. Figs. 23, 25, 32). There does not appear to be any indication of sharp compositional breaks

in any of the plots of this type with the exception of hornblende in the Rainier Mesa Member where the CaO and Al_2O_3 histograms for hornblende indicate two distinct compositions (Figs. 33, 34). Thus, variable phenocryst composition as a function of increasing magmatic evolution does not lend unequivocal support to a layered magma chamber model. Alternatively, the TiO_2 composite histograms for both the Rainier Mesa Member and Ammonia Tanks Member could be interpreted as showing bimodal to trimodal phenocryst populations for each member respectively (Figs. 24, 26). Bimodal distributions within the glass data (SiO_2 and Al_2O_3) for the Rainier Mesa Member and Ammonia Tanks Member cannot be used to either support or reject the presence of compositional gaps in the magma chamber (Figs. 7, 9, 39, 40). Although the composite histograms again show even better defined modes, there are samples with data that are transitional in concentration between the modes. Thus depending upon the bias of the observer, a case may be made for either a layered system, or, for a zoned system.

Based on the geochemical and mineralogical data for the Timber Mountain Tuff, there is no a priori evidence for distinct compositional magmatic interfaces in the parental magma chamber(s). Much of the data is consistent with the interpretation that some sort of magmatic discontinuities, as defined by geochemical compositional

gaps and potentially bimodal phenocryst data, did exist in the parental chamber(s).

Geothermometric Considerations

The temperature distribution for the Rainier Mesa Member and Ammonia Tanks Member is consistent with the model of a zoned magma chamber in which the hotter, more mafic magma is overlain by cooler, progressively more silicic magma (Smith, 1979; Hildreth, 1981)(Fig. 43). The thermal gradient in the Rainier Mesa magmatic system from the trachyandesite to the high-silica rhyolite appears to have been lower than the thermal gradient in the Ammonia Tanks magmatic system (Fig. 43). No evidence exists for sharp thermal interfaces within the Rainier Mesa Member magmatic system. Fe-Ti oxide temperature and oxygen fugacity data for the Rainier Mesa Member can be interpreted however, to suggest that a separate magma chamber existed for the high-Nb, high-silica rhyolite. On Figures 43 and 44, the two high-Nb, high-silica rhyolite samples plot well away from the dominant trend of the Rainier Mesa Member data. Although these data lie within the Ammonia Tanks Member data field, the pumice fragments from which the data were derived cannot represent xenoliths from the Ammonia Tanks Member due to the stratigraphic relationship of the two members, nor can they be of Ammonia Tanks affinity based on their chemical

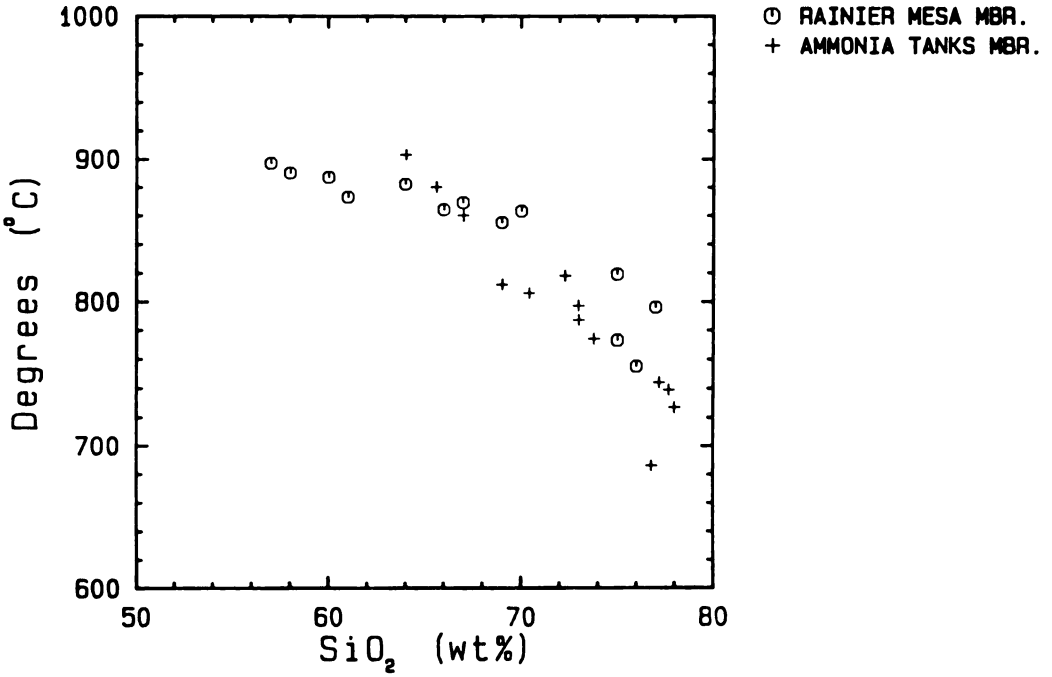


Figure 43. SiO_2 versus temperature for the Timber Mountain Tuff.

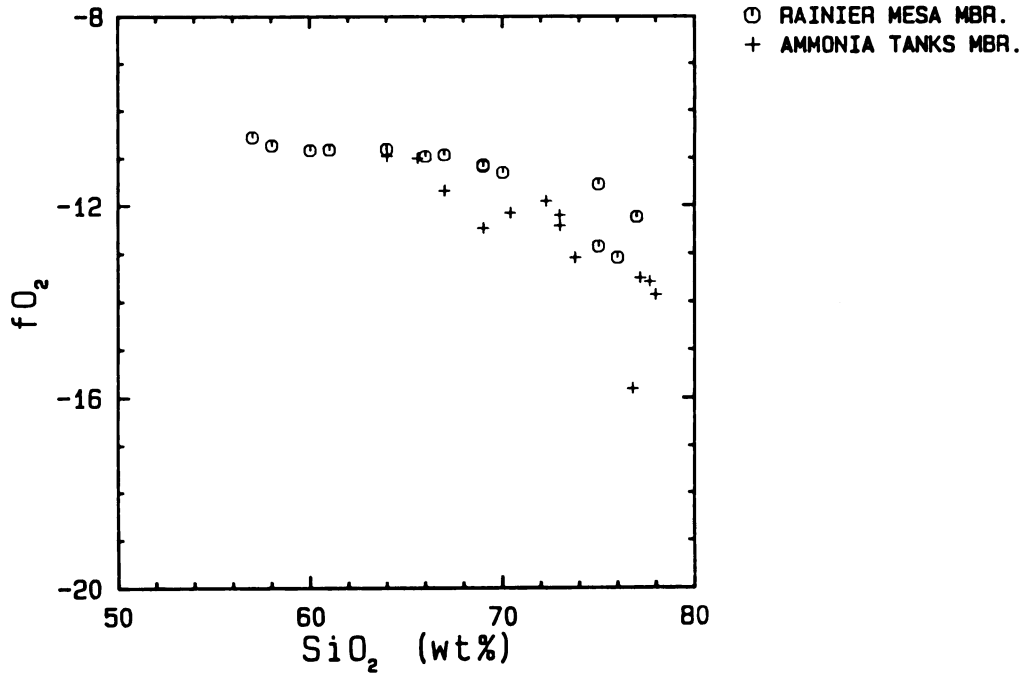


Figure 44. SiO_2 versus $-fO_2$ for the Timber Mountain Tuff.

and mineralogical compositions. There are several implications to this point. First, the lack of an obvious thermal interface implies that the magma types present in the Rainier Mesa Member system immediately prior to the eruptive event, were not thermally distinct magmas brought together immediately preceding eruption. Secondly, if the magma types present in the chamber did originate as thermally discrete magma bodies, and were subsequently brought together prior to eruption, then enough time must have elapsed for the equilibration of thermal discontinuities and for the development of a smooth thermal profile via conduction and/or convection of the excess heat. Additionally, re-equilibration of the magnetite/ilmenite compositions should have occurred. Finally, in light of models in which magmatic injection is called upon to initiate eruption (cf. Hildreth, 1981, 1983), it is possible that a new, thermally distinct magma was injected into the system prior to eruption, and may have even been the driving force for the eruption. This type of phenomena may have been recorded in the Ammonia Tanks Member as the trachydacite to trachyandesite temperature gradient is steeper than that for the Rainier Mesa Member. However, either this magma was not tapped during the eruption or it was volumetrically insignificant within the Rainier Mesa or Ammonia Tanks magmatic systems. Only a small amount of evidence for a uniquely basaltic

component exists within the Rainier Mesa Member and occurs as a few mafic glass and phenocryst analyses in samples R8-25 and R11-5 (Figs. 39, 40). Warren, et al., (1989) support this observation.

In the Ammonia Tanks Member magmatic system, there is no evidence for the presence of thermal interfaces or separate magma bodies. Complicating this evaluation however is the lack of thermal data for the trachyandesite magmatic component in the Ammonia Tanks Member due to the lack of ilmenite in the mafic pumice samples.

Oxygen Fugacity and Sphene-Ilmenite Stability

A comparison of the oxygen fugacity for the Rainier Mesa and Ammonia Tanks Members must be done with caution as no data for the trachyandesite pumice are available for the Ammonia Tanks Member due to the absence of ilmenite. Data plotted on a SiO_2 vs. log fO_2 diagram (Fig. 44) are indicative of a lower oxygen fugacity for the rhyolite to trachydacite of the Ammonia Tanks Member as compared to the Rainier Mesa Member. Trachyandesite magmas of the Ammonia Tanks Member on the other hand, may have had a *higher* oxygen fugacity than the trachyandesite of the Rainier Mesa Member.

Lipman (1971), in his work on compositionally zoned ash-flow sheets of the Southwestern Nevada Volcanic Field, interpreted the presence of sphene in samples of the Tiva

Canyon Member and Ammonia Tanks Member, and the absence of sphene in samples of the Topopah Spring Member and Rainier Mesa Member, as due to oxygen fugacity variations within the respective magmatic systems (Topopah Spring Member and Tiva Canyon Member = Paintbrush Tuff). His interpretations were based on previous studies of the sphene-ilmenite phase relationships by Verhoogen (1962) and Wones (1966), and on the sphene-ilmenite thermodynamic calculations of Carmichael and Nicholls (1967), and Smith (1970). The sphene-ilmenite reaction proposed by the above workers is:

$$3CaTiSiO_5 + Fe_3O_4 = 3FeTiO_3 + 3CaSiO_3 + 0.5O_2$$

where excess oxygen reacts with ilmenite and pyroxene to form sphene and Ti-poor magnetite. More recently, Haggerty (1976) in a review of opaque mineral oxides in terrestrial igneous rocks, citing studies by Carmichael and co-workers, summarizes their work by noting that not only is the oxygen fugacity important for the phase transition, but that the silica activity must also be taken into account (see references of Haggerty, (1976) pgs. 169-172). Haggerty (1976) summarizes the problem by stating that;

> ". . . the demise of ilmenite and the depletion of Ti in Mt_{ss} can be related to $aSiO_2$ and fO_2. If $aSiO_2$ is considered alone, Mt_{ss} + perovskite will form in preference to Mt_{ss} + sphene at low values of $aSiO_2$ ($CaSiTiO_5 = CaTiO_3 + SiO_2$). If fO_2 is considered in addition, high fO_2 and high $aSiO_2$ will favor sphene; lower fO_2 and lower $aSiO_2$ will favor perovskite . . . i.e., for any given fO_2 sphene or perovskite are dependent on $aSiO_2$."

For the Timber Mountain Tuff however, the data are antithetic to Haggerty's summary. Based upon the data presented in Figure 44, the Rainier Mesa Member has a higher oxygen fugacity than that the Ammonia Tanks Member at any given composition. Theoretically then, the Rainier Mesa Member should be sphene bearing, not the Ammonia Tanks Member. For the Timber Mountain magmatic system then, there must be additional controlling factors at work besides oxygen fugacity and silica activity which controlled the crystallization of sphene as opposed to ilmenite.

In conclusion, geothermometric and oxygen fugacity data for the Timber Mountain Tuff does not support an interpretation for a layered magmatic system in either member. The data for the Rainier Mesa Member are consistent however, with at least a two chamber model in which the high-Nb, high-silica rhyolite is separated from the dominant volume magma body. The data for the Ammonia Tanks Member are consistent with a single magma chamber model.

Geobarometry

Based on the distribution of data in Figure 42, it could be inferred that the magmas of the Timber Mountain system resided in a mid-crustal chamber at a depth between 13.2 and 21 km (4.4 and 7 kbars respectively). The anomalous data points which occur at 1.7, 3.0, and 8.9 kbars may reflect either poorly constrained phenocryst compositions, or, phenocrysts which equilibrated under different geobarometric conditions. The latter interpretation seems unlikely however and it is inferred here that the phenocryst compositions are suspect. It should be emphasized that interpretation of the data in Figure 41b is speculative at best in light of the small number of data points, error associated with the pressure estimates, and discordance between the feldspar and Fe-Ti oxide temperature calculations.

The calculated pressures of formation based on the hornblende/quartz geobarometer of Hammarstrom and Zen (1986) (4.8 to 3.9 kbars) are relatively consistent however with the pressures derived from coexisting feldspar/Fe-Ti oxide estimates (4.5 kb to 8.9 kb, avg = 6.3 kb for Fe-Ti oxide/co-existing feldspar)(Fig. 41). Calibration of the Hammarstrom and Zen (1986) hornblende geobarometer by Hollister, et al., (1987) and experimental

studies on the Fish Canyon Tuff by Johnson and Rutherford (1989) indicate an accuracy of +/- 1.0 kbar.

PETROGENESIS

Overview

Fractional crystallization and magma mixing are used in the following section to evaluate possible origins of the compositional range of the Rainier Mesa Member and Ammonia Tanks Member of the Timber Mountain Tuff.

All of the major and most of the trace element data (Figs. 7, 8, 9, 10) for both members of the Timber Mountain Tuff exhibit a systematic compositional variation from approximately 58 wt% SiO_2 to 78 wt% SiO_2 with significant SiO_2 gaps occurring between the trachydacite and rhyolite of each member. The span of compositions could be the result of one or more processes acting on the magmatic system, for example; fractional crystallization of parental trachyandesite, mixing of felsic and mafic magmas, assimilation of country rock, and/or different degrees of partial melting of crustal rock. Testing of these processes however is restricted to fractional crystallization, magma mixing, and partial melting due to the availability of necessary data. Whole pumice and phenocryst analyses for the Timber Mountain Tuff permitted investigation of fractional crystallization and magma mixing models. Rigorous quantitative assimilation and

partial melting models however could not be tested due to the lack of geochemical data on the composition of potential crustal source rocks in the Timber Mountain region. Geochemical data from this study and new Nd isotopic data from Tegtmeyer, et al., (1989) are used to qualitatively evaluate the role of partial melting and assimilation in the origin of the Timber Mountain magmatic system.

Fractional Crystallization

Rainier Mesa Member

Major-element multiple linear regression modelling was used to determine whether fractional crystallization could produce the observed compositional change from trachyandesite to either the low-Nb or high-Nb, high-silica rhyolite in the Rainier Mesa Member. Testing of Rayleigh fractionation using the trace element data was also performed to either support or reject the major element regressions.

Major-element multiple linear regression was done in a stepwise fashion with each model spanning a range of 4 to 7 wt% SiO_2. Stepwise modelling was particularly important for determining if crystal fractionation could account not only for the increasing magmatic evolution from trachyandesite to high-silica rhyolite but also whether or not the SiO_2 gaps observed in the data set

represented compositional interfaces within the magma chamber. If a layered magmatic system existed in the chamber, then a reasonable fractional crystallization model would be unlikely as the magmas at the interface should not be related by crystal fractionation. If the SiO_2 gaps do not prevent modelling of fractional crystallization then perhaps some other process such as sample bias, eruption dynamics, or magmatic fluid dynamics is needed to explain the SiO_2 gaps.

A total of seven models were tested for the Rainier Mesa Member (Table 6). Models 1 thru 4 consecutively evaluated the change in composition from the least evolved magmatic composition (sample R21-13, 57 wt% SiO_2) to a low-Nb rhyolite at 70 wt% SiO_2 (sample R18-2). Models 5 thru 7 were used to evaluate the formation of the high-Nb, high-silica rhyolite (sample R11-7, 78 wt% SiO_2) from the low-silica rhyolite, and, from the trachyandesite. The major-element regression models were performed using the compositions of whole-pumice samples and their corresponding phenocryst assemblages. These data are presented in Table 7. The least evolved pumice sample (sample R21-13) was used as the starting composition and was regressed against a slightly more evolved pumice sample using various combinations of major phenocryst phases present in the parental pumice fragment (trace phenocryst phases such as allanite, apatite and chevkinite

TABLE 6. Rainier Mesa Member: Major-element Multiple Linear Regression Models

---

Model 1

R21-13 = -0.185 +0.755 R11-5 + 0.0641 PLG + 0.173 HRN + 0.012 MT + 0.00856 ILM

R^2 = 100 SS = 0.09

Model 2

R11-5 = -0.202 + 0.806 R23-26 + 0.102 PLG + 0.0276 BIO + 0.0583 CPX + 0.0170 MT + 0.00759 ILM

R^2 = 100 SS = 0.15

Model 3

R23-26 = 0.0039 + 0.504 R23-13 + 0.259 PLG + 0.175 KSP + 0.0191 BIO + 0.0280 CPX + 0.0152 MT + 0.00180 ILM

R^2 = 100 SS = 0.04

Model 4

R23-13 = 0.481 + 0.777 R18-2 + 0.0864 PLG + 0.0852 KSP + 0.0056 CPX + 0.0130 MT - 0.0078 ILM

R^2 = 100 SS = 0.15

Model 5

R23-13 = 0.0163 + 0.638 R18-16 + 0.164 PLG + 0.147 KSP + 0.0418 BIO + 0.00769 MT + 0.0001 ILM

R^2 = 100 SS = 0.00

Model 6

R23-13 = 0.107 + 0.726 R11-7 + 0.184 PLG + 0.063 KSP + 0.027 BIO + 0.011 MT

R^2 =100 SS = 0.09

Model 7

R18-16 = 0.051 + 0.861 R11-7 + 0.045 PLG + 0.111 QTZ + 0.002 MT

R^2 = 100 SS = 0.10

Table 7. Phenocryst and pumice block compositions used in fractional crystallization modelling for the Rainier Mesa Member of the Timber Mountain Tuff.

Sample	Mineral	ID #	SiO_2	Al_2O_3	FeO	MgO	CaO	Na_2O	K_2O	TiO_2	MnO	P_2O_5	BaO	NiO	Cr_2O_3
R21-13	PLG	1	55.56	28.57	0.30	0.00	9.51	5.55	0.40	0.03	0.04	0	0.04	-	-
57%SiO_2	BIO	2	37.65	14.61	15.73	14.60	0.04	0.68	9.32	6.01	0.34	0	0.59	0.43	-
		3	37.95	15.61	13.68	15.62	0.05	1.02	8.71	5.69	0.20	0	1.44	0.02	-
	HRN	4	43.61	13.00	12.61	14.00	9.88	2.64	0.65	3.29	0.30	-	0	0	-
	MT_1	5	-	3.45	83.63	2.29	-	-	-	9.82	0.81	-	-	0	0.0
	MT_2	6	-	2.92	84.22	2.68	-	-	-	9.14	1.04	-	-	-	0.0
	ILM	7	-	0.35	56.82	3.05	-	-	-	39.02	0.76	-	-	-	0.0
	Glass	8	70.00	16.42	1.44	0.50	1.41	4.23	5.18	0.45	0.11	0.09	0.17	-	-
	Pumice	9	56.80	17.24	7.25	3.47	5.86	3.66	3.23	1.59	0.14	0.74	1365	0	7.5
R11-5	PLG	10	53.60	29.88	0	0.02	10.55	5.26	0.44	0.05	0.07	0	0.14	-	-
61%SiO_2		11	55.69	28.65	0	0.03	9.12	5.74	0.53	0.07	0.04	0	0.13	-	-
	KSP	12	63.00	20.35	0	0.22	0.66	4.25	9.60	0.03	0	0.02	1.86	-	-
	BIO	13	38.41	14.61	15.09	14.87	0.07	0.66	8.81	6.37	0.25	-	0.86	0	-
	HRN	14	43.49	11.46	12.57	13.55	11.10	2.66	1.01	3.57	0.42	-	0.15	0	-
	CPX	15	52.41	1.70	8.11	13.92	22.28	0.55	0	0.42	0.60	-	0	0	-
	MT	16	-	2.36	86.41	1.64	-	-	-	8.33	1.23	-	-	-	0.04
	ILM	17	-	0.29	56.92	1.79	-	-	-	39.76	1.25	-	-	-	0.0
	Glass	18	70.70	16.79	0.97	0.25	1.06	4.36	5.25	0.35	0.08	0.05	0.14	-	-
	Pumice	19	60.92	17.99	4.98	1.84	4.34	4.03	4.30	0.93	0.12	0.56	1827	0	0
R23-26	PLG	20	60.83	24.28	0.37	0	4.93	7.70	1.65	0.03	0	0.06	0.16	-	-
64%SiO_2	KSP	21	63.15	20.35	0.14	0.01	0.71	4.18	9.69	0.05	0.00	0.00	1.71	-	-
	BIO	22	37.16	15.53	15.58	14.03	0	0.51	8.93	6.45	0.25	-	1.73	0.03	-
	CPX	23	52.54	1.37	8.41	14.42	21.43	0.67	0.02	0.31	0.84	-	0	0	-
	OPX	24	53.82	0.36	19.65	22.50	0.89	0.07	0	0.14	2.51	-	0.05	0	-
	MT_1	25	-	1.89	84.88	1.65	-	-	-	10.37	1.17	-	-	-	0.04
	MT_2	26	-	1.38	88.47	1.66	-	-	-	7.26	1.26	-	-	-	0.03
	ILM	27	-	0.32	55.73	2.05	-	-	-	40.86	1.04	-	-	-	0.00
	Glass	28	70.98	15.72	1.23	0.21	0.83	4.20	6.27	0.28	0.09	0.08	0.08	-	-
	Pumice	29	64.25	18.11	3.01	1.08	2.79	4.66	5.19	0.60	0.09	0.20	2883	0	8.5

Table 7. Continued.

Sample	Mineral	ID #	SiO_2	Al_2O_3	FeO	MgO	CaO	Na_2O	K_2O	TiO_2	MnO	P_2O_5	BaO	NiO	Cr_2O_3
R23-13	PLG	30	60.20	24.14	0.38	0.04	6.73	7.19	1.14	0.01	0.02	0.02	0.14	-	-
70%SiO_2		31	62.02	23.35	0.27	0.02	4.40	7.94	1.91	0	0.06	0	0.04	-	-
	KSP	32	63.87	20.04	0.52	0	0.45	4.46	10.06	0.04	0.04	0.04	0.47	-	-
	BIO	33	38.24	15.07	15.11	14.49	0.03	0.66	9.41	5.85	0.34	-	0.75	0.03	-
	HRN	34	42.75	12.47	12.30	13.58	11.32	2.58	0.93	3.64	0.33	-	0.08	0.02	-
	CPX	35	53.16	1.04	8.63	13.85	21.42	0.60	0	0.22	1.06	-	0	0.01	-
	OPX	36	53.87	0.39	20.10	22.07	0.95	0	0.01	0.09	2.50	-	0.2	0	-
	MT_1	37	-	1.51	87.61	1.06	-	-	-	8.36	1.47	-	-	-	0.0
	MT_2	38	-	2.36	85.13	1.49	-	-	-	10.16	0.87	-	-	-	0.0
	ICM	39	-	0.24	57.26	1.99	-	-	-	39.40	1.11	-	-	-	0.0
	Glass	40	74.35	14.45	0.60	0.06	0.49	3.54	5.91	0.29	0.02	0.17	0.11	-	-
	Pumice	41	70.03	15.64	1.92	0.76	1.52	3.83	5.67	0.43	0.07	0.12	1271	0	9.7
R18-2	PLG	42	62.75	22.82	0.59	0.01	3.66	8.93	1.16	0.02	0.02	0.05	0	-	-
77%SiO_2	KSP	43	65.69	18.97	0.08	0.04	0.24	4.08	10.78	0.04	0	0	0.08	-	-
	BIO	44	39.21	14.33	16.10	14.68	0.02	0.48	9.36	4.19	0.45	-	1.17	0	-
	MT	45	-	1.24	89.88	0.81	-	-	-	6.29	1.79	-	-	-	0.0
	ILM	46	-	0.10	51.97	1.70	-	-	-	43.79	2.43	-	-	-	0.0
	Glass	47	76.78	13.20	0.24	0.0	0.51	3.16	5.93	0.07	0.00	0.07	0.03	-	-
	Pumice	48	75.17	14.85	0.80	0.50	0.53	2.65	5.26	0.17	0.05	0.02	0	0	0
R18-16	PLG	49	62.76	23.21	0.23	0	3.96	8.49	1.25	0	0.03	0	0.07	-	-
77%SiO_2	KSP	50	64.87	19.64	0.07	0	0.30	4.08	10.98	0	0	0	0.05	-	-
	BIO	51	41.07	14.38	16.34	14.00	0.07	0.47	8.77	4.49	0.42	-	0	0	-
	MT	52	-	1.39	88.30	0.96	-	-	-	6.31	3.02	-	-	-	0.02
	IL	53	-	0.10	53.54	1.46				42.46	2.47	-	-	-	0.0
	Glass	54	76.79	12.87	0.44	0.04	0.51	3.50	5.66	0.10	0.05	0.04	0	-	-
	Pumice	55	76.98	12.65	0.73	0.18	0.59	2.99	5.65	0.16	0.05	0.02	0	0	0
R11-7	PLG	56	64.79	22.51	0.13	0.01	2.73	9.53	1.34	0	0	0.11	0.03	0	0
76.06%SiO_2	KSP	57	65.46	19.53	0	0	0.22	4.28	10.73	0	0.01	0	0	0	0
	QTZ	58	92.46	3.87	0.12	0.07	0.42	1.30	0.96	0.02	0	0	0	0	0
	BIO	59	37.23	13.42	15.55	13.85	0.18	0.49	8.10	3.86	0.64	-	0.02	0.02	-
	MT	60	-	1.19	84.46	0.52	-	-	-	4.91	1.93	-	-	-	0
	IL	61	-	0.06	47.31	1.16	-	-	-	42.89	3.94	-	-	-	0
	HRN	62	41.68	11.92	12.60	12.90	11.19	2.62	0.80	3.63	0.37	-	0	0	0
	Glass	63	74.15	12.62	0.15	0.03	0.37	2.81	6.05	0.12	0.07	0.07	0	-	-
	Pumice	64	74.08	12.98	0.53	0.27	0.43	2.59	6.24	0.11	0.10	0.02	0	0.01	0

were not used in the models as these phases were not chemically analyzed with the microprobe, and, because these phases have little affect on the major element regression).

For each model, the selection of the best fit was based on several criteria: 1) a correlation coefficient (R^2) of 0.99 to 1.0 , 2) a sum of the square of the residuals (SS) less than 0.3 , 3) a phenocryst assemblage similar to that of the parental pumice fragment and 4) geologically reasonable percentages of each fractionating phase. For each model, several phenocryst assemblages were geologically viable and produced reasonable statistical results. These best fit models were then rigorously tested by using the Rayleigh trace element concentrations for each regression assemblage.

Using the major element linear regression technique, it was found that the entire compositional range observed in the Rainier Mesa Member could be modelled by pure crystal fractionation. Each major element regression was successful at producing a statistically and geologically reasonable fractionating mineral assemblage. These best fit models and their statistics are presented in Table 6.

Plagioclase and magnetite are consistently present as fractionating phases while potassium feldspar, biotite, clinopyroxene, and ilmenite are commonly present.

Hornblende and quartz are fractionated only in the first and last steps respectively, but are the dominant fractionating phase in each of these steps (Table 6).

Of interest in these models is the apparent fractionation of hornblende before clinopyroxene. Rose (1988) notes a similar effect for the Ammonia Tanks Member but discounts hornblende as an initial fractionating phase due to the limited occurrence and paucity of hornblende in the Ammonia Tanks Member. Additionally, many of the hornblende grains in the Ammonia Tanks Member have resorption textures. The Rainier Mesa Member is different in that hornblende is ubiquitous in pumice samples over a considerable range of whole pumice compositions (Table 2). Clinopyroxene was tested as a fractionating phase in model 1 but consistently resulted in very poor statistics (SS > 2.0) and a negative coefficient (fractionated from daughter composition).

Trace element testing provides a more rigorous test of the major element linear regression models. For this study Rayleigh fractionation was assumed. The Rayleigh fractionation equation taken from Cox, et al., (1979) is given below:

$$C_D = C_P F^{(D-1)}$$

where: C_D = trace element conc. in daughter magma
C_P = trace element conc. in parent magma
F = fraction of melt remaining
D = bulk distribution coefficient

Rayleigh fractionation assumes perhaps somewhat ideally, but not unrealistically, that the phenocryst phases fractionated are completely removed from the system (or contact with the melt). Thus phenocrysts will not undergo any re-equilibration as they pass through magma of slightly to significantly different compositions on the way to their final resting place. Some analyzed trace elements for the Rainier Mesa Member behave compatibly with increasing SiO_2 and thus are unusable for fractionation modelling. With the Rainier Mesa Member spanning such a large compositional range it was unlikely to expect most elements to be incompatible through the complete magmatic compositional range. Thus trace elements were chosen if they exhibited incompatible behavior for at least a portion of the compositional range. Only Rb appears to steadily increase in concentration continuously across the entire compositional span of the Rainier Mesa Member (Fig. 8). Rb however, does not behave as a perfectly incompatible element as the final concentration in the high-silica rhyolite should be 609 ppm as compared to 168 ppm in sample R11-7 (high-Nb, high-silica rhyolite) based on Rayleigh fractionation (an initial concentration of 67 ppm (C_p) in the least evolved pumice sample R21-13, a residual melt volume of 11% (F), and a bulk D of 0.0). Rb in the Rainier Mesa Member is

most likely buffered by the removal of sanidine and biotite ($K_{d\ max}$ = 2.4 to 5.3 respectively). Thus, the trace elements ultimately chosen for testing were Th, Sc, Rb, La, Ce, Yb and Lu.

Ideally, distribution coefficients should be analytically determined for each individual magmatic system as elemental distribution is directly controlled by temperature, pressure, volatile partial pressure, and chemical concentrations (cf. Greenland, 1970; Hart and Allegre, 1980). For the Timber Mountain Tuff, phenocryst abundance and sample preparation time proved too restrictive to permit for individual K_d analyses. Thus distribution coefficients for this study were compiled from Arth and Hanson (1975), Arth (1976), Henderson (1982), Mahood and Hildreth (1983), Hyndman (1985), Nash and Crecraft (1985), Bacon, et al., (1987), and Spell and Kyle (1989). Distribution coefficients were selected from these sources with consideration given to choosing K_d values for appropriate magmatic compositions and to ensure that the maximum K_d range of an element was noted for a given magmatic composition. For Nb and Y however, K_d values for the feldspars, magnetite and ilmenite are only available for high-silica rhyolites and thus were used by default for the more mafic fractionation models. The K_d values used in this study are presented in Table 8.

Table 8. Distribution coefficients used for fractional crystallization modelling in the Rainier Mesa Member of the Timber Mountain Tuff.

	Magma Composition			
	Andesite	Dacite		Rhyolite
Plagioclase				
Th			0.01 - 0.14	
Sc			0.01 - 0.06	
Rb	0.4	0.048	0.016 - 0.46	0.041
Nb	--[1]	--		--
Y	0.26		0.04 - 0.29	
La	0.02 - 0.3		0.24 - 0.49	
Ce	0.085 - 0.24	0.24	0.11 - 0.40	0.27
Yb	0.02 - 0.031	0.077	0.02 - 0.91	
Lu	0.032	0.062	0.03 - 1.4	0.046
Sanidine				
Th			0.01 - 0.03	
Sc			0.01 - 0.06	
Rb			0.11 - 2.4	
Nb	--	--		--
Y	--	--		--
La			0.037 - 0.11	
Ce			0.02 - 0.10	
Yb			0.005 - 0.04	
Lu			0.006 - 0.07	
Quartz				
Th				0.006 - 0.010
Sc				0.010 - 0.015
Rb				0.012 - 0.016
Nb	--	--		--
Y	--	--		--
La				0.012 - 0.018
Ce				0.006 - 0.018
Yb				0.012 - 0.025
Lu				0.002 - 0.024
Biotite				
Th			0.27 - 2.0	
Sc			4.9 - 20.0	
Rb		3.26	2.24 - 5.3	2.24
Nb			4.0 - 9.5	
Y			1.0 - 1.4	
La			0.39 - 15.1	
Ce		0.037	0.037 - 11.0	0.31
Yb		0.43	0.18 - 3.0	0.18
Lu		0.19	0.19 - 3.4	0.33

[1] Distribution coefficients currently not available.

Table 8. Continued.

	Magma Composition			
	Andesite	Dacite		Rhyolite
Hornblende				
Th	0.18		0.13 - 0.22	
Sc	12		2.1 - 20	
Rb	0.05 - 0.5	0.3	0.0077 - 0.014	
Nb	0.8		1.3	4.0
Y	1.0		2.5	6.0
La	0.05 - 0.39		0.34 - 0.49	
Ce	0.2 - 0.63		0.68 - 1.77	1.52
Yb	0.25 - 2.1	4.89	1.3 - 8.38	7.45 - 9
Lu	0.43 - 2.3	4.53	1.4 - 6.3	5.5
Clinopyroxene				
Th			0.01 - 6.56	
Sc	18		18 - 96	
Rb	0.4		0.003 - 0.5	0.032
Nb		0.3	0.3 - 0.8	0.8
Y		1.5	1.5 - 4.0	4.0
La	0.26		0.45 - 13.1	
Ce	0.44		0.5 - 11.3	0.5
Yb	1.8		1.5 - 11.6	1.5
Lu	2.1		2.0 - 10.7	1.54
Orthopyroxene				
Th			0.11 - 0.15	
Sc	4.5		7.1 - 9.8	
Rb	0.045 - 0.02	--		0.01 - 0.04
Nb	--	--		--
Y			<1.1	
La	0.22		0.34 - 0.74	<0.4
Ce	0.28		0.45 - 0.89	<0.4
Yb	0.64 - 0.77		0.90 - 1.4	
Lu	0.71		1.0 - 1.5	
Magnetite				
Th			0.04 - 0.32	
Sc			1.5 - 15.6	
Rb				0.07 - 0.7
Nb	--	--		--
Y	--	--		--
La			0.24 - 1.9	
Ce			0.28 - 2.7	
Yb			0.20 - 2.2	
Lu			0.20 - 1.5	

Table 8. Continued.

	Magma Composition		
	Andesite	Dacite	Rhyolite
Ilmenite			
Th		0.43 - 7.5	
Sc		5.9 - 18.5	
Rb			0.07 - 0.7
Nb	--	--	--
Y	--	--	--
La		1.31 - 32	
Ce		1.19 - 26	
Yb		0.55 - 4.1	
Lu		0.74 - 3.6	
Apatite			
Th	--	--	--
Sc		0.22	
Rb		0.0	
Nb		0.1	
Y		20 - 40	
La		8.6 - 28.2	
Ce		18 - 52	
Yb		13 - 37	
Lu		11.2 - 30.2	
Zircon			
Th		62.4 - 91.2	
Sc		60 - 77	
Rb	--	--	--
Nb	--	--	--
Y	--	--	--
La		1.14 - 26.6	
Ce		1.17 - 23.5	
Yb		128 - 564	
Lu		196 - 689	

If crystal fractionation of the parental magma was the method by which the more evolved daughter magma formed, then the predicted and actual trace element concentrations should match for the daughter magma. Review of the data in Table 9 reveals that for all of the models with the exception of model 4, relatively few of the actual trace element concentrations coincided with the predicted results in any given model. In model 4 (rhyolite (70 wt% SiO_2) to form high-silica rhyolite (75 wt% SiO_2)) three of the four incompatible trace elements (Th, Rb and Lu) match well, while Yb is close to the acceptable concentration range. None of the predicted incompatible trace element concentrations in model 6 however encompassed the actual daughter magma concentrations. On this basis, model 6 is unequivocally rejected.

Models 1-3, 5 and 7 are equivocal as only one or two of the predicted element concentration ranges encompasses the actual concentration. This may be due to the use of K_d's from other chemically and thermodynamically distinct magmatic systems, the fractionation of significant quantities of trace phases such as chevkinite, monazite or sphene, or, may in turn be used as evidence to suggest that crystal fractionation was not the dominant process responsible for the observed compositional diversity in the Rainier Mesa Member. At this time, it is not clear

Table 9. Rayleigh fractionation modelling for the Rainier Mesa Member of the Timber Mountain Tuff.

Sample #	R21-13 - R11-5	R11-5 - R23-26	R23-26 - R23-13	R23-13 - R18-2	R23-13 - R18-16	R23-13 - R11-7	R18-16 - R11-7
SiO_2 %	57 - 61 SiO_2	61 - 64 SiO_2	64 - 70 SiO_2	70 - 75 SiO_2	70 - 77 SiO_2	70 - 76 SiO_2	77 - 76 SiO_2
Model #	1	2	3	4	5	6	7
Th	16.19 - 1.71 18.84	22.66 - 21.38 21.80 23.31 - 21.04	43.26 - 35.91 25.23	37.02 - 33.31 33.72 37.16 - 35.58	39.28 - 35.50 31.47	34.64 - 33.82 21.11	36.54 - 36.51 21.11
Sc	9.38 - 8.64 9.43	9.31 - 8.75 5.26 9.07 - 7.70	6.75 - 1.02 4.13	4.75 - 1.64 1.61 5.12 - 1.87	5.84 - 4.13 3.0	5.42 - 4.50 4.10	3.48 - 3.47 4.10
Rb	88.43 - 86.07 123.12	146.85 - 146.17 76.66 148.63 - 145.42	146.36 - 96.36 113.07	164.87 - 137.12 155.22 168.73 - 135.17	168.68 - 131.74 144.77	152.24 - 137.46 238.42	168.09 - 167.54 238.42
Nb	- 16.15 - 13.14	15.55 - 15.49 11.98 15.61 - 15.02	21.56 - 19.87 13.42	19.28 - 19.17 20.42 19.18 - 17.38	19.14 - 17.26 11.12	17.62 - 16.79 31.16	12.90 31.16
Y	- 38.97 - 22.97	26.99 - 26.49 13.26 27.56 - 26.68	24.74 - 22.30 14.04	20.02 - 19.26 22.56 21.07 - 20.15	21.32 - 20.77 18.17	19.02 - 18.68 32.17	21.09 - 21.06 32.17
La	113.87 - 102.23 96.04	115.72 - 111.27 101.15 118.36 - 104.06	189.41 - 109.16 80.68	116.25 - 90.58 31.40 121.97 - 81.40	122.87 - 89.06 36.68	109.01 - 93.78 23.67	42.52 - 42.42 23.67
Ce	201.42 - 182.92 190.55	227.87 - 220.77 173.35 234.03 - 207.72	334.19 - 207.58 143.67	208.13 - 167.63 79.44 220.81 - 159.20	221.97 - 201.26 85.23	196.25 - 173.55 60.34	98.90 - 98.62 60.34
Yb	2.99 - 2.69 3.23	3.83 - 3.75 1.83 3.91 - 3.79	3.52 - 2.30 1.40	2.01 - 1.69 2.13 2.15 - 1.75	2.18 - 1.92 2.01	1.92 - 1.76 2.21	2.33 - 2.32 2.21
Lu	0.55 - 0.49 0.48	0.57 - 0.56 0.39 0.58 - 0.57	0.74 - 0.46 0.28	0.40 - 0.34 0.33 0.43 - 0.34	0.44 - 0.37 0.25	0.38 - 0.34 0.28	0.29 - 0.29 0.28

how significant a role crystal fractionation played in producing the observed magmatic compositions. Preliminary data from phenocryst glass inclusion studies by Vogel (1991, unpublished data) indicate that the melt major element compositions match almost exactly with those of the glass composing the inclusion. This may be further evidence that fractional crystallization was not responsible for generating the wide range of magmatic compositions observed in the Timber Mountain system. Additional evidence against fractional crystallization comes from the recent work by Tegtmeyer, et al., (1989). These workers suggest that Nd isotope data indicate that up to 10% crustal assimilation may have occurred to modify the observed magmatic compositions.

Examination of the data plotted on the spidergrams in Figure 12b and enrichment diagram in Figure 13 reveals the consistent decrease in concentration in the more silicic magmas of all the trace elements plotted except for Rb, Th, K and Nb. The increase in Rb, Th, K and Nb is consistent with fractional crystallization as these elements may behave incompatibly with increasing magmatic evolution. The other trace elements are more compatible with the modal phenocryst phases present in the system, thus the decrease in concentration of these elements may reflect the formation and removal of phenocryst phases *within* the various magmatic groups (Figs. 4, 5a).

Ammonia Tanks Member

Fractionation and magma mixing were tested by Rose (1988) as possible processes by which the compositional range of the Ammonia Tanks Member could be formed. The fundamental methods and conclusions drawn by Rose (1988) are sound and do not need to be repeated here in detail. Thus a brief synopsis of Rose's (1988) discussion and conclusions are presented below. Data used by Rose (1988) are reproduced in this manuscript for completeness.

As with the Rainier Mesa Member, pure crystal fractionation was tested as a model for the origin of the compositional range (59 wt% to 78 wt% SiO_2) of the Ammonia Tanks Member. Both major element multiple linear regression and Rayleigh fractionation techniques were used. Chemical analyses of whole pumice may be found in Appendix 2. Chemical analyses of phenocrysts are presented in Table 10. Distribution coefficients for Rayleigh fractionation modelling were compiled from the literature and are presented in Table 11 (see references from the Rainier Mesa Member section).

The major element multiple linear regression technique was done in six steps beginning with the least evolved pumice sample (59 wt% SiO_2) and proceeded consecutively through more evolved magma compositions and finally to a high-silica rhyolite composition (78 wt% SiO_2). The resulting regression equations were

Table 10. Mineral analyses used in regressions for crystal fractionation models in the Ammonia Tanks Member. From Rose (1988).

Plagioclase

Sample	A5-75	A5-63	A5-72	A5-71	A5-58	A5-35
Step	1	2	3	4	5	6
Mineral ID	92	38	77	61	15	27
SiO_2	55.17	58.15	58.84	57.77	61.28	63.95
Al_2O_3	28.86	26.26	25.33	26.51	23.70	22.59
FeO	0.20	0.32	0.84	0.40	0.38	0.26
MgO	0.05	0.01	0.00	0.03	0.00	0.00
CaO	9.65	6.67	6.57	6.84	4.68	2.77
Na_2O	5.25	6.78	6.77	6.94	8.34	8.71
K_2O	0.54	1.27	1.38	1.01	1.40	1.72
BaO	0.18	0.34	0.25	0.39	0.10	0.00
Total	99.90	99.80	99.98	99.89	99.88	100.00

Sanidine

Sample	A5-71	A5-58	A5-35
Step	4	5	6
Mineral ID	65	14	28
SiO_2	65.21	64.34	65.48
Al_2O_3	19.89	20.01	19.29
FeO	0.24	0.27	0.09
MgO	0.00	0.00	0.00
CaO	0.64	0.52	0.38
Na_2O	4.84	5.77	5.16
K_2O	9.17	8.59	9.33
BaO	0.00	0.38	0.25
Total	99.99	99.88	99.98

Clinopyroxene

Sample	A5-75	A5-63	A5-72	A5-71	A5-58
Step	1	2	3	4	5
Mineral ID	86	35	72	57	12
SiO_2	51.86	52.29	53.52	52.95	52.54
Al_2O_3	2.14	2.13	2.40	2.06	1.17
FeO	7.94	7.52	7.89	7.86	8.26
MgO	15.90	15.49	15.45	15.02	13.64
CaO	20.31	20.76	18.67	20.16	21.94
Na_2O	0.65	0.58	0.59	0.64	0.76
K_2O	0.00	0.01	0.00	0.00	0.00
TiO_2	0.47	0.58	0.52	0.48	0.28
MnO	0.69	0.55	0.93	0.80	1.35
P_2O_5	0.00	0.00	0.00	0.00	0.00
BaO	0.04	0.09	0.03	0.00	0.05
Total	100.00	100.00	100.00	100.00	99.99

Table 10. Continued.

Magnetite

Sample	A5-75	A5-63	A5-72	A5-71	A5-58	A5-35
Step	1	2	3	4	5	6
Mineral ID	97	42	83	69	32	20
Cr_2O_3	0.04	0.00	0.03	0.09	0.03	0.02
Al_2O_3	3.61	2.85	2.43	1.47	1.01	0.82
MgO	3.25	3.76	2.77	1.66	1.27	0.73
FeO	84.20	80.58	81.55	79.54	87.65	90.14
TiO_2	8.05	11.81	11.75	15.35	7.75	6.46
MnO	0.85	1.01	1.47	1.90	2.29	1.83
Total	100.00	100.01	100.00	100.01	100.00	100.00

Biotite

Sample	A5-35
Step	6
Mineral ID	25
SiO_2	40.58
Al_2O_3	13.67
FeO	15.06
MgO	16.56
CaO	0.28
Na_2O	0.58
K_2O	8.00
TiO_2	4.59
MnO	0.43
BaO	0.24
Total	99.99

Table 11. Distribution coefficients used for Rayleigh fractionation modelling of the Ammonia Tanks Member of the Timber Mountain Tuff. From Rose (1988).

	Plagioclase		Sanidine		Clinopyroxene	
	max	min	max	min	max	min
Sc	0.20	0.01	0.059	0.01	172	18
Rb	0.46	0.016	2.4	0.11	0.09	0.032
Sr	33	1.45	26	3.6	0.516	
Ba	3.3	0.3	24	1.0	2.3	0.131
Ce	0.4	0.11	0.095	0.02	21.6	0.36
Yb	0.3	0.049	0.04	0.005	11.6	1.14
Th	0.09	0.01	0.03	0.0095	6.56	0.01

	Biotite		Magnetite	
	max	min	max	min
Sc	20	4.9	15.6	1.5
Rb	5.3	2.24	0	
Sr	0.53	0.12	0	
Ba	36	3.7	0.08	0.05
Ce	11.0	0.037	22.9	0.28
Yb	3.0	0.179	2.2	0.2
Th	2.0	0.27	5.04	0.04

geologically reasonable and statistically sound (R^2 > 99%, SS < 0.19) which support an origin for the evolved magmas by fractional crystallization (Table 12). Testing of the major element linear regression models by Rayleigh fractionation of trace elements also provide favorable results and again are consistent with crystal fractionation (Table 13).

The presence of disequilibrium phenocrysts in many of the pumice samples led Rose (1988) to evaluate the possibility of combined fractional crystallization and magma mixing as a possible origin for the magmatic suite. Testing of this model by major element multiple linear regression again produced geologically and statistically reasonable results (R^2 = 100%, SS < 0.25)(Table 14).

Based upon this evidence, Rose (1988) concluded that the evolved magmas of the Ammonia Tanks Member were derived by a combination of fractional crystallization and mixing of a high-silica rhyolite and trachyandesite.

Thus for the Timber Mountain Tuff, fractional crystallization does not appear to be the sole mechanism for the generation of the wide range of compositions observed in the Rainier Mesa Member or Ammonia Tanks Member. The modelling does appear to be consistent however with a fractional crystallization/assimilation or fractional crystallization/mixing component for the Ammonia Tanks Member.

Table 12. Major element multiple linear regression models for the Ammonia Tanks Member of the Timber Mountain Tuff. From Rose (1988).

Step 1.

Parent = A5-75 (59 wt% SiO_2)
Daughter = A5-63 (62 wt% SiO_2)

A5-75 = 0.0869 + 0.848 A5-63 + 0.0923 Plag + 0.0316 Cpx + 0.0175 Mt

R^2 = 1.00 SS = 0.1576

Step 2.

Parent = A5-63 (62 wt% SiO_2)
Daughter = A5-72 (64 wt% SiO_2)

A5-63 = 0.0890 + 0.896 A5-72 +0.0614 Plag + 0.0212 Cpx + 0.0096 Mt

R^2 = 1.00 SS = 0.1321

Step 3.

Parent = A5-72 (64 wt% SiO_2)
Daughter = A5-71 (67 wt% SiO_2)

A5-72 = -0.0091 + 0.764 A5-71 + 0.193 Plag + 0.0285 Cpx + 0.0161 Mt

R^2 = 1.00 SS = 0.1814

Step 4.

Parent = A5-71 (67 wt% SiO_2)
Daughter = A5-58 (69 wt% SiO_2)

A5-71 = 0.0225 + 0.719 A5-58 + 0.22 Ksp + 0.0396 Plag + 0.00888 Cpx + 0.00896 Mt

R^2 = 1.00 SS = 0.07865

Step 5.

Parent = A5-58 (69 wt% SiO_2)
Daughter = A5-35 (73 wt% SiO_2)

A5-58 = 0.0547 + 0.672 A5-35 + 0.294 Ksp + 0.0109 Plag + 0.0181 Cpx + 0.0144 Mt

R^2 = 1.00 SS = 0.004290

Step 6.

Parent = A5-35 (73 wt% SiO_2)
Daughter = A5-3 (78 wt% SiO_2)

A5-35 = -0.0067 + 0.696 A5-3 + 0.0503 Plag + 0.231 Ksp + 0.0176 Bio + 0.00607 Mt

R^2 = 1.00 SS = 0.06226

Table 13. Rayleigh fractionation trace element models for the Ammonia Tanks Member of the Timber Mountain Tuff. From Rose (1988).

Step		1	2	3	4
Parent		A5-75	A5-63	A5-72	A5-71
Daughter		A5-63	A5-72	A5-71	A5-58
Sc	predicted	0.02-4.9	0.14-5.0	0.02-4.5	1.2-7.2
	observed	6.9	6.3	6.4	3.4
Rb	predicted	75-79	80-82	95-104	65-120
	observed	75	80	89	122
Sr	predicted	35-811	80-610	0.5-496	0.06-83
	observed	615	524	164	138
Ba	predicted	3641-5288	3373-4298	2090-4352	2.8-1230
	observed	3990	3560	1168	709
Ce	predicted	75-245	120-247	93-300	328-534
	observed	228	238	393	222
Yb	predicted	1.7-2.7	2.0-3.2	2.0-3.2	2.8-3.2
	observed	2.4	2.4	2.4	2.7
Th	predicted	9.6-13.3	12.6-17.4	12.6-17.4	23.7-27.0
	observed	12.1	13.3	19.6	20.17

Step		5	6
Parent		A5-58	A5-35
Daughter		A5-35	A5-3
Sc	predicted	0.1-3.9	1.9-3.0
	observed	2.3	1.3
Rb	predicted	65-120	77-177
	observed	164	216
Sr	predicted	0.01-56	0.01-43
	observed	88	7
Ba	predicted	0.2-742	0.3-390
	observed	394	74
Ce	predicted	134-329	120-184
	observed	129	58
Yb	predicted	3.0-3.9	3.5-3.9
	observed	2.7	2.9
Th	predicted	23.7-30.2	32.0-34.7
	observed	24.3	30.0

Table 14. Magma mixing models for the Ammonia Tanks Member of the Timber Mountain Tuff. From Rose (1988).

A. Magma mixing and crystal fractionation to produce rhyolite.

A5-35 = -0.0442 + 0.539 A5-71 + 0.513 A5-3 - 0.0372 Ksp - 0.00754 Plag - 0.00266 Cpx

R^2 = 1.00 SS = 0.04616

Hybrid = A5-35 (73 wt% SiO_2)
Magma 1: A5-71 (67 wt% SiO_2)
Magma 2: A5-3 (78 wt% SiO_2)

B. Mixing of end-member magma compositions to produce rhyolite.

A5-35 = 0.022 + 0.501 A5-75 + 0.704 A5-3 - 0.0584 Cpx - 0.135 Plag - 0.014 Mt

R^2 = 1.00 SS = 0.2469

Hybrid = A5-35 (73 wt% SiO_2)
Magma 1: A5-75 (59 wt% SiO_2)
Magma 2: A5-3 (78 wt% SiO_2)

Mineral Compositions for Part A.

	Plagioclase	Sanidine	Clinopyroxene
SiO_2	63.95	65.48	52.75
Al_2O_3	22.59	19.29	0.81
FeO	0.26	0.09	9.01
MgO	0.00	0.00	13.23
CaO	2.77	0.38	21.43
Na_2O	8.71	5.16	0.67
K_2O	1.72	9.33	0.02
BaO	0.00	0.25	0.09
TiO_2	NA[1]	NA	0.20
MnO	NA	NA	1.76
NiO	NA	NA	0.04
Total	100.00	99.98	100.01

Mineral Compositions for Part B[2].

	Clinopyroxene		Magnetite
SiO_2	52.50	Cr_2O_3	0.02
Al_2O_3	0.93	Al_2O_3	0.82
FeO	7.74	MgO	0.71
MgO	14.96	FeO	90.14
CaO	22.52	TiO_2	6.46
Na_2O	0.45	MnO	1.83
K_2O	0.00	Total	99.98
BaO	0.00		
TiO_2	0.20		
MnO	0.70		
NiO	0.00		
Total	100.00		

1 NA = Not analyzed.
2 Plagioclase in Part B is the same composition as in Part A.

Although Rose's (1988) modelling by fractionation and mixing is plausible, the model preferred here is that fractionation, assimilation and mixing were responsible for modifying and expanding the range of composition of individual magma batches in an initially layered system prior to eruption of the Rainier Mesa Member. Continued fractionation, assimilation, mixing and input of new magma into the system prior to eruption of the Ammonia Tanks Member 'blurred' the initial layering and produced a system which now appears to be continuously zoned based on a cursory examination of the geochemical, mineralogical and geothermometric data.

Examination of the data plotted on the spidergrams in Figure 15b and enrichment diagram in Figure 16 reveals the consistent decrease in concentration of all the trace elements plotted except for Rb, Th, K and Nb. The increase in Rb, Th, K and Nb is consistent with fractional crystallization as these elements may behave incompatibly with increasing magmatic evolution. The other trace elements are more compatible with the modal phenocryst phases present in the system, thus the decrease in concentration of these elements may reflect the formation and removal of phenocryst phases within *specific* magmatic groups (Figs. 4, 5a) from the Ammonia Tanks Member.

Magma Mixing

The origin of intermediate magmas in both members of the Timber Mountain Tuff could have potentially formed from the mixing of rhyolite and trachyandesite. Simple variation diagrams of both major (i.e. Al_2O_3 vs. SiO_2; Figs. 7, 9) and trace elements (i.e. Ba or Zr vs. SiO_2; Figs. 8, 10; Ce or Eu vs. SiO_2; Figs. 8, 10) quickly eliminate mixing as a possible hybridization mechanism as both parental and mixed compositions should lie on a straight line (Figs. 7, 8, 9, 10).

Initial examination of major and trace element variation diagrams and REE plots of the rhyolites for the Rainier Mesa Member and Ammonia Tanks Member led to the observation that the Ammonia Tanks Member high-silica rhyolite had an intermediate composition between the two high-silica rhyolites of the Rainier Mesa Member. This led to the hypothesis that the Ammonia Tanks Member high-silica rhyolite was a product of mixing of the Rainier Mesa Member high-silica rhyolitic magmas during or after eruption of the Rainier Mesa Member. Testing of this hypothesis using a variation plot of the two incompatible elements Nb and Rb reveals that the high-silica rhyolite of the Ammonia Tanks Member has a higher concentration of Nb at similar concentrations of Rb than the high-silica rhyolites of the Rainier Mesa Member (Fig. 45). Thus the high-silica rhyolite of the Ammonia Tanks Member could not

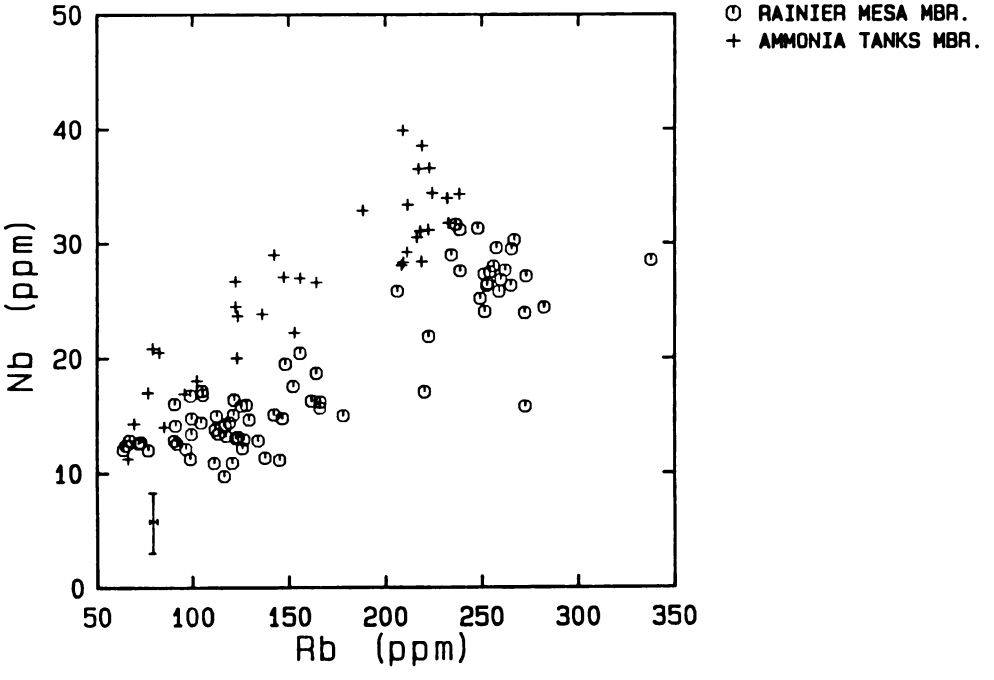


Figure 45. Rb versus Nb for the Timber Mountain Tuff.

have originated by magma mixing of the two Rainier Mesa Member high-silica rhyolites as concentrations for the Ammonia Tanks Member should lie intermediate to the end member Rainier Mesa Member concentrations. However, Th and Yb trace element data for the Ammonia Tanks Member seem to reveal the presence of two high-silica rhyolites.

Examination of the spidergrams of the Rainier Mesa Member high-silica rhyolites and the Ammonia Tanks Member rhyolite reveals that the Ammonia Tanks Member rhyolite is more similar in trace element composition to the high-Nb, rhyolite of the Rainier Mesa Member than the low-Nb, rhyolite of the Rainier Mesa Member (Figs. 12, 15). An overlay of the two spidergrams (Ammonia Tanks rhyolite and high-Nb Rainier Mesa Member rhyolite) shows a striking similarity in normalized element abundances (Fig. 46). Enrichment diagrams which compare trace element concentrations in both the Rainier Mesa Member high-silica rhyolites (high-Nb and low-Nb) to the trace element concentration in the Ammonia Tanks Member do not unequivocally relate any of the rhyolites to one another (Figs. 16, 17). Based on the spidergrams however, it is interpreted here that the high-silica rhyolite of the Ammonia Tanks Member may represent modified, residual high-Nb, high-silica rhyolite of the Rainier Mesa Member. Modification of the residual rhyolite may have occurred through fractional crystallization of the existing

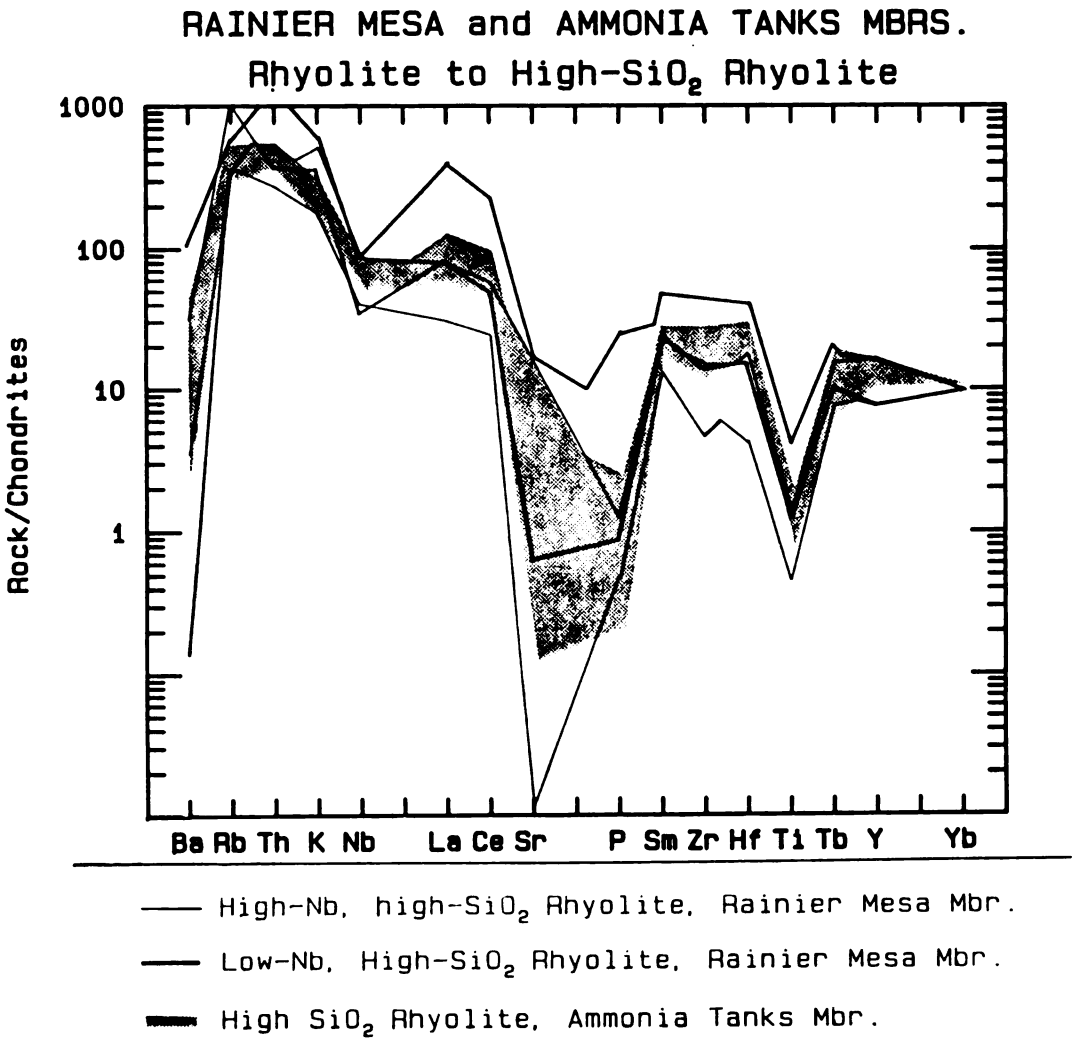


Figure 46. Overlay of the spidergrams for the high-silica rhyolites of the Rainier Mesa Member (low-Nb and high-Nb) and the high-silica rhyolite of the Ammonia Tanks Member.

rhyolite, input of new high-silica rhyolite from a parent chamber deeper within the crust or continued partial melting of upper crustal country rock. The short time interval between the eruption of the two high-silica rhyolites (less than 100,000 years; Sawyer, 1990, pers. comm.) is supportive and consistent with the hypothesis of a significant residual component being present after eruption of the Rainier Mesa Member. Such a short time span between eruptive events would most likely not allow for the generation of large volumes of rhyolitic magma through crystal fractionation or assimilation.

Partial Melting/Assimilation

Trachyandesite and Trachydacite

The enrichment diagram presented in Figure 47 compares the concentration of trace elements in the trachyandesite of the Rainier Mesa Member with the concentration of trace elements in the trachyandesite of the Ammonia Tanks Member. Analysis of the data reveals that there are negligible to significant differences in the concentrations of trace elements in the two members. Interpretation of the enrichment data for the trachyandesite of each member are consistent with the interpretation that the trachyandesites were generated by different degrees of partial melting of a lithologically

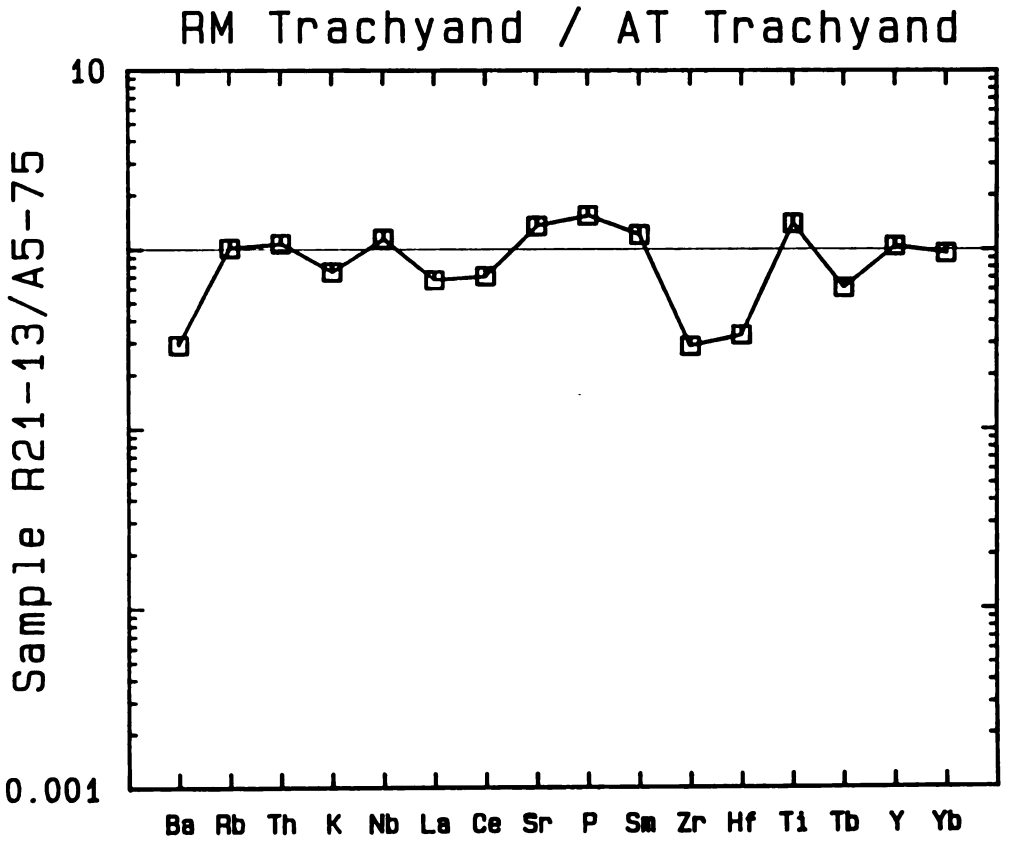


Figure 47. Enrichment diagram comparing trace element enrichment in the Rainier Mesa Member and Ammonia Tanks Member trachyandesites.

similar source rock in the lower crust. This model will be tested and discussed in more detail below.

Nd isotopic data from the initial work of Tegtmeyer, et al., (1989) indicates that the magmatic bodies for both the Rainier Mesa Member and the Ammonia Tanks Member were zoned with respect to Nd and epsilon Nd and behaved as open systems with respect to wallrock interaction (Fig. 48). Significant differences in epsilon Nd vs. 1/Nd values for both members provide supporting evidence for different degrees of crustal melting for the origin of the Rainier Mesa Member and Ammonia Tanks Member mafic magmas, and, for magmas of the Paintbrush Tuff (Fig. 48).

The origin of the mafic magmas of the Timber Mountain Tuff and the Paintbrush Tuff can be at least qualitatively evaluated using trace element data from the two tuffs. Using the relatively compatible elements Zr, Eu and the relatively incompatible elements Th, Yb and plotting them against SiO_2 where only data from trachyandesitic to trachydacitic whole-pumice samples are included, it can be observed that data from the four major ash-flow tuffs (Topopah Spring Member, Tiva Canyon Member, Rainier Mesa Member, and Ammonia Tanks Member) occur as geochemically distinct groups (Fig. 49). These groups of data are used to infer that the four ash-flow tuffs originated as separate magma batches from either different degrees of partial melting of the same source rock or from partial

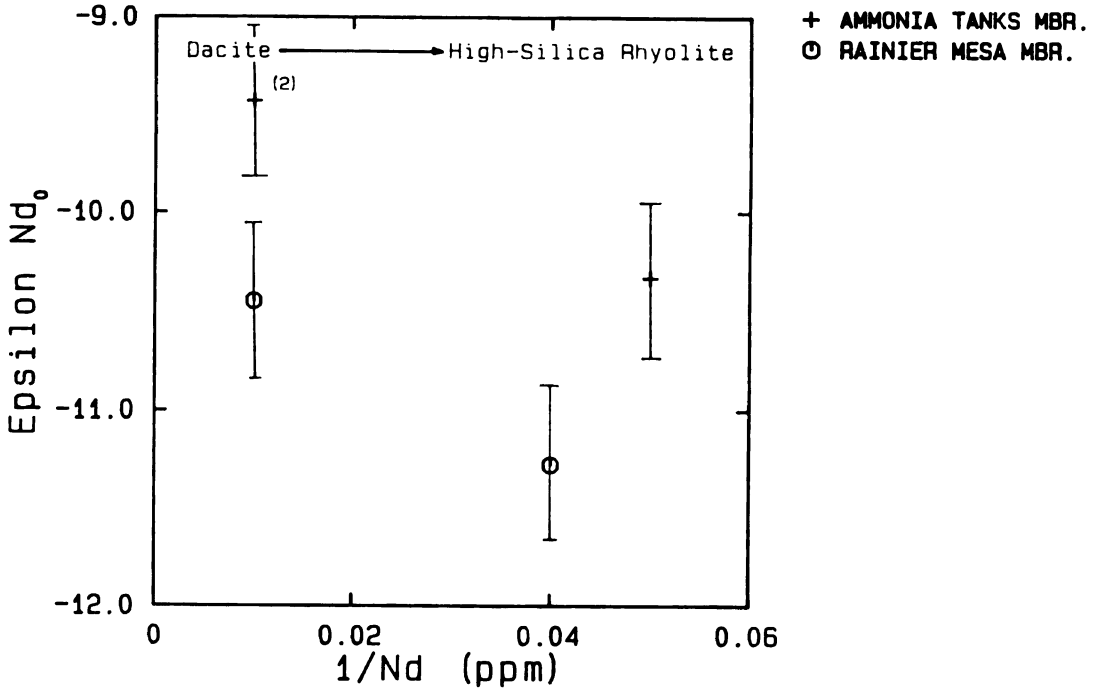


Figure 48. Nd versus 1/Nd data from Tegtmeyer, et al., (1989) for the Timber Mountain Tuff.

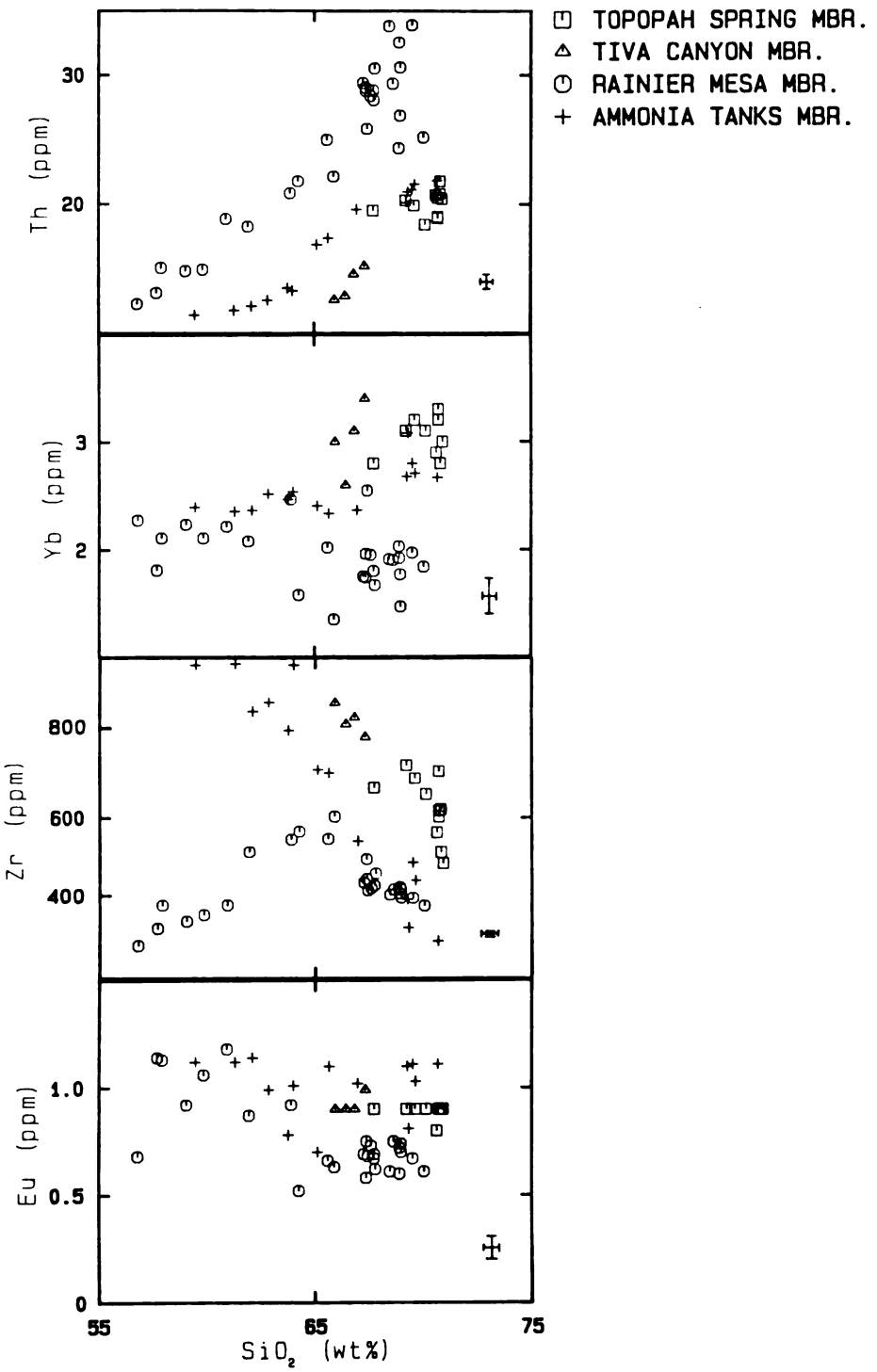


Figure 49. SiO_2 versus Th, Yb, Zr and Eu for the Paintbrush Tuff and Timber Mountain Tuff. Trachyandesite and trachydacite data only.

melting of different compositional regions within the crust and do not represent a long lived, continuously evolving magma body (Fig. 49). A plot of Yb/Th vs. Th, where both elements are at least partially incompatible, produces a series of data trends that can only be explained by different degrees of partial melting of a similar source rock, or, partial melting of compositionally heterogeneous source rock. Crystal fractionation cannot be used to explain the large range in data for each tuff as 60% fractionation of a common trachyandesite parent can only produce a small portion of the observed range in data (Fig. 50). Alternatively, a ratio plot using the partially compatible elements Zr or Eu, can be used to evaluate whether or not crystal fractionation has occurred. Zr and Eu ratio plots again show the distinct groups of data of each of the mafic end-members (trachyandesites and trachydacites) of the major ash-flow tuff sheets (Fig. 51). This data can be used to infer that within each major ash-flow tuff, fractionation is a plausible mechanism for the origin of the variation in the various elemental ratios *within each group* (such as zircon fractionation being responsible for the variation in the Zr/Th ratio shown in Figure 51). Similar plots using other element ratios (i.e. Zr/Rb) produce similar results. Thus, these ratio plots can be used to infer that the overall variation in composition between various

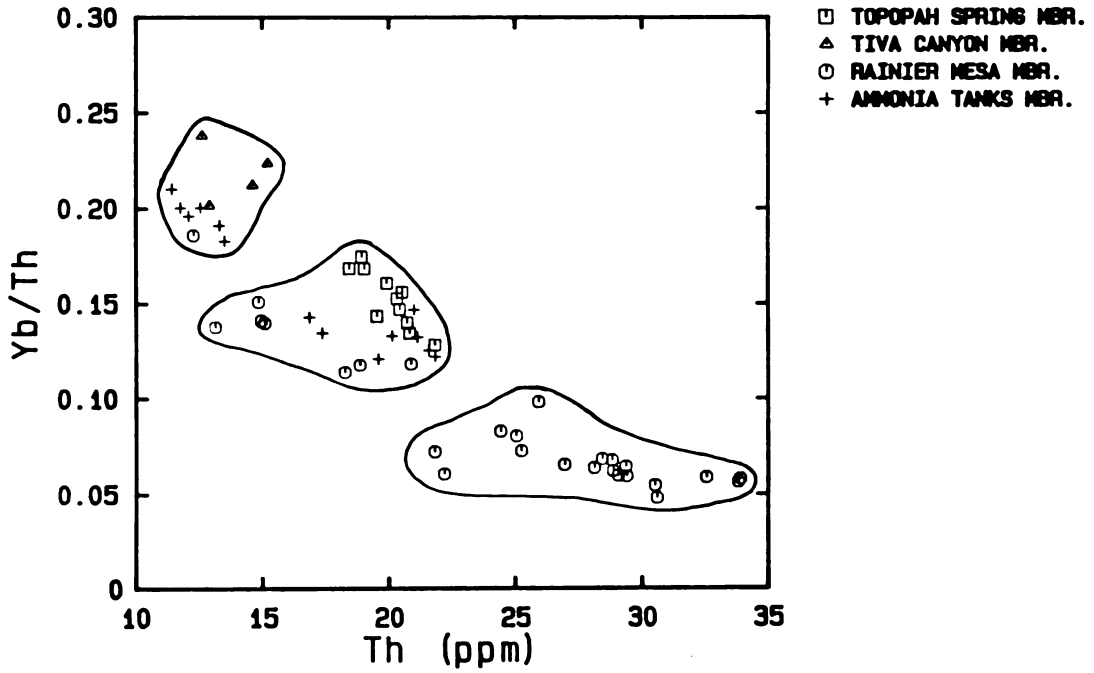


Figure 50. Yb/Th versus Th for the Paintbrush Tuff and the Timber Mountain Tuff.

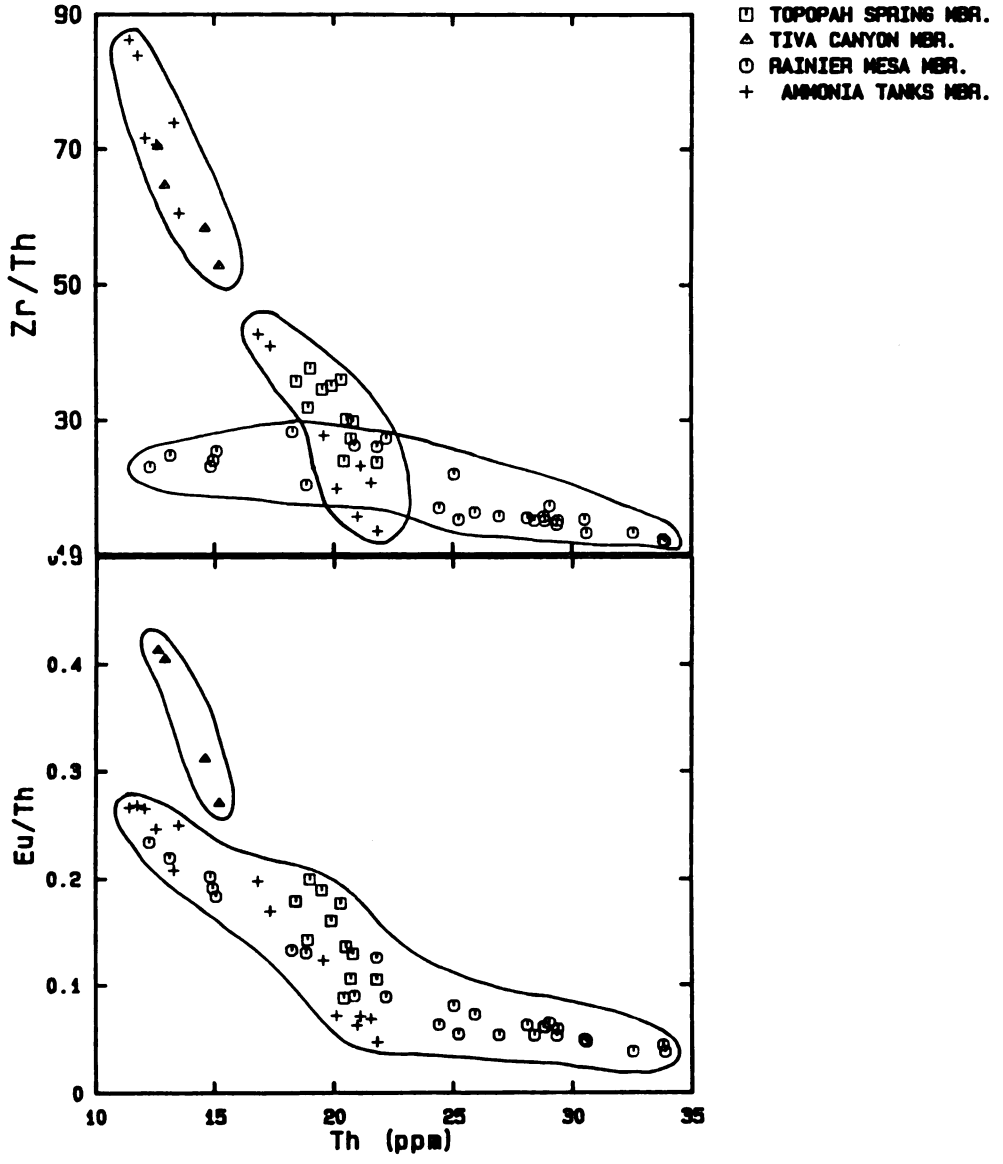


Figure 51. Zr/Th and Eu/Th versus Th for the Paintbrush Tuff and Timber Mountain Tuff. Trachyandesite and trachydacite data only.

mafic magmas cannot be explained by crystal fractionation. The variation in composition of the most mafic magmas of the four ash-flow tuffs is most likely due to a difference in degrees of partial melting of a similar source rock, or, partial melting of compositionally heterogeneous source rock.

Rhyolites

Origin of the rhyolitic magmas of the Rainier Mesa Member and Ammonia Tanks Member is more difficult to resolve. Pure fractional crystallization in the Rainier Mesa Member can account only for the formation of the low-Nb, high-silica rhyolite from rhyolite (R23-13 RH to R18-2 HSR; Model 4). Attempts to model the origin of the high-silica rhyolites from more mafic magmatic components or other dacitic to rhyolitic magmatic components by fractional crystallization fail completely. The extreme enrichment of Rb, Nb and Th in the high-Nb, high-silica rhyolites versus the concentration of these elements in the lower-silica rhyolite or low-Nb, high-silica rhyolite of the Rainier Mesa Member cannot be explained by simple fractional crystallization. The origin of the low-Nb, high-silica rhyolite may be related to fractional crystallization of the trachydacitic magma with some crustal assimilation occurring, while the high-Nb, high-

silica rhyolite most likely represents a separate melt derived from Nb-enriched crustal material.

Rhyolites of the Ammonia Tanks Member most likely represent modified residual rhyolite remaining after eruption of the Rainier Mesa Member. This residual rhyolite to high-silica rhyolite (both low-Nb and high-Nb) was probably modified by input of new crustal melt, fractional crystallization, assimilation and perhaps some mixing of the two Rainier Mesa Member high-silica rhyolites. Although Rose's (1988) modelling is permissive for generation of the rhyolites by fractional crystallization of more mafic trachydacite to trachyandesite, the geochemical and mineralogical data are more consistent with an independent source for these magmas. Nd isotopic evidence from Tegtmeyer, et al., (1989) again are consistent with a model of an open system where all levels of the magmatic system were open to wallrock interaction.

MAGMATIC WATER CONTENTS

Preliminary H_2O and CO_2 contents calculated by Vogel, et al., (1989) for the Ammonia Tanks Member based on infrared spectrographic analyses of over 250 melt inclusions in feldspar and quartz phenocrysts range from 1.0 wt% to 2.1 wt% H_2O in trachydacitic pumice fragments (64.97 wt% SiO_2) and 3.2 wt% to 5.9 wt% H_2O in more siliceous trachydacitic to rhyolitic pumice fragments (67.08 wt% to 70.42 wt% SiO_2). CO_2 concentrations in the lower-silica trachydacite pumice contained from 78 ppm to 106 ppm CO_2 while phenocrysts from higher-silica pumice contained 23 ppm to 102 ppm CO_2 (Vogel, 1990, unpublished data).

Using the theoretical closed-system degassing curves for H_2O and CO_2 derived by Newman, et al., (1988) for obsidian from the Mono Craters, California, data from the Ammonia Tanks Member appear to fall along two trends (Fig. 52). Volatile data from the higher-silica trachydacitic to rhyolitic pumice fall to the right of the closed system degassing curve of Newman, et al., (1988) for initial H_2O and CO_2 contents of 5.0 wt% and 1.2 wt% respectively. The more mafic pumice fragment phenocryst data fall to the left of the Newman, et al., (1988) initial degassing curve. Although only two data points are available for the mafic pumice phenocrysts, this data can be used to

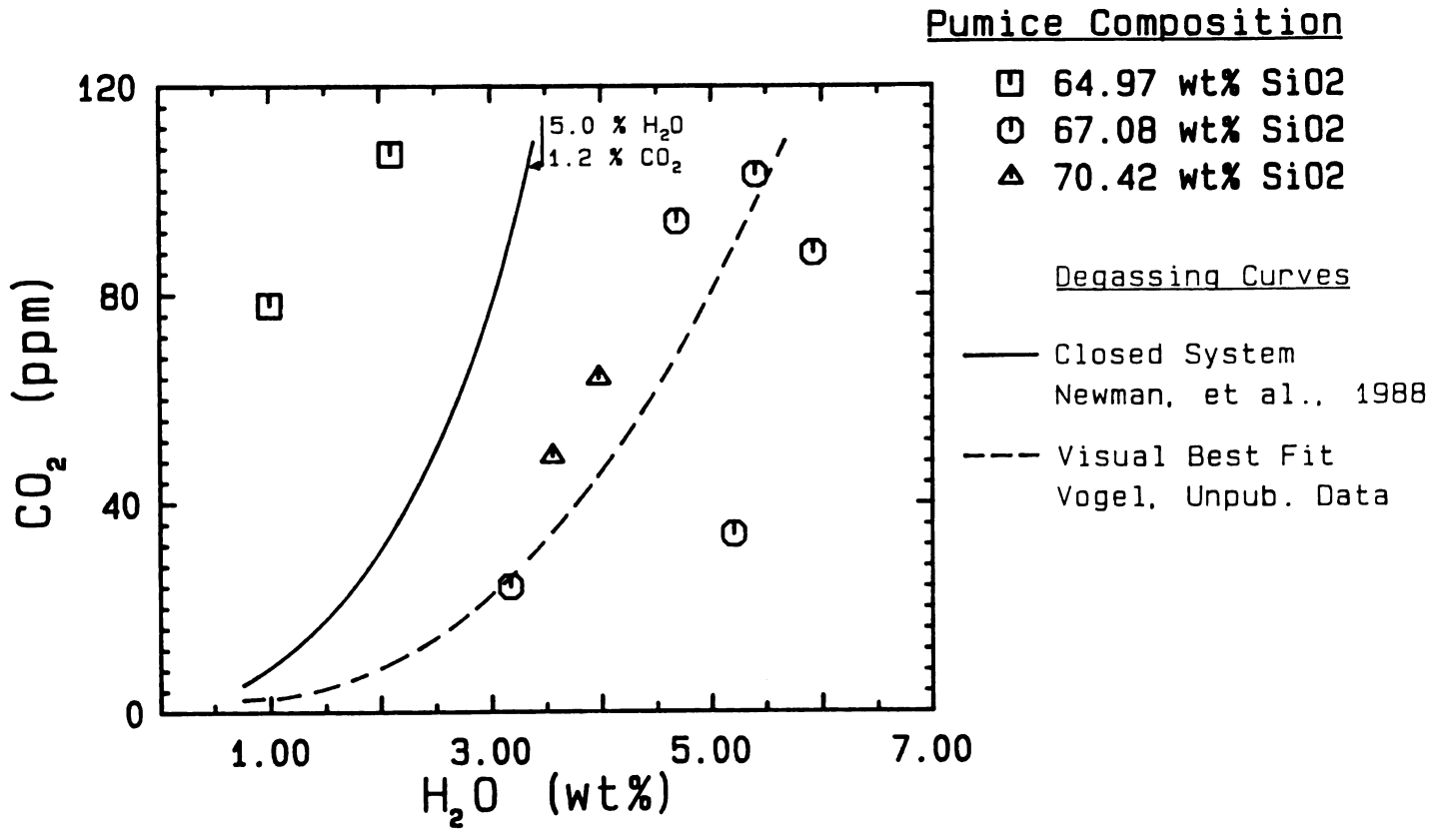


Figure 52. H_2O versus CO_2 concentrations for the Ammonia Tanks Member showing the separate degassing paths for the trachydacites and rhyolite using the degassing curves of Newman, et al., (1988).

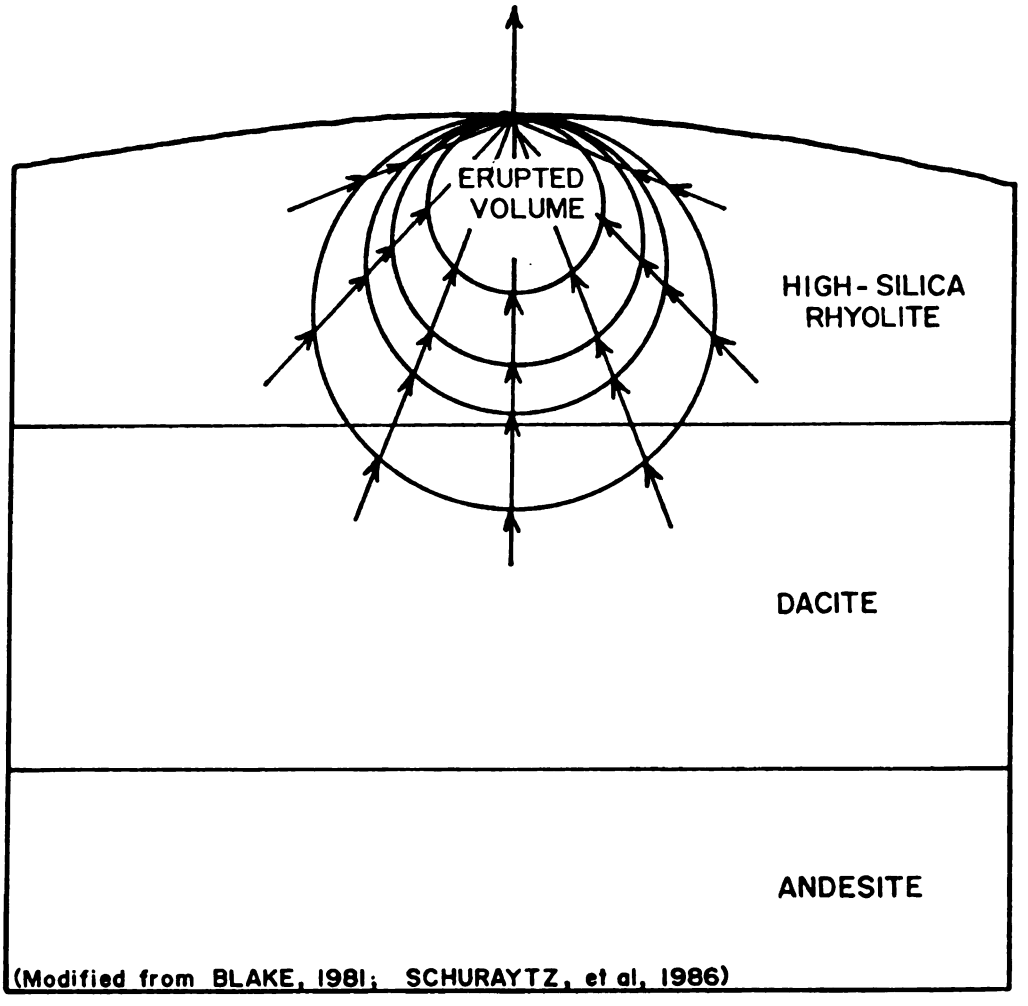
suggest, albeit somewhat cautiously, that the more mafic magma experienced a separate closed-system degassing path from the more silicic magma (Fig. 52). Preliminary volatile data from the Rainier Mesa Member indicate that the trachyandesitic to trachydacitic magmas were independently zoned with respect to the rhyolitic magmas. Although still preliminary in nature, this data is supportive of an independent source model for the various magmatic compositions present in the Rainier Mesa system.

Initial major element data from the glass inclusions and that of the pumice matrix glass, is almost exactly identical for all the samples thus far studied (trachyandesite to high-silica rhyolite)(Vogel, 1991; pers. comm.). This data would indicate then that the melt compositions were not being significantly modified by fractional crystallization.

ERUPTION DYNAMICS

Early work by Lipman (1967), and more recently work by Blake (1981), Hildreth (1983), Wolff and Storey (1984), Schuraytz, et al., (1989) and Flood, et al., (1989a) has shown that the zonation within ash-flow tuffs is more complex than the whole rock chemistry would imply. Analyses of individual pumice fragments collected from the base to the top of a stratigraphic section have systematic variations in chemistry, mineralogy, and thermal gradients when analyzed as a group. However, analyses of pumice fragments collected laterally over distances of a few meters also show discrete and sometimes large variations in composition between the individual pumice fragments (Figs. 2a, 2b, 3)(Lipman, 1967; Wolff and Storey, 1984; Schuraytz, et al., 1986, 1989; Rose, 1988; Flood, et al., 1989a).

Recognition of this compositional heterogeneity in pumice fragments has forced a review of how magma is erupted from a chamber. Blake (1981) undertook a mathematical analysis of eruption dynamics for Newtonian fluids and found that the evacuation of a magma chamber could be modelled by circular eruption isochrons (Fig. 53). In this way, Blake (1981) suggested that compositional heterogeneities in pumice fragments should be observed within ash-flow sheets assuming compositional layering existed in the magma body. This heterogeneity



HYPOTHETICAL MAGMA CHAMBER

Figure 53. Schematic diagram of evacuation isochrons as modelled by Blake (1981) for a liquid of homogeneous density and viscosity being drained from a single vent.

would result from simultaneous tapping of different compositional zones of magma at any instant in time. The effect of discrete magma layers with density/viscosity variations however was not taken into account (Blake and Ivey, 1986). Re-analysis of the problem in light of density/viscosity differences in the fluid layers has shown that withdrawal of the deeper, more dense, less viscous fluid can occur rapidly after initial evacuation begins, and before complete removal of the upper layer has occurred. Tapping of the lower, more dense layer is primarily dependent upon the thickness and viscosity of the overlying layer (Blake and Ivey, 1986)(Fig. 54). The theoretical models suggest that withdrawal of compositionally zoned and/or layered magma can produce compositional heterogeneities similar to those observed in the pumice fragments of ash-flow tuffs whether the magma body is zoned and/or layered.

Both the Rainier Mesa Member and Ammonia Tanks Member exhibit compositional heterogeneity in pumice fragment composition both vertically and laterally in any given stratigraphic section (with the exception of most the basal unwelded zones which are composed of high-silica rhyolite)(Figs. 2a, 2b, 3). In many localities the basal unwelded tuff may be relatively homogeneous and contain pumice fragments with a composition of high-silica rhyolite. This homogeneous zone however, quickly becomes

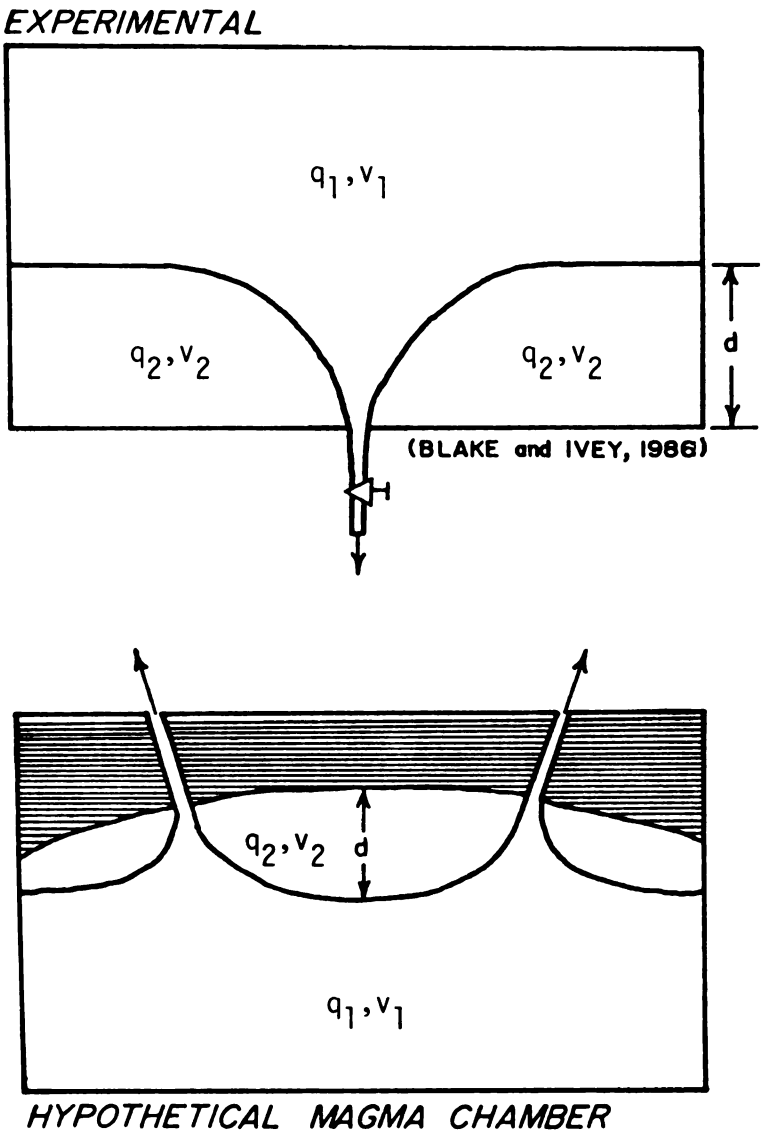


Figure 54. Schematic diagram of the evacuation profile for two liquids of contrasting density (q_1,q_2) and viscosity (v_1,v_2) being drained from a single vent (modified from Blake and Ivey, 1986).

heterogeneous however with respect to pumice fragment composition within 10 cm to 100 cm up section. In the upper unwelded zone of the ash-flow sheet, the compositional range defined by pumice fragments found in the lower portions of the sheet is found within this upper zone. This phenomena is consistent with the findings of Schuraytz, et al., (1986, 1989) for the Topopah Spring Tuff.

If simple vertical drawdown of a zoned magma body had occurred, pumice fragments in the ash-flow tuff would be relatively homogeneous at any given stratigraphic horizon and would exhibit a systematic change from more evolved compositions at the base to more mafic compositions at the top. The data for the Rainier Mesa Member and Ammonia Tanks Member is not consistent with this model. The data is consistent with the model of Blake and Ivey (1986).

SUMMARY AND CONCLUSIONS

Geochemical and mineralogical analyses of glassy pumice fragments from the Rainier Mesa Member and Ammonia Tanks Member of the Timber Mountain Tuff reveal that the parental magmatic systems from which the tuffs originated, were composed of magma ranging in composition from trachyandesite (57 wt% SiO_2 and 59 wt% SiO_2 in the Rainier Mesa and Ammonia Tanks Members respectively) to high-silica rhyolite (78 wt% SiO_2 for both members). Based on the geochemical similarity of the two magmatic systems, it is inferred that magmas of the Ammonia Tanks Member originated as a combination of; residual magmas leftover after eruption of the Rainier Mesa Member, assimilation of wallrock, input of new, perhaps slightly alkaline magma as evidenced by the elevated concentrations of Ba, Zr, Hf, Nb and La in the trachyandesitic pumice and a steepening of the paleomagmatic temperature gradient with respect to that of the Rainier Mesa Member.

Within the Rainier Mesa magmatic system, there is evidence from the trace element chemistry and geothermometry of Fe-Ti oxides for at least two separate magma batches; one, the dominant volume magma body ranging in composition from trachyandesite to low-Nb, high-silica rhyolite, and two, a separate, smaller volume body of high-Nb, high-silica rhyolite. Data for the Ammonia Tanks Member does not reveal any unequivocal

evidence for the existence of separate magma bodies. Th and Yb trace element data however may indicate the presence of two high-silica rhyolites. These rhyolites may represent chemically modified, residual high-silica rhyolites left over after eruption of the Rainier Mesa Member.

Although compositional gaps do occur in the major and trace element data in both members, the geochemical, mineralogical and geothermometric data are not entirely consistent with the model of a single, layered magma chamber for either member ***at the time of eruption***. The data are more consistent however with a model of a zoned magmatic system where the more mafic trachyandesite is overlain by progressively more silicic magma which eventually grades into high-silica rhyolite at the chamber cupola.

The origin of the geochemical gaps is somewhat enigmatic. The compositional gaps are inferred in this study to represent initial compositional boundaries which were present prior to eruption of the Rainier Mesa Member. The gaps originated as individual magma batches were brought together to form a dominant volume, layered, magmatic system prior to eruption of the Rainier Mesa Member.

Various mineral phases in each member of the Timber Mountain Tuff, i.e. biotite or plagioclase feldspar

exhibit gradual compositional changes as the magma composition evolves from trachyandesite to high-silica rhyolite. The phenocrysts do not reveal any sharp differences in composition across the geochemical gaps. Glass compositions of the pumice fragments also indicate gradual compositional changes from the mafic to felsic magmatic compositions. Composite histograms for the phenocryst data do in many cases reveal bimodal to trimodal phenocryst populations. The modal populations are interpreted here to represent phenocryst compositions that were present in the original magma bodies. Reequilibration of the phenocrysts, modification of the magmatic compositions by fractional crystallization, assimilation and possible magma mixing blurred the compositional boundaries between the magma bodies resulting in a magmatic system that under cursory examination now appears to have been continuously zoned. The geothermometric data do not reveal any thermal discontinuities for magmatic compositions on either side of the geochemical gaps. This is interpreted to signify that a long enough period of time must have elapsed such that the temperature gradient, as reflected by the Fe-Ti oxide compositons, reequilibrated to the new magmatic configuration.

The origin of the magmas in the Timber Mountain system appears to have been the result of several

processes. Comparison and analysis of trace element data using ratio plots of incompatible elements for trachyandesites and trachydacites of the Timber Mountain Tuff and those of the 12.9 to 13.4 million year old Paintbrush Tuff indicate that the mafic magmas originated from either different degrees of partial melting of the same crustal source rock, or, formed from partial melting of compositionally heterogeneous crustal source rocks. The compositional range from trachyandesite to trachydacite however, can be explained by the fractionation of phenocryst phases observed within the tuffs based on these ratio plots. Thus the possibility that there was a common trachyandesitic parental magma body which continuously supplied magma to the Timber Mountain and Paintbrush magmatic systems can be ruled out based on the trace element evidence.

Within the Timber Mountain magmatic system, and for each member, petrogenetic modelling using fractional crystallization and assimilation gave mixed results for the origin of the more evolved trachydacitic to high-silica rhyolite magmas. In the Rainier Mesa Member, fractional crystallization cannot be used to explain the observed compositional range. The lack of specific distribution coefficients (K_D) for the various mineral phases present in the Timber Mountain magmatic system, and reliance on published K_D values for other magmatic systems

for the modelling, may have contributed to the difficulty in producing viable petrogenetic models, *if* crystal fractionation was the dominant differentiation process acting on the magmatic system. Rose (1988) however was able to model the observed compositional range in the Ammonia Tanks Member by using both a fractional crystallization model and a fractional crystallization/magma mixing model. Rose (1988) preferred the fractionation/mixing model as it best explains the presence of ubiquitous disequilibrium phenocrysts. Although this model is permissive, it is preferred in this study to call upon the model where originally compositionally discrete magma batches were modified internally by fractional crystallization, assimilation and input of new magma which expanded the compositional range of each magma batch. Some mixing may have occurred upon eruption of the Rainier Mesa Member to form some of the intermediate magmas in the Ammonia Tanks Member, however, current modelling has been inconclusive.

Partial melting of crustal rock was probably responsible for the formation of the high-Nb, high-silica rhyolite of the Rainier Mesa Member based on the high concentrations of trace elements, particularly Th, Nb and Rb. Crystal fractionation of a more mafic magma in the Rainier Mesa magmatic system could not produce the observed concentrations of the these elements in this

particular rhyolite. Trace element signatures on rare-earth element plots, spidergrams and enrichment diagrams indicate that the high-silica rhyolite of the Ammonia Tanks Member is similar to, but not comagmatic with, the high-Nb, high-silica rhyolite of the Rainier Mesa Member. Thus it is interpreted here that the high-silica rhyolite of the Ammonia Tanks Member most likely represents an unknown amount of residual magma from the Rainier Mesa magmatic system (as evidenced by the Th and Yb trace element data for the Ammonia Tanks Member), continued magmatic input from partial melting of crustal material and fractional crystallization.

Geobarometric data determined by two separate methods indicates a range in the equilibrium pressure of phenocryst formation from 2 kbars to 6 kbars (Hammarstrom and Zen (1986) amphibole-quartz geobarometer; 3.9 to 4.8 kbars for rhyolite of the Rainier Mesa Member: Stormer and Whitney (1985) two feldspar/Fe-Ti oxide geobarometer; 2 kbars to 6 kbars for both members of the Timber Mountain Tuff). From this data it is interpreted that phenocrysts in magmas of the Timber Mountain magmatic system were at equilibrium at a mid-crustal level.

Measured H_2O and CO_2 concentrations in melt inclusions in feldspar and quartz phenocrysts in the Ammonia Tanks Member indicate that trachydacitic magma (64 wt% SiO_2) contained higher initial H_2O and CO_2 contents

than the more silicic trachydacitic (67 wt% SiO_2) and rhyolitic magma (70 wt% SiO_2). The more mafic and volatile-rich trachydacitic magma followed a separate degassing path than the less volatile-rich, more silicic trachydacite and rhyolite, indicating that the parental magma body was zoned with respect to H_2O and CO_2. Preliminary H_2O and CO_2 data for the Rainier Mesa Member indicates that the trachyandesitic to trachydacitic magmas were independently zoned with respect to the rhyolitic magmas. This type of zonation would support the model of an independent source for each magma batch.

The distribution of compositionally heterogeneous pumice fragments within the ash-flow sheets is consistent with the eruption dynamic models of Blake and Ivey (1986) for density and viscosity stratified magma bodies.

Thus, in conclusion, the magmatic system that erupted the Timber Mountain Tuff initially formed by coalascence of compositionally heterogeneous magma bodies which originated from the partial melting of lower to mid-crustal rock. The initial dominant volume magma body was layered from a basal trachyandesite to trachydacite to an intermediate trachydacite to rhyolite to an upper rhyolite to high-silica rhyolite. A prolonged residence time of the layered magma body at a mid-crustal level allowed each of these layers to become chemically, mineralogically and thermally modified through fractional crystallization and

assimilation of wallrock. Partial melting of upper crustal rock may have been responsible for forming a second high-silica rhyolite magma in close proximity to the dominant volume chamber. The magmatic system just prior to eruption of the Rainier Mesa Member more closely resembled a chemically, mineralogically and thermally zoned system. Relict layering of the magmatic system was reflected in the volatile gradients, geochemical compositional gaps, bimodal to trimodal phenocryst populations and trace element partitioning. Injection of new more mafic magma may have triggered the eruption of the Rainier Mesa Member. Incomplete evacuation of the dominant volume chamber (and perhaps the secondary high-silica rhyolite chamber), input of new mafic magma and wallrock assimilation resulted in the formation of a magmatic system which quickly reestablished chemical, mineralogical, thermal and volatile gradients. Crystal fractionation, assimilation and possible magma mixing from eruption of the Rainier Mesa Member continued to modify the magmatic compositions present in the chamber resulting in slightly different mineral assemblages, geochemical makeup and thermal and volatile gradients. Either volatile exsolution or input of new magma or both resulted in eruption of the Ammonia Tanks Member. Eruption of both members of the Timber Mountain Tuff probably did not occur as simple vertical drawdown of magma from the chamber, but

from a more complex process of a rapidly growing, spherical evacuation front as evidenced by stratigraphic, pumice fragment compositional heterogeneity in the ash-flow tuffs.

LIBRARY
Michigan State
University

PLACE IN RETURN BOX to remove this checkout from your record.
TO AVOID FINES return on or before date due.

DATE DUE	DATE DUE	DATE DUE

MSU Is An Affirmative Action/Equal Opportunity Institution
c:\circ\datedue.pm3-p.1

THE TIMBER MOUNTAIN TUFF, SOUTHWESTERN NEVADA VOLCANIC FIELD: GEOCHEMISTRY, MINERALOGY AND PETROGENESIS

Volume II

By

James Gordon Mills, Jr.

A DISSERTATION

Submitted to
Michigan State University
in partial fulfillment of the requirements
for the degree of

DOCTOR OF PHILOSOPHY

Department of Geological Sciences

1991

APPENDICES

APPENDIX 1

Description of Sampling Locations

Appendix 1. Locations of samples collected from the Timber Mountain Tuff.

SAMPLES[1]	STRATIGRAPHIC INTERVAL[2]	LOCATION	USGS MAP
R8-1 to R8-19 R8-20 to R8-31 R8-32 to R8-49	LRM VRM URM	Southeast Rainier Mesa, Area 12, N. Rainier Mesa Rd., 0.5 km (0.45 miles) due east of drill hole UE12t-1. Latitude: 37° 13' 08" Longitude: 116° 10' 11.5"	I-754
R11-1 to R11-23	URM	Near Test Well #8 (GTW-8), 0.35 km (0.25 miles) NE of GTW-8 (mapped as Tmf). Latitude: 37° 10' 02" Longitude: 116° 17' 10"	GQ-638
R18-1 to R18-17 R18-18 to R18-24	LRM VRM	Silent Butte area, Area 19 Site overlooks Silent Canyon. Latitude: 37° 19' 33" Longitude: 116° 23' 53"	GQ-493
R21-1 to R21-16 R21-27 A21-17 to A21-26	URM LAT?	Echo Peak Rd., South Silent Canyon, Area 19. Latitude: 37° 15' 32" Longitude: 116° 20' 51"	GQ-614
R21-28 to R21-30	URM	Latitude: 37° 15' 08" Longitude: 116° 21' 08"	
R21-31 to R21-44	URM	Latitude: 37° 15' 32" Longitude: 116° 20' 51"	
R23-1 to R23-27	URM	Pahute Mesa Rd., Area 19 2.4 km (1.5 miles) NW of drill hole UE-19c. Latitude: 37° 16' 52" Longitude: 116° 20' 32"	GQ-614

[1] Not all samples chemically analyzed

[2] LRM = Lower Rainier Mesa Mbr. VRM = Vitrophyre, Rainier Mesa Mbr. URM = Upper Rainier Mesa Mbr. LAT = Lower Ammonia Tanks Mbr. MAT = Middle Ammonia Tanks Mbr. UAT = Upper Ammonia Tanks

Appendix 1. Continued.

SAMPLES[1]	STRATIGRAPHIC INTERVAL[2]	LOCATION	USGS MAP
R25-1 to R25-21	URM	SE of intersection of Pahute Mesa Rd. and Road 19-03, Area 19. West side of road on bulldozed equipment pad. Latitude: 37° 16' 22" Longitude: 116° 23' 01"	GQ-493
R26-3 to R26-11	URM	N. Buckboard Mesa Rd., 1.5 km (1 mile) south of Pahute Mesa Rd. junction. East side of road. Latitude: 37° 13' 39" Longitude: 116° 27' 08"	GQ-695
R26-12 to R26-24	LRM	N. Buckboard Mesa Rd. 2.5 km (1.5 miles) south of Pahute Mesa Rd. junction. East side of road. Latitude: 37° 13' 00" Longitude: 116° 27' 21"	
A4-1 to A4-37 A4-38 to A4-85	LAT UAT	Silent Butte area, Area 19 0.75 km (0.5 miles) north on Road 19-03 from Pahute Mesa Road junction. East side of road. Latitude: 37° 16' 49" Longitude: 116° 22' 54"	GQ-493
A5-1 to A5-13 A5-14 to A5-20 A5-21 to A5-40 A5-41 to A5-55 A5-56 to A5-68 A5-69 to A5-84	LAT (1)[3] LAT (10) LAT (30) MAT (50) UAT (90) UAT (100)	Silent Butte area, Area 19 1.5 km (1 mile) west on Pahute Mesa Rd. from junction with Road 19-03. South side of road. Latitude: 37° 16' 19" Longitude: 116° 24' 01"	GQ-493

[3] Feet above basal contact with bedded air-fall unit

APPENDIX 2

Geochemical Data for Glassy Pumice Samples; Major and Trace Elements (XRF and INAA)

Appendix 2. Major and trace element analyses of whole pumice samples in the Rainier Mesa Member and Ammonia Tanks Member of the Timber Mountain Tuff.

Rainier Mesa Member								
Sample Number								
	R8-1	R8-2	R8-3	R8-6	R8-7	R8-9	R8-10	R8-11
Weight Percent Oxide (wt %)								
SiO_2	76.08	75.99	75.75	75.86	76.30	75.48	74.69	73.93
TiO_2	0.10	0.11	0.10	0.11	0.11	0.10	0.09	0.09
Al_2O_3	11.95	12.03	11.89	12.09	12.00	12.09	12.20	12.48
FeO	0.40	0.52	0.55	0.44	0.58	0.52	0.42	0.39
MnO	0.07	0.07	0.06	0.07	0.06	0.07	0.07	0.07
MgO	0.00	0.00	0.00	0.00	0.00	0.01	0.00	0.00
CaO	0.40	0.40	0.48	0.42	0.48	0.43	0.40	0.44
Na_2O	2.94	2.91	2.52	3.08	2.52	2.69	3.48	3.54
K_2O	5.29	5.34	5.69	5.16	5.70	5.54	5.04	5.05
P_2O_5	0.01	0.01	0.01	0.01	0.01	0.01	0.01	0.01
Total	97.24	97.38	97.05	97.24	97.76	96.94	96.40	96.00
X-ray Fluorescence (ppm)								
Cr	14.40	7.10	0.50	10.70	12.80	7.30	0.00	0.00
Ni	0.00	0.00	1.90	0.00	10.00	0.00	0.00	7.40
Cu	0.00	10.80	0.00	0.00	0.00	0.00	0.00	0.00
Zn	30.10	34.30	16.30	36.10	14.80	28.30	26.80	16.90
Rb	265.12	258.56	264.80	257.16	271.90	266.50	255.72	259.50
Sr	2.67	0.00	4.55	0.19	0.00	4.96	3.65	3.48
Y	30.11	33.38	31.32	31.28	26.01	32.00	32.10	29.77
Zr	68.54	89.26	73.64	78.21	80.16	70.78	59.80	62.01
Nb	29.46	25.72	26.26	29.57	23.85	30.25	27.96	26.77
La	35.09	20.14	41.66	48.36	28.14	22.19	44.95	16.44
Ba	132	100	190	86	169	87	88	229
INAA (ppm)								
Sc	3.82	4.25	4.17	4.14	3.34	4.59	4.21	3.76
Hf	3.52	3.90	3.44	2.62	2.31	2.90	3.29	3.35
Th	25.46	25.22	21.80	16.64	11.69	15.58	22.14	21.81
La	21.36	21.10	21.34	19.64	20.32	24.11	18.72	18.91
Ce	51.06	58.68	48.81	44.91	36.33	40.07	44.20	45.19
Sm	5.55	6.26	5.77	5.51	5.22	5.50	5.22	5.60
Eu	0.12	0.18	0.17	0.14	0.19	0.20	0.12	0.14
Tb	0.66	0.63	0.61	0.56	0.52	0.55	0.62	0.61
Yb	4.38	3.54	2.81	2.87	1.67	2.15	4.08	3.79
Lu	0.42	0.36	0.30	0.32	0.24	0.26	0.42	0.41
Strat	15	15	15	15	15	15	15	15

Appendix 2. Continued.

Rainier Mesa Member							
Sample Number							
R8-14	R8-15	R8-16	R8-20	R8-21	R8-22	R8-23	R8-24
Weight Percent Oxide (wt %)							
SiO_2 75.54	75.45	73.77	66.46	65.71	63.61	65.43	65.57
TiO_2 0.10	0.10	0.12	0.43	0.46	0.60	0.49	0.46
Al_2O_3 12.21	12.16	12.86	16.09	16.45	16.99	16.68	16.10
FeO 0.42	0.46	0.74	1.89	2.32	2.88	2.24	2.14
MnO 0.07	0.07	0.08	0.08	0.09	0.13	0.08	0.08
MgO 0.04	0.00	0.52	0.71	0.74	0.95	0.74	0.71
CaO 0.41	0.43	0.41	1.61	2.09	2.40	2.01	1.89
Na_2O 2.73	2.52	2.51	4.34	4.41	4.44	4.24	4.33
K_2O 5.41	5.83	4.92	5.38	5.15	4.77	5.09	5.33
P_2O_5 0.01	0.01	0.02	0.11	0.15	0.22	0.13	0.13
Total 96.94	97.03	95.95	97.10	97.57	96.99	97.13	96.74
X-ray Fluorescence (ppm)							
Cr 1.40	0.00	2.90	0.40	0.00	0.00	0.40	0.00
Ni 6.60	0.00	13.00	0.00	0.00	4.30	0.00	0.00
Cu 0.00	0.00	0.00	5.70	0.00	8.50	0.00	0.00
Zn 15.90	18.50	186.80	44.90	50.20	66.30	46.70	47.90
Rb 261.78	281.95	252.21	125.43	90.32	165.76	91.47	98.60
Sr 0.00	0.00	14.09	335.24	453.25	559.40	438.70	414.22
Y 31.56	28.00	45.77	19.14	20.82	24.34	20.46	20.95
Zr 71.89	72.43	107.22	407.99	497.25	547.93	447.71	461.52
Nb 27.61	24.32	26.24	12.14	16.03	15.67	12.55	16.75
La 15.24	9.33	35.86	129.53	111.00	127.84	116.51	123.38
Ba 203	88	268	1319	1900	1939	1551	1715
INAA (ppm)							
Sc 4.11	3.44	3.56	3.77	3.66	3.35	3.36	3.41
Hf 3.50	3.27	4.02	9.47	10.99	12.81	10.69	10.00
Th 22.83	22.74	24.43	33.81	29.05	25.04	28.81	30.51
La 18.62	16.91	16.34	132.40	125.02	114.45	121.79	118.80
Ce 47.79	48.97	61.18	212.82	194.08	179.99	191.40	189.35
Sm 5.25	5.29	5.83	6.70	7.16	7.14	7.00	6.83
Eu 0.17	0.17	0.28	1.49	1.89	2.03	1.77	1.51
Tb 0.62	0.61	0.63	0.67	0.64	0.62	0.66	0.65
Yb 3.84	3.65	3.99	1.92	1.74	2.04	1.97	1.66
Lu 0.35	0.36	0.49	0.20	0.20	0.23	0.25	0.21
Strat 15	15	15	70	70	70	70	70

Appendix 2. Continued.

Rainier Mesa Member							
Sample Number							
	R8-25	R8-26	R8-27	R8-32a	R8-32b	R8-35	R8-37
Weight Percent Oxide (wt %)							
SiO_2	65.08	65.87	65.63	73.09	74.22	75.62	62.16
TiO_2	0.49	0.46	0.47	0.21	0.25	0.20	0.70
Al_2O_3	16.36	16.24	16.22	12.84	12.35	11.72	17.44
FeO	2.28	2.18	2.18	0.86	1.01	0.87	3.41
MnO	0.08	0.08	0.08	0.05	0.06	0.04	0.09
MgO	0.74	0.68	0.66	0.12	0.15	0.03	1.36
CaO	1.99	1.90	1.90	0.79	0.81	0.51	3.31
Na_2O	4.36	4.40	4.35	2.82	2.67	2.18	3.98
K_2O	5.26	5.31	5.30	5.85	5.68	6.10	4.56
P_2O_5	0.15	0.14	0.14	0.03	0.03	0.02	0.29
Total	96.79	97.26	96.93	96.66	97.23	97.29	97.30
X-ray Fluorescence (ppm)							
Cr	0.00	0.00	3.70	7.10	5.40	0.00	3.90
Ni	7.10	0.00	0.00	18.90	0.00	0.00	0.00
Cu	1.50	0.00	13.90	0.00	0.00	6.70	0.00
Zn	44.90	45.30	56.00	11.30	33.30	32.60	70.90
Rb	96.23	105.07	104.15	116.65	117.04	141.98	110.90
Sr	435.86	428.10	411.38	74.99	58.69	34.59	837.38
Y	18.87	15.26	19.48	16.95	18.10	21.34	27.36
Zr	439.29	431.54	430.68	168.08	183.27	153.51	546.11
Nb	12.10	16.83	14.40	14.09	13.22	15.09	10.86
La	142.76	117.16	125.88	82.39	74.55	79.83	106.70
Ba	1704	1664	1530	485	189	157	2322
INAA (ppm)							
Sc	3.62	4.06	2.84	1.81	1.81	1.97	4.83
Hf	10.63	9.92	9.86	5.78	5.78	4.71	12.84
Th	29.39	28.10	28.84	35.23	35.23	33.45	20.86
La	124.37	121.27	117.94	80.23	80.23	68.72	105.79
Ce	198.32	183.21	185.97	129.64	129.64	110.48	171.40
Sm	7.13	6.68	6.83	5.69	5.69	6.04	8.45
Eu	1.75	1.77	1.75	0.73	0.73	0.59	1.88
Tb	0.65	0.65	0.65	0.68	0.68	0.68	0.63
Yb	1.76	1.80	1.81	1.81	1.81	1.66	2.52
Lu	0.21	0.23	0.21	0.19	0.19	0.16	0.36
Strat	70	70	70	95	95	95	95

Appendix 2. Continued.

Rainier Mesa Member						
Sample Number						
	R8-39	R8-40	R8-41	R8-42	R8-44	R8-45
Weight Percent Oxide (wt %)						
SiO_2	65.63	73.53	73.54	74.19	66.00	64.06
TiO_2	0.48	0.20	0.22	0.27	0.45	0.58
Al_2O_3	16.81	12.83	12.95	12.59	15.96	16.82
FeO	2.23	0.81	0.88	1.02	2.07	2.96
MnO	0.07	0.04	0.05	0.05	0.08	0.08
MgO	0.75	0.07	0.12	0.15	0.88	0.91
CaO	2.07	0.73	0.78	0.75	1.66	2.55
Na_2O	3.72	2.83	2.61	2.86	3.40	3.95
K_2O	5.47	5.93	6.08	5.67	5.57	5.14
P_2O_5	0.11	0.03	0.03	0.03	0.11	0.19
Total	97.34	97.00	97.26	97.58	96.18	97.24
X-ray Fluorescence (ppm)						
Cr	2.60	5.70	6.30	0.00	13.00	10.10
Ni	2.70	0.00	1.00	0.00	0.00	0.00
Cu	0.00	0.00	0.00	0.00	4.90	8.60
Zn	42.70	26.80	16.10	20.90	52.20	70.00
Rb	147.90	112.09	125.06	121.20	146.37	90.15
Sr	490.00	62.92	72.58	68.19	359.18	607.49
Y	26.50	21.25	23.85	21.10	27.16	25.32
Zr	419.00	152.99	169.47	193.70	421.32	603.40
Nb	19.50	14.96	15.85	16.39	14.76	12.81
La	137.54	76.09	82.36	89.85	148.23	132.45
Ba	1917	263	454	433	1379	2070
INAA (ppm)						
Sc	3.20	1.62	1.73	1.95	3.25	4.32
Hf	9.53	4.40	4.87	5.42	8.92	12.54
Th	25.90	29.19	33.19	37.56	29.35	22.17
La	134.01	62.90	83.79	86.51	135.98	112.08
Ce	166.24	98.98	122.99	138.12	160.15	159.21
Sm	8.10	5.32	7.15	6.43	7.30	6.98
Eu	1.89	0.80	0.92	0.69	1.56	1.98
Tb	0.63	0.64	0.68	0.69	0.66	0.60
Yb	2.60	1.48	1.83	1.47	1.91	1.33
Lu	0.25	0.17	0.17	0.10	0.23	0.21
Strat	95	95	95	95	95	95

Appendix 2. Continued.

Rainier Mesa Member						
Sample Number						
	R11-2	R11-3	R11-5	R11-7	R11-9	R11-20
Weight Percent Oxide (wt %)						
SiO_2	67.01	73.97	59.14	74.08	60.01	72.16
TiO_2	0.44	0.11	0.90	0.11	0.75	0.26
Al_2O_3	14.82	12.53	17.46	12.98	17.86	13.40
FeO	1.86	0.50	4.83	0.53	4.03	1.18
MnO	0.08	0.05	0.12	0.10	0.11	0.05
MgO	0.55	0.25	1.79	0.27	1.54	0.16
CaO	1.89	0.67	4.21	0.43	3.79	0.78
Na_2O	3.44	2.41	3.91	2.59	4.30	2.39
K_2O	6.19	6.39	4.17	6.24	4.10	7.13
P_2O_5	0.14	0.02	0.54	0.02	0.40	0.05
Total	96.42	96.90	97.07	97.35	96.89	97.56
X-ray Fluorescence (ppm)						
Cr	9.20	0.00	0.00	0.00	0.00	0.00
Ni	0.00	1.40	0.00	13.00	1.20	0.00
Cu	0.00	0.00	0.00	0.00	4.80	0.00
Zn	49.00	16.30	106.50	8.00	99.20	20.10
Rb	126.35	247.68	123.12	238.42	118.70	165.90
Sr	282.09	0.23	858.78	4.40	917.42	97.46
Y	17.88	28.76	22.94	32.17	20.26	16.30
Zr	400.17	78.50	381.98	78.68	515.36	210.82
Nb	12.92	31.28	13.14	31.16	14.40	16.21
La	135.90	0.00	105.40	36.80	82.90	85.60
Ba	938	0.00	1826	0.00	2067	408
INAA (ppm)						
Sc	3.21	3.66	9.43	4.10	6.35	2.08
Hf	7.85	3.27	8.39	3.09	9.94	4.57
Th	33.89	22.26	18.84	21.11	18.24	31.26
La	123.46	21.81	96.04	23.67	95.82	82.03
Ce	214.54	58.25	190.55	60.34	171.38	135.50
Sm	7.58	5.58	9.41	5.39	7.87	6.03
Eu	1.33	0.12	2.57	0.13	2.43	0.60
Tb	0.58	0.48	1.48	0.44	1.09	0.06
Yb	1.94	2.24	3.23	2.21	2.70	1.18
Lu	0.23	0.31	0.48	0.28	0.40	0.09
Strat	100	100	100	100	100	100

Appendix 2. Continued.

Rainier Mesa Member							
Sample Number							
	R18-1	R18-2	R18-3	R18-4	R18-8	R18-12	R18-16
Weight Percent Oxide (wt %)							
SiO_2	76.12	72.72	74.98	75.58	75.07	75.11	75.42
TiO_2	0.10	0.16	0.11	0.11	0.18	0.12	0.16
Al_2O_3	12.30	14.36	13.03	12.38	12.92	12.49	12.39
FeO	0.56	0.77	0.56	0.53	0.81	0.63	0.72
MnO	0.07	0.05	0.07	0.07	0.05	0.06	0.05
MgO	0.01	0.48	0.25	0.00	0.37	0.04	0.18
CaO	0.39	0.51	0.41	0.42	0.58	0.46	0.58
Na_2O	3.51	2.56	3.05	3.58	2.53	3.41	2.93
K_2O	4.65	5.09	5.10	4.86	5.22	5.20	5.54
P_2O_5	0.01	0.02	0.01	0.01	0.23	0.01	0.02
Total	97.72	96.72	97.57	97.54	97.96	97.53	97.99
X-ray Fluorescence (ppm)							
Cr	0.00	0.00	0.00	0.00	0.00	0.00	0.00
Ni	0.00	0.00	0.00	0.00	0.00	0.00	0.00
Cu	0.00	0.00	0.00	0.00	0.00	0.00	0.00
Zn	26.90	44.10	36.40	33.50	49.60	30.70	28.00
Rb	251.00	155.22	238.56	252.75	151.73	222.31	144.77
Sr	1.88	10.96	0.00	0.47	23.87	0.00	21.61
Y	29.94	22.56	31.77	31.04	20.07	25.65	18.17
Zr	67.21	112.18	80.92	73.46	112.39	83.07	109.77
Nb	27.26	20.42	27.54	26.43	17.56	21.82	11.12
La	27.40	33.60	10.30	36.20	22.00	40.90	39.60
Ba	0.00	0.00	0.00	0.00	0.00	0.00	13
INAA (ppm)							
Sc	4.50	1.61	2.66	0.94	3.63	3.50	3.00
Hf	3.26	4.53	1.96	3.79	4.15	3.93	3.50
Th	21.44	33.72	20.88	23.29	34.49	25.06	31.47
La	26.58	31.40	16.70	31.54	38.23	27.96	36.68
Ce	42.75	79.44	48.70	47.33	88.54	57.59	85.23
Sm	5.37	5.40	5.13	5.43	5.12	5.51	4.97
Eu	0.07	0.17	0.13	0.01	0.25	0.16	0.32
Tb	0.52	0.39	0.49	0.49	0.37	0.40	0.50
Yb	2.94	2.13	1.83	2.75	2.03	2.41	2.01
Lu	0.44	0.33	0.37	0.47	0.26	0.41	0.25
Strat	5.0	5.0	5.0	5.0	5.0	5.0	5.0

Appendix 2. Continued.

Rainier Mesa Member					
Sample Number					
R18-18	R18-19	R18-20	R18-21	R18-22	R18-23
Weight Percent Oxide (wt %)					
SiO_2 76.22	75.41	73.97	75.40	75.00	75.35
TiO_2 0.12	0.11	0.23	0.10	0.12	0.10
Al_2O_3 12.02	12.48	12.64	12.24	12.37	12.35
FeO 0.60	0.48	0.93	0.47	0.56	0.48
MnO 0.05	0.07	0.05	0.07	0.06	0.07
MgO 0.00	0.00	0.17	0.02	0.00	0.04
CaO 0.49	0.43	0.65	0.41	0.50	0.42
Na_2O 3.36	3.53	3.37	3.50	3.52	3.59
K_2O 4.93	4.94	5.23	4.88	5.04	5.03
P_2O_5 0.01	0.01	0.03	0.01	0.01	0.01
Total 97.80	97.46	97.27	97.10	97.18	97.44
X-ray Fluorescence (ppm)					
Cr 0.00	2.00	0.30	0.00	0.00	0.00
Ni 0.00	0.00	0.00	0.00	0.00	0.00
Cu 0.00	0.00	0.00	0.00	0.00	0.00
Zn 24.60	30.30	49.30	36.20	29.70	26.90
Rb 177.93	251.26	127.58	254.47	206.00	253.88
Sr 6.97	0.00	45.52	3.51	6.65	5.27
Y 19.92	27.99	14.28	30.04	23.99	28.15
Zr 87.20	71.32	169.42	68.30	81.61	72.21
Nb 15.01	23.96	15.94	29.33	25.75	27.45
La 51.00	22.30	56.20	4.40	30.10	15.80
Ba 1.0	0.00	94	21	0.00	0.00
INAA (ppm)					
Sc 3.17	3.04	1.86	NA[1]	3.60	3.10
Hf 3.42	3.87	5.10	NA	3.62	3.82
Th 25.72	22.34	33.30	NA	26.16	21.93
La 30.19	29.06	56.73	NA	33.34	28.81
Ce 61.88	46.64	122.61	NA	62.65	45.59
Sm 5.06	5.05	5.99	NA	5.17	5.26
Eu 0.08	0.05	0.54	NA	0.03	0.03
Tb 0.23	0.53	0.30	NA	0.37	0.42
Yb 2.36	3.16	2.16	NA	2.64	2.98
Lu 0.41	0.53	0.32	NA	0.42	0.55
Strat 12.0	12.0	12.0	12.0	12.0	12.0

NA[1] = Not analyzed

Appendix 2. Continued.

Rainier Mesa Member						
Sample Number						
R21-1	R21-5	R21-6	R21-8	R21-9	R21-12	R21-13
Weight Percent Oxide (wt %)						
SiO_2 67.08	73.48	74.20	65.21	74.91	74.52	54.98
TiO_2 0.46	0.27	0.24	0.47	0.20	0.21	1.54
Al_2O_3 15.84	12.72	12.74	16.94	12.34	12.21	16.69
FeO 2.06	1.18	0.98	2.12	0.79	0.85	7.02
MnO 0.10	0.07	0.06	0.11	0.06	0.05	0.14
MgO 0.65	0.61	0.09	0.61	0.08	0.34	3.36
CaO 1.60	0.82	0.67	1.79	0.61	0.59	5.67
Na_2O 3.76	2.89	2.98	3.65	2.81	2.54	3.54
K_2O 5.69	5.38	5.45	5.42	5.55	5.48	3.13
P_2O_5 0.12	0.05	0.03	0.17	0.02	0.03	0.72
Total 97.36	97.47	97.44	96.49	97.37	96.82	96.79
X-ray Fluorescence (ppm)						
Cr 1.10	1.00	0.40	7.10	0.00	0.00	7.50
Ni 0.00	0.00	0.00	0.00	0.00	0.00	0.00
Cu 10.10	5.40	1.10	9.90	3.50	0.30	22.70
Zn 57.10	55.90	37.80	73.60	34.60	32.70	130.90
Rb 99.02	99.18	111.49	90.77	122.20	133.75	67.01
Sr 298.01	66.79	59.29	369.30	31.54	26.96	1099
Y 16.17	14.96	14.86	18.94	14.51	13.94	31.05
Zr 427.13	205.05	187.38	424.95	150.12	166.75	281.58
Nb 13.39	14.76	13.78	14.14	13.01	12.81	12.83
La 154.90	103.94	76.27	153.10	74.03	92.15	104.53
Ba 961	277	263	1321	35	55	1365
INAA (ppm)						
Sc 2.98	1.70	1.87	2.97	2.45	1.79	13.14
Hf 9.18	5.28	5.43	10.25	4.35	5.05	6.16
Th 32.54	32.20	34.69	28.41	31.54	32.43	12.27
La 133.89	76.52	78.50	124.39	69.46	72.62	86.02
Ce 207.74	130.81	135.81	197.11	111.06	118.15	153.48
Sm 7.66	6.63	5.76	8.26	5.38	5.92	10.72
Eu 1.25	0.59	0.60	1.52	0.40	0.40	2.87
Tb 0.72	0.74	0.74	0.73	0.75	0.75	0.68
Yb 1.92	1.84	1.85	1.95	1.86	1.93	2.28
Lu 0.28	0.18	0.25	0.28	0.24	0.28	0.42
Strat 20	20	20	20	20	30	30

Appendix 2. Continued.

Rainier Mesa Member						
Sample Number						
	R21-27	R21-34	R21-35	R21-40	R21-43	R21-44
Weight Percent Oxide (wt %)						
SiO_2	70.27	72.90	67.32	76.13	55.97	74.40
TiO_2	0.33	0.24	0.46	0.13	1.41	0.24
Al_2O_3	14.59	13.23	15.79	11.99	16.80	12.83
FeO	1.51	0.98	2.17	0.61	6.70	1.06
MnO	0.06	0.05	0.08	0.05	0.13	0.05
MgO	0.34	0.20	0.70	0.00	2.90	0.13
CaO	1.12	0.72	1.69	0.51	5.53	0.75
Na_2O	3.60	3.24	3.96	2.88	3.76	3.03
K_2O	5.34	5.72	5.42	5.29	3.13	5.47
P_2O_5	0.07	0.04	0.13	0.01	0.67	0.03
Total	97.23	97.32	97.72	97.60	97.00	97.99
X-ray Fluorescence (ppm)						
Cr	4.10	0.00	6.20	0.00	5.70	11.80
Ni	0.00	0.00	0.00	0.00	0.00	0.00
Cu	0.00	0.00	0.00	0.00	12.80	0.00
Zn	64.30	37.50	57.30	75.60	102.00	45.50
Rb	106.20	122.87	98.67	163.87	65.16	116.25
Sr	228.35	93.50	371.48	22.03	1139.00	69.91
Y	14.48	13.67	11.66	15.31	25.61	14.52
Zr	296.89	187.85	410.88	95.80	324.13	186.51
Nb	12.79	13.57	11.22	18.69	12.38	9.71
La	107.20	78.63	93.37	48.65	92.59	82.90
Ba	945	389	1561	134	1517	258
INAA (ppm)						
Sc	NA	NA	2.89	2.66	11.78	1.73
Hf	NA	NA	7.25	2.66	7.28	3.66
Th	NA	NA	24.40	20.96	13.13	24.06
La	NA	NA	109.72	40.47	70.14	73.02
Ce	NA	NA	162.34	55.41	125.83	87.38
Sm	NA	NA	6.64	5.18	9.14	5.25
Eu	NA	NA	1.47	0.16	2.95	0.55
Tb	NA	NA	0.46	0.33	1.76	0.33
Yb	NA	NA	1.68	0.99	3.54	0.66
Lu	NA	NA	0.23	0.11	0.70	0.07
Strat	10	1000	1000	1000	1000	1000

Appendix 2. Continued.

Rainier Mesa Member							
Sample Number							
	R23-1	R23-4	R23-5	R23-6	R23-11	R23-13	R23-15
Weight Percent Oxide (wt %)							
SiO_2	75.40	74.99	75.39	74.75	75.74	68.37	73.91
TiO_2	0.10	0.20	0.10	0.19	0.10	0.42	0.24
Al_2O_3	11.95	12.07	12.03	12.46	12.20	15.27	12.62
FeO	0.49	0.79	0.47	0.91	0.51	1.87	0.95
MnO	0.06	0.04	0.05	0.04	0.06	0.07	0.05
MgO	0.00	0.11	0.00	0.20	0.07	0.74	0.09
CaO	0.47	0.61	0.40	0.61	0.40	1.48	0.62
Na_2O	2.69	2.58	2.64	2.80	3.15	3.75	3.20
K_2O	5.75	5.45	5.98	5.75	5.16	5.54	5.56
P_2O_5	0.01	0.02	0.01	0.02	0.01	0.12	0.03
Total	96.92	96.86	97.07	97.73	97.40	97.63	97.27
X-ray Fluorescence (ppm)							
Cr	8.10	5.20	0.00	0.00	5.10	9.70	8.30
Ni	0.00	0.00	0.00	0.00	14.90	0.00	0.00
Cu	0.00	0.00	1.90	0.00	0.00	1.90	0.00
Zn	13.50	20.00	15.80	36.60	18.70	42.30	30.30
Rb	234.03	120.78	236.26	131.89	239.27	113.07	120.31
Sr	16.72	84.45	6.26	52.25	2.70	319.06	52.71
Y	28.70	14.56	27.32	12.07	29.93	14.04	12.32
Zr	72.13	145.54	69.53	141.96	76.20	380.66	177.42
Nb	28.95	15.07	31.63	18.85	28.52	13.42	10.86
La	25.60	43.70	36.10	36.20	12.30	98.40	64.10
Ba	0.00	207	56	257	0.00	1271	234
INAA (ppm)							
Sc	1.94	1.31	2.72	NA	NA	4.13	1.06
Hf	1.22	3.72	1.66	NA	NA	7.22	3.26
Th	18.51	26.73	20.48	NA	NA	25.23	30.46
La	18.20	59.99	21.35	NA	NA	80.68	61.32
Ce	42.80	95.64	47.83	NA	NA	143.67	110.08
Sm	4.99	5.93	5.13	NA	NA	6.60	5.60
Eu	0.13	0.51	0.13	NA	NA	1.41	0.34
Tb	0.37	0.29	0.42	NA	NA	0.50	0.21
Yb	1.61	1.11	1.74	NA	NA	1.40	0.87
Lu	0.33	0.23	0.37	NA	NA	0.28	0.18
Strat	100	100	100	100	100	100	100

Appendix 2. Continued.

Rainier Mesa Member							
Sample Number							
	R23-16	R23-17	R23-21	R23-22	R23-23	R23-24	R23-26
Weight Percent Oxide (wt %)							
SiO_2	66.82	57.36	72.17	75.29	76.09	58.08	62.73
TiO_2	0.46	1.18	0.23	0.10	0.14	1.11	0.59
Al_2O_3	15.60	16.97	13.53	12.31	11.83	17.03	17.68
FeO	2.08	5.81	1.02	0.50	0.65	5.59	2.94
MnO	0.08	0.13	0.05	0.06	0.05	0.12	0.09
MgO	0.68	2.59	0.24	0.00	0.07	2.46	1.06
CaO	1.71	5.05	0.89	0.42	0.49	4.66	2.73
Na_2O	3.86	3.87	3.34	3.19	2.89	3.89	4.55
K_2O	5.48	3.57	5.53	5.46	5.32	3.56	5.07
P_2O_5	0.13	0.61	0.05	0.01	0.01	0.55	0.20
Total	96.90	97.14	97.05	97.34	97.54	97.05	97.64
X-ray Fluorescence (ppm)							
Cr	0.00	8.10	4.80	8.80	2.80	0.00	8.50
Ni	0.00	0.00	0.00	14.70	0.00	0.00	0.00
Cu	0.00	7.70	0.00	0.00	0.00	10.80	4.70
Zn	51.80	90.90	27.20	19.70	25.30	90.60	53.70
Rb	104.57	71.48	129.09	248.90	160.36	72.73	76.66
Sr	327.61	1063	133.31	17.38	10.06	1064	676.21
Y	16.60	26.41	13.23	29.42	17.54	21.28	13.26
Zr	400.66	341.62	194.75	71.29	89.69	357.69	566.44
Nb	17.16	12.57	14.65	25.11	19.50	12.67	11.98
La	125.70	69.90	77.20	33.00	57.20	80.00	113.50
Ba	1129	1746	470	0.00	0.00	1798	2883
INAA (ppm)							
Sc	3.95	10.26	0.88	3.20	NA	9.38	5.26
Hf	9.24	9.68	3.40	1.31	NA	10.47	13.29
Th	30.59	14.83	25.43	19.61	NA	14.94	21.80
La	119.52	80.92	61.00	17.83	NA	80.43	101.15
Ce	198.84	153.76	106.20	44.98	NA	149.70	173.35
Sm	7.79	9.39	5.67	5.33	NA	9.18	7.44
Eu	1.60	2.94	0.59	0.13	NA	2.79	2.49
Tb	0.66	1.43	0.28	0.40	NA	1.28	0.73
Yb	1.60	2.88	0.85	1.64	NA	2.67	1.83
Lu	0.34	0.58	0.20	0.37	NA	0.54	0.39
Strat	100	100	100	100	100	100	100

Appendix 2. Continued.

Rainier Mesa Member						
Sample Number						
	R23-27	R25-1	R25-11	R25-12	R25-14	R25-16
Weight Percent Oxide (wt %)						
SiO_2	56.66	75.97	72.32	75.27	73.86	75.68
TiO_2	1.36	0.13	0.29	0.11	0.24	0.15
Al_2O_3	17.05	11.64	13.82	12.45	12.90	12.19
FeO	6.63	0.74	1.15	0.42	0.86	0.56
MnO	0.13	0.10	0.06	0.05	0.05	0.04
MgO	2.84	0.18	0.31	0.03	0.28	0.08
CaO	5.38	0.50	0.81	0.38	0.56	0.50
Na_2O	3.65	2.84	3.22	2.78	3.05	2.77
K_2O	3.46	5.76	5.26	5.55	5.30	5.54
P_2O_5	0.67	0.10	0.06	0.01	0.03	0.01
Total	97.83	97.96	97.30	97.05	97.13	97.52
X-ray Fluorescence (ppm)						
Cr	0.90	0.00	0.00	1.40	0.00	0.00
Ni	0.00	12.40	0.00	0.00	1.70	0.00
Cu	15.60	0.00	0.00	0.00	0.00	0.00
Zn	90.70	32.80	156.80	95.00	108.00	32.70
Rb	63.69	240.85	161.35	272.61	272.23	220.07
Sr	1083	7.45	84.66	0.00	47.10	9.22
Y	26.31	40.46	18.99	30.88	14.72	25.63
Zr	381.54	127.96	239.99	82.73	186.98	104.17
Nb	12.03	35.00	16.28	27.09	15.80	17.07
La	82.00	19.80	82.60	12.40	76.70	40.90
Ba	1418	0.00	288	0.00	154	0.00
INAA (ppm)						
Sc	NA	1.93	2.44	3.47	2.00	2.47
Hf	NA	4.48	5.18	3.16	4.41	3.25
Th	NA	31.12	31.59	21.75	31.22	28.46
La	NA	33.51	93.86	23.06	70.44	42.30
Ce	NA	79.59	156.19	57.22	125.41	81.96
Sm	NA	6.13	6.37	5.07	5.43	5.35
Eu	NA	0.26	0.72	0.13	0.49	0.17
Tb	NA	0.40	0.38	0.43	0.24	0.21
Yb	NA	2.33	1.64	2.14	1.40	1.33
Lu	NA	0.30	0.17	0.28	0.13	0.14
Strat	100	100	100	100	100	100

Appendix 2. Continued.

Rainier Mesa Member					
Sample Number					
R25-20	R25-21	R26-3	R26-6	R26-7	R26-9
Weight Percent Oxide (wt %)					
SiO_2 76.07	66.77	74.12	74.06	74.13	73.22
TiO_2 0.10	0.43	0.19	0.20	0.20	0.21
Al_2O_3 12.48	16.13	12.37	12.72	12.17	12.91
FeO 0.35	1.90	0.77	0.78	0.86	0.86
MnO 0.05	0.07	0.05	0.05	0.05	0.05
MgO 0.01	0.66	0.09	0.17	0.12	0.13
CaO 0.36	1.76	0.54	0.58	0.59	0.60
Na_2O 2.94	4.01	2.78	2.65	2.83	2.88
K_2O 5.50	5.00	6.08	6.42	5.91	6.44
P_2O_5 0.01	0.11	0.02	0.03	0.03	0.03
Total 97.87	96.84	97.01	97.66	96.89	97.33
X-ray Fluorescence (ppm)					
Cr 0.00	0.00	0.00	0.00	0.00	0.00
Ni 7.00	5.50	0.00	0.00	0.00	4.60
Cu 0.00	0.00	0.00	0.00	0.00	0.00
Zn 59.90	85.90	15.90	14.40	22.40	16.30
Rb 337.53	137.21	151.87	148.76	130.48	131.31
Sr 0.00	326.07	27.53	34.36	26.15	51.02
Y 28.26	16.22	15.17	13.27	14.58	13.62
Zr 68.25	420.57	149.89	138.09	152.76	159.44
Nb 28.50	11.31	14.10	11.49	13.81	11.28
La 11.40	110.40	48.40	43.70	48.20	65.80
Ba 31	1168	28	0.00	0.00	218
INAA (ppm)					
Sc 3.88	3.71	NA	NA	NA	NA
Hf 2.90	7.52	NA	NA	NA	NA
Th 19.28	26.92	NA	NA	NA	NA
La 22.27	120.84	NA	NA	NA	NA
Ce 49.76	186.42	NA	NA	NA	NA
Sm 4.98	6.93	NA	NA	NA	NA
Eu 0.06	1.41	NA	NA	NA	NA
Tb 0.43	0.56	NA	NA	NA	NA
Yb 1.92	1.68	NA	NA	NA	NA
Lu 0.26	0.23	NA	NA	NA	NA
Strat 100	100	100	100	100	100

Appendix 2. Continued.

Rainier Mesa Member							
Sample Number							
	R26-11	R26-13	R26-16	R26-17	R26-18	R26-22	R26-24
Weight Percent Oxide (wt %)							
SiO_2	73.92	71.87	75.27	73.68	73.41	75.07	75.23
TiO_2	0.22	0.32	0.16	0.20	0.18	0.18	0.16
Al_2O_3	12.47	13.45	12.06	13.22	13.07	12.13	12.26
FeO	0.91	1.38	0.74	0.99	1.01	0.86	0.76
MnO	0.05	0.06	0.05	0.04	0.05	0.05	0.04
MgO	0.25	0.38	0.10	0.57	0.39	0.17	0.14
CaO	0.80	0.88	0.55	0.48	0.54	0.51	0.50
Na_2O	2.89	2.98	2.91	2.58	2.37	2.46	2.53
K_2O	6.02	5.96	5.59	5.03	5.88	6.03	6.04
P_2O_5	0.03	0.05	0.02	0.02	0.02	0.02	0.01
Total	97.56	97.33	97.45	96.81	96.92	97.48	97.67
X-ray Fluorescence (ppm)							
Cr	0.00	0.00	0.00	0.00	0.00	0.00	0.00
Ni	4.30	0.00	0.00	0.00	0.00	0.00	11.40
Cu	0.00	0.00	0.00	0.00	0.00	0.00	0.00
Zn	17.50	35.70	23.10	26.00	31.60	30.00	19.60
Rb	119.75	118.19	154.90	123.87	156.20	151.23	142.02
Sr	53.31	86.26	14.90	18.41	29.10	11.44	23.84
Y	15.79	18.16	18.68	17.32	21.43	19.86	12.71
Zr	167.97	249.67	114.03	136.51	127.08	133.34	116.68
Nb	11.37	10.50	13.55	15.28	17.36	15.61	14.48
La	66.70	81.10	28.60	28.20	63.30	62.00	48.20
Ba	73	286	0.00	20	0.00	0.00	64
INAA (ppm)							
Sc	NA	NA	NA	NA	NA	NA	NA
Hf	NA	NA	NA	NA	NA	NA	NA
Th	NA	NA	NA	NA	NA	NA	NA
La	NA	NA	NA	NA	NA	NA	NA
Ce	NA	NA	NA	NA	NA	NA	NA
Sm	NA	NA	NA	NA	NA	NA	NA
Eu	NA	NA	NA	NA	NA	NA	NA
Tb	NA	NA	NA	NA	NA	NA	NA
Yb	NA	NA	NA	NA	NA	NA	NA
Lu	NA	NA	NA	NA	NA	NA	NA
Strat	100	3	3	3	3	3	3

Appendix 2. Continued.

Rainier Mesa Member						
Sample Number						
	R26-2A	R26-4A	R26-6A	R26-7A	R26-9A	R26-10A
Weight Percent Oxide (wt %)						
SiO_2	68.01	75.89	68.87	66.94	73.85	67.70
TiO_2	0.44	0.17	0.36	0.46	0.22	0.42
Al_2O_3	14.89	11.90	15.13	15.32	13.25	15.09
FeO	1.93	0.65	1.60	1.96	0.96	1.67
MnO	0.08	0.04	0.07	0.09	0.05	0.08
MgO	0.73	0.42	0.44	0.85	0.16	0.55
CaO	1.49	0.73	1.21	1.63	0.67	1.31
Na_2O	3.51	2.47	3.65	3.44	3.02	3.78
K_2O	6.15	6.10	6.21	6.02	6.09	6.13
P_2O_5	0.14	0.11	0.08	0.13	0.03	0.10
Total	97.37	98.48	97.62	96.84	98.30	96.83
X-ray Fluorescence (ppm)						
Cr	0.00	0.00	0.40	0.00	0.00	0.00
Ni	0.00	0.00	2.40	0.00	13.30	6.60
Cu	0.00	0.00	0.00	0.00	0.00	0.00
Zn	46.40	16.00	26.70	47.10	12.80	29.20
Rb	110.27	131.28	103.75	101.88	120.43	100.07
Sr	199.46	31.84	158.72	247.00	48.61	191.37
Y	15.61	18.44	16.63	19.18	16.26	17.00
Zr	376.25	128.13	311.97	419.79	147.71	384.84
Nb	13.09	16.53	16.00	16.65	15.41	14.62
La	118.10	42.60	136.70	149.60	48.70	126.20
Ba	803	35	695	1064	92	640
INAA (ppm)						
Sc	NA	NA	NA	NA	NA	NA
Hf	NA	NA	NA	NA	NA	NA
Th	NA	NA	NA	NA	NA	NA
La	NA	NA	NA	NA	NA	NA
Ce	NA	NA	NA	NA	NA	NA
Sm	NA	NA	NA	NA	NA	NA
Eu	NA	NA	NA	NA	NA	NA
Tb	NA	NA	NA	NA	NA	NA
Yb	NA	NA	NA	NA	NA	NA
Lu	NA	NA	NA	NA	NA	NA
Strat	100	100	100	100	100	100

Appendix 2. Continued.

Rainier Mesa Member				
Sample Number				
	R26-13A	R26-14A	R26-16A	R26-17A
Weight Percent Oxide (wt %)				
SiO_2	75.35	74.45	66.01	70.59
TiO_2	0.17	0.09	0.46	0.25
Al_2O_3	12.12	12.40	15.22	12.63
FeO	0.87	0.51	2.02	1.02
MnO	0.05	0.06	0.08	0.06
MgO	0.11	0.00	0.87	1.00
CaO	0.61	0.53	2.01	1.77
Na_2O	2.40	3.06	3.52	2.78
K_2O	6.32	5.90	6.13	5.88
P_2O_5	0.05	0.01	0.17	0.12
Total	98.05	97.01	96.49	96.10
X-ray Fluorescence (ppm)				
Cr	0.00	0.00	0.00	0.00
Ni	10.10	9.10	1.20	3.10
Cu	0.00	0.00	0.00	0.00
Zn	17.50	5.70	42.70	23.00
Rb	139.62	243.58	97.66	105.89
Sr	22.82	0.00	272.98	103.66
Y	17.77	32.73	18.52	17.76
Zr	116.87	69.83	428.09	200.05
Nb	16.07	34.68	14.81	12.01
La	46.50	12.40	126.80	77.60
Ba	217	0.00	1264	245
INAA (ppm)				
Sc	NA	NA	NA	NA
Hf	NA	NA	NA	NA
Th	NA	NA	NA	NA
La	NA	NA	NA	NA
Ce	NA	NA	NA	NA
Sm	NA	NA	NA	NA
Eu	NA	NA	NA	NA
Tb	NA	NA	NA	NA
Yb	NA	NA	NA	NA
Lu	NA	NA	NA	NA
Strat	100	100	100	100

Appendix 2. Continued.

Ammonia Tanks Member							
Sample Number							
	A4-6	A4-12	A4-14	A4-16	A4-17	A4-53	A4-55
Weight Percent Oxide (wt %)							
SiO_2	75.53	76.15	76.11	63.35	75.94	74.77	67.90
TiO_2	0.13	0.14	0.14	0.68	0.13	0.17	0.36
Al_2O_3	11.71	11.90	11.95	17.24	11.69	12.23	15.98
FeO	0.65	0.73	0.66	2.81	0.62	0.72	1.47
MnO	0.08	0.09	0.08	0.16	0.08	0.07	0.09
MgO	0.08	0.21	0.00	0.84	0.00	0.00	0.32
CaO	0.43	0.41	0.42	2.14	0.36	0.41	1.15
Na_2O	3.53	3.27	3.68	4.64	3.19	2.95	4.53
K_2O	4.90	5.15	4.90	5.26	5.20	6.08	6.12
P_2O_5	0.01	0.01	0.01	0.16	0.01	0.01	0.06
Total	97.05	98.06	97.95	97.28	97.22	97.41	97.98
X-ray Fluorescence (ppm)							
Cr	2.00	0.00	0.00	5.00	10.10	0.00	0.30
Ni	4.50	5.40	0.00	0.00	0.00	6.90	0.00
Cu	0.00	0.00	0.00	0.00	0.00	0.00	0.00
Zn	38.80	38.80	37.10	193.20	25.00	23.90	40.20
Rb	217.22	232.69	231.81	122.62	238.23	188.06	123.01
Sr	7.75	4.77	0.00	372.13	3.09	2.48	180.90
Y	31.46	28.57	34.19	28.88	31.31	39.27	28.80
Zr	123.24	123.00	126.23	720.86	118.65	165.32	326.08
Nb	36.50	31.75	33.92	20.01	34.26	32.84	23.61
La	15.86	46.80	44.25	170.42	38.74	65.34	116.07
Ba	136	197	296	2478	193	169	852
INAA (ppm)							
Sc	1.57	1.62	1.89	6.98	1.59	1.29	3.46
Hf	3.73	3.68	5.24	15.62	3.59	5.73	8.77
Th	23.48	24.59	34.32	16.85	23.99	27.73	20.97
La	29.65	34.31	34.50	200.17	32.30	48.07	103.28
Ce	49.24	51.12	68.46	295.39	49.62	85.75	171.53
Sm	5.20	5.39	6.45	10.61	4.92	8.12	8.62
Eu	0.11	0.14	0.26	3.34	0.08	0.39	1.32
Tb	0.42	0.38	0.68	0.57	0.36	0.65	0.61
Yb	1.35	1.42	4.31	2.45	1.25	3.73	3.17
Lu	0.20	0.24	0.41	0.40	0.20	0.36	0.33
Strat	10	10	10	10	10	160	160

Appendix 2. Continued.

Ammonia Tanks Member						
Sample Number						
	A4-69	A4-70	A4-75	A5-2	A5-3	A5-4
Weight Percent Oxide (wt %)						
SiO_2	75.04	70.42	61.38	67.52	75.87	68.71
TiO_2	0.13	0.32	0.75	0.43	0.13	0.30
Al_2O_3	11.81	14.35	16.90	15.51	11.80	14.47
FeO	0.67	1.35	3.16	1.53	0.56	1.26
MnO	0.08	0.09	0.12	0.11	0.08	0.09
MgO	0.03	0.19	1.61	0.61	0.00	0.91
CaO	0.37	0.91	2.52	0.91	0.35	1.78
Na_2O	2.89	3.74	4.21	4.15	3.17	3.66
K_2O	5.95	6.02	5.27	6.12	5.35	5.97
P_2O_5	0.01	0.05	0.33	0.06	0.01	0.07
Total	96.98	97.44	96.25	96.95	97.32	97.22
X-ray Fluorescence (ppm)						
Cr	5.80	4.20	5.90	0.00	0.00	4.40
Ni	6.00	0.00	0.00	0.00	0.00	0.00
Cu	0.00	0.00	0.00	0.00	0.00	0.00
Zn	23.90	31.00	67.70	52.90	66.10	44.00
Rb	211.58	146.89	82.29	135.91	211.29	155.14
Sr	0.00	131.08	478.56	77.62	2.42	174.17
Y	32.08	30.57	33.08	32.96	33.08	33.23
Zr	128.86	296.78	818.33	444.30	116.99	292.77
Nb	33.35	27.02	20.49	23.77	29.21	26.92
La	35.59	78.59	146.16	140.14	51.53	76.19
Ba	131	620	3820	366	74	622
INAA (ppm)						
Sc	1.63	2.71	6.87	4.00	1.34	2.67
Hf	5.06	5.70	16.70	11.21	4.77	8.87
Th	32.46	18.21	13.52	21.57	29.94	21.83
La	31.78	74.21	150.94	148.65	29.71	89.98
Ce	64.26	103.41	228.98	240.96	59.71	149.84
Sm	5.56	7.83	9.75	10.95	5.63	8.24
Eu	0.31	0.80	3.38	1.54	0.21	1.03
Tb	0.67	0.58	0.56	0.73	0.74	0.74
Yb	3.72	1.43	2.52	2.71	2.91	2.67
Lu	0.37	0.25	0.34	0.46	0.52	0.48
Strat	175	175	175	1	1	1

Appendix 2. Continued.

Ammonia Tanks Member							
Sample Number							
	A5-8	A5-9	A5-25	A5-29	A5-30	A5-31	A5-35
Weight Percent Oxide (wt %)							
SiO_2	75.72	69.13	75.29	75.12	63.36	61.03	70.85
TiO_2	0.16	0.41	0.14	0.14	0.69	0.82	0.28
Al_2O_3	12.27	15.22	12.12	12.25	16.89	17.54	14.10
FeO	0.58	1.65	0.63	0.55	2.39	3.61	1.21
MnO	0.08	0.11	0.08	0.08	0.11	0.12	0.08
MgO	0.00	0.36	0.02	0.00	0.84	1.47	0.25
CaO	0.37	1.00	0.37	0.39	1.63	2.86	0.73
Na_2O	3.28	4.02	2.94	3.24	4.47	4.76	3.60
K_2O	5.49	6.22	5.61	5.48	5.97	4.58	5.98
P_2O_5	0.01	0.06	0.01	0.01	0.18	0.32	0.04
Total	97.96	98.18	97.21	97.26	96.53	97.11	97.12
X-ray Fluorescence (ppm)							
Cr	0.00	0.06	2.50	0.00	1.60	3.90	2.70
Ni	0.00	0.00	0.00	0.00	0.00	0.00	0.00
Cu	0.00	0.00	0.00	0.00	0.00	0.00	0.00
Zn	31.80	54.10	29.00	28.60	103.30	135.30	42.10
Rb	219.01	141.94	216.29	224.34	95.47	102.16	163.95
Sr	0.00	128.69	2.88	0.00	250.47	574.35	81.93
Y	34.04	32.11	34.23	37.00	29.10	37.22	32.28
Zr	144.44	381.08	132.74	126.18	712.34	887.96	250.88
Nb	38.52	28.98	30.49	34.36	16.90	18.04	26.55
La	11.38	106.56	56.44	36.30	240.41	146.97	66.75
Ba	121	691	90	0.00	2128	3616	394
INAA (ppm)							
Sc	1.71	4.18	1.43	1.46	6.14	6.28	2.31
Hf	5.98	11.60	5.26	4.97	16.09	19.11	7.98
Th	33.89	23.17	32.09	32.10	17.36	12.57	24.33
La	35.94	116.42	34.61	29.89	225.00	148.31	71.04
Ce	75.67	196.41	65.02	61.59	382.56	235.16	130.78
Sm	6.90	10.07	5.71	6.12	12.41	10.39	8.62
Eu	0.35	1.33	0.25	0.18	3.20	3.36	0.64
Tb	0.72	0.72	0.73	0.74	0.70	0.72	0.74
Yb	3.24	2.80	2.88	2.99	2.34	2.52	2.72
Lu	0.63	0.53	0.55	0.54	0.41	0.47	0.47
Strat	1	1	30	30	30	30	30

Appendix 2. Continued.

Ammonia Tanks Member							
Sample Number							
	A5-37	A5-56	A5-58	A5-63	A5-65	A5-68	A5-69
Weight Percent Oxide (wt %)							
SiO_2	75.51	75.61	67.38	60.23	67.97	72.31	59.43
TiO_2	0.14	0.14	0.38	0.87	0.44	0.23	0.96
Al_2O_3	11.86	11.89	15.67	17.47	15.60	13.83	17.45
FeO	0.68	0.55	1.42	3.72	1.62	1.02	4.30
MnO	0.08	0.06	0.10	0.12	0.11	0.08	0.12
MgO	0.00	0.00	0.32	1.51	0.27	0.11	1.70
CaO	0.35	0.30	1.11	3.15	0.93	0.72	3.29
Na_2O	3.10	2.97	4.18	4.63	4.15	3.72	4.48
K_2O	5.47	5.83	6.67	4.93	6.63	5.93	4.81
P_2O_5	0.01	0.00	0.06	0.34	0.07	0.03	0.39
Total	97.20	97.36	97.29	96.97	97.79	97.98	96.93
X-ray Fluorescence (ppm)							
Cr	0.00	0.00	1.20	0.00	0.00	0.00	8.20
Ni	0.00	0.00	0.00	0.00	0.00	0.00	8.30
Cu	0.00	0.00	0.00	0.00	0.00	0.00	0.00
Zn	28.90	25.20	38.40	94.50	46.40	33.60	99.50
Rb	222.81	208.80	121.80	78.89	122.17	152.68	69.31
Sr	0.00	0.00	126.21	613.65	71.98	70.15	652.52
Y	33.55	34.46	31.75	31.61	34.90	32.23	32.20
Zr	128.55	129.91	396.32	865.57	488.43	223.42	985
Nb	36.58	39.85	26.63	20.81	24.41	22.15	14.30
La	0.64	30.12	125.34	118.57	169.76	37.36	136.53
Ba	0.00	46	709	3990	499	373	4073
INAA (ppm)							
Sc	1.74	1.42	3.93	6.87	4.18	1.28	7.29
Hf	4.84	5.05	11.00	18.88	12.74	6.98	19.58
Th	31.55	32.45	20.12	12.09	21.12	23.02	11.77
La	31.91	31.76	120.76	137.60	146.14	52.72	133.86
Ce	61.62	66.39	223.31	228.70	264.81	102.78	228.11
Sm	6.03	5.64	10.22	10.35	10.49	6.81	9.88
Eu	0.18	0.21	1.49	3.50	1.57	0.50	3.44
Tb	0.74	0.74	0.74	0.72	0.72	0.75	0.72
Yb	2.91	3.05	2.68	2.37	2.80	2.66	2.36
Lu	0.52	0.56	0.44	0.40	0.53	0.46	0.41
Strat	30	90	90	90	90	90	100

Appendix 2. Continued.

Ammonia Tanks Member						
Sample Number						
	A5-71	A5-72	A5-75	A5-79	A21-18	A21-19
Weight Percent Oxide (wt %)						
SiO_2	65.02	61.86	57.68	74.90	75.11	74.52
TiO_2	0.54	0.69	1.11	0.13	0.14	0.13
Al_2O_3	16.61	17.58	17.69	12.16	12.13	12.63
FeO	1.84	3.01	4.90	0.64	0.72	0.72
MnO	0.10	0.11	0.12	0.07	0.08	0.08
MgO	0.52	1.11	2.17	0.21	0.00	0.32
CaO	1.31	2.52	4.08	0.47	0.41	0.35
Na_2O	4.28	4.27	4.60	2.74	3.55	2.99
K_2O	6.77	5.28	4.20	6.21	5.07	5.30
P_2O_5	0.11	0.23	0.47	0.01	0.01	0.01
Total	97.10	96.66	97.02	97.54	97.22	97.05
X-ray Fluorescence (ppm)						
Cr	4.20	2.30	0.00	1.20	0.00	0.00
Ni	0.00	0.00	0.00	0.00	0.00	0.00
Cu	0.00	0.00	0.00	0.00	1.00	0.00
Zn	47.30	78.20	96.00	28.00	53.30	55.90
Rb	85.11	76.50	66.18	208.29	218.76	208.97
Sr	155.05	520.88	819.54	4.03	3.80	0.00
Y	28.21	30.17	29.77	29.47	30.06	27.64
Zr	542.25	819	982	125.44	131.30	128.13
Nb	14.01	17.01	11.23	28.04	28.38	28.30
La	242.35	131.41	107.46	23.49	50.51	51.70
Ba	1168	3560	4703	24	0.00	25
INAA (ppm)						
Sc	6.37	6.27	8.06	0.97	1.34	1.54
Hf	12.26	17.78	18.60	4.91	5.22	3.92
Th	19.58	13.30	11.41	30.52	29.95	24.19
La	232.94	134.56	128.25	29.75	34.67	28.48
Ce	393.01	238.70	217.23	56.80	64.01	49.65
Sm	13.12	9.61	8.93	5.22	5.80	5.51
Eu	2.60	2.99	3.30	0.13	0.09	0.12
Tb	0.72	0.73	0.72	0.75	0.76	0.47
Yb	2.37	2.54	2.40	2.97	3.11	1.30
Lu	0.49	0.44	0.31	0.51	0.55	0.22
Strat	100	100	100	100	3	3

Appendix 2. Continued.

Ammonia Tanks Member		
	Sample Number	
	A21-23	A21-26
	Weight Percent Oxide (wt %)	
SiO_2	74.57	75.49
TiO_2	0.13	0.13
Al_2O_3	12.41	12.09
FeO	0.69	0.71
MnO	0.08	0.08
MgO	0.01	0.00
CaO	0.37	0.37
Na_2O	3.75	3.60
K_2O	4.70	4.99
P_2O_5	0.01	0.00
Total	96.72	97.46
	X-ray Fluorescence (ppm)	
Cr	0.00	0.00
Ni	0.00	0.00
Cu	1.60	0.00
Zn	55.30	54.20
Rb	217.90	222.23
Sr	4.79	2.42
Y	27.16	34.00
Zr	120.08	125.52
Nb	31.03	31.15
La	44.27	34.22
Ba	128	104
	INAA (ppm)	
Sc	1.58	1.69
Hf	5.31	5.58
Th	31.96	32.76
La	33.06	32.04
Ce	57.84	69.90
Sm	5.24	6.13
Eu	0.17	0.16
Tb	0.75	0.74
Yb	2.76	2.98
Lu	0.50	0.55
Strat	3	3

APPENDIX 3

Analytical Techniques
Major and Trace Elements (XRF)
Trace Elements (INAA)
Phenocryst Compositions
Magnetite/Ilmenite Analyses

ANALYTICAL TECHNIQUE

Major and Trace Elements (XRF)

Over 130 glassy pumice fragments from the Timber Mountain Tuff were prepared for x-ray fluorescence analysis. All of the weathered rind and ashy matrix was cleaned off of each sample. The pumice fragments were then coarse crushed into 3 mm to 5 mm sized pieces in a ceramic mortar and pestle. The crushed sample (including fines) was then boiled for 30 minutes in a carbonate leach solution (13.5 ml glacial acetic acid, 41 g sodium acetate, and 470 ml distilled water) to remove any secondary carbonate mineralization (Jackson, 1979). The residue was then oven dried, hand ground in an agate mortar and pestle to -200 mesh, and stored in polyvinyl vials. Before fusing, the samples were vacuum-oven dried at 110 ^{o}C for 24 hours. Finally, each sample was fused in platinum-gold alloy crucibles and molded into a glass wafer. For each wafer, a mixture of 9.0 g $Li_2B_4O_7$, 1.0 g sample, and 0.16 g NH_3NO_4 was used (all weights +/- 0.0005 g).

For all samples, all major-element oxides and eleven trace elements were collected by an automated Rigaku (S-Max) X-ray fluorescence (XRF) spectrometer at Michigan State University. The Criss matrix absorption parameter was used to correct all major-element XRF analyses (Criss, 1980). U.S. Geological Survey (USGS) whole-rock standards

were run with each sample set as both known and unknown samples. Results of the USGS standards run as unknowns are listed in Table A3a (major elements) and Table A3b (trace elements) along with the published concentrations. Trace elements determined by XRF include Cr, Ni, Cu, Zn, Rb, Sr, Y, Zr, Nb, La, and Ba. Trace element concentrations were determined by linear regression on analyzed USGS standards. Matrix adsorption effects during trace element analysis were corrected for by using the Compton peak as an internal reference peak correction factor as described by Reynolds (1963, 1967) and Wilband (1975).

All major element data cited in this study has been recalculated to 100% anhydrous conditions with the exception of the raw data in Appendix 2. Iron is reported as FeO_{total} and H_2O^- and H_2O^+ were not determined.

Trace Elements (INAA)

Most samples of the Timber Mountain Tuff were analyzed by INAA (Instrumental Neutron Activation Analysis). Each sample consisted of a one gram split of the XRF powder (see preparation technique above). Each sample was then heat sealed in a polyvinyl rabbit and then irradiated.

Most samples were activated with the Triga Mark III reactor at Michigan State University under a neutron flux

Table A3a. X-ray fluorescence major element concentrations of USGS standards run as unknowns compared to the reported concentrations in Govindaraju (1984).

AGV-1	SiO2	Al2O3	FeO	MgO	CaO	Na2O	K2O	TiO2	P2O5	MnO	Total
Reported	59.25	17.15	6.53	1.53	4.94	4.25	2.90	1.06	0.48	0.01	
Analysis 1	59.96	17.12	6.19	1.51	4.96	4.30	2.94	1.07	0.51	0.10	98.66
Analysis 2	60.41	17.44	6.15	1.50	5.00	4.31	2.94	1.07	0.51	0.10	99.44
Analysis 3	60.02	17.09	6.16	1.56	4.99	4.23	2.94	1.09	0.51	0.10	98.69
Uncertainty	1.16	0.29	0.38	0.03	0.06	0.06	0.04	0.03	0.03	0.00	

BCR-1	SiO2	Al2O3	FeO	MgO	CaO	Na2O	K2O	TiO2	P2O5	MnO	Total
Reported	54.35	13.63	12.47	3.45	6.95	3.27	1.69	2.22	0.37	0.19	
Analysis 1	54.87	13.59	12.01	3.79	6.95	3.20	1.71	2.25	0.38	0.19	98.96
Uncertainty	0.52	0.04	0.46	0.34	0.00	0.07	0.02	0.03	0.01	0.00	

GSP-1	SiO2	Al2O3	FeO	MgO	CaO	Na2O	K2O	TiO2	P2O5	MnO	Total
Reported	67.37	15.16	4.06	0.99	2.04	2.80	5.51	0.66	0.28	0.04	
Analysis 1	67.29	14.93	3.79	1.00	2.07	2.80	5.52	0.67	0.29	0.04	98.39
Uncertainty	0.08	0.23	0.27	0.01	0.03	0.00	0.01	0.01	0.01	0.00	

G-1	SiO2	Al2O3	FeO	MgO	CaO	Na2O	K2O	TiO2	P2O5	MnO	Total
Reported	72.46	14.23	1.85	0.39	1.38	3.33	5.48	0.25	0.09	0.03	
Analysis 1	71.75	14.24	1.88	0.39	1.33	3.37	5.50	0.26	0.09	0.03	98.83
Uncertainty	0.71	0.01	0.03	0.00	0.05	0.04	0.02	0.01	0.00	0.00	

G-2	SiO2	Al2O3	FeO	MgO	CaO	Na2O	K2O	TiO2	P2O5	MnO	Total
Reported	69.04	15.14	2.52	0.76	1.97	4.07	4.49	0.50	0.14	0.03	
Analysis 1	69.61	15.44	2.38	0.74	1.98	4.07	4.48	0.49	0.13	0.03	99.35
Analysis 2	69.62	15.46	2.36	0.79	1.99	4.12	4.48	0.48	0.14	0.03	99.47
Analysis 3	69.74	15.60	2.36	0.76	1.99	4.14	4.48	0.50	0.14	0.03	99.75
Analysis 4	69.26	15.18	2.37	0.77	2.00	4.06	4.48	0.50	0.14	0.03	98.77
Analysis 5	69.62	15.34	2.35	0.74	2.00	4.04	4.48	0.49	0.14	0.03	99.22
Uncertainty	0.70	0.46	0.17	0.03	0.03	0.07	0.01	0.02	0.01	0.00	

Table A3a. Continued.

W-1											
	SiO2	Al2O3	FeO	MgO	CaO	Na2O	K2O	TiO2	P2O5	MnO	Total
Reported	52.55	14.99	10.21	6.62	10.94	2.13	0.64	1.07	0.14	0.17	
Analysis 1	52.38	14.89	10.13	6.69	10.97	2.15	0.64	1.10	0.14	0.17	99.27
Analysis 2	52.72	15.08	9.93	6.60	10.87	2.09	0.63	1.08	0.15	0.17	99.32
Uncertainty	0.22	0.10	0.28	0.07	0.07	0.04	0.01	0.03	0.01	0.00	

Table A3b. X-ray fluorescence trace element concentrations of USGS standards run as unknowns compared to reported concentrations in Govindaraju (1984).

AGV-1

	Cr	Ni	Cu	Zn	Rb	Sr	Y	Zr	Nb	La	Ba
Reported	12	17	60	88	67	660	21	225	15	37	1220
Analysis 1	19.5	12.8	66.2	83	78	667	24.8	229	18.7	51.0	1444
Analysis 2	26.0	4.1	65.7	91	68	665	25.0	227	10.2	32.9	1249
Analysis 3	16.7	5.2	56.1	88	70	662	25.2	227	7.5	58.8	1184
Analysis 4	25.1	2.2	64.4	94	69	662	24.7	227	8.4	40.2	1108
Analysis 5	7.3	3.3	48.5	90	72	663	25.1	231	14.1	43.1	1382
Analysis 6	21.4	0.2	50.6	91	72	658	25.3	231	11.5	0.0	1092
Analysis 7	21.4	0.2	50.6	91	72	658	25.3	231	11.5	0.0	1092
Analysis 8	7.3	3.3	48.5	90	72	663	25.1	214	14.1	43.1	1387
Analysis 9	17.6	11.6	64.1	89	72	657	27.1	228	11.0	34.3	1104
Analysis 10	14.3	13.4	62.0	85	68	663	26.7	230	9.7	45.9	1193
Analysis 11	6.6	14.0	61.2	92	70	663	24.8	228	8.1	38.4	1169
Analysis 12	15.1	20.5	58.6	87	70	664	24.4	226	6.8	38.8	1287
Uncertainty	14.0	16.8	11.5	6	11	7	6.1	11	8.2	37.0	224
Mean	16.5	7.6	58.0	89	71	662	25.3	227	11.0	35.5	1224
Std. dev.	6.7	6.6	6.9	3	3	3	0.8	5	3.4	18.0	125
SEMean	1.9	1.9	2.0	1	1	1	0.2	1	1.0	5.2	36

BCR-1

	Cr	Ni	Cu	Zn	Rb	Sr	Y	Zr	Nb	La	Ba
Reported	16	13	18	129	47	330	39	191	14	25	678
Analysis 1	35.5	8.8	14.1	125	51	328	25.5	176	12.7	30.6	682
Analysis 2	43.1	13.6	16.5	129	54	330	32.0	178	17.6	31.4	586
Analysis 3	47.2	10.1	16.7	125	52	330	32.8	178	13.5	24.1	714
Analysis 4	31.4	25.5	8.1	128	55	332	30.0	180	12.4	46.1	809
Analysis 5	37.1	19.0	3.8	125	48	327	30.5	178	10.6	8.1	743
Uncertainty	31.2	12.5	14.2	4	8	3	13.5	15	3.6	21.1	131
Mean	38.9	15.4	11.8	126	52	329	30	178	13.4	28.1	707
Std. dev.	6.3	6.9	5.7	2	3	2	2.8	1	2.6	13.8	82
SEMean	2.8	3.1	2.5	1	1	1	1.3	1	1.2	6.2	37

Table A3b. Continued.

G-1

	Cr	Ni	Cu	Zn	Rb	Sr	Y	Zr	Nb	La	Ba
Reported	20	<1	12	45	215	249	13	201	20	104	1080
Analysis 1	16.1	0.0	12.2	44	213	244	27.1	198	18.0	117.5	911
Analysis 2	23.6	0.0	16.4	46	213	251	38.1	201	24.1	94.2	887
Analysis 3	14.5	1.4	16.3	44	213	249	36.8	201	23.6	116.4	979
Analysis 4	26.7	1.1	8.1	47	214	246	34.4	197	21.6	88.7	1149
Analysis 5	19.4	10.0	10.7	43	212	243	33.0	196	20.2	80.4	1086
Analysis 6	0.0	18.2	15.6	40	202	241	33.2	198	16.3	80.5	1130
Uncertainty	20.0	18.2	4.4	5	13	8	25.1	5	4.1	24.5	193
Mean	16.7	5.1	13.2	44	211	246	33.8	199	20.6	96.3	1024
Std. dev.	9.4	7.5	3.4	3	5	4	3.8	2	3.1	16.8	113
SEMean	3.8	3.0	1.4	1	2	2	1.6	1	1.3	6.9	46

G-2

	Cr	Ni	Cu	Zn	Rb	Sr	Y	Zr	Nb	La	Ba
Reported	9	5	11	85	170	478	11.4	300	13	90	1880
Analysis 1	10.3	28.6	6.4	93	175	477	25.9	306	17.4	75.5	2126
Analysis 2	37.5	25.5	17.9	103	174	475	26.3	307	5.8	80.9	1714
Analysis 3	18.1	19.7	4.6	96	172	474	26.0	305	12.4	83.1	1922
Analysis 4	16.6	22.5	11.2	98	172	473	26.1	306	12.1	97.4	1824
Analysis 5	13.4	17.3	0.0	96	172	475	26.2	306	14.4	67.6	2055
Analysis 6	13.4	17.3	0.0	96	172	475	26.2	310	14.4	67.6	2041
Analysis 7	22.5	19.9	7.3	91	174	472	32.5	304	8.3	97.3	1869
Analysis 8	9.4	20.8	7.9	94	170	469	30.8	306	9.9	71.0	1866
Analysis 9	6.8	22.9	3.8	96	173	471	29.7	305	7.8	92.1	1877
Analysis 10	13.4	29.0	0.1	90	170	470	29.1	305	7.3	67.3	2137
Uncertainty	28.5	23.6	11.0	18	5	9	21.1	10	7.2	22.7	257
Mean	16.1	22.4	5.9	95	172	473	27.9	306	11.0	80.0	1943
Std. dev.	8.8	4.2	5.7	4	2	3	2.4	2	3.8	12.2	140
SEMean	2.8	1.3	1.8	1	1	1	0.8	1	1.2	3.8	44

Table A3b. Continued.

GSP-1

	Cr	Ni	Cu	Zn	Rb	Sr	Y	Zr	Nb	La	Ba
Reported	13	10	34	103	254	234	29	530	26	185	1310
Analysis 1	17.3	9.1	62.8	107	257	218	29.4	494	25.9	211.8	1223
Analysis 2	2.7	12.9	51.7	98	256	221	29.2	497	23.8	177.4	1243
Analysis 3	9.0	11.7	52.7	100	254	226	48.0	496	26.7	194.7	1379
Analysis 4	15.5	14.3	59.1	105	259	227	46.7	495	28.5	175.2	1400
Analysis 5	9.8	18.9	56.9	102	255	225	43.2	497	25.3	179.7	1330
Analysis 6	2.4	18.9	56.1	99	256	220	43.0	503	25.2	152.7	1379
Uncertainty	10.6	8.9	28.8	5	5	16	19.0	36	2.5	26.8	90
Mean	9.5	14.3	56.6	102	256	223	39.9	497	25.9	181.9	1326
Std. Dev.	6.2	4.0	4.1	4	2	4	8.5	3	1.6	19.9	76
SEMean	2.5	1.6	1.7	2	1	2	3.5	1	0.7	8.1	31

MRG-1

	Cr	Ni	Cu	Zn	Rb	Sr	Y	Zr	Nb	La	Ba
Reported	450	195	135	190	8	260	16	105	20	10	50
Analysis 1	449.1	193.6	67.6	188	7	269	23.2	113	23.5	11.4	164
Uncertainty	0.9	1.4	67.4	2	1	9	7.2	8	3.5	1.4	114

RGM-1

	Cr	Ni	Cu	Zn	Rb	Sr	Y	Zr	Nb	La	Ba
Reported	4	6	11	36	155	100	25	200	9.4	23	800
Analysis 1	8.3	0.0	33.3	28	146	108	35.8	198	12.4	26.1	761
Analysis 2	0.0	0.0	25.9	33	153	107	33.7	200	15.0	43.2	667
Analysis 3	3.2	0.0	39.4	29	150	102	33.4	197	7.8	10.4	715
Analysis 4	0.0	8.8	23.0	26	138	98	30.9	197	10.6	25.3	861
Uncertainty	4.3	6.0	28.4	10	17	8	10.8	3	5.6	20.2	133
Mean	2.9	2.2	30.4	29	147	104	33.5	198	11.5	26.3	751
Std. dev.	3.9	4.4	7.4	3	7	5	2.0	1	3.0	13.4	83
SEMean	2.0	2.2	3.7	2	3	2	1.0	1	1.5	6.7	41

Table A3b. Continued.

STM-1

	Cr	Ni	Cu	Zn	Rb	Sr	Y	Zr	Nb	La	Ba
Reported	4	3	4	240	120	700	46	1300	220	150	560
Analysis 1	0.8	8.4	86.1	240	119	707	45.8	1056	269.7	146.6	587
Analysis 2	3.5	2.0	82.5	239	116	704	45.9	1063	269.6	162.2	522
Analysis 3	14.1	10.7	81.2	237	120	704	40.9	1066	269.7	163.6	543
Analysis 4	1.2	3.8	3.8	239	116	709	39.6	1067	272.5	150.2	524
Uncertainty	10.1	7.7	82.1	3	4	9	6.4	244	52.5	13.6	38
Mean	4.9	6.2	63.4	239	118	706	43.1	1063	270.4	155.7	544
Std. dev.	6.3	4.0	39.8	1	2	3	3.3	5	1.4	8.5	30
SEMean	3.1	2.0	19.9	1	1	1	1.6	3	0.7	4.3	15

W-1

	Cr	Ni	Cu	Zn	Rb	Sr	Y	Zr	Nb	La	Ba
Reported	120	75	114	84	21	187	26	100	8	11	162
Analysis 1	129.1	81.4	109.4	77	33	194	24.3	101	19.8	12.4	280
Analysis 2	123.7	71.5	107.6	83	22	189	24.4	97	10.8	1.1	140
Analysis 3	122.0	76.8	119.7	91	19	184	24.2	100	9.3	26.9	143
Analysis 4	119.4	69.5	92.2	84	23	193	24.3	103	13.9	0.0	314
Analysis 5	119.4	69.5	92.2	84	23	193	24.3	49	13.9	0.0	348
Analysis 6	120.8	78.1	104.6	80	22	189	23.5	100	10.6	18.7	189
Analysis 7	116.1	74.6	107.4	79	22	192	24.2	101	7.9	20.2	183
Analysis 8	115.8	70.5	109.5	78	20	189	23.2	102	11.2	9.2	246
Analysis 9	116.8	72.5	111.6	76	20	188	22.3	97	11.8	7.4	30
Uncertainty	9.1	6.4	21.8	8	12	7	3.7	51	11.8	15.9	186
Mean	120.3	73.8	106.0	81	23	190	23.9	94	12.1	10.7	208
Std. dev.	4.2	4.2	8.9	5	4	3	0.7	17	3.5	9.7	99
SEMean	1.4	1.4	3.0	2	1	1	0.2	6	1.2	3.2	33

W-2

	Cr	Ni	Cu	Zn	Rb	Sr	Y	Zr	Nb	La	Ba
Reported	92	70	106	80	21	192	23	100	6.8	10.4	174
Analysis 1	89.4	72.8	107.9	75	19	194	24.2	99	12.9	3.0	227
Analysis 2	89.3	66.3	113.8	77	17	200	23.6	100	9.8	16.6	147
Analysis 3	96.7	70.2	112.7	76	23	198	23.2	98	11.1	1.5	212
Analysis 4	94.7	71.0	108.8	72	20	197	22.3	101	10.8	0.5	175
Analysis 5	99.4	70.4	113.7	74	15	193	23.2	100	9.4	3.6	64
Uncertainty	7.4	3.7	7.8	8	6	8	1.2	2	6.1	9.9	110
Mean	93.9	70.1	111.4	75	19	196	23.3	100	10.8	5.0	165
Std. dev.	4.5	2.4	2.8	2	3	3	0.7	1	1.4	6.6	65
SEMean	2.0	1.1	1.3	1	1	1	0.3	1	0.6	2.9	29

of 10^{12} for 15 hours. The remainder of the samples were activated with the Triga reactor at the University of Illinois, Urbana-Champaign under a neutron flux of 10^{15} for 4 hours. All samples were counted at Michigan State University using a GeLi detector and a Canberra Series 35 Plus Multichannel Analyzer. Sm, La, Na, and Sc were counted 7-8 days after activation and Th, Hf, Ce, Eu, Tb, Yb, and Lu were counted 14-16 days after activation (see Gordon, et al., 1968 for counting parameters). The INAA data reduction programs "MCA" and "NEUTRON" used in this study were written by Dr. J.T. Wilband of Michigan State University. Five to six international whole-rock standards were run in conjunction with the samples. Analyzed standard concentrations and their published values are presented in Table A3c.

Phenocryst Compositions

Most phenocryst compositions were determined by automated electron microprobe analysis (JEOL 733A Superprobe) at the Lawrence Livermore National Laboratory (LLNL). Several additional samples from the Ammonia Tanks Member were analyzed on a Cameca microprobe at the University of Michigan, Ann Arbor (UM).

Phenocrysts were separated from the glassy pumice fragments by gently hand crushing the pumice in a ceramic mortar and pestle and sieving the resulting powders.

Table A3c. Analytical errors for INAA trace element analyses based on linear regression of analyzed USGS (BIR-1, G-1, G-2, QLO-1, RGM-1, STM-1 and W-2), Canadian (MRG-1 and SY-2) and Japanese (JG-1a) rock standards.

Element	Intercept	Mean square residuals	Std. Error of Estimate	Degrees Freedom	Correlation Coefficient
Sc	-0.263	0.152	0.390	14	0.990
	-0.308	--	0.471	13	0.999
	-0.521	--	0.355	10	0.999
	-0.967	1.513	1.230	10	0.999
Hf	0.269	0.167	0.409	18	0.972
	-0.377	0.125	0.354	13	0.999
	-0.503	--	0.417	13	0.999
	-1.489	0.025	0.159	7	0.985
	5.952	0.352	0.593	10	0.998
Th	0.514	0.994	0.997	13	0.999
	-0.194	0.257	0.507	13	0.999
	-0.426	--	0.678	13	0.999
	-3.762	4.926	2.219	10	0.993
	-6.514	0.746	0.863	10	0.999
La	-1.891	18.959	4.350	18	0.994
	-17.560	6.202	2.490	7	0.999
	-1.917	--	2.008	13	0.999
	-0.535	--	1.839	10	0.999
	-1.770	67.524	8.217	10	0.979
Ce	-0.860	35.580	5.965	14	0.996
	-6.041	9.619	3.101	13	0.999
	-5.460	--	7.312	10	0.997
	-19.329	137.173	11.712	7	0.983
	-24.179	6.026	2.455	7	0.999
Sm	-0.862	0.123	0.351	14	0.973
	-1.204	0.644	0.802	13	0.983
	-0.348	--	0.440	13	0.992
	-0.386	--	0.305	10	0.997
	-0.194	0.043	0.207	3	0.999
Eu	0.055	0.005	0.068	17	0.984
	-0.088	0.006	0.075	13	0.998
	-0.853	--	0.234	10	0.982
	-0.001	0.010	0.098	10	0.955
	-0.015	0.001	0.034	7	0.996

Table A3c. Continued.

Tb	0.452	0.034	0.183	18	0.984
	-0.621	0.040	0.199	10	0.983
	0.091	0.055	0.234	10	0.845
	-0.132	0.015	0.122	10	0.958
Yb	-0.249	0.065	0.255	14	0.914
	0.815	0.119	0.344	13	0.961
	-0.005	0.049	0.222	10	0.974
	-2.414	0.232	0.481	7	0.952
	-0.112	0.019	0.136	10	0.990
Lu	-0.051	0.001	0.026	10	0.986
	-0.096	0.003	0.059	13	0.954
	-0.071	0.001	0.034	13	0.987
	-0.072	0.003	0.053	13	0.967
	0.020	0.000	0.015	10	0.997

These powders (-60 to +140 mesh fraction) were then concentrated into light (feldspar/glass) and heavy mineral (ferromagnesian and magnetite/ilmenite) fractions by bromoform heavy liquid separation. The light and heavy fractions were then mounted in standard metallurgical epoxy discs and polished. Whole phenocrysts were hand picked from the coarsely crushed pumice fragments and mounted in epoxy disks. This was done to preserve large scale zonation features in the feldspar and ferromagnesian minerals for potential analysis. Thin sections of each sample were also used for phenocryst and glass matrix composition analyses. The small percentage of phenocrysts present in the thin sections precluded the sole use of thin sections for compositional studies. The element codes and corresponding beam parameters used for the different mineral types are listed in Table A3d.
For each mineral grain, one to two spots were analyzed to check for homogeneity. Most grains were analyzed near the edge of the grain. For zoned grains such as the plagioclase feldspars, one analysis was taken on the rim of the grain and another in the center of the grain. Due to the random orientation of the mineral grains, the grain center analysis only represents a minimum range in composition when compared to the rim analysis if the mineral grain was zoned.

Table A3d. Electron microprobe beam parameters and analyzed oxides for various phenocryst compositions.

Feldspar and glass, I = 10 nA, V = 15 Kev, B = 100 um^2

LLNL - Feldspar and Glass
SiO_2, TiO_2, Al_2O_3, FeO, MnO, MgO, CaO, Na_2O, K_2O, P_2O_5, BaO

UM - Feldspar
SiO_2, Al_2O_3, Fe_2O_3, CaO, Na_2O, K_2O, BaO

UM - Glass
SiO_2, TiO_2, Al_2O_3, Fe_2O_3, MnO, MgO, CaO, Na_2O, K_2O, P_2O_5, F, Cl

Ferromagnesian minerals, I = 15 nA, V = 15 Kev, B = point

LLNL
SiO_2, TiO_2, Al_2O_3, FeO, MnO, MgO, CaO, Na_2O, K_2O, NiO, BaO

UM
SiO_2, TiO_2, Al_2O_3, Fe_2O_3, MnO, MgO, CaO, Na_2O, K_2O, BaO

Magnetite/Ilmenite, I = 15 nA, V = 15 Kev, B = point

LLNL
TiO_2, Al_2O_3, FeO, MnO, MgO, Cr_2O_3

UM
SiO_2, TiO_2, Al_2O_3, Fe_2O_3, MnO, MgO, CaO, Cr_2O_3

(I = current, V = voltage, B = beam size)

For magnetite and ilmenite phenocrysts, grains with more than one analysis were averaged. For each sample, grain averages with similar compositions were then averaged together. If the mineral grain averages were variable in composition, then several grain averages for each sample were computed.

Oxide and silicate mineral standards were run periodically for system calibration. The Bence-Albee correction procedure was applied to all quantitative analyses (Bence and Albee, 1968). Analyzed standards, their published values, and elemental detection limits are listed in Table A3e. ZAF corrections were made to all raw data resulting from analysis of phenocrysts at UM.

Magnetite/Ilmenite Analyses

A total of 31 samples were analyzed for Fe-Ti oxide geothermometry from the Timber Mountain Tuff. From these samples, temperature and oxygen fugacity were determined for 14 samples of the Rainier Mesa Member and 13 samples of the Ammonia Tanks Member. The remaining 4 samples, all from the Ammonia Tanks Member, were devoid of ilmenite. Of the 27 samples used for geothermometry, 9 samples from the Rainier Mesa Member and 7 samples from the Ammonia Tanks Member contained exsolved magnetite grains, and two samples from the Rainier Mesa Member contained exsolved ilmenite (Table 5).

As noted by Schuraytz (1988) for the Topopah Spring Member of the Paintbrush Tuff, many of the pumice samples in the Timber Mountain Tuff contained both exsolved and unexsolved magnetite grains. If post-depositional oxidation or reduction was responsible for exsolution, then all the grains within a sample should have been

Table A3e. Electron microprobe analyses of mineral standards.

A. Feldspar, ferromagnesium silicates and glass analyses

Element	Mineral Standard	Counting Time (seconds)
SiO_2	Orthoclase, Diopside	(5)
Al_2O_3	Orthoclase	(20)
TiO_2	Spessartine garnet	(20)
FeO	Diopside	(20)
MgO	Diopside	(20)
CaO	Diopside	(10)
Na_2O	Orthoclase	(10)
K_2O	Orthoclase	(20)
MnO	Spessartine garnet, Diopside	(20)
P_2O_5	None	(20)
BaO	Orthoclase	(20)

Diopside

	Reported Concentrations	Mean of Analyses (n=18)	Std. Dev. of Mean	Std. Error of Mean
SiO_2	54.98	54.95	0.65	0.15
FeO	1.87	1.98	0.17	0.04
MgO	17.09	17.14	0.25	0.06
CaO	25.66	24.99	0.83	0.20
MnO	0.21	0.18	0.06	0.01

Orthoclase

	Reported Concentrations	Mean of Analyses (n=18)	Std. Dev. of Mean	Std. Error of Mean
SiO_2	64.65	64.10	0.84	0.20
Al_2O_3	17.04	16.78	0.15	0.04
Na_2O	0.94	0.99	0.06	0.02
K_2O	15.40	15.30	0.37	0.09
BaO	0.05	0.05	0.03	0.01

Spessartine Garnet

	Reported Concentrations	Mean of Analyses (n=10)	Std. Dev. of Mean	Std. Error of Mean
TiO_2	0.11	0.19	0.29	0.09
MnO	40.31	38.97	0.37	0.12

Table A3e. Continued.

B. Magnetite and ilmenite analyses

Element	Mineral Standard	Counting Time (seconds)
Al_2O_3	Orthoclase, Diopside	(5)
FeO	Diopside, Orthoclase	(20)
MgO	Diopside	(20)
MnO	Spessartine Garnet	(10)
TiO_2	Spessartine Garnet	(20)
Cr_2O_3	None	(20)

Diopside

Reported Concentrations		Mean of Analyses (n=10)	Std. Dev. of Mean	Std. Error of Mean
Al_2O_3	0.16	0.21	0.04	0.01
FeO	1.87	1.92	0.08	0.03
MgO	17.09	16.76	0.24	0.08

Orthoclase

Reported Concentrations		Mean of Analyses (n=10)	Std. Dev. of Mean	Std. Error of Mean
Al_2O_3	17.04	16.98	0.56	0.18
FeO	1.87	1.67	0.12	0.04

Spessartine Garnet

Reported Concentrations		Mean of Analyses (n=10)	Std. Dev. of Mean	Std. Error of Mean
MnO	40.31	38.97	0.37	0.12
TiO_2	0.11	0.19	0.29	0.09

similarly affected. Thus, exsolution of the magnetite grains in the Timber Mountain Tuff appears to be a primary magmatic phenomena as many grains are unaltered. The Mg/Mn partitioning test for testing of equilibrium between coexisting Fe-Ti oxide phenocrysts developed by Bacon and Hirschmann (1988) was employed in this study (Figs. A3-1, A3-2). Grains that did not plot within the 2σ standard deviation lines were not used for temperature calculations.

Where possible, only chemically homogeneous grains were used for temperature and oxygen fugacity calculations. Analytical totals for the magnetite grains typically averaged 96 wt% to 97 wt%. Due to the ubiquitous occurrence of exsolved grains, at least two analyses per grain were collected with a 100 um^2 rastered beam. These analyses were then averaged to try to approximate the original unexsolved composition. Analyses of magnetites performed in this fashion gave noticeably low analytical totals ranging from 91 wt% to 95 wt% (Appendix 4). Ilmenite analyses consistently ranged from 96 wt% to 99 wt%. Within a particular sample, FeO, TiO_2, and MnO concentrations vary by approximately 5% for exsolved magnetite versus homogeneous magnetite (Appendix 4). In light of the presence of exsolved phenocrysts, all temperature and oxygen fugacity data for this study should be used with caution.

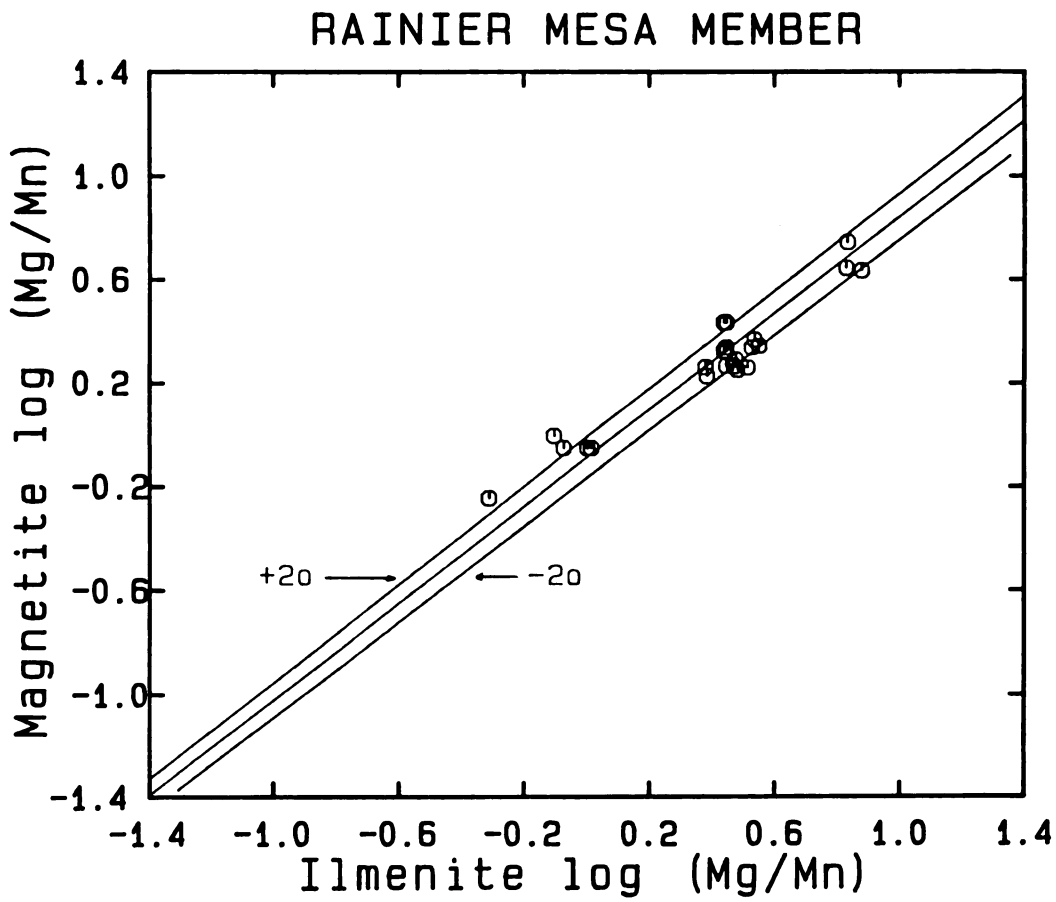


Figure A3-1. Mg/Mn partitioning for magnetite and ilmenite phenocrysts in the Rainier Mesa Member.

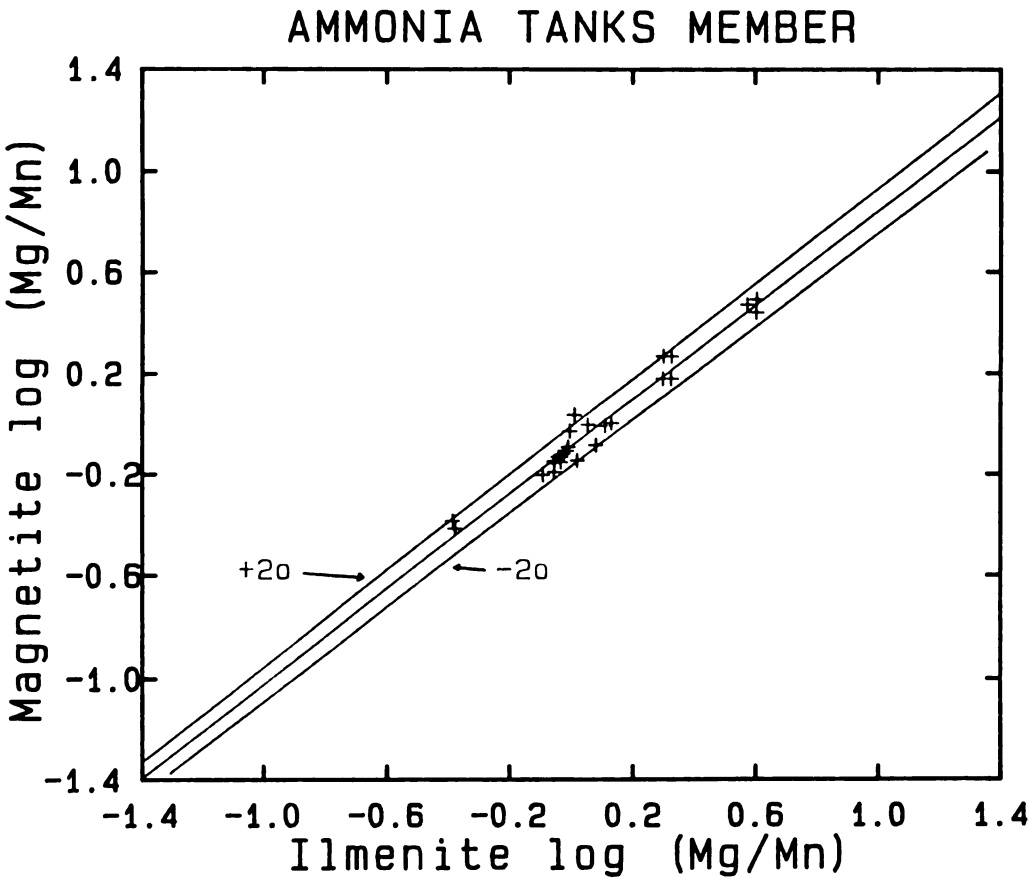


Figure A3-2. Mg/Mn partitioning for magnetite and ilmenite phenocrysts in the Ammonia Tanks Member.

Approximately 10-15 grains of magnetite and ilmenite were measured per sample. After averaging individual grain analyses, the resulting analysis for each grain was compared with other grains in that sample. Grains of similar composition were then combined and averaged. In this fashion, one to several magnetite and ilmenite compositions were determined for each sample. Magnetite grains with analytical totals less than 90.0 wt% were not used. Usp and Ilm mole fractions were calculated using the methods of Lindsley and Spencer (1982) and Stormer (1983). If at all possible, magnetite and ilmenite phenocryst pairs with common grain boundaries were analyzed as these phenocryst pairs provide the most reliable data. It is inferred that these phases crystallized coevally within the magma body. If magnetite and ilmenite phenocrysts with common grain boundaries were not found within a sample, all possible combinations of the Usp-Ilm mole fractions for a given sample were used to calculate temperature and oxygen fugacity.

All temperatures and oxygen fugacities were calculated with the Basic program NEWSTFO2 (Anderson and Lindsley, 1985).

APPENDIX 4

Electron Microprobe Data for Phenocrysts of the Timber Mountain Tuff

Explanation of Table Symbols for Appendix 4

R8-44

R = Sample from the Rainier Mesa Member
A = Sample from the Ammonia Tanks Member
8 = Stratigraphic section number
44 = Sample number

Whole Grain An uncrushed phenocryst was hand picked from the pumice sample and mounted in standard metallurgical epoxy mount with several other hand-picked phenocrysts.

Thin Section Phenocryst analyses from a polished thin section

Grain Mount Phenocrysts separated in heavy liquids after crushing of the host pumice fragment. The phenocrysts were then mounted in a standard metallurgical epoxy mount.

Position

E = Analysis of the phenocryst edge
NE = Near edge analysis
NC = Near center analysis
C = Grain center analysis
+ = Possible disequilibrium phenocryst. May have exhibited resorbtion texture.
p1 = Analyses of a magnetite and ilmenite phenocryst pair. The grains were attached along a common grain boundary and were assumed to be in equilibrium with each other.

Appendix 4. Mineral and glass compositions determined by electron microprobe analysis for the Timber Mountain Tuff.

GLASS ANALYSES

Rainier Mesa Member

Sample Id	SiO_2	Al_2O_3	FeO	MgO	CaO	Na_2O	K_2O	TiO_2	MnO	P_2O_5	BaO	Total
R8-25	70.01	15.13	0.23	0.03	0.45	3.76	5.85	0.34	0.00	0.07	0.08	95.96
	67.50	14.50	0.62	0.11	0.62	3.38	6.33	0.31	0.06	0.08	0.08	93.60
	67.60	14.52	0.25	0.10	0.63	3.80	5.79	0.29	0.00	0.07	0.09	93.15
	68.26	14.11	2.26	0.25	0.97	4.01	5.64	0.37	0.09	0.00	0.13	96.09
	69.37	14.50	0.42	0.21	0.85	3.89	5.82	0.34	0.32	0.02	0.03	95.78
	67.94	14.67	0.87	0.19	0.75	4.08	6.00	0.31	0.04	0.09	0.12	95.04
	64.76	13.95	3.39	0.83	1.61	4.33	5.61	0.44	0.08	0.02	0.07	95.08
	69.80	15.02	0.24	0.06	0.45	3.97	6.04	0.35	0.00	0.07	0.02	96.02
R8-44	69.12	12.14	0.28	0.02	0.43	1.62	6.40	0.21	0.02	0.07	0.00	90.31
	71.07	13.59	0.29	0.02	0.49	2.78	6.06	0.22	0.06	0.00	0.00	94.58
	71.78	13.95	0.75	0.02	0.45	3.21	5.61	0.20	0.07	0.04	0.02	96.10
	72.01	14.77	0.39	0.06	0.57	2.59	6.38	0.24	0.03	0.11	0.04	97.19
	72.30	14.28	0.31	0.05	0.46	2.99	6.05	0.22	0.03	0.06	0.00	96.75
	68.99	13.18	0.31	0.04	0.45	3.24	6.59	0.17	0.00	0.06	0.00	93.03
	68.33	13.10	0.27	0.02	0.50	2.22	6.47	0.22	0.04	0.04	0.00	91.21
	66.16	13.85	0.43	0.20	0.61	2.82	5.50	0.29	0.02	0.11	0.00	89.99
	69.20	14.83	0.28	0.13	0.51	3.33	5.64	0.23	0.02	0.11	0.00	94.28
	66.55	13.89	0.46	0.10	0.56	2.68	5.81	0.24	0.06	0.11	0.03	90.49
R8-45	68.71	15.21	1.05	0.04	0.67	3.28	5.87	0.25	0.83	0.00	0.10	96.01
	65.95	14.54	0.44	0.05	0.70	2.92	6.22	0.28	0.00	0.00	0.10	91.20
	67.94	14.71	1.20	0.08	0.68	3.73	5.66	0.28	0.00	0.00	0.16	94.44
	68.99	15.02	1.01	0.06	0.59	3.61	5.89	0.28	0.00	0.00	0.10	95.55
	68.68	14.87	1.24	0.16	0.79	3.85	5.90	0.28	0.00	0.00	0.12	95.89
	66.92	14.98	1.20	0.13	0.78	3.86	5.74	0.24	0.00	0.00	0.10	93.95
	66.84	14.56	1.33	0.07	0.61	3.37	6.00	0.26	0.00	0.00	0.08	93.12
	66.63	14.34	1.17	0.12	0.72	3.42	5.85	0.27	0.00	0.00	0.13	92.65
	68.40	14.72	0.90	0.11	0.63	3.32	6.21	0.26	0.00	0.05	0.21	94.81
	68.07	14.87	1.33	0.13	0.63	3.96	5.89	0.28	0.00	0.00	0.05	95.21
	68.84	15.32	1.05	0.07	0.74	3.69	5.80	0.27	0.00	0.00	0.17	95.95
	67.86	15.10	0.64	0.08	0.89	2.79	6.64	0.21	0.00	0.00	0.09	94.30
	67.92	15.02	1.18	0.04	0.68	3.50	5.85	0.28	0.00	0.00	0.09	94.56
	68.84	14.78	1.26	0.12	0.85	3.84	5.83	0.30	0.03	0.00	0.05	95.90
	68.58	15.08	1.37	0.09	0.69	3.59	5.87	0.23	0.05	0.03	0.00	95.58

Appendix 4. Continued.

GLASS ANALYSES

Rainier Mesa Member

Sample Id	SiO_2	Al_2O_3	FeO	MgO	CaO	Na_2O	K_2O	TiO_2	MnO	P_2O_5	BaO	Total
R11-5	66.78	15.75	1.03	0.27	1.07	3.76	5.13	0.35	0.04	0.04	0.22	94.44
	67.33	15.99	0.92	0.24	1.01	4.15	5.00	0.33	0.08	0.05	0.13	95.23
	66.45	15.44	1.22	0.25	1.04	4.37	5.53	0.34	1.29	0.12	0.16	96.21
	66.31	15.29	1.57	0.37	1.18	3.83	5.11	0.37	0.12	0.09	0.17	94.41
	67.03	15.40	0.93	0.23	0.95	3.89	5.61	0.34	0.09	0.08	0.11	94.66
	67.03	15.52	0.84	0.20	0.90	4.29	5.21	0.34	0.04	0.06	0.15	94.58
	66.49	15.27	0.58	0.19	0.93	3.69	5.59	0.30	0.04	0.07	0.15	93.30
	61.91	16.61	1.47	0.18	0.84	3.52	5.08	0.27	0.06	0.05	0.13	90.12
	65.19	15.07	1.58	0.26	0.91	4.03	5.36	0.35	0.05	0.05	0.04	92.89
	65.09	14.85	1.38	0.28	1.04	3.55	5.64	0.33	0.09	0.00	0.10	92.35
	64.12	15.31	1.77	0.25	1.03	3.81	4.99	0.32	0.11	0.09	0.11	91.91
R11-7	74.13	12.38	0.15	0.02	0.36	3.10	5.31	0.12	0.05	0.00	0.00	95.62
	72.98	12.34	0.16	0.02	0.38	3.00	5.54	0.12	0.05	0.02	0.04	94.65
	73.88	12.62	0.16	0.02	0.37	3.14	5.60	0.12	0.08	0.10	0.00	96.09
	72.79	12.62	0.18	0.03	0.30	3.10	5.40	0.09	0.07	0.00	0.00	94.58
	73.84	12.60	0.24	0.02	0.32	3.11	5.61	0.07	0.09	0.04	0.05	95.99
	74.28	12.49	0.13	0.03	0.32	3.17	5.29	0.07	0.08	0.07	0.00	95.93
	74.15	12.62	0.15	0.03	0.37	2.81	6.05	0.12	0.07	0.07	0.00	96.44
	72.71	12.55	0.38	0.03	0.37	2.72	5.76	0.09	0.05	0.07	0.00	94.73
	73.20	12.60	0.20	0.05	0.35	2.98	5.99	0.11	0.03	0.05	0.04	95.60
	72.03	12.52	0.16	0.02	0.33	3.05	5.47	0.09	0.09	0.00	0.00	93.76
	72.75	12.20	0.16	0.04	0.31	2.64	5.96	0.07	0.08	0.04	0.00	94.25
	72.64	12.67	0.13	0.03	0.34	4.19	5.51	0.09	0.09	0.05	0.00	95.74
	73.11	13.17	0.20	0.02	0.06	3.44	5.81	0.06	0.03	0.04	0.04	95.98
	74.17	12.87	0.13	0.02	0.05	2.12	7.39	0.09	0.00	0.00	0.04	96.88
	73.73	12.31	0.45	0.03	0.06	2.38	6.83	0.14	0.00	0.00	0.08	96.01
	64.38	16.20	2.56	1.55	0.93	3.21	3.17	0.73	0.00	0.05	0.22	93.00
	67.30	14.52	0.34	0.11	1.70	4.92	2.44	0.00	0.00	0.08	0.00	91.41
	74.22	11.44	0.79	0.25	1.03	3.72	2.74	0.54	0.06	0.10	0.08	94.97
	70.94	16.01	0.41	0.07	2.71	5.83	1.12	0.11	0.05	0.00	0.05	97.30
	70.98	15.24	0.34	0.10	1.87	5.22	2.44	0.10	0.00	0.00	0.06	96.35
	73.07	12.55	0.67	0.03	0.10	3.05	6.27	0.17	0.00	0.00	0.14	96.05
	74.17	12.21	0.18	0.07	0.23	3.06	5.43	0.09	0.00	0.00	0.03	95.47
	75.02	11.90	0.20	0.07	0.29	3.05	5.64	0.12	0.00	0.00	0.00	96.29
	72.97	11.26	0.19	0.04	0.20	2.87	5.72	0.07	0.02	0.00	0.03	93.37
	72.70	11.40	0.21	0.04	0.17	3.08	5.75	0.05	0.00	0.00	0.03	93.43

Appendix 4. Continued.

GLASS ANALYSES

Rainier Mesa Member

Sample Id	SiO_2	Al_2O_3	FeO	MgO	CaO	Na_2O	K_2O	TiO_2	MnO	P_2O_5	BaO	Total
R18-2	74.60	12.60	0.20	0.02	0.43	2.65	6.01	0.12	0.04	0.03	0.02	96.73
	75.09	12.27	0.56	0.06	0.44	3.40	4.86	0.09	0.04	0.00	0.05	96.86
	75.20	12.68	0.52	0.05	0.47	3.59	4.70	0.07	0.01	0.03	0.03	97.37
	73.62	12.66	0.23	0.00	0.49	3.03	5.69	0.07	0.00	0.07	0.03	95.88
	74.57	12.67	0.30	0.04	0.46	2.74	6.01	0.12	0.06	0.00	0.00	96.98
	74.81	12.69	0.44	0.06	0.47	3.60	5.14	0.09	0.00	0.09	0.05	97.45
	74.10	12.67	0.42	0.08	0.48	3.11	5.57	0.10	0.05	0.03	0.02	96.61
	75.17	12.99	0.33	0.07	0.49	3.09	5.73	0.12	0.01	0.07	0.00	98.08
	73.38	12.65	0.30	0.06	0.41	2.93	6.07	0.10	0.00	0.03	0.06	96.01
	71.27	12.33	0.11	0.02	0.40	2.47	6.38	0.08	0.02	0.05	0.03	93.15
	73.58	12.79	0.49	0.07	0.48	3.52	4.82	0.14	0.05	0.05	0.04	96.01
	74.18	12.87	0.26	0.03	0.41	2.70	5.78	0.12	0.02	0.09	0.00	96.48
	74.87	12.67	0.46	0.05	0.42	3.63	4.77	0.14	0.00	0.00	0.03	97.04
R18-16	75.32	12.56	0.56	0.05	0.47	3.41	5.04	0.13	0.06	0.07	0.00	97.67
	73.93	12.34	0.53	0.03	0.44	3.48	4.99	0.15	0.07	0.10	0.00	96.06
	74.51	12.42	0.40	0.02	0.39	3.15	5.47	0.12	0.08	0.00	0.02	96.58
	74.57	12.08	0.57	0.05	0.38	3.64	4.96	0.12	0.04	0.08	0.00	96.49
	73.28	12.52	0.57	0.06	0.49	3.35	4.77	0.14	0.02	0.00	0.00	95.20
	74.03	12.58	0.42	0.05	0.46	3.23	5.26	0.10	0.03	0.06	0.00	96.22
	72.74	12.61	0.50	0.04	0.46	3.67	5.06	0.11	0.02	0.06	0.00	95.27
	74.73	12.50	0.54	0.05	0.43	3.37	5.00	0.14	0.03	0.06	0.00	96.85
	74.47	12.38	0.60	0.04	0.46	3.46	4.93	0.13	0.07	0.00	0.00	96.54
	75.19	12.49	0.58	0.06	0.47	3.56	4.78	0.10	0.05	0.08	0.07	97.43
	75.25	12.61	0.43	0.04	0.50	3.43	5.55	0.10	0.05	0.04	0.00	98.00
	74.34	12.85	0.52	0.05	0.43	3.42	4.86	0.14	0.05	0.00	0.00	96.66
	75.01	12.83	0.50	0.05	0.44	3.51	4.85	0.14	0.06	0.04	0.00	97.43
	74.92	12.56	0.58	0.06	0.43	3.43	5.05	0.21	0.06	0.02	0.06	97.38
	75.13	12.61	0.65	0.05	0.50	3.61	5.01	0.15	0.09	0.04	0.06	97.90
R21-1	70.14	13.83	0.98	0.12	0.56	3.47	5.67	0.22	0.11	0.00	0.00	95.10
	69.22	13.70	0.90	0.11	0.61	3.42	5.76	0.20	0.04	0.00	0.00	93.96
	68.55	13.84	0.79	0.11	0.64	3.40	5.80	0.19	0.06	0.00	0.00	93.38
	68.40	13.62	0.93	0.12	0.64	3.47	5.78	0.30	0.04	0.05	0.00	93.35
	69.41	13.67	0.99	0.11	0.64	3.31	5.50	0.21	0.04	0.00	0.00	93.88

Appendix 4. Continued.

GLASS ANALYSES

Rainier Mesa Member

Sample Id	SiO_2	Al_2O_3	FeO	MgO	CaO	Na_2O	K_2O	TiO_2	MnO	P_2O_5	BaO	Total
R21-5	73.76	12.51	0.47	0.08	0.46	2.96	5.25	0.16	0.00	0.00	0.09	95.74
	73.96	12.41	0.37	0.04	0.44	2.75	5.46	0.12	0.02	0.00	0.04	95.61
	73.67	12.37	0.61	0.10	0.45	3.05	5.21	0.14	0.60	0.00	0.03	96.23
	72.06	12.37	0.69	0.07	0.43	3.10	5.07	0.13	0.00	0.04	0.00	93.96
	72.63	12.08	0.66	0.09	0.46	3.05	5.23	0.16	0.00	0.00	0.04	94.40
R21-13	68.22	16.12	1.40	0.41	1.24	3.93	4.89	0.35	0.06	0.06	0.12	96.80
	67.16	15.84	1.43	0.38	1.29	3.89	4.82	0.37	0.07	0.02	0.22	95.49
	66.27	15.70	1.66	0.43	1.55	3.92	5.04	0.37	0.09	0.10	0.20	95.33
	67.33	15.98	1.06	0.36	1.45	4.25	4.97	0.35	0.11	0.07	0.14	96.08
	66.83	15.59	1.46	0.45	1.49	4.05	4.95	0.37	0.04	0.07	0.17	95.47
	66.72	15.90	1.15	0.39	1.40	3.76	5.03	0.42	0.03	0.11	0.22	95.12
	67.11	15.74	1.38	0.48	1.35	4.06	4.97	0.43	0.11	0.09	0.16	95.87
	67.06	15.87	1.59	0.47	1.51	3.74	4.92	0.33	0.08	0.09	0.15	95.81
	66.78	15.54	1.73	0.41	1.22	4.11	4.91	0.34	0.10	0.12	0.23	95.49
R23-13	73.30	12.31	0.67	0.07	0.47	2.95	4.88	0.10	0.05	0.08	0.00	94.88
	68.13	13.70	0.74	0.05	0.49	3.31	5.77	0.21	0.02	0.04	0.05	92.51
	66.90	15.70	0.88	0.13	1.18	4.30	4.82	0.14	0.09	0.04	0.00	94.18
	68.04	14.05	0.98	0.09	0.52	3.68	5.26	0.19	0.04	0.07	0.00	92.92
	69.38	12.84	0.43	0.05	0.45	3.07	5.62	0.17	0.03	0.07	0.00	92.11
	72.88	12.24	0.52	0.05	0.34	2.97	5.24	0.17	0.02	0.00	0.00	94.43
	71.61	12.19	0.60	0.05	0.32	2.96	5.26	0.18	0.41	0.10	0.06	93.74
	68.12	14.87	1.41	0.32	0.82	3.77	5.60	0.32	0.08	0.07	0.09	95.47
	68.21	14.02	1.08	0.11	0.74	3.48	5.49	0.27	0.00	0.06	0.07	93.53
	66.53	13.37	0.55	0.08	0.38	3.31	5.34	0.26	0.04	0.08	0.04	89.98
	68.19	14.59	1.15	0.10	0.60	3.79	5.31	0.28	0.02	0.04	0.09	94.16
	69.35	13.48	0.56	0.06	0.46	3.30	5.51	0.27	0.02	0.16	0.10	93.27
R23-24	65.48	15.06	1.43	0.65	1.56	3.85	4.60	0.45	0.19	0.05	0.21	93.53
	68.82	16.06	0.78	0.27	1.44	4.23	4.72	0.35	0.08	0.00	0.14	96.89
	64.80	15.25	0.78	0.23	1.28	4.26	4.45	0.37	0.04	0.00	0.17	91.63
	67.98	15.82	1.28	0.34	1.53	4.29	4.80	0.36	0.13	0.07	0.15	96.75
	66.62	16.32	0.96	0.33	1.52	4.18	4.69	0.42	0.04	0.12	0.26	95.46
	68.06	15.88	0.49	0.17	1.32	4.08	4.74	0.37	0.06	0.00	0.17	95.34
	68.20	16.53	0.88	0.29	1.59	4.29	4.38	0.44	0.03	0.05	0.24	96.92
	65.70	15.41	1.10	0.31	1.36	4.28	4.64	0.41	0.09	0.02	0.17	93.49

Appendix 4. Continued.

GLASS ANALYSES

Rainier Mesa Member

Sample Id	SiO_2	Al_2O_3	FeO	MgO	CaO	Na_2O	K_2O	TiO_2	MnO	P_2O_5	BaO	Total
R23-26	69.63	15.37	1.20	0.21	0.72	3.84	6.02	0.33	0.04	0.05	0.07	97.47
	67.46	15.77	1.24	0.22	1.39	4.23	5.38	0.23	0.00	0.06	0.16	96.13
	67.62	15.15	1.27	0.17	0.64	3.54	6.06	0.29	0.02	0.09	0.06	94.91
	68.96	15.15	1.19	0.24	0.85	3.89	6.14	0.32	0.03	0.12	0.11	96.98
	64.90	14.43	1.13	0.31	0.94	3.29	5.61	0.26	0.03	0.03	0.08	91.00
	68.23	14.90	1.25	0.15	0.87	4.08	6.00	0.28	0.03	0.09	0.15	96.03
	68.90	15.26	1.19	0.20	0.81	4.08	6.09	0.27	0.09	0.08	0.08	97.07
	68.08	15.57	1.24	0.20	0.83	4.03	5.95	0.22	0.00	0.10	0.10	96.31
	68.80	15.24	1.21	0.19	0.85	4.02	6.13	0.25	0.03	0.07	0.10	96.89
	67.10	15.14	1.14	0.16	0.81	3.72	6.13	0.26	0.04	0.06	0.14	94.71
	67.58	15.08	0.69	0.15	0.68	3.84	6.34	0.25	0.01	0.00	0.12	94.75
	68.52	15.10	1.29	0.18	0.88	3.66	6.06	0.21	0.01	0.05	0.05	96.00
R23-27	67.40	15.65	0.83	0.00	1.78	3.78	4.96	0.37	0.02	0.13	0.19	95.11
	66.93	15.44	0.97	0.00	1.51	4.16	4.84	0.41	0.03	0.00	0.21	94.49
	66.14	16.00	1.58	0.00	1.55	4.41	4.61	0.42	0.05	0.08	0.11	94.97
	69.16	16.34	0.66	0.00	1.31	4.58	5.15	0.36	0.06	0.12	0.14	97.90
	64.52	15.11	0.61	0.00	1.48	3.71	4.89	0.38	0.02	0.00	0.07	90.79
	67.72	15.79	1.07	0.00	0.91	4.29	5.32	0.40	0.00	0.07	0.11	95.68
	67.11	15.74	0.87	0.00	1.23	3.92	5.27	0.42	0.04	0.04	0.06	94.69
	65.60	15.41	0.45	0.00	1.28	3.71	5.46	0.40	0.04	0.08	0.13	92.56
	64.26	15.09	0.53	0.00	1.33	3.43	5.16	0.34	0.04	0.11	0.09	90.38
	69.27	16.63	0.49	0.00	1.13	4.04	5.65	0.38	0.03	0.10	0.16	97.89
	67.55	15.80	1.20	0.00	1.59	4.15	5.23	0.36	0.02	0.10	0.17	96.17

Appendix 4. Continued.

GLASS ANALYSES

Ammonia Tanks Member

Sample Id	SiO_2	Al_2O_3	FeO	MgO	CaO	Na_2O	K_2O	TiO_2	MnO	P_2O_5	BaO	Total
A4-70	76.73	13.64	0.89	0.08	0.34	2.09	3.82	0.14	0.00	0.00	0.00	97.98
	75.22	13.36	0.62	0.06	0.26	2.50	3.98	0.18	0.04	0.00	0.00	96.51
	75.83	13.40	0.74	0.07	0.31	2.54	4.04	0.26	0.00	0.00	0.00	97.53
	75.98	13.43	0.50	0.04	0.21	2.51	4.19	0.10	0.00	0.01	0.00	97.31
	75.38	13.32	0.49	0.03	0.24	2.08	4.43	0.18	0.12	0.01	0.00	96.53
A5-3	72.97	12.32	0.72	0.10	0.39	3.85	5.34	0.19	0.13	0.04	0.13	96.18
	73.58	11.99	0.68	0.16	0.43	3.04	5.36	0.06	0.15	0.00	0.00	95.44
	71.77	11.81	0.65	0.03	0.31	2.89	5.09	0.09	0.13	0.04	0.00	92.82
	71.08	12.18	0.62	0.05	0.37	3.14	5.23	0.10	0.03	0.00	0.04	92.83
	69.47	11.41	0.50	0.04	0.33	2.84	5.24	0.11	0.06	0.03	0.02	90.04
A5-9	73.57	13.34	0.68	0.01	0.37	2.52	5.93	0.18	0.06	0.00	0.00	96.95
	72.89	13.19	0.53	0.01	0.32	3.24	5.66	0.26	0.00	0.01	0.00	96.36
	72.51	13.34	0.65	0.01	0.33	3.48	5.51	0.22	0.00	0.00	0.00	96.31
	73.34	13.35	0.57	0.01	0.34	3.45	5.71	0.28	0.05	0.01	0.00	97.20
	71.90	13.45	0.34	0.03	0.35	2.82	5.70	0.22	0.00	0.01	0.00	94.93
A5-29	75.62	11.68	0.58	0.04	0.32	3.00	4.91	0.00	0.06	0.01	0.00	96.70
	75.05	11.94	0.47	0.05	0.37	3.15	4.87	0.00	0.07	0.00	0.00	96.29
	75.03	11.84	0.80	0.06	0.37	3.20	5.04	0.00	0.11	0.05	0.00	96.62
	75.34	12.02	0.34	0.01	0.33	3.17	5.10	0.01	0.07	0.00	0.00	96.54
	71.85	11.19	0.34	0.02	0.26	2.70	5.05	0.08	0.08	0.02	0.00	91.82
A5-30	68.03	16.05	0.98	0.22	0.04	4.63	0.16	0.10	0.07	0.03	0.00	90.77
	67.47	15.66	1.95	0.17	0.82	4.54	6.07	0.51	0.02	0.08	0.00	97.69
	67.10	15.78	1.82	0.20	0.88	4.67	5.78	0.25	0.16	0.05	0.00	97.08
	66.68	15.79	2.05	0.22	0.73	4.61	5.96	0.29	0.05	0.10	0.00	96.81
	67.16	15.86	1.83	0.27	0.89	4.59	5.84	0.44	0.04	0.06	0.00	97.57
	67.85	15.82	1.76	0.19	0.87	4.61	5.70	0.32	0.13	0.06	0.00	97.63
A5-31	62.46	20.99	0.92	0.00	2.43	6.46	4.86	0.00	0.00	0.07	0.00	98.20
	64.30	19.65	0.83	0.02	2.09	6.88	3.56	0.20	0.00	0.06	0.00	97.64
	65.70	19.89	0.96	0.03	2.70	6.99	3.36	0.01	0.00	0.08	0.00	99.96
	63.57	22.23	0.42	0.00	0.24	7.90	0.07	0.00	0.00	0.05	0.00	94.66
	64.56	20.17	0.67	0.01	1.72	5.80	6.50	0.00	0.00	0.06	0.00	99.64

Appendix 4. Continued.

GLASS ANALYSES

Ammonia Tanks Member

Sample Id	SiO_2	Al_2O_3	FeO	MgO	CaO	Na_2O	K_2O	TiO_2	MnO	P_2O_5	BaO	Total
A5-35	72.84	12.90	0.64	0.03	0.38	3.18	5.80	0.16	0.03	0.00	0.02	95.98
	71.62	12.49	0.37	0.00	0.33	3.14	5.92	0.21	0.00	0.04	0.00	94.12
	71.47	12.93	0.77	0.03	0.35	3.48	5.83	0.16	0.00	0.00	0.00	95.02
	72.58	13.03	0.59	0.00	0.36	3.53	5.80	0.17	0.05	0.00	0.00	96.11
A5-37	71.77	11.81	0.65	0.03	0.31	2.89	5.09	0.09	0.13	0.04	0.00	92.81
	71.08	12.18	0.62	0.05	0.37	3.14	5.23	0.10	0.03	0.00	0.04	92.84
	69.47	11.41	0.50	0.04	0.33	2.84	5.24	0.11	0.06	0.03	0.02	90.05
A5-56	75.49	11.88	0.64	0.04	0.24	2.75	5.29	0.09	0.04	0.03	0.00	96.76
	75.33	12.03	0.33	0.02	0.13	2.48	5.27	0.20	0.08	0.00	0.00	96.07
	73.74	11.83	0.41	0.03	0.20	2.82	5.31	0.09	0.07	0.00	0.00	94.71
	76.07	11.96	0.66	0.05	0.19	2.95	5.29	0.02	0.01	0.01	0.00	97.20
A5-58	65.19	19.98	0.20	0.00	0.70	8.35	4.50	0.05	0.00	0.06	0.05	99.08
	63.51	21.36	0.22	0.00	1.99	7.89	4.16	0.07	0.00	0.06	0.05	99.31
	63.08	21.16	0.65	0.02	2.68	8.33	2.12	0.19	0.05	0.22	0.63	99.13
	68.84	14.15	0.00	0.09	0.53	3.51	6.60	0.25	0.67	0.12	0.03	94.79
A5-63	62.80	16.95	2.17	0.66	1.63	4.49	5.71	0.54	0.09	0.13	0.38	95.55
	62.56	16.68	2.26	0.59	1.56	4.69	5.81	0.55	0.07	0.11	0.36	95.24
	64.07	16.54	3.32	0.64	1.65	4.90	5.70	0.51	0.09	0.08	0.40	97.90
	63.03	16.67	2.27	0.57	1.42	4.73	5.69	0.52	0.11	0.00	0.42	95.43
	63.07	16.69	2.29	0.59	1.48	4.69	5.95	0.56	0.10	0.12	0.36	95.90
A5-68	75.04	12.10	0.52	0.03	0.36	2.90	5.51	0.02	0.07	0.03	0.00	96.86
	75.41	12.03	0.37	0.02	0.30	2.92	5.50	0.00	0.06	0.05	0.00	96.82
	74.76	11.97	0.61	0.03	0.34	2.85	5.04	0.18	0.09	0.01	0.00	96.03
	75.71	12.20	0.67	0.04	0.32	3.10	5.10	0.09	0.20	0.04	0.00	98.00
	76.31	12.24	0.47	0.02	0.30	2.96	5.50	0.07	0.12	0.00	0.00	98.14

Appendix 4. Continued.

GLASS ANALYSES

Ammonia Tanks Member

Sample Id	SiO_2	Al_2O_3	FeO	MgO	CaO	Na_2O	K_2O	TiO_2	MnO	P_2O_5	BaO	Total
A5-69	61.35	17.27	2.67	0.79	1.89	4.42	5.57	0.60	0.12	0.23	0.31	95.22
	61.36	16.77	2.65	0.80	1.94	4.67	5.70	0.58	0.08	0.20	0.37	95.12
	62.20	16.69	2.04	0.58	1.56	4.55	5.64	0.54	0.09	0.28	0.36	94.53
	62.69	16.56	2.15	0.61	1.58	4.56	5.85	0.54	0.11	0.13	0.25	95.03
	62.91	16.60	2.16	0.59	1.63	6.27	5.83	0.54	0.08	0.16	0.32	97.09
A5-71	58.43	21.28	1.17	0.21	0.75	2.86	6.03	0.29	0.11	0.06	0.04	91.23
	65.71	15.48	1.29	0.24	0.87	3.29	6.77	0.36	0.12	0.00	0.00	94.13
	66.56	15.17	1.28	0.20	0.75	3.64	6.94	0.34	0.14	0.04	0.00	95.06
	65.88	15.47	1.30	0.17	0.71	3.79	6.53	0.30	0.17	0.00	0.04	94.36
	67.04	15.11	1.30	0.18	0.71	3.63	6.44	0.33	0.09	0.00	0.01	94.84
	64.33	15.06	1.29	0.19	0.82	3.40	6.67	0.36	0.09	0.04	0.06	92.31
	65.57	15.29	2.18	0.29	0.81	3.63	6.64	0.38	0.07	0.00	0.00	94.86
A5-72	61.09	16.49	2.15	0.48	1.26	3.66	6.55	0.53	0.10	0.24	0.26	92.81
	64.10	15.89	1.41	0.25	0.84	4.62	6.35	0.40	0.05	0.09	0.18	94.18
	61.16	16.45	2.13	0.53	1.28	3.65	6.19	0.57	0.13	0.13	0.31	92.53
	64.11	16.35	1.88	0.46	1.20	4.35	6.20	0.55	0.05	0.15	0.31	95.61
A5-75	61.49	16.75	2.57	0.77	1.87	4.70	5.25	0.63	0.12	0.11	0.29	94.55
	61.13	16.97	2.37	0.73	1.78	4.51	4.94	0.59	0.10	0.16	0.32	93.60
	61.07	16.89	3.02	0.82	1.94	4.82	5.33	0.60	0.51	0.10	0.31	95.41
	61.42	16.85	2.00	0.61	1.70	4.60	5.49	0.54	0.09	0.17	0.37	93.84
	61.63	16.57	2.68	0.93	2.15	4.78	5.40	0.55	0.09	0.06	0.29	95.13
	61.16	17.14	2.39	0.77	1.88	4.54	5.44	0.60	0.09	0.16	0.29	94.46
A5-79	73.62	11.93	0.33	0.01	0.26	2.60	5.35	0.05	0.00	0.00	0.00	94.27
	65.78	19.13	0.22	0.06	0.41	7.77	5.26	0.07	0.00	0.00	0.00	98.71
	73.55	11.95	0.62	0.02	0.28	2.91	5.24	0.45	0.00	0.00	0.00	95.06
	73.84	11.79	0.60	0.04	0.30	2.96	5.19	0.08	0.00	0.00	0.00	95.11
	73.61	11.75	0.56	0.03	0.34	2.80	5.06	0.18	0.00	0.01	0.00	94.50

Appendix 4. Continued.

FELDSPAR ANALYSES

Rainier Mesa Member

Sample Type	Grain #	Pos.	SiO_2	Al_2O_3	FeO	MgO	CaO	Na_2O	K_2O	TiO_2	MnO	P_2O_5	BaO	Total
R8-25														
Whole	1	E	63.65	20.27	0.15	0.00	0.69	5.43	8.26	0.02	0.00	0.05	1.23	99.75
Grain	1	NE	65.31	19.19	0.09	0.00	0.32	4.13	10.81	0.00	0.00	0.07	0.14	100.06
	1	C	64.40	19.43	0.10	0.00	0.33	4.16	10.90	0.00	0.01	0.07	0.23	99.63
	2	E	65.39	19.23	0.11	0.00	0.28	4.69	10.08	0.00	0.02	0.06	0.07	99.93
	2	C	64.94	19.32	0.06	0.00	0.31	4.20	10.92	0.03	0.00	0.00	0.07	99.85
	3	E	65.20	19.90	0.16	0.00	0.45	5.14	9.38	0.00	0.00	0.00	0.18	100.41
	3	C	64.28	19.11	0.15	0.00	0.42	4.42	10.32	0.05	0.00	0.05	0.33	99.13
	4	E	60.81	23.88	0.31	0.00	5.18	7.78	1.44	0.00	0.00	0.04	0.19	99.63
	4	NE	56.99	26.94	0.23	0.00	8.21	6.58	0.74	0.02	0.00	0.02	0.16	99.89
	4	C	59.14	25.91	0.26	0.00	6.54	7.50	1.10	0.01	0.00	0.05	0.19	100.70
	5	E	63.19	20.33	0.15	0.00	0.60	4.41	9.54	0.06	0.00	0.06	2.05	100.39
	5	C	63.15	20.68	0.16	0.00	0.66	4.04	9.51	0.05	0.00	0.12	2.45	100.82
	6	E	63.77	20.25	0.18	0.00	0.52	4.36	9.57	0.00	0.00	0.00	1.29	99.94
	6	E	57.71	26.34	0.31	0.00	7.51	6.67	0.77	0.02	0.00	0.07	0.18	99.58
Thin	7	E	60.26	22.86	0.36	0.00	4.92	7.61	1.50	0.00	0.00	0.00	0.16	97.67
Section	7	E	60.52	24.11	0.41	0.00	5.24	8.00	1.64	0.03	0.04	0.00	0.08	100.07
	7	C	57.99	25.50	0.09	0.00	6.89	7.07	0.86	0.00	0.02	0.00	0.00	98.42
	8	E	55.46	27.36	0.01	0.01	9.13	6.00	0.49	0.00	0.04	0.00	0.00	98.50
	8	C	59.72	25.36	0.33	0.03	5.79	7.47	1.11	0.00	0.03	0.00	0.27	100.11
	9	E	60.80	24.92	0.30	0.03	5.31	7.54	1.28	0.00	0.00	0.02	0.20	100.40
	9	C	60.99	24.24	0.23	0.00	4.83	7.74	1.71	0.00	0.10	0.02	0.18	100.04
	10	E*	57.17	27.74	0.31	0.00	8.01	6.54	0.70	0.05	0.02	0.00	0.21	100.75
Grain	11		58.86	25.00	0.28	0.07	6.15	7.61	1.11	0.10	0.00	0.06	0.10	99.34
Mount	12		61.26	25.00	0.27	0.05	5.63	8.04	1.32	0.08	0.05	0.00	0.16	101.86
	13		60.36	24.40	0.59	0.17	5.54	7.83	0.98	0.11	0.18	0.07	0.03	100.26
	14		60.60	24.60	0.30	0.08	5.60	7.86	1.36	0.10	0.00	0.00	0.15	100.65
	15		60.93	24.62	0.31	0.08	5.57	7.93	1.20	0.10	0.00	0.03	0.22	100.99
	16		59.76	25.42	0.31	0.04	6.40	7.51	1.15	0.11	0.00	0.00	0.17	100.87
	17		61.08	24.17	0.31	0.06	4.91	7.75	1.70	0.05	0.00	0.03	0.13	100.19
	18		59.53	24.50	0.40	0.02	5.66	7.74	0.74	0.05	0.02	0.03	0.18	98.87
	19		58.35	24.59	0.33	0.12	6.13	8.27	0.75	0.10	0.00	0.06	0.19	98.89
	20		58.84	24.12	0.38	0.00	5.85	8.23	0.51	0.05	0.00	0.00	0.00	97.98

Appendix 4. Continued.

FELDSPAR ANALYSES

Rainier Mesa Member

Sample Type	Grain #	Pos.	SiO_2	Al_2O_3	FeO	MgO	CaO	Na_2O	K_2O	TiO_2	MnO	P_2O_5	BaO	Total
R8-44														
Grain	1		57.34	24.72	0.27	0.03	6.14	7.40	1.17	0.00	0.00	0.00	0.14	97.21
Mount	2		60.10	25.27	0.30	0.00	5.74	7.67	1.25	0.00	0.00	0.03	0.15	100.51
	3		64.19	23.58	0.20	0.00	4.36	8.82	1.43	0.00	0.00	0.09	0.00	102.67
	4		60.36	24.42	0.24	0.03	5.43	7.94	1.48	0.01	0.00	0.00	0.06	99.97
	5		64.67	20.23	0.14	0.00	0.54	4.65	9.83	0.04	0.00	0.00	0.89	100.99
	6		62.28	20.06	0.19	0.00	0.59	4.01	9.69	0.04	0.00	0.05	1.93	98.84
	7		60.80	26.30	0.30	0.02	6.67	7.71	1.04	0.00	0.00	0.09	0.16	103.09
	8		60.95	24.77	0.26	0.02	5.34	7.96	1.31	0.00	0.00	0.02	0.11	100.74
	9		63.90	19.39	0.16	0.02	0.37	4.46	10.37	0.00	0.00	0.00	0.27	98.94
	10		63.67	19.55	0.15	0.00	0.45	4.35	10.45	0.00	0.00	0.06	0.31	98.99
	11		59.28	24.62	0.33	0.00	5.48	7.76	1.27	0.00	0.25	0.00	0.06	99.05
	12		64.82	19.10	0.15	0.01	0.37	4.40	10.41	0.03	0.00	0.00	0.19	99.48
	13		58.11	26.74	0.30	0.03	7.45	7.68	0.58	0.00	0.00	0.00	0.09	100.98
	14		62.84	20.13	0.21	0.02	0.60	4.29	9.57	0.04	0.54	0.06	1.52	99.82
	15		60.16	25.06	0.31	0.00	5.69	7.56	1.32	0.02	0.00	0.06	0.11	100.29
	16		59.34	25.92	0.31	0.00	5.47	7.57	1.38	0.01	0.00	0.00	0.13	100.13
	17		61.84	24.63	0.29	0.03	5.10	7.93	1.60	0.00	0.00	0.00	0.12	101.54
	18		62.60	20.47	0.20	0.00	0.53	4.17	9.59	0.04	0.00	0.06	1.71	99.37
	19		72.87	12.80	0.78	0.07	0.50	3.30	5.14	0.05	0.05	0.07	0.02	95.65
	20		63.38	20.47	0.16	0.00	0.56	4.04	9.57	0.07	0.00	0.00	1.93	100.18
	21		64.81	19.65	0.17	0.00	0.33	4.05	10.71	0.00	0.00	0.05	0.10	99.87
Whole	22	E	64.72	19.40	0.09	0.00	0.28	3.97	10.79	0.03	0.75	0.00	0.39	100.42
Grain	22	C	64.86	19.24	0.13	0.00	0.28	4.03	10.65	0.04	0.00	0.00	0.09	99.32
	23	E	59.28	24.11	0.30	0.00	5.26	7.88	1.45	0.04	0.00	0.00	0.22	98.54
	23	C	59.68	24.86	0.24	0.00	5.65	7.84	1.19	0.09	0.00	0.00	0.25	99.80
	24	E	60.37	23.77	0.25	0.00	4.92	7.83	1.45	0.05	0.00	0.00	0.09	98.73
	24	C	59.23	24.40	0.34	0.00	5.57	7.51	1.23	0.06	0.00	0.02	0.20	98.56
	25	E	59.41	24.25	0.24	0.00	5.55	7.48	1.36	0.02	0.00	0.00	0.17	98.48
	25	NE	57.10	25.72	0.27	0.00	7.32	6.87	0.83	0.04	0.00	0.05	0.10	98.30
	25	C	59.63	24.39	0.31	0.00	4.99	7.62	1.51	0.07	0.00	0.05	0.21	98.78
	26	E	62.02	23.09	0.22	0.00	3.98	8.60	1.54	0.03	0.00	0.03	0.05	99.56
	26	C	61.76	23.80	0.15	0.00	4.68	8.51	1.18	0.02	0.00	0.00	0.06	100.16
	27	E	55.26	28.98	0.08	0.00	9.62	5.97	0.43	0.00	0.00	0.00	0.06	100.40
	27	C	62.44	23.41	0.51	0.00	4.00	8.60	1.46	0.03	0.00	0.00	0.09	100.54
	28	E	62.54	19.95	0.15	0.00	0.56	4.39	9.61	0.00	0.00	0.00	1.19	98.39
	28	C	62.92	19.63	0.20	0.00	0.53	3.98	9.90	0.06	0.00	0.06	1.10	98.38
	29	E	65.07	19.63	0.12	0.00	0.32	4.56	9.88	0.04	0.00	0.00	0.28	99.90
	29	C	64.85	19.48	0.03	0.00	0.35	4.27	10.38	0.00	0.00	0.00	0.07	99.43
	30	E	63.46	19.77	0.18	0.00	0.51	4.30	9.79	0.02	0.00	0.00	1.12	99.15
	30	C	65.00	19.32	0.08	0.00	0.28	4.20	10.56	0.02	0.00	0.00	0.07	99.53

Appendix 4. Continued.

FELDSPAR ANALYSES

Rainier Mesa Member

Sample Type	Grain #	Pos.	SiO_2	Al_2O_3	FeO	MgO	CaO	Na_2O	K_2O	TiO_2	MnO	P_2O_5	BaO	Total
R8-44														
Thin	31	E	61.42	25.30	0.33	0.00	5.70	7.71	1.28	0.00	0.00	0.04	0.27	102.05
Section	31	NE	58.22	26.34	0.33	0.00	6.93	6.97	1.02	0.00	0.01	0.00	0.20	100.02
	31	C	58.50	26.78	0.40	0.00	7.06	6.90	0.91	0.03	0.00	0.06	0.12	100.76
	32	E	64.96	20.49	0.24	0.00	0.52	4.35	9.79	0.05	0.03	0.00	0.91	101.34
	32	NE	64.58	20.20	0.24	0.00	0.59	4.32	9.87	0.00	0.03	0.00	0.95	100.78
	32	C	64.39	19.92	0.25	0.00	0.49	4.23	9.83	0.00	0.03	0.00	1.02	100.16
	33	E	60.41	25.15	0.34	0.00	5.60	7.60	1.38	0.02	0.01	0.00	0.09	100.60
	33	NE	60.90	24.51	0.30	0.00	5.85	7.70	1.31	0.04	0.16	0.00	0.10	100.87
	33	C	61.45	24.22	0.33	0.00	5.33	7.99	1.51	0.02	0.00	0.00	0.12	100.97
	34	E	59.82	24.93	0.39	0.00	5.80	7.54	1.25	0.00	0.03	0.05	0.29	100.10
	34	C	60.44	24.85	0.37	0.00	5.67	7.71	1.31	0.00	0.00	0.00	0.10	100.45
	35	E	65.29	19.34	0.14	0.00	0.34	4.27	10.36	0.00	0.00	0.00	0.07	99.81
	35	C	65.19	19.79	0.17	0.00	0.43	4.47	9.99	0.00	0.00	0.00	0.22	100.26
	36	NC	61.07	23.84	0.35	0.00	4.82	7.60	1.82	0.04	0.03	0.00	0.10	99.67
	36	E	61.51	25.05	0.36	0.00	5.48	7.99	1.47	0.03	0.01	0.06	0.03	101.99
	36	C	61.31	24.53	0.36	0.00	5.04	7.92	1.50	0.03	0.00	0.00	0.03	100.72
R8-45														
Grain	1		58.03	25.85	0.37	0.03	6.45	7.62	1.04	0.03	0.00	0.05	0.14	99.61
Mount	2		60.29	24.70	0.27	0.02	5.29	7.89	1.45	0.04	0.00	0.00	0.19	100.14
	3	+	61.72	24.42	0.31	0.02	4.87	8.14	1.61	0.04	0.00	0.02	0.10	101.25
	4		61.40	24.23	0.25	0.03	4.96	8.07	1.60	0.02	0.00	0.00	0.06	100.62
	5	+	55.54	28.44	0.27	0.02	9.30	6.14	0.65	0.07	0.00	0.07	0.07	100.57
	6		59.76	24.78	0.38	0.02	5.54	7.69	1.42	0.03	0.00	0.00	0.18	99.80
	7	+	59.96	26.30	0.77	0.03	6.24	7.74	1.14	0.02	0.00	0.00	0.16	102.36
	8		59.78	24.96	0.32	0.01	5.43	7.83	1.42	0.05	0.00	0.00	0.23	100.03
	9	E	59.52	24.69	0.23	0.03	5.01	8.12	1.53	0.06	0.00	0.02	0.21	99.42
	10	E	59.44	25.76	0.44	0.05	5.99	7.69	1.29	0.04	0.00	0.00	0.26	100.96
	10	C	58.69	25.64	0.41	0.02	5.79	7.46	1.37	0.00	0.00	0.06	0.32	99.76
	11	+	57.30	26.13	0.38	0.04	7.10	7.02	0.91	0.04	0.00	0.00	0.21	99.13
	12	E	59.29	23.76	0.37	0.00	5.11	7.81	1.56	0.06	0.00	0.00	0.29	98.25
	13		62.36	19.99	0.24	0.02	0.29	4.19	10.41	0.02	0.00	0.00	0.83	98.35
	14		61.01	20.42	0.17	0.00	0.74	4.15	9.27	0.06	0.00	0.02	1.80	97.64
	15		67.83	15.20	1.21	0.13	0.68	3.80	5.77	0.28	0.00	0.00	0.07	94.97
	16		61.10	19.98	0.22	0.01	0.53	4.14	9.63	0.07	0.00	0.00	1.64	97.32
	17		61.57	20.01	0.20	0.00	0.49	4.07	9.79	0.09	0.04	0.00	1.98	98.24

Appendix 4. Continued.

FELDSPAR ANALYSES

Rainier Mesa Member

Sample Type	Grain #	Pos.	SiO_2	Al_2O_3	FeO	MgO	CaO	Na_2O	K_2O	TiO_2	MnO	P_2O_5	BaO	Total
R8-45														
Whole	18	E	62.69	19.52	0.17	0.00	0.51	3.96	9.74	0.05	0.00	0.00	1.56	98.20
Grain	18	C	62.90	19.73	0.14	0.00	0.69	4.19	9.63	0.03	0.00	0.00	1.47	98.78
	19	E	57.39	25.49	0.30	0.00	6.18	7.14	1.10	0.06	0.00	0.00	0.24	97.90
	19	NE	55.52	27.31	0.33	0.00	8.17	6.51	0.74	0.02	0.00	0.00	0.13	98.73
	19	NC	57.00	26.09	0.30	0.03	7.10	7.25	0.85	0.06	0.00	0.00	0.23	98.91
	19	C	57.91	27.20	0.27	0.00	6.81	6.99	0.92	0.00	0.00	0.04	0.25	100.39
	20	E	62.35	20.05	0.19	0.00	0.64	4.30	9.51	0.04	0.00	0.00	1.66	98.74
	20	C	62.57	20.12	0.18	0.00	0.66	4.32	9.52	0.05	0.00	0.00	1.65	99.07
	21	E	60.22	24.46	0.24	0.00	5.15	7.77	1.45	0.00	0.00	0.00	0.18	99.47
	21	NE	54.86	27.92	0.31	0.00	8.65	6.00	0.54	0.02	0.00	0.00	0.11	98.41
	21	C	58.43	25.78	0.34	0.00	6.32	7.21	1.07	0.05	0.00	0.00	0.20	99.40
	22	E	63.00	19.93	1.28	0.00	0.59	4.34	9.76	0.05	0.00	0.00	1.62	100.57
	22	C	62.38	20.23	0.19	0.00	0.67	4.32	9.32	0.05	0.00	0.00	1.90	99.06
	23	E+	60.47	24.55	0.18	0.00	5.50	7.51	1.51	0.02	0.00	0.00	0.18	99.92
	23	C+	59.22	24.96	0.28	0.02	5.84	7.31	1.21	0.00	0.00	0.00	0.13	98.97
	24	E	60.29	24.51	0.29	0.00	5.26	7.71	1.47	0.02	0.00	0.00	0.15	99.70
	24	C	60.15	24.25	0.26	0.00	5.34	8.01	1.48	0.06	0.00	0.00	0.16	99.71
	25	E	61.82	20.40	0.18	0.00	0.69	5.82	9.33	0.05	0.00	0.00	2.25	100.54
Thin	26	E	59.32	25.47	0.39	0.00	5.94	7.48	1.23	0.04	0.00	0.04	0.15	100.06
Section	26	NE	58.64	24.76	0.29	0.00	6.31	7.51	1.20	0.06	0.00	0.02	0.14	98.93
	26	C	60.36	25.36	0.37	0.00	5.58	7.70	1.37	0.03	0.00	0.00	0.15	100.92
	27	E	64.22	20.00	0.25	0.00	0.60	4.22	9.80	0.12	0.00	0.00	1.19	100.40
	27	C	64.83	20.54	0.24	0.00	0.61	4.52	9.66	0.10	0.80	0.00	1.35	102.65
	28	E	61.08	23.72	0.34	0.00	5.17	8.02	1.45	0.05	0.02	0.04	0.17	100.06
	28	C	58.23	25.10	0.32	0.02	7.02	7.28	0.80	0.04	0.02	0.02	0.08	98.93
	29	E	61.49	24.80	0.33	0.02	5.37	8.18	1.50	0.04	0.00	0.02	0.16	101.91
	29	C	60.97	24.98	0.36	0.01	5.59	7.51	1.28	0.03	0.00	0.00	0.19	100.92
	30	E	60.58	24.82	0.30	0.02	5.24	7.89	1.35	0.06	0.00	0.00	0.17	100.43
	30	C	61.15	25.13	0.34	0.03	5.68	7.87	1.35	0.06	0.03	0.05	0.25	101.94
	31	E	62.82	20.06	0.24	0.02	0.79	4.17	9.28	0.13	0.02	0.02	2.11	99.66
	31	C	64.23	20.25	0.23	0.00	0.55	4.24	10.03	0.05	0.00	0.04	1.29	100.91
	32	E	62.89	23.70	0.26	0.05	4.18	7.94	2.14	0.02	0.03	0.06	0.13	101.40
	32	C	60.47	24.68	0.16	0.00	5.26	7.93	1.50	0.00	0.00	0.00	0.09	100.09

Appendix 4. Continued.

FELDSPAR ANALYSES

Rainier Mesa Member

Sample Type	Grain #	Pos.	SiO_2	Al_2O_3	FeO	MgO	CaO	Na_2O	K_2O	TiO_2	MnO	P_2O_5	BaO	Total
R11-5														
Grain	1		58.56	25.10	0.31	0.03	6.29	7.53	0.84	0.03	0.00	0.08	0.20	98.97
Mount	2	E+	56.96	26.58	0.38	0.00	8.00	6.78	0.64	0.03	0.02	0.12	0.11	99.62
	3	+	56.75	25.93	0.30	0.03	6.68	7.01	1.06	0.05	0.10	0.07	0.22	98.20
	4	E+	52.05	29.33	0.37	0.03	10.79	4.85	0.32	0.07	0.01	0.00	0.10	97.92
	5	E	56.53	26.66	0.40	0.02	7.37	6.90	0.72	0.03	0.03	0.05	0.09	98.80
	6		57.02	26.26	0.28	0.01	6.77	7.11	0.80	0.00	0.02	0.00	0.07	98.34
	7	E+	55.81	26.96	0.43	0.02	8.16	6.46	0.57	0.03	0.04	0.09	0.08	98.65
	8		56.36	25.50	0.39	0.04	6.53	7.37	0.83	0.03	0.03	0.00	0.19	97.27
	9		62.26	20.18	0.17	0.00	0.52	4.13	9.41	0.04	0.02	0.00	1.66	98.39
	10		60.96	20.70	0.24	0.00	0.66	4.15	8.72	0.07	0.04	0.10	2.77	98.41
	11		54.50	28.82	0.45	0.03	10.47	5.33	0.39	0.06	0.02	0.09	0.09	100.25
	12		53.26	29.03	0.37	0.02	10.26	5.24	0.41	0.05	0.03	0.07	0.07	98.81
Thin	1	E+	58.12	27.06	0.00	0.08	7.34	7.04	0.67	0.02	0.00	0.00	0.14	100.47
Section	1	NE+	56.93	26.97	0.00	0.02	7.74	6.93	0.68	0.07	0.00	0.02	0.11	99.47
	1	C+	57.84	26.69	0.00	0.03	7.35	7.00	0.78	0.05	0.00	0.00	0.14	99.88
	2	E	55.95	27.47	0.00	0.00	8.75	6.40	0.59	0.02	0.04	0.04	0.11	99.37
	2	C	53.76	28.93	0.00	0.04	9.84	5.68	0.45	0.07	0.04	0.08	0.14	99.03
	3	E	58.92	26.55	0.00	0.00	7.43	7.04	0.88	0.01	0.00	0.00	0.04	100.87
	4	E	58.38	26.17	0.00	0.00	7.40	6.87	0.74	0.03	0.00	0.04	0.11	99.74
	5	E	58.62	25.37	0.00	0.02	7.15	7.08	0.78	0.04	0.01	0.00	0.11	99.18
	5	C	56.79	27.50	0.00	0.02	8.24	6.60	0.70	0.03	0.00	0.00	0.13	100.01
	6	E	56.48	28.03	0.00	0.01	8.65	6.61	0.69	0.04	0.05	0.00	0.08	100.64
	6	C	54.18	30.13	0.00	0.00	10.90	5.27	0.42	0.09	0.04	0.00	0.16	101.19
	7	E	54.18	30.21	0.00	0.02	10.66	5.32	0.44	0.05	0.07	0.00	0.14	101.09
	7	C	54.89	30.00	0.00	0.02	10.95	5.24	0.43	0.05	0.00	0.09	0.07	101.74
	8	E	58.97	26.55	0.00	0.04	7.18	7.04	0.94	0.02	0.02	0.00	0.08	100.84
	9	E	56.05	28.84	0.00	0.03	9.18	5.78	0.53	0.07	0.04	0.00	0.13	100.65
	10	E	57.67	27.89	0.00	0.02	8.23	6.57	0.65	0.08	0.04	0.00	0.12	101.27
	10	NE	49.81	33.10	0.39	0.05	14.28	3.11	0.17	0.07	0.03	0.00	0.11	101.12
	10	C	48.07	34.06	0.00	0.01	15.81	2.43	0.14	0.06	0.00	0.05	0.11	100.74
	11	E	57.29	26.08	0.00	0.03	7.15	6.69	0.89	0.04	0.04	0.00	0.10	98.31
	12	E	57.79	27.00	0.00	0.50	7.71	6.88	0.82	0.07	0.37	0.00	0.20	101.34
	13	E+	59.06	26.70	0.00	0.01	7.12	7.14	0.69	0.03	0.02	0.00	0.19	100.96
	13	C+	57.97	25.94	0.00	0.02	6.90	7.30	0.75	0.03	0.02	0.04	0.19	99.16

Appendix 4. Continued.

FELDSPAR ANALYSES

Rainier Mesa Member

Sample Type	Grain #	Pos.	SiO_2	Al_2O_3	FeO	MgO	CaO	Na_2O	K_2O	TiO_2	MnO	P_2O_5	BaO	Total
R11-7														
Grain	1		65.16	19.61	0.07	0.00	0.16	4.38	10.71	0.00	0.00	0.00	0.00	100.09
Mount	2		65.59	19.18	0.10	0.01	0.37	4.83	9.29	0.02	0.00	0.04	0.00	99.43
	3	E	65.63	19.42	0.14	0.00	0.22	4.28	10.31	0.00	0.00	0.02	0.00	100.02
	4		65.01	19.34	0.09	0.00	0.22	4.10	10.92	0.00	0.00	0.04	0.00	99.72
	5		63.52	19.03	0.07	0.00	0.13	4.25	10.65	0.00	0.00	0.05	0.00	97.70
	6		72.88	12.19	0.42	0.04	0.35	3.05	5.21	0.10	0.06	0.00	0.00	94.30
	7		65.41	18.90	0.10	0.00	0.20	4.66	10.54	0.00	0.00	0.00	0.00	99.81
	8		64.41	19.39	0.10	0.00	0.21	4.25	10.82	0.00	0.04	0.00	0.00	99.22
	9	E	59.08	24.29	0.36	0.00	5.60	7.28	1.28	0.02	0.00	0.00	0.15	98.06
	10	E	64.72	19.35	0.06	0.00	0.27	3.79	11.19	0.00	0.00	0.02	0.00	99.40
	11		63.34	22.32	0.12	0.00	2.85	9.34	1.15	0.00	0.00	0.00	0.00	99.12
	12	E	65.51	19.44	0.13	0.00	0.21	4.22	10.65	0.01	0.00	0.00	0.00	100.17
Thin	13	E	64.79	22.51	0.13	0.01	2.73	9.53	1.34	0.00	0.00	0.11	0.03	101.18
Section	13	NE	65.10	22.05	0.18	0.00	2.96	9.74	1.43	0.00	0.00	0.02	0.03	101.51
	13	C	65.54	22.39	0.15	0.00	2.54	9.57	1.58	0.03	0.03	0.00	0.02	101.85
	14	E	66.23	18.38	0.09	0.02	0.19	4.38	10.64	0.00	0.04	0.04	0.04	100.05
	14	C	65.33	19.15	0.11	0.00	0.18	4.43	10.62	0.03	0.00	0.00	0.07	99.92
	15	E	64.66	22.71	0.16	0.00	2.92	9.10	1.20	0.02	0.02	0.02	0.00	100.81
	15	C	64.59	23.17	0.19	0.01	3.40	9.22	1.11	0.01	0.00	0.00	0.07	101.77
	16	E	63.12	24.09	0.25	0.01	4.32	8.47	1.26	0.00	0.00	0.00	0.05	101.57
	16	C	62.64	23.93	0.23	0.01	4.35	8.83	1.42	0.01	0.00	0.00	0.03	101.45
	17	E	56.69	28.48	0.44	0.04	8.97	6.24	0.46	0.03	0.00	0.00	0.14	101.49
R18-2														
Grain	1		66.28	19.74	0.10	0.00	0.22	4.04	11.05	0.03	0.00	0.00	0.12	101.58
Mount	2		63.69	23.39	0.17	0.00	4.13	8.99	1.17	0.02	0.00	0.00	0.00	101.56
	3		62.68	22.60	0.16	0.00	3.41	8.76	1.34	0.02	0.00	0.00	0.00	98.97
	4		64.01	19.12	0.09	0.00	0.24	4.79	9.75	0.00	0.00	0.00	0.04	98.04
	5	E	58.95	26.97	0.12	0.00	7.21	7.29	0.53	0.03	0.03	0.08	0.07	101.28
	6		65.26	19.55	0.09	0.00	0.16	3.73	11.19	0.06	0.00	0.02	0.00	100.06
	7		66.33	19.38	0.16	0.00	0.21	4.08	11.34	0.03	0.05	0.00	0.04	101.62
	8		64.00	19.57	0.13	0.00	0.26	4.08	11.28	0.00	0.01	0.00	0.11	99.44
	9		63.06	23.34	0.24	0.00	3.82	8.71	1.20	0.00	0.00	0.00	0.00	100.37
	10		63.17	23.29	0.14	0.00	3.69	8.65	1.21	0.02	0.00	0.00	0.00	100.17
	11		60.42	23.67	0.13	0.00	5.51	7.93	0.83	0.02	0.03	0.08	0.04	98.66
	12		63.78	19.48	0.13	0.00	0.20	3.87	11.27	0.02	0.08	0.00	0.23	99.06

Appendix 4. Continued.

FELDSPAR ANALYSES

Rainier Mesa Member

Sample Type	Grain #	Pos.	SiO_2	Al_2O_3	FeO	MgO	CaO	Na_2O	K_2O	TiO_2	MnO	P_2O_5	BaO	Total
R18-2														
Whole	13	E	64.17	23.34	0.60	0.01	3.74	9.13	1.19	0.02	0.02	0.05	0.00	102.27
Grain	13	NE	63.72	22.40	0.12	0.05	2.99	9.01	1.59	0.05	0.00	0.00	0.00	99.93
	13	C	63.40	22.61	0.14	0.00	3.13	9.14	1.29	0.05	0.07	0.00	0.00	99.83
	14	E	65.29	18.85	0.08	0.04	0.24	4.06	10.71	0.04	0.00	0.00	0.08	99.39
	14	C	65.44	19.50	0.05	0.04	0.21	4.05	11.07	0.04	0.03	0.00	0.05	100.48
	15	E+	64.61	19.42	0.14	0.02	0.22	3.94	11.02	0.06	0.03	0.02	0.15	99.63
	15	C+	64.78	19.61	0.09	0.00	0.26	4.01	10.96	0.04	0.04	0.00	0.11	99.90
	16	E+	64.41	19.55	0.09	0.03	0.26	3.88	11.02	0.08	0.04	0.02	0.18	99.56
	16	C+	64.72	19.13	0.08	0.02	0.24	3.88	11.21	0.05	0.04	0.00	0.05	99.42
	17	E+	63.34	18.93	0.02	0.01	0.22	3.99	11.03	0.05	0.00	0.00	0.03	97.62
	17	C+	64.75	19.21	0.09	0.00	0.21	4.13	11.01	0.07	0.03	0.00	0.00	99.50
Thin	18	E+	66.50	19.56	0.10	0.00	0.23	4.01	10.99	0.00	0.00	0.04	0.15	101.58
Section	18	C+	66.87	19.85	0.06	0.00	0.26	3.91	11.04	0.00	0.00	0.04	0.02	102.05
	19	E	63.50	23.26	0.16	0.00	4.00	9.04	1.13	0.00	0.00	0.00	0.00	101.09
	20	E	63.93	23.55	0.22	0.00	3.76	8.83	1.26	0.00	0.00	0.05	0.03	101.63
	20	C	64.92	23.53	0.19	0.00	3.87	9.09	1.26	0.00	0.14	0.06	0.04	103.10
	21	E	63.43	23.48	0.12	0.00	3.82	9.05	1.28	0.00	0.00	0.02	0.00	101.20
	22	E	65.86	19.58	0.05	0.00	0.29	3.92	10.90	0.00	0.00	0.00	0.17	100.77
	22	C	65.97	19.69	0.05	0.00	0.28	3.93	11.05	0.00	0.00	0.00	0.00	100.97
R18-16														
Grain	1	E	65.06	20.06	0.10	0.00	0.28	4.24	11.06	0.03	0.07	0.00	0.22	101.12
Mount	2		63.75	23.03	0.36	0.00	3.53	8.99	1.61	0.05	0.00	0.00	0.00	101.32
	3		65.19	19.69	0.10	0.00	0.26	4.09	11.28	0.08	0.03	0.06	0.08	100.86
	4		65.21	19.51	0.06	0.00	0.26	4.19	11.37	0.05	0.03	0.00	0.03	100.71
	5		64.83	19.93	0.07	0.00	0.28	4.19	11.09	0.05	0.00	0.00	0.13	100.57
	6		62.56	23.60	0.16	0.00	3.85	8.76	1.33	0.04	0.00	0.00	0.02	100.32
Whole	7	E	64.33	19.48	0.07	0.00	0.30	4.05	10.89	0.00	0.00	0.00	0.05	99.17
Grain	7	C	65.12	19.31	0.11	0.00	0.24	3.94	10.80	0.00	0.00	0.02	0.00	99.54
	8	E	63.54	19.13	0.13	0.00	0.25	3.92	10.93	0.00	0.00	0.00	0.06	97.96
	8	C	64.34	19.02	0.06	0.00	0.25	3.98	11.20	0.00	0.00	0.00	0.00	98.85
	9	E	64.96	19.14	0.15	0.00	0.25	3.82	11.08	0.00	0.02	0.00	0.02	99.44
	9	C	64.73	19.37	0.05	0.00	0.25	3.87	11.01	0.00	0.00	0.00	0.00	99.28
	10	E	64.61	19.60	0.16	0.00	0.25	4.01	10.84	0.00	0.00	0.02	0.08	99.57
	10	C	64.90	19.46	0.05	0.00	0.28	3.85	10.90	0.00	0.01	0.00	0.03	99.48
	11	E	59.90	24.82	0.21	0.00	5.61	8.24	0.86	0.00	0.00	0.00	0.00	99.64
	11	NE	59.31	25.91	0.13	0.00	6.39	7.74	0.73	0.00	0.01	0.00	0.00	100.22

Appendix 4. Continued.

FELDSPAR ANALYSES

Rainier Mesa Member

Sample Type	Grain #	Pos.	SiO_2	Al_2O_3	FeO	MgO	CaO	Na_2O	K_2O	TiO_2	MnO	P_2O_5	BaO	Total
R18-16														
Thin	12	E	64.40	19.59	0.14	0.00	0.24	3.98	11.14	0.05	0.03	0.00	0.14	99.71
Section	13	C	63.79	23.44	0.21	0.00	4.30	8.81	1.22	0.04	0.00	0.00	0.04	101.85
	14	E	64.37	23.81	0.24	0.00	4.06	8.71	1.28	0.00	0.03	0.00	0.07	102.57
	14	C	56.71	26.77	0.15	0.00	9.27	6.07	0.38	0.00	0.06	0.00	0.02	99.43
	15	E	65.88	17.97	0.21	0.00	0.22	3.77	11.28	0.04	0.00	0.00	0.11	99.48
	15	C	65.04	19.53	0.15	0.00	0.28	3.97	10.89	0.00	0.02	0.00	0.12	100.00
	16	E	63.43	23.16	0.23	0.00	4.05	8.48	1.29	0.03	0.00	0.00	0.07	100.74
	16	C	65.19	22.72	0.21	0.00	3.40	9.11	1.65	0.01	0.00	0.00	0.00	102.29
	17	E	65.82	19.59	0.09	0.00	0.21	3.81	10.99	0.03	0.00	0.00	0.17	100.71
	17	C	66.12	19.78	0.08	0.00	0.21	4.08	11.47	0.02	0.00	0.00	0.02	101.78
	18	E	65.70	19.19	0.19	0.00	0.24	3.76	11.22	0.01	0.06	0.00	0.14	100.51
	18	C	64.44	19.42	0.12	0.00	0.25	3.78	11.16	0.04	0.04	0.07	0.19	99.51
	19	E	63.49	23.68	0.22	0.00	3.90	8.45	1.39	0.04	0.05	0.00	0.04	101.26
R23-13														
Grain	1		62.15	19.77	0.22	0.00	0.49	4.03	9.68	0.04	0.19	0.02	1.41	98.00
Mount	2		64.44	19.24	0.15	0.00	0.25	3.82	10.83	0.02	0.05	0.00	0.13	98.93
	3	E	60.75	23.64	0.36	0.00	4.51	7.67	1.81	0.02	0.02	0.00	0.10	98.88
	4		58.86	24.92	0.28	0.00	5.35	7.79	1.34	0.05	0.02	0.04	0.18	98.83
	5		62.52	19.16	0.23	0.00	0.38	4.22	10.22	0.03	0.02	0.00	0.33	97.11
	6	+	57.96	25.85	0.34	0.00	6.60	6.74	1.02	0.04	0.03	0.04	0.31	98.93
	7		57.50	25.30	1.05	0.00	5.89	7.52	1.19	0.06	0.02	0.08	0.24	98.85
	8		52.14	29.19	0.35	0.03	10.37	5.19	0.27	0.06	0.04	0.00	0.06	97.70
	9	E	61.43	23.02	0.27	0.00	4.10	8.33	1.52	0.04	0.03	0.00	0.07	98.81
	9	C	54.74	27.77	0.43	0.04	8.66	5.96	0.58	0.02	0.02	0.04	0.19	98.45
	10		60.61	24.17	0.29	0.03	4.62	7.99	1.47	0.00	0.03	0.06	0.10	99.37
	11	E	59.95	24.25	0.42	0.03	5.06	7.90	1.34	0.03	0.02	0.06	0.09	99.15
	12	E	64.61	19.47	0.12	0.00	0.32	5.17	9.10	0.00	0.03	0.07	0.06	98.95
Whole	13	E	62.80	19.69	0.18	0.00	0.47	4.25	10.08	0.02	0.01	0.00	0.53	98.03
Grain	13	C	63.79	19.96	0.17	0.00	0.46	4.40	10.32	0.00	0.00	0.04	0.62	99.76
	14	E	63.08	20.40	0.19	0.00	0.60	4.22	9.90	0.00	0.05	0.00	1.43	99.87
	14	C	65.43	19.82	0.08	0.00	0.31	4.25	10.53	0.00	0.02	0.00	0.05	100.49
	15	E	64.61	20.27	0.53	0.00	0.46	4.51	10.18	0.04	0.04	0.04	0.48	101.16
	15	C	65.61	19.82	0.10	0.00	0.28	4.06	10.83	0.00	0.05	0.00	0.00	100.75
	16	E	63.32	20.68	0.20	0.00	0.51	4.09	9.58	0.02	0.09	0.00	2.11	100.60
	16	C	64.04	20.08	0.18	0.00	0.60	4.38	10.04	0.00	0.03	0.05	0.79	100.19
	17	E	66.03	19.96	0.12	0.00	0.32	4.24	10.79	0.00	0.00	0.00	0.00	101.46
	17	C	65.13	19.69	0.10	0.00	0.32	4.06	11.02	0.00	0.02	0.00	0.00	100.34

Appendix 4. Continued.

FELDSPAR ANALYSES

Rainier Mesa Member

Sample Type	Grain #	Pos.	SiO_2	Al_2O_3	FeO	MgO	CaO	Na_2O	K_2O	TiO_2	MnO	P_2O_5	BaO	Total
R23-13														
Thin	18	E	61.66	23.21	0.27	0.02	4.37	7.89	1.90	0.00	0.06	0.00	0.04	99.42
Section	18	C	58.51	25.74	0.32	0.04	7.65	6.79	0.75	0.02	0.05	0.00	0.10	99.97
	19	E	60.88	23.65	0.36	0.03	4.77	7.53	1.69	0.02	0.03	0.00	0.02	98.98
	19	C	61.18	24.25	0.31	0.03	5.32	7.64	1.31	0.05	0.03	0.02	0.10	100.24
	20	E+	59.06	25.75	0.27	0.03	7.66	7.02	0.51	0.03	0.04	0.00	0.09	100.46
	20	C+	57.29	26.62	0.30	0.02	8.49	6.99	0.43	0.03	0.00	0.00	0.09	100.26
	21	E	60.37	24.21	0.38	0.04	6.75	7.21	1.14	0.01	0.02	0.02	0.14	100.29
	22	E	62.84	23.64	0.31	0.02	4.89	7.92	1.75	0.04	0.05	0.00	0.07	101.53
	22	C	56.42	28.21	0.31	0.05	9.46	5.99	0.52	0.00	0.08	0.00	0.09	101.13
	23	E+	63.12	20.31	0.26	0.03	0.60	4.20	9.69	0.08	0.06	0.02	2.39	100.76
	23	C+	64.75	19.92	0.18	0.02	0.49	4.40	10.04	0.05	0.02	0.04	0.99	100.90
	24	E	61.13	24.87	0.29	0.02	5.70	7.46	1.30	0.00	0.06	0.00	0.17	101.00
	24	C	57.52	27.27	0.28	0.05	8.32	6.70	0.69	0.03	0.03	0.06	0.19	101.14
R23-24														
Thin	1	E+	58.89	26.48	0.34	0.01	7.19	7.17	0.72	0.03	0.00	0.00	0.25	101.08
Section	1	NE+	59.16	26.35	0.38	0.03	7.33	7.20	0.66	0.05	0.60	0.04	0.21	102.01
	1	C+	58.53	26.08	0.29	0.03	7.19	6.73	0.70	0.03	0.00	0.00	0.17	99.75
	2	E	54.57	29.24	0.37	0.03	10.32	5.26	0.38	0.07	0.00	0.02	0.12	100.38
	2	C	54.64	29.70	0.46	0.05	11.05	4.78	0.36	0.04	0.00	0.00	0.09	101.17
	3	E+	55.62	28.77	0.36	0.03	10.18	5.32	0.37	0.02	0.00	0.00	0.16	100.83
	3	C+	55.52	27.89	0.39	0.04	10.10	5.80	0.39	0.03	0.00	0.04	0.15	100.35
	4	E+	55.57	27.10	0.32	0.03	9.18	5.87	0.43	0.03	0.00	0.08	0.12	98.73
	4	C+	54.17	28.00	0.50	0.05	11.01	5.22	0.26	0.06	0.00	0.00	0.07	99.34
	5	E	58.69	26.92	0.34	0.05	8.01	6.84	0.55	0.00	0.02	0.04	0.16	101.62
	5	C	57.35	27.70	0.41	0.00	8.49	6.19	0.46	0.03	0.00	0.00	0.10	100.73
	6	E+	57.39	28.23	0.36	0.03	9.03	6.16	0.45	0.06	0.00	0.00	0.06	101.77
Grain	7	E	55.36	29.02	0.41	0.02	9.89	5.93	0.36	0.09	0.02	0.02	0.00	101.12
Mount	8		54.14	30.12	0.51	0.06	11.06	5.31	0.35	0.05	0.00	0.06	0.00	101.66
	9	E	53.50	28.35	0.37	0.00	9.86	5.54	0.46	0.08	0.02	0.04	0.00	98.22
	10	E	55.12	28.54	0.49	0.00	9.19	6.07	0.49	0.07	0.00	0.00	0.00	99.97
	11	E	55.05	28.88	0.33	0.01	9.86	5.64	0.34	0.06	0.02	0.07	0.00	100.26
	12	E	56.85	28.12	0.41	0.00	8.74	6.26	0.46	0.03	0.04	0.06	0.00	100.97
	13	E	55.11	28.90	0.33	0.01	9.65	6.19	0.37	0.02	0.00	0.00	0.00	100.58
	14	E+	57.80	26.91	0.32	0.00	7.34	7.10	0.67	0.06	0.03	0.00	0.04	100.27
	15	E+	57.32	27.21	0.34	0.00	8.02	6.83	0.54	0.05	0.00	0.08	0.00	100.39
	16	E+	54.40	28.57	0.35	0.02	10.11	5.91	0.40	0.06	0.00	0.00	0.02	99.84

Appendix 4. Continued.

FELDSPAR ANALYSES

Rainier Mesa Member

Sample Type	Grain #	Pos.	SiO_2	Al_2O_3	FeO	MgO	CaO	Na_2O	K_2O	TiO_2	MnO	P_2O_5	BaO	Total
R23-24														
Whole	17	E	56.72	27.55	0.37	0.03	8.61	6.31	0.50	0.06	0.00	0.00	0.03	100.18
Grain	17	C	56.67	27.63	0.32	0.04	8.41	6.02	0.43	0.09	0.02	0.06	0.14	99.83
R23-26														
Whole	1	E	64.11	19.82	0.19	0.04	0.40	4.11	10.31	0.05	0.04	0.02	1.09	100.18
Grain	1	C	64.13	19.50	0.13	0.01	0.51	4.18	10.10	0.07	0.00	0.00	0.48	99.11
	2	E	64.36	19.87	1.57	0.02	0.40	4.33	10.33	0.10	0.02	0.00	0.70	101.70
	2	C	63.30	19.96	0.14	0.02	0.47	4.21	10.17	0.08	0.03	0.00	1.13	99.51
	3	E+	62.78	20.20	0.17	0.02	0.64	4.03	9.55	0.09	0.03	0.02	1.79	99.32
	3	C+	62.63	19.43	0.20	0.02	0.43	4.21	10.16	0.04	0.05	0.00	0.97	98.14
	4	E	62.10	20.01	0.14	0.01	0.70	4.11	9.53	0.05	0.00	0.00	1.68	98.33
	4	C	62.96	19.94	0.16	0.01	0.51	4.43	10.01	0.09	0.05	0.00	1.39	99.55
	5	E	60.76	25.14	0.26	0.00	5.16	7.59	1.65	0.12	0.02	0.00	0.14	100.84
	5	C	60.97	24.22	0.35	0.00	5.09	7.60	1.60	0.10	0.00	0.00	0.27	100.20
	6	E	59.65	24.42	0.35	0.03	5.52	7.45	1.44	0.05	0.04	0.00	0.14	99.09
	7	E	58.86	25.50	1.09	0.03	5.98	7.51	1.22	0.06	0.07	0.00	0.29	100.61
	7	C	58.03	26.29	0.37	0.02	7.29	6.85	0.94	0.10	0.05	0.00	0.15	100.09
Grain	8		63.82	20.52	0.20	0.00	0.65	4.19	9.90	0.00	0.00	0.03	1.83	101.14
Mount	9		63.89	20.20	0.23	0.00	0.60	4.10	9.60	0.00	0.00	0.02	1.87	100.51
	10		61.16	23.47	0.34	0.00	5.66	7.63	1.44	0.00	0.00	0.00	0.10	99.80
	11		60.80	24.29	0.40	0.00	5.91	7.28	1.38	0.00	0.00	0.00	0.11	100.17
	12		61.36	24.67	0.27	0.00	5.52	7.55	1.48	0.00	0.00	0.00	0.11	100.96
	13	E	59.48	25.19	0.32	0.00	6.62	7.31	1.12	0.00	0.00	0.00	0.13	100.17
	14	E	61.31	24.32	0.29	0.00	5.00	7.86	1.71	0.00	0.00	0.00	0.05	100.54
	15		63.06	20.22	1.17	0.00	0.93	3.83	9.33	0.03	0.00	0.07	2.71	101.35
	16		61.73	24.24	0.30	0.00	5.40	7.64	1.58	0.00	0.00	0.00	0.16	101.05
	17		61.85	24.77	0.37	0.04	5.62	7.51	1.32	0.00	0.00	0.02	0.07	101.57
	18		63.70	20.25	0.16	0.00	0.73	4.12	9.67	0.03	0.00	0.00	1.79	100.45
	19		60.95	24.19	0.32	0.02	5.59	7.46	1.40	0.00	0.00	0.00	0.15	100.08
	20		63.53	20.10	0.20	0.00	0.62	3.98	9.75	0.04	0.00	0.00	1.58	99.80
	21		61.69	24.36	0.37	0.03	5.26	7.58	1.70	0.00	0.00	0.06	0.13	101.18
	22		60.95	24.28	0.58	0.00	5.54	7.45	1.44	0.00	0.00	0.00	0.12	100.36

Appendix 4. Continued.

FELDSPAR ANALYSES

Rainier Mesa Member

Sample Type	Grain #	Pos.	SiO_2	Al_2O_3	FeO	MgO	CaO	Na_2O	K_2O	TiO_2	MnO	P_2O_5	BaO	Total
R23-26														
Thin	23	E	61.64	24.60	0.37	0.00	5.00	7.80	1.67	0.03	0.00	0.06	0.16	101.33
Section	23	C	55.20	28.74	0.36	0.00	10.21	5.40	0.53	0.04	0.00	0.00	0.07	100.55
	24	E	60.65	24.65	0.41	0.00	5.65	7.52	1.41	0.00	0.00	0.02	0.19	100.50
	24	NE	55.75	27.98	0.53	0.01	8.85	5.95	0.62	0.08	0.03	0.00	0.17	99.97
	24	C	56.65	27.51	0.45	0.02	8.79	6.44	0.68	0.07	0.02	0.08	0.14	100.85
	25	E+	60.93	25.12	0.36	0.00	5.97	7.66	1.28	0.00	0.00	0.05	0.07	101.44
	25	C+	60.81	25.60	0.40	0.00	6.01	7.79	1.39	0.02	0.00	0.00	0.08	102.10
	26	E+	59.86	25.46	0.39	0.32	6.22	7.33	1.20	0.03	0.00	0.00	0.16	100.97
	27	E	59.96	27.39	0.35	0.01	8.09	6.46	0.83	0.03	0.00	0.00	0.08	103.20
	27	C	57.43	26.56	0.42	0.03	7.94	6.71	1.05	0.06	0.00	0.00	0.11	100.31
	28	E+	59.93	24.17	0.34	0.00	5.32	7.36	1.51	0.00	0.73	0.07	0.11	99.54
	28	C+	61.85	24.47	0.32	0.00	5.12	7.79	1.60	0.04	0.00	0.05	0.06	101.30
R23-27														
Grain	1		53.22	30.13	0.31	0.01	11.03	4.96	0.25	0.00	0.00	0.02	0.11	100.04
Mount	2		54.13	28.23	0.34	0.29	10.29	5.34	0.31	0.02	0.00	0.00	0.08	99.03
	3		58.59	26.02	0.28	0.00	6.80	7.56	0.81	0.05	0.00	0.00	0.26	100.37
	4		57.85	27.24	0.31	0.00	7.64	7.14	0.54	0.00	0.00	0.00	0.10	100.82
	5		56.41	27.83	0.33	0.00	8.86	6.42	0.46	0.00	0.00	0.08	0.08	100.47
	6		56.88	24.46	0.26	0.00	7.81	6.57	0.61	0.03	0.00	0.00	0.17	96.79
	7	E	57.37	27.29	0.37	0.00	8.27	6.80	0.53	0.01	0.00	0.02	0.17	100.83
	7	C	57.42	26.82	0.32	0.00	7.99	6.48	0.55	0.02	0.00	0.00	0.04	99.64
	8	E+	57.27	27.61	0.35	0.02	8.65	6.68	0.47	0.00	0.01	0.00	0.04	101.10
	8	C+	57.46	28.13	0.29	0.01	8.47	6.80	0.47	0.00	0.00	0.02	0.18	101.83
	9		67.12	15.83	1.57	0.30	1.13	4.56	5.01	0.33	0.01	0.00	0.15	96.01
Whole	10	E	56.60	28.04	0.33	0.01	8.87	6.36	0.47	0.09	0.00	0.02	0.09	100.88
Grain	10	NE	57.54	27.98	0.34	0.02	8.58	6.65	0.46	0.05	0.00	0.02	0.11	101.75
	10	NC	56.41	27.93	0.28	0.03	8.90	6.40	0.46	0.11	0.00	0.04	0.17	100.73
	11	E	57.13	27.32	0.36	0.03	8.42	6.61	0.50	0.08	0.02	0.00	0.13	100.60
	11	C	53.81	29.64	0.40	0.02	10.99	5.29	0.28	0.08	0.02	0.04	0.13	100.70
	12	E	55.62	27.83	0.33	0.19	9.25	6.25	0.48	0.07	0.00	0.04	0.14	100.20
	12	C	56.34	27.54	0.37	0.03	8.49	6.40	0.58	0.08	0.06	0.00	0.18	100.07
	13	E	57.21	26.02	0.38	0.18	7.62	7.32	0.67	0.10	0.03	0.04	0.24	99.81
	13	C	57.50	26.07	0.31	0.02	7.46	6.97	0.74	0.08	0.04	0.04	0.24	99.47

Appendix 4. Continued.

FELDSPAR ANALYSES

Rainier Mesa Member

Sample Type	Grain #	Pos.	SiO_2	Al_2O_3	FeO	MgO	CaO	Na_2O	K_2O	TiO_2	MnO	P_2O_5	BaO	Total
R23-27														
Thin	14	E	59.79	28.70	0.33	0.01	8.37	6.97	0.50	0.06	0.00	0.00	0.16	104.89
Section	14	C	57.31	27.81	0.34	0.00	8.74	6.23	0.49	0.05	0.00	0.00	0.17	101.14
	15	E	54.24	26.80	0.31	0.00	8.59	6.39	0.47	0.07	0.00	0.04	0.10	97.01
	15	C	55.80	27.00	0.33	0.00	8.72	6.40	0.50	0.06	0.00	0.00	0.07	98.88
	16	E	56.03	28.06	0.36	0.00	9.67	6.02	0.42	0.09	0.04	0.05	0.10	100.84
	17	E+	56.58	27.11	0.38	0.00	9.03	5.96	0.41	0.06	0.03	0.02	0.13	99.71
	17	C+	55.58	29.02	0.39	0.45	10.80	5.47	0.32	0.07	0.03	0.06	0.10	102.29
	18	E	52.37	25.19	1.93	0.00	9.46	5.35	0.43	0.23	0.38	0.38	0.08	95.80
R21-1														
Grain	1	E	61.94	20.13	0.84	0.00	0.42	3.86	9.95	0.07	0.00	0.05	1.16	98.42
Mount	2	E	62.96	19.37	0.12	0.00	0.35	3.97	10.02	0.05	0.02	0.00	0.40	97.26
	3	E	63.13	18.96	0.07	0.00	0.21	3.65	10.47	0.00	0.02	0.00	0.10	96.61
	4	E	63.51	19.06	0.12	0.00	0.27	3.85	10.65	0.02	0.00	0.00	0.16	97.64
	4	C	64.24	19.20	0.15	0.00	0.26	3.78	10.61	0.05	0.00	0.00	0.13	98.42
	5	E	61.91	19.07	0.13	0.00	0.37	3.79	9.93	0.05	0.00	0.00	0.64	95.89
	6	E	63.07	19.11	0.11	0.00	0.18	3.65	10.53	0.02	0.00	0.00	0.05	96.72
	7	E	62.26	19.38	0.15	0.00	0.56	4.05	9.45	0.05	0.05	0.00	1.02	96.97
	8	E	59.30	24.34	0.14	0.02	5.42	7.76	1.37	0.00	0.00	0.05	0.02	98.42
	9	E	60.00	24.22	0.21	0.00	4.89	8.04	1.56	0.00	0.00	0.11	0.06	99.09
	10	C	58.83	25.36	0.23	0.00	6.11	7.66	1.19	0.00	0.01	0.00	0.15	99.54
	11	E	50.78	25.04	0.31	0.00	7.07	6.84	0.81	0.03	0.03	0.00	0.20	91.11
	11	C	59.68	24.71	0.18	0.01	5.40	7.66	1.52	0.01	0.00	0.00	0.23	99.40
	12	E	59.83	23.74	0.16	0.00	4.56	7.67	1.59	0.00	0.05	0.00	0.10	97.70
	13	E	59.87	23.81	0.16	0.00	4.79	7.80	1.56	0.00	0.00	0.02	0.20	98.21
	14	E+	60.13	23.80	0.11	0.00	4.73	7.97	1.52	0.00	0.02	0.00	0.09	98.37
	14	C+	58.34	25.01	0.12	0.00	6.45	7.20	1.02	0.00	0.07	0.00	0.21	98.42
	15	E+	61.43	24.49	0.16	0.00	4.92	7.90	1.53	0.00	0.00	0.00	0.07	100.50
	16	C+	63.11	19.13	0.03	0.00	0.33	3.94	10.82	0.00	0.05	0.08	0.44	97.93

Appendix 4. Continued.

FELDSPAR ANALYSES

Rainier Mesa Member

Sample Type	Grain #	Pos.	SiO_2	Al_2O_3	FeO	MgO	CaO	Na_2O	K_2O	TiO_2	MnO	P_2O_5	BaO	Total
R21-13														
Grain	1	E	55.71	29.38	0.29	0.00	10.03	5.74	0.37	0.02	0.02	0.06	0.08	101.70
Mount	1	C	52.29	30.31	0.38	0.00	11.76	4.65	0.25	0.02	0.06	0.06	0.00	99.78
	2	E	54.55	28.05	0.29	0.00	9.34	5.45	0.39	0.03	0.04	0.00	0.04	98.18
	2	C	53.00	30.07	0.37	0.00	11.42	4.55	0.28	0.01	0.00	0.04	0.02	99.76
	3	E	53.43	26.82	0.49	0.00	9.12	5.24	0.38	0.02	0.00	0.05	0.05	95.60
	3	C	51.98	31.25	0.37	0.03	12.01	4.37	0.27	0.07	0.00	0.06	0.07	100.48
	4	E	53.29	30.09	0.37	0.01	11.50	4.62	0.25	0.00	0.00	0.06	0.03	100.22
	4	C	52.46	30.11	0.43	0.02	11.37	4.56	0.30	0.04	0.00	0.00	0.00	99.29
	5	E	51.17	28.08	0.35	0.00	10.66	4.86	0.34	0.02	0.04	0.00	0.03	95.55
	5	C	48.81	32.53	0.39	0.03	14.42	3.21	0.14	0.00	0.00	0.09	0.03	99.65
Zoned	1	E	50.58	26.69	0.47	0.04	9.80	4.67	0.40	0.08	0.03	0.00	0.11	92.87
Plag	1	NE	50.57	30.41	0.53	0.05	12.03	4.35	0.24	0.05	0.00	0.04	0.09	98.36
Grain	1	C	48.02	33.23	0.67	0.07	15.05	2.88	0.11	0.08	0.00	0.00	0.04	100.15
	1	NC	47.69	32.44	0.56	0.06	15.08	2.83	0.18	0.04	0.00	0.09	0.07	99.04
	1	NE	48.53	32.47	0.49	0.06	14.91	3.03	0.14	0.03	0.00	0.11	0.03	99.80
R21-5														
Grain	1	E	38.17	16.52	0.27	0.00	3.25	7.25	1.62	0.02	0.03	0.08	0.05	67.26
Mount	2	E	61.99	23.09	0.23	0.00	3.98	8.44	1.62	0.02	0.00	0.02	0.09	99.48
	3	E	62.63	23.19	0.25	0.00	3.97	8.46	1.62	0.08	0.00	0.00	0.00	100.20
	4	E	61.38	22.50	0.21	0.00	3.60	8.53	1.67	0.03	0.04	0.00	0.06	98.02
	4	C	55.36	28.32	0.16	0.00	9.39	6.19	0.45	0.01	0.04	0.02	0.14	100.08
	5	E	62.98	24.04	0.27	0.00	4.15	8.63	1.67	0.02	0.03	0.02	0.09	101.90
	5	C	60.56	23.54	0.25	0.00	4.50	8.28	1.36	0.00	0.02	0.05	0.02	98.58
	6	E	62.67	23.53	0.26	0.00	4.20	8.44	1.56	0.02	0.04	0.04	0.06	100.82
	6	C	61.55	23.64	0.19	0.00	4.26	8.62	1.57	0.00	0.02	0.00	0.00	99.85
	7	E	62.50	23.48	0.28	0.00	4.10	8.52	1.58	0.00	0.02	0.08	0.02	100.58
	7	C	57.27	27.24	0.51	0.00	8.27	6.95	0.56	0.01	0.04	0.00	0.07	100.92
	8	E	61.87	22.59	0.29	0.00	3.79	8.58	1.60	0.02	0.08	0.00	0.00	98.82
	9	E	61.53	23.64	0.27	0.00	3.89	8.64	1.66	0.02	0.01	0.06	0.10	99.82
	10	E	62.11	23.41	0.20	0.00	4.04	8.13	1.58	0.00	0.24	0.10	0.00	99.81
	11	E	61.86	23.11	0.26	0.00	3.77	8.55	1.74	0.04	0.03	0.00	0.04	99.40
	11	NE	61.23	24.42	0.24	0.00	4.75	7.97	1.29	0.02	0.04	0.05	0.00	100.01
	11	C	62.21	23.69	0.84	0.00	3.92	8.59	1.59	0.02	0.04	0.00	0.07	100.97

Appendix 4. Continued.

FELDSPAR ANALYSES

Rainier Mesa Member

Sample Type	Grain #	Pos.	SiO_2	Al_2O_3	FeO	MgO	CaO	Na_2O	K_2O	TiO_2	MnO	P_2O_5	BaO	Total
R21-5														
Grain	12	E	63.18	19.09	0.07	0.00	0.29	3.92	10.06	0.00	0.02	0.00	0.17	96.80
Mount	13	E	63.87	19.45	0.13	0.00	0.31	4.03	9.87	0.05	0.00	0.04	0.30	98.05
	14	E	62.83	19.27	0.12	0.00	0.34	4.06	9.81	0.00	0.00	0.04	0.08	96.55
	15	E	62.54	18.69	0.10	0.00	0.26	3.97	9.75	0.00	0.00	0.00	0.10	95.41
	16	E	62.31	19.06	0.13	0.00	0.35	3.93	9.92	0.01	0.00	0.04	0.07	95.82
	17	E	62.83	19.07	0.17	0.00	0.32	4.00	10.04	0.03	0.02	0.05	0.14	96.67

Appendix 4. Continued.

FELDSPAR ANALYSES

Ammonia Tanks Member

Sample Type	Grain #	Pos.	SiO_2	Al_2O_3	FeO	MgO	CaO	Na_2O	K_2O	TiO_2	MnO	P_2O_5	BaO	Total
A5-3														
Grain	1	E	65.40	19.53	0.14	0.00	0.37	5.54	8.53	0.04	0.01	0.00	0.03	99.59
Mount	1	C	66.26	19.54	0.14	0.00	0.35	5.35	8.59	0.03	0.00	0.02	0.00	100.28
	2	E	62.98	18.70	0.24	0.03	0.33	5.64	8.42	0.06	0.04	0.05	0.20	96.69
	2	C	54.31	25.97	0.23	0.05	7.79	6.78	0.43	0.06	0.05	0.01	0.21	95.89
A5-35														
Grain	1	E	62.03	19.25	0.16	0.00	0.44	5.26	8.64	0.03	0.02	0.00	0.16	95.99
Mount	2	E	63.01	18.74	0.16	0.00	0.44	5.17	8.87	0.02	0.00	0.05	0.16	96.62
	3	E	64.34	18.86	0.16	0.00	0.32	5.30	9.03	0.06	0.00	0.00	0.00	98.07
	4	E	62.66	19.17	0.17	0.00	0.54	4.99	8.59	0.03	0.00	0.05	0.47	96.67
	5	E	67.84	12.22	0.66	0.06	0.34	3.65	5.11	0.14	0.02	0.06	0.03	90.13
	6	E	64.07	19.35	0.13	0.00	0.36	5.11	8.92	0.03	0.00	0.07	0.07	98.11
	7	E	61.55	18.86	0.15	0.00	0.48	5.00	9.11	0.04	0.03	0.04	0.29	95.55
	8	E	64.21	19.48	0.16	0.00	0.49	5.25	8.81	0.04	0.00	0.00	0.18	98.62
	9	E	63.91	18.83	0.09	0.00	0.37	5.03	9.11	0.00	0.00	0.02	0.24	97.60
	9	E	60.70	18.35	0.14	0.30	0.41	4.73	8.62	0.05	0.03	0.08	0.13	93.54
	9	NE	63.82	19.19	0.15	0.00	0.38	5.06	9.08	0.02	0.03	0.07	0.07	97.87
	9	C	63.76	19.37	0.16	0.00	0.32	5.02	9.20	0.06	0.05	0.07	0.07	98.08
	10	E	56.43	26.55	0.24	0.00	7.56	6.79	0.46	0.00	0.00	0.00	0.08	98.11
	10	E	55.91	26.75	0.31	0.00	7.61	6.89	0.45	0.05	0.04	0.00	0.08	98.09
	10	NE	58.15	25.24	0.29	0.00	6.18	7.47	0.74	0.04	0.03	0.00	0.25	98.39
	10	C	57.41	24.62	0.26	0.00	6.30	7.20	0.73	0.03	0.04	0.14	0.26	96.99
A5-58														
Grain	1	E	62.83	21.13	0.25	0.00	1.74	7.53	4.68	0.00	0.00	0.04	0.15	98.35
Mount	2	E	63.26	20.10	0.22	0.00	0.96	6.04	7.55	0.02	0.02	0.08	0.38	98.63
	3	E	64.23	19.83	0.19	0.00	0.74	6.16	7.69	0.00	0.00	0.00	0.23	99.07
	4	E	63.00	19.59	0.26	0.00	0.50	5.65	8.42	0.00	0.00	0.12	0.37	97.91
	5	E	63.02	19.37	0.21	0.00	0.65	5.57	8.06	0.06	0.00	0.07	0.08	97.09
	6	E	58.42	22.59	0.36	0.00	4.46	7.95	1.34	0.03	0.04	0.04	0.10	95.33
	6	NE	60.38	23.92	0.30	0.01	4.84	7.81	1.31	0.03	0.03	0.04	0.09	98.76
	6	C	55.47	27.42	0.41	0.02	8.42	6.58	0.53	0.00	0.00	0.07	0.10	99.02

Appendix 4. Continued.

FELDSPAR ANALYSES

Ammonia Tanks Member

Sample Type	Grain #	Pos.	SiO_2	Al_2O_3	FeO	MgO	CaO	Na_2O	K_2O	TiO_2	MnO	P_2O_5	BaO	Total
A5-63														
Grain	1	E	35.82	14.60	12.33	15.30	0.14	0.88	8.67	7.03	0.20	0.00	1.96	96.93
Mount	1	C	36.10	14.61	12.79	15.03	0.06	0.85	8.49	7.00	0.21	0.05	1.62	96.81
	2	E	34.60	14.79	12.86	14.71	0.08	0.78	7.92	7.18	0.18	0.05	3.03	96.18
	3	E	58.25	26.30	0.32	0.01	6.78	6.79	1.27	0.00	0.03	0.07	0.34	100.16
	3	C	58.02	25.89	0.40	0.00	6.77	6.90	1.30	0.03	0.00	0.00	0.47	99.78
	4	E	57.36	25.75	0.36	0.01	6.98	6.58	1.23	0.04	0.00	0.07	0.32	98.70
	4	C	57.81	26.09	0.31	0.00	7.18	6.45	1.20	0.01	0.00	0.13	0.39	99.57
	5	E	56.84	24.98	0.43	0.01	6.58	6.36	1.24	0.02	0.02	0.00	0.27	96.75
	5	C	58.37	25.49	0.33	0.00	6.57	6.95	1.27	0.02	0.04	0.06	0.39	99.49
	6	E	54.63	24.03	0.36	0.00	6.52	6.97	1.33	0.02	0.00	0.00	0.44	94.30
	7	E	57.23	26.30	0.38	0.03	6.95	6.77	1.08	0.05	0.00	0.08	0.37	99.24
	7	C	56.69	26.42	0.37	0.00	7.13	6.58	1.10	0.04	0.57	0.00	0.32	99.22
A5-69														
Grain	1	E	59.12	24.57	0.40	0.00	5.33	7.22	1.81	0.05	0.00	0.00	0.43	98.93
Mount	1	C	59.61	24.78	0.37	0.00	5.16	7.21	1.83	0.06	0.00	0.00	0.35	99.37
	2	E	58.71	24.60	0.36	0.00	5.34	7.03	1.81	0.03	0.00	0.00	0.29	98.17
	2	C	58.84	24.44	0.44	0.00	5.53	7.14	1.82	0.06	0.01	0.00	0.32	98.60
	3	E	57.00	26.07	0.43	0.03	6.79	6.88	1.11	0.05	0.00	0.00	0.32	98.68
	3	C	54.71	25.53	0.50	0.02	8.38	6.13	0.92	0.07	0.00	0.00	0.26	96.52
	4	E	59.55	24.67	1.14	0.00	5.09	7.67	1.88	0.09	0.96	0.00	0.30	101.35
	4	C	57.64	25.79	0.54	0.02	6.74	6.76	1.34	0.07	0.02	0.00	0.44	99.36
	5	E+	57.52	25.96	0.40	0.02	7.11	6.94	1.10	0.07	0.04	0.00	0.30	99.46
	5	C+	56.70	25.72	0.45	0.05	6.94	6.64	1.10	0.06	0.02	0.00	0.41	98.09
	6	E	58.00	26.26	0.46	0.02	6.73	6.90	1.12	0.07	0.00	0.00	0.41	99.97
	6	C	57.86	26.29	0.42	0.01	6.56	6.92	1.28	0.05	0.56	0.00	0.28	100.23
	7	E	65.00	19.46	0.22	0.00	0.36	6.09	8.17	0.00	0.04	0.00	0.00	99.34
	8	E	64.23	19.54	0.22	0.00	0.35	6.00	7.83	0.01	0.00	0.00	0.06	98.24
	9	E+	63.88	19.28	0.21	0.00	0.36	5.86	8.38	0.04	0.00	0.00	0.06	98.07
	10	E	65.18	19.79	0.25	0.01	0.42	6.27	7.57	0.00	0.00	0.00	0.02	99.51
	11	E+	54.35	29.11	0.42	0.04	9.81	5.64	0.61	0.07	0.00	0.04	0.19	100.28

Appendix 4. Continued.

FELDSPAR ANALYSES

Ammonia Tanks Member

Sample Type	Grain #	Pos.	SiO_2	Al_2O_3	FeO	MgO	CaO	Na_2O	K_2O	TiO_2	MnO	P_2O_5	BaO	Total
A5-71														
Grain	1	E	64.60	20.54	0.25	0.00	0.91	5.82	8.26	0.10	0.08	0.00	0.26	100.82
Mount	2	E	62.12	21.19	0.35	0.00	2.44	7.51	4.27	0.07	0.00	0.00	0.07	98.02
	2	C	58.23	25.51	0.36	0.03	6.42	7.34	0.97	0.05	0.00	0.00	0.32	99.23
	3	E	57.95	26.59	0.41	0.03	6.86	6.97	1.01	0.06	0.00	0.05	0.39	100.32
	3	C	59.60	26.40	0.41	0.03	6.38	7.32	1.07	0.09	0.00	0.03	0.19	101.52
	4	E	61.16	23.96	0.27	0.03	4.89	7.81	1.75	0.06	0.00	0.00	0.37	100.30
	4	C	61.15	23.90	0.40	0.03	4.60	7.83	1.82	0.07	0.00	0.00	0.27	100.07
	5	E	59.84	25.72	0.36	0.00	6.15	7.39	0.99	0.09	0.00	0.00	0.34	100.88
	5	C	59.63	25.17	0.36	0.03	5.88	7.27	1.10	0.08	0.00	0.00	0.22	99.74
	6	E	65.31	20.15	0.36	0.00	0.56	5.12	9.08	0.05	0.00	0.00	0.16	100.79
	7	E	63.79	20.06	0.28	0.02	0.79	5.34	8.62	0.13	0.00	0.07	0.65	99.75
	8	NE	57.48	26.89	0.91	0.03	7.43	6.91	0.99	0.08	0.00	0.00	0.38	101.10
	8	C	59.32	25.49	0.49	0.04	5.81	7.46	1.57	0.08	0.00	0.00	0.40	100.66
	9	E	65.97	20.12	0.24	0.00	0.65	4.90	9.28	0.02	0.00	0.00	0.00	101.18
	10	E	65.17	20.06	0.26	0.00	0.74	5.24	8.39	0.04	0.00	0.00	0.02	99.92
	11	E	64.74	20.88	0.21	0.00	0.95	5.26	8.76	0.08	0.00	0.00	0.59	101.47
	12	E	65.98	20.67	0.25	0.00	0.87	5.46	8.35	0.04	0.00	0.00	0.07	101.69
	12	C	65.61	20.36	0.32	0.00	0.89	5.67	8.39	0.08	0.00	0.00	0.03	101.35
Thin	13	E	62.52	21.86	0.36	0.00	2.62	7.05	4.60	0.06	0.06	0.00	0.23	99.36
Section	13	C	61.62	24.00	0.30	0.00	4.12	7.80	2.32	0.06	0.00	0.04	0.20	100.46
	14	E	48.44	1.03	8.25	13.07	21.16	0.52	0.02	0.40	1.36	0.06	0.02	94.33
	14	C	51.81	1.05	7.94	14.45	21.70	0.77	0.00	0.40	1.29	0.08	0.02	99.51
	15	E	59.38	23.92	0.37	0.00	5.07	7.83	1.45	0.00	0.03	0.08	0.05	98.18
	15	C	60.72	24.32	0.28	0.00	4.70	7.79	1.77	0.02	0.03	0.00	0.02	99.65
	16	E+	63.36	20.20	0.22	0.00	0.94	5.74	8.04	0.06	0.03	0.06	0.08	98.73
	16	C+	62.63	20.45	0.25	0.00	0.88	5.82	8.52	0.06	0.00	0.06	0.10	98.77
	17	E	63.35	20.25	0.28	0.00	0.88	5.70	8.23	0.06	0.02	0.02	0.06	98.85
	18	NE	56.35	26.87	0.34	0.00	7.95	6.65	0.70	0.04	0.05	0.04	0.21	99.20
	18	C	53.65	25.02	0.34	0.00	7.10	6.96	0.94	0.07	0.00	0.07	0.15	94.30
	19	NE	58.35	24.09	0.36	0.00	5.36	7.07	1.34	0.13	0.03	0.00	0.40	97.13
	19	C	58.46	24.97	0.46	0.00	5.74	7.59	1.25	0.06	0.00	0.00	0.33	98.86

Appendix 4. Continued.

FELDSPAR ANALYSES

Ammonia Tanks Member

Sample Type	Grain #	Pos.	SiO_2	Al_2O_3	FeO	MgO	CaO	Na_2O	K_2O	TiO_2	MnO	P_2O_5	BaO	Total
A5-72														
Grain	1	E	61.13	20.63	0.26	0.00	0.87	4.49	8.32	0.06	0.00	0.00	2.42	98.18
Mount	2	E	57.84	23.15	0.38	0.00	5.01	6.45	1.90	0.00	0.00	0.00	0.40	95.13
	2	C	56.82	23.81	0.31	0.00	5.36	6.47	1.65	0.01	0.00	0.08	0.28	94.79
	3	E	56.30	24.23	0.80	0.00	6.29	6.48	1.32	0.02	0.00	0.00	0.24	95.68
	3	C	52.97	26.85	0.31	0.00	8.95	5.17	0.57	0.00	0.00	0.08	0.14	95.04
	4	E	59.75	20.37	0.22	0.00	1.01	4.29	8.07	0.03	0.00	0.06	3.47	97.27
	5	E	60.40	20.55	0.15	0.00	0.88	4.45	8.31	0.07	0.00	0.08	2.86	97.75
	5	C	61.39	20.34	0.24	0.00	0.92	4.21	8.37	0.06	0.00	0.00	2.44	97.97
	6	E	61.02	20.47	0.19	0.00	0.93	4.50	8.24	0.05	0.00	0.05	2.04	97.49
	7	E	61.87	20.34	0.26	0.00	0.76	4.58	8.88	0.05	0.00	0.02	2.11	98.87
	7	C	61.40	20.13	0.24	0.00	0.80	4.26	8.71	0.04	0.00	0.00	2.10	97.68
	8	E	56.66	24.49	0.37	0.00	5.78	6.38	1.48	0.00	0.00	0.07	0.44	95.67
	8	C	56.61	25.26	0.21	0.00	6.64	6.29	1.15	0.03	0.00	0.00	0.04	96.23
	9	E	59.77	23.47	0.34	0.00	4.73	7.02	2.04	0.00	0.00	0.05	0.24	97.66
	9	C	57.78	24.49	0.38	0.00	5.62	7.23	1.54	0.03	0.00	0.06	0.28	97.41
	10	E	58.54	21.07	0.22	0.00	1.10	4.28	7.45	0.12	0.00	0.00	4.00	96.78
	11	E	57.29	25.57	0.37	0.00	6.36	6.71	1.19	0.00	0.00	0.11	0.43	98.03
	11	C	56.56	27.02	0.30	0.00	7.59	6.07	0.87	0.00	0.00	0.00	0.37	98.78
A5-75														
Grain	1	E	59.12	28.81	0.20	0.05	8.85	6.06	0.76	0.04	0.02	0.00	0.34	104.25
Mount	1	C	56.52	30.83	0.17	0.05	11.09	5.22	0.52	0.05	0.00	0.14	0.19	104.78
	2	E	52.33	35.07	0.31	0.04	15.42	3.09	0.21	0.00	0.02	0.10	0.00	106.59
	2	C	58.39	28.52	0.26	0.04	9.73	5.70	0.75	0.05	0.03	0.03	0.25	103.75
	3	E	58.17	29.42	0.19	0.03	9.62	5.97	0.82	0.00	0.01	0.11	0.16	104.50
	3	C	57.81	25.87	0.31	0.04	6.90	6.31	1.03	0.00	0.00	0.02	0.31	98.60
	4	E	55.07	26.99	0.21	0.04	8.51	5.62	0.75	0.01	0.00	0.00	0.22	97.42
	4	C	56.01	26.54	0.18	0.01	7.86	6.05	0.94	0.06	0.00	0.00	0.30	97.95
	5	E	58.42	24.59	0.11	0.02	5.33	6.76	1.79	0.00	0.03	0.07	0.30	97.42
	5	C	57.82	25.41	0.13	0.01	6.24	6.63	1.39	0.03	0.00	0.09	0.34	98.09
	6	E	58.60	24.91	0.14	0.00	5.98	6.70	1.58	0.05	0.00	0.06	0.30	98.32
	6	C	58.17	25.23	0.21	0.00	6.21	6.41	1.52	0.02	0.00	0.09	0.24	98.10
	7	E	53.77	27.35	0.12	0.03	8.63	5.49	0.75	0.00	0.02	0.07	0.15	96.38
	8	E	54.43	26.84	0.18	0.03	8.34	5.79	0.80	0.05	0.00	0.02	0.24	96.72
	8	C	55.93	25.96	0.25	0.03	7.82	6.07	0.93	0.00	0.00	0.09	0.26	97.34
	9	E	54.21	28.36	0.20	0.05	9.48	5.16	0.53	0.03	0.00	0.07	0.18	98.27

Appendix 4. Continued.

FELDSPAR ANALYSES

Ammonia Tanks Member

Sample Type	Grain #	Pos.	SiO_2	Al_2O_3	FeO	MgO	CaO	Na_2O	K_2O	TiO_2	MnO	P_2O_5	BaO	Total
A21-18														
Grain	1	E	63.24	18.63	0.13	0.00	0.36	5.19	8.12	0.00	0.00	0.00	0.03	95.70
Mount	2	E	63.13	20.98	0.15	0.00	1.75	8.47	2.03	0.00	0.00	0.00	0.02	96.53
	3	C	55.71	26.96	0.14	0.00	7.92	6.37	0.34	0.00	0.00	0.00	0.03	97.47
	4	E	63.48	19.25	0.15	0.00	0.37	5.51	7.43	0.00	0.00	0.02	0.02	96.23
	5	E	64.73	19.47	0.15	0.00	0.37	5.50	7.77	0.00	0.00	0.05	0.05	98.09
	6	E	63.16	19.16	0.17	0.00	0.39	5.22	8.05	0.00	0.00	0.00	0.00	96.15
	7	E	64.75	19.61	0.17	0.00	0.31	5.38	7.96	0.00	0.00	0.09	0.00	98.27
	8	C	64.92	19.71	0.12	0.00	0.35	5.61	7.82	0.00	0.00	0.05	0.03	98.61
	9	E	64.52	21.41	0.19	0.00	2.05	9.27	1.82	0.00	0.00	0.00	0.03	99.29
	9	C	64.35	21.36	0.18	0.00	2.12	8.93	1.80	0.00	0.84	0.00	0.05	99.63

FELDSPAR ANALYSES -- University of Michigan

Ammonia Tanks Member

Sample Type	Grain #	Pos.	SiO_2	Al_2O_3	FeO	CaO	Na_2O	K_2O	BaO	Total
A4-70										
Thin	1	E	63.30	19.40	0.16	0.46	5.32	8.90	0.06	97.59
Sec.	2	E	62.94	19.71	0.29	0.38	5.02	9.05	1.54	98.93
	3	E	64.52	19.44	0.17	0.45	5.38	8.87	0.20	99.02
	3	C	58.19	25.99	0.31	7.36	7.41	0.54	0.15	99.95
	4	E	64.90	19.72	0.31	0.52	5.51	8.93	0.14	100.04
	5	E	63.55	21.44	0.28	2.43	8.43	3.15	0.11	99.39
	6	E	64.80	19.31	0.16	0.46	5.41	8.81	0.20	99.14
	7	E	61.62	21.82	0.26	2.91	8.96	1.56	0.20	97.34
A5-9										
Thin	1	E	62.04	18.97	0.32	0.64	4.76	7.61	0.20	94.54
Sec.	2	E	63.04	19.27	0.33	0.62	5.63	8.40	0.14	97.44
	2	C	63.65	19.23	0.28	0.54	5.38	8.61	0.28	97.96
	3	E	62.09	21.34	0.43	2.77	8.60	1.93	0.12	97.28
	4	E	63.15	19.46	0.35	0.67	5.62	8.24	0.17	97.66
	4	C	59.85	23.58	0.32	4.74	8.29	1.09	0.11	97.98
	5	E	61.17	22.54	0.47	3.80	8.49	1.33	0.00	97.80

Appendix 4. Continued.

FELDSPAR ANALYSES -- University of Michigan

Ammonia Tanks Member

Sample Type	Grain #	Pos.	SiO_2	Al_2O_3	FeO	CaO	Na_2O	K_2O	BaO	Total
A5-29										
Thin	1	E	64.00	19.29	0.20	0.32	5.77	8.20	0.03	97.81
Sec.	1	C	63.73	18.77	0.13	0.35	5.67	8.11	0.00	96.76
	2	E	63.46	18.85	0.17	0.31	5.81	8.28	0.09	96.98
	2	C	64.22	19.07	0.13	0.33	5.79	8.02	0.15	97.71
	3	E	64.50	19.37	0.11	0.29	5.90	8.27	0.03	98.48
	4	E	64.29	18.93	0.17	0.31	5.64	8.48	0.11	97.93
A5-30										
Thin	1	E	63.03	19.91	0.23	0.75	5.25	8.81	0.49	98.47
Sec.	1	C	63.18	19.80	0.28	0.74	4.95	9.18	0.32	98.45
	2	E	56.22	22.22	0.33	4.74	7.02	1.63	0.11	92.26
	3	E	64.23	19.92	0.17	0.88	5.31	8.66	0.29	99.45
	4	E	60.89	23.60	0.42	4.78	7.69	1.99	0.35	99.73
	5	E	61.31	22.77	0.34	3.94	7.81	2.59	0.14	98.89
	6	E	58.62	24.44	0.27	6.01	7.21	1.44	0.18	98.17
A5-31										
Thin	1	E	60.94	19.92	0.33	0.64	3.96	8.93	2.69	97.41
Sec.	2	E	57.59	25.60	0.54	7.02	6.86	1.18	0.18	98.96
	3	E	58.39	24.43	0.36	5.79	7.18	1.74	0.28	98.16
	4	E	56.71	26.06	0.56	7.47	6.61	1.08	0.12	98.62
	5	C	57.48	25.95	0.44	7.52	6.62	1.08	0.34	99.44
	5	NE	59.67	25.06	0.41	6.14	7.07	1.51	0.41	100.29
	5	E	63.32	19.40	0.38	0.60	4.94	9.36	0.23	98.24
A5-56										
Thin	1	E	64.26	19.19	0.15	0.36	5.84	8.46	0.05	98.30
Sec.	2	E	64.34	19.09	0.13	0.37	5.85	8.26	0.05	98.09
	3	E	64.55	19.41	0.21	0.38	5.95	7.89	0.00	98.39
	3	C	65.27	19.41	0.22	0.40	6.11	8.08	0.06	99.56
A5-68										
Thin	1	E	64.27	19.36	0.18	0.49	6.06	7.91	0.06	98.34
Sec.	2	E	64.84	19.47	0.16	0.53	6.11	7.98	0.03	99.12

Appendix 4. Continued.

FELDSPAR ANALYSES -- University of Michigan

Ammonia Tanks Member

Sample Type	Grain #	Pos.	SiO_2	Al_2O_3	FeO	CaO	Na_2O	K_2O	BaO	Total
A5-79										
Thin	1	E	63.26	19.21	0.25	0.44	5.92	8.00	0.00	97.08
Sec.	2	E	63.89	20.88	0.18	2.02	9.28	1.85	0.00	98.10
	3	E	63.96	18.99	0.15	0.25	5.57	8.35	0.00	97.27
	4	E	63.07	18.97	0.08	0.31	5.70	8.32	0.03	96.49

Appendix 4. Continued.

BIOTITE ANALYSES

Rainier Mesa Member

Sample	Grain #	Pos.	Na_2O	Al_2O_3	MgO	CaO	K_2O	TiO_2	MnO	FeO	NiO	SiO_2	BaO	Total
R8-25	1	E	0.33	14.26	13.96	0.20	6.35	5.74	0.32	3.59	0.00	34.92	0.87	90.54
	1	C	0.40	13.88	14.32	0.33	5.79	5.80	0.33	14.05	0.00	34.12	1.10	90.12
	2	E	0.42	14.78	13.33	0.02	8.93	6.24	0.28	14.37	0.13	36.57	1.62	96.69
	2	C	0.66	14.31	13.89	0.03	8.86	5.85	0.31	14.19	0.00	35.97	0.75	94.82
	3	E	0.34	13.51	14.07	0.17	6.65	5.17	0.23	13.36	0.00	36.84	0.16	90.50
	3	C	0.50	13.19	14.20	0.19	7.49	5.40	0.33	14.21	0.00	36.18	0.02	91.71
	4	E	0.68	14.76	13.53	0.01	8.96	5.93	0.35	15.63	0.00	36.25	0.78	96.88
	4	C	0.64	13.49	14.56	0.00	9.19	5.62	0.27	14.66	0.00	37.51	0.10	96.04
	5	E	0.60	14.53	13.40	0.08	8.23	6.09	0.30	14.81	0.00	35.32	1.58	94.94
	6	E	0.62	14.45	13.33	0.04	8.44	6.24	0.37	14.82	0.00	35.41	1.79	95.51
	7	E	0.60	14.39	14.44	0.00	8.92	5.70	0.34	14.50	0.00	36.31	0.53	95.73
	8	C	0.59	14.51	13.97	0.00	8.78	6.10	0.52	14.78	0.00	36.00	1.08	96.33
	9	E	0.67	14.28	13.26	0.09	8.51	6.12	0.27	15.86	0.00	36.16	1.27	96.49
	9	E	0.60	14.41	14.06	0.06	8.80	5.94	0.32	15.27	0.03	36.16	0.95	96.60
	10	E	0.57	13.69	13.98	0.07	8.62	5.94	0.28	14.25	0.04	35.96	0.59	93.99
	11	E	0.54	14.33	13.66	0.05	8.74	6.18	0.29	14.71	0.00	36.37	1.03	95.90
	12	E	0.49	13.48	14.40	0.19	7.34	5.79	0.30	14.48	0.00	35.32	0.44	92.23
R8-44	1	E	0.63	13.82	11.44	0.13	7.96	5.91	0.23	13.29	0.00	37.25	1.05	91.71
	1	C	0.80	13.81	11.96	0.16	7.42	5.97	0.27	13.94	0.00	36.01	1.06	91.40
	2	E	0.65	13.80	15.77	0.01	9.18	4.79	0.34	14.39	0.00	38.95	0.14	98.02
	2	C	0.60	13.64	15.12	0.02	9.15	4.95	0.26	13.77	0.00	38.43	0.00	95.93
	3	E	0.48	14.08	12.57	0.27	7.50	6.03	0.21	13.65	0.01	37.35	0.63	92.78
	4	E	0.48	14.11	12.25	0.15	7.55	6.08	0.31	14.72	0.00	37.57	1.22	94.44
	5	E	0.56	14.12	14.17	0.01	8.92	6.12	0.30	14.58	0.00	36.57	0.57	95.92
	6	E	0.45	13.65	13.46	0.18	7.53	5.41	0.25	13.75	0.00	39.16	0.04	93.88
	7	E	0.63	14.67	14.13	0.06	8.64	6.24	0.55	15.37	0.00	36.32	1.42	98.03
R8-45	1	E	0.70	14.40	13.99	0.06	8.62	6.03	0.33	15.35	0.00	36.39	1.52	97.39
	2	E	0.62	13.90	13.45	0.11	8.53	5.80	0.30	14.63	0.00	36.68	0.54	94.56
	2	C	0.55	14.12	14.02	0.10	8.79	5.94	0.28	14.35	0.00	37.54	0.69	96.38
	3	E	0.71	14.72	13.84	0.08	8.78	5.92	0.26	14.81	0.02	36.51	1.52	97.17
	3	C	0.63	14.38	13.56	0.05	8.67	5.95	0.26	14.99	0.00	35.58	1.33	95.40
	4	E	0.71	14.68	13.20	0.05	8.67	6.39	0.30	15.08	0.04	35.89	1.96	96.97
	5	E	0.56	14.10	13.71	0.17	8.39	6.10	0.32	14.75	0.00	36.37	0.85	95.32
	6	E	0.39	13.99	13.75	0.26	7.49	5.69	0.18	14.04	0.01	37.00	0.63	93.43
	7	E	0.66	14.59	14.19	0.15	8.79	5.84	0.27	14.83	0.04	36.92	0.55	96.83
	8	E	0.61	14.67	14.06	0.11	8.41	6.27	0.31	15.54	0.03	36.57	1.17	97.75

Appendix 4. Continued.

BIOTITE ANALYSES

Rainier Mesa Member

Sample	Grain #	Pos.	Na_2O	Al_2O_3	MgO	CaO	K_2O	TiO_2	MnO	FeO	NiO	SiO_2	BaO	Total
R11-5	1	E	0.63	14.96	13.99	0.07	7.99	5.80	0.30	13.50	0.02	36.60	1.11	94.97
	1	C	0.59	15.04	13.05	0.18	7.88	5.47	0.21	13.33	0.00	36.83	0.91	93.49
	2	E	0.68	14.60	14.10	0.55	7.74	5.42	0.20	13.09	0.03	36.29	0.46	93.16
	3	E	0.46	13.69	13.34	0.12	7.51	5.73	0.26	13.74	0.03	35.74	0.36	90.98
	4	E	0.71	14.89	13.65	0.02	8.13	5.58	0.28	13.97	0.02	36.60	0.52	94.37
	5	E	1.48	14.47	14.33	0.11	7.47	5.54	0.28	13.17	0.00	36.35	1.08	94.28
	6	E	0.78	15.36	14.09	0.00	8.15	5.64	0.25	13.55	0.15	36.41	1.31	95.69
	6	C	0.65	15.06	13.49	0.04	7.61	5.48	0.23	13.31	0.02	36.77	0.76	93.42
	7	E	0.62	13.76	14.00	0.07	8.30	6.00	0.24	14.21	0.00	36.17	0.81	94.18
	8	E	0.51	14.02	13.60	0.20	7.98	5.72	0.19	13.81	0.00	36.13	0.88	93.04
	9	E	0.49	14.65	13.63	0.36	7.46	5.72	0.24	14.15	0.00	35.83	1.07	93.60
	9	E	0.40	14.56	13.37	0.30	7.65	5.69	0.20	13.52	0.00	36.17	0.96	92.82
R11-7	1	E	0.66	13.64	14.44	0.03	9.27	3.59	0.74	15.88	0.00	37.51	0.05	95.81
	2	E	0.34	12.90	12.81	0.34	7.13	3.71	0.54	16.47	0.00	37.31	0.06	91.61
	3	E	0.41	13.83	13.77	0.31	6.74	5.91	0.20	14.26	0.02	35.43	0.59	91.47
	4	E	0.41	13.27	13.36	0.27	7.67	3.60	0.53	15.23	0.02	36.83	0.03	91.22
	5	E	0.50	14.09	13.30	0.10	8.71	3.71	0.64	14.60	0.00	37.77	0.12	93.54
	6	E	0.49	13.42	13.85	0.18	8.10	3.86	0.64	15.55	0.02	37.23	0.02	93.36
	6	C	0.43	13.02	13.86	0.42	7.34	3.50	0.79	15.46	0.00	36.88	0.45	92.15
	7	E	0.60	13.56	14.02	0.02	9.16	3.83	0.59	16.44	0.00	37.42	0.02	95.66
	8	E	0.58	13.26	14.33	0.03	9.24	3.64	0.67	16.14	0.00	37.16	0.00	95.05
	9	E	0.37	13.37	13.75	0.36	7.21	3.48	0.67	15.01	0.01	36.81	0.02	91.06
	10	E	0.32	12.89	13.44	0.32	7.68	3.16	0.57	14.90	0.00	37.58	0.02	90.88
	10	E	0.30	13.18	13.90	0.30	7.50	3.47	0.64	15.60	0.08	37.64	0.07	92.68
	11	E	0.35	13.84	14.16	0.34	7.41	5.24	0.33	14.27	0.00	37.20	0.22	93.36
	12	E	0.39	13.39	12.96	0.23	7.68	5.62	0.29	14.47	0.02	35.52	0.71	91.28
	12	E	0.37	13.85	13.36	0.23	7.54	5.07	0.31	14.45	0.00	36.20	0.33	91.71
R18-2	1	E	0.51	13.04	13.73	0.02	9.07	4.08	0.48	15.30	0.00	37.32	0.13	93.68
	2	E	0.46	13.33	13.48	0.05	9.05	4.06	0.48	15.59	0.00	36.93	0.00	93.43
	3	E	0.53	13.82	13.54	0.05	9.10	4.29	0.52	15.39	0.00	37.58	0.02	94.84
	4	E	0.46	13.68	14.01	0.02	8.93	4.00	0.43	15.37	0.00	37.42	1.12	95.44
	5	E	0.55	14.03	14.45	0.01	9.25	4.16	0.43	15.21	0.00	37.35	0.05	95.49
	5	C	0.49	13.54	14.06	0.05	9.03	3.92	0.43	15.01	0.00	36.71	0.00	93.24
	6	E	0.51	13.18	13.58	0.15	8.52	4.09	0.55	15.05	0.00	37.33	0.00	92.96
	6	C	0.56	13.31	13.99	0.20	8.28	4.17	0.49	15.00	0.00	37.79	1.84	95.63

Appendix 4. Continued.

BIOTITE ANALYSES

Rainier Mesa Member

Sample	Grain #	Pos.	Na_2O	Al_2O_3	MgO	CaO	K_2O	TiO_2	MnO	FeO	NiO	SiO_2	BaO	Total
R18-16	1	E	0.53	15.07	13.39	0.04	9.17	4.64	0.42	16.85	0.06	36.54	0.49	97.20
	2	E	0.44	13.59	13.23	0.07	8.29	4.24	0.40	15.45	0.00	38.82	0.00	94.53
	3	E	0.33	12.28	13.27	0.17	7.75	4.04	0.33	14.54	0.00	38.38	0.02	91.11
	4	E	0.61	14.60	13.51	0.00	9.25	4.69	0.43	16.15	0.04	35.96	0.43	95.67
	4	C	0.63	14.63	13.06	0.05	8.99	4.81	0.44	16.09	0.00	36.39	0.43	95.52
	5	E	0.51	13.21	14.09	0.28	8.47	4.08	0.31	14.43	0.00	38.50	0.08	93.96
	5	NE	0.43	13.46	12.92	1.16	7.74	3.98	0.30	13.56	0.00	37.52	0.00	91.07
	5	C	0.31	13.31	14.17	0.15	8.60	4.21	0.32	13.83	0.00	39.64	0.04	94.59
	6	E	0.33	12.88	13.61	0.10	8.39	4.33	0.32	14.74	0.02	38.09	0.00	92.81
	7	E	0.47	13.15	14.34	0.03	9.12	4.23	0.37	14.69	0.05	37.49	0.02	93.96
	7	C	0.43	13.25	13.89	0.02	8.85	4.22	0.37	14.62	0.00	36.55	0.14	92.34
R23-13	1	E	0.65	14.86	14.29	0.03	9.28	5.77	0.34	14.90	0.03	37.70	0.74	98.59
	1	C	0.55	14.29	14.47	0.03	8.93	5.98	0.42	15.22	0.03	37.27	0.40	97.59
	2	E	0.52	14.49	13.17	0.05	8.81	6.24	0.35	15.08	0.04	36.42	1.33	96.50
	3	E	0.57	14.83	13.28	0.04	8.59	6.16	0.43	15.39	0.03	36.53	1.63	97.48
	4	E	0.56	15.02	13.58	0.04	8.60	6.23	0.34	15.21	0.48	35.97	1.66	97.69
	5	E	0.50	14.45	14.35	0.04	9.03	5.91	0.37	15.16	0.04	36.70	0.38	96.93
	6	E	0.42	14.99	14.08	0.00	8.85	6.14	0.33	15.00	0.04	37.39	0.92	98.16
	7	E	0.53	14.15	13.78	0.08	8.99	5.52	0.33	14.57	0.03	36.91	0.44	95.33
R23-24	1	E	0.80	14.88	14.61	0.01	8.19	5.37	0.21	13.02	0.00	34.87	1.41	93.37
	2	E	0.88	14.99	15.17	0.03	8.33	5.45	0.21	13.14	0.00	36.78	1.58	96.56
	3	E	0.95	14.80	14.80	0.02	7.83	5.16	0.16	12.73	0.00	34.90	1.58	92.93
	4	E	0.73	14.39	14.32	0.02	8.67	5.66	0.21	13.86	0.02	35.61	0.94	94.43
	5	E	0.84	14.91	14.52	0.02	7.93	5.49	0.19	12.88	0.00	35.20	1.66	93.64
	5	C	0.86	14.63	14.31	0.00	8.05	5.50	0.19	12.82	0.00	34.97	1.81	93.14
	6	E	0.99	14.72	15.31	0.03	7.64	5.04	0.14	12.49	0.00	34.52	1.51	92.39
	7	E	0.99	15.09	14.89	0.03	8.21	5.22	0.17	12.83	0.00	35.35	1.53	94.31
R23-26	1	E	0.58	14.83	13.31	0.00	8.76	6.29	0.25	15.17	0.00	34.98	1.54	95.71
	2	E	0.64	14.64	13.74	0.02	8.55	6.42	0.28	14.85	0.00	35.37	1.48	95.99
	3	E	0.60	14.09	13.44	0.00	8.58	5.86	0.28	14.52	0.00	35.19	0.89	93.45
	4	E	0.49	14.73	13.48	0.00	8.58	6.20	0.24	14.97	0.03	35.70	1.66	96.08
	5	E	0.67	14.89	13.76	0.00	8.57	6.29	0.32	14.83	0.00	34.86	1.63	95.82
	5	C	0.57	14.93	13.58	0.02	8.67	6.26	0.49	15.15	0.00	35.43	1.56	96.66
	5	E	0.55	14.17	13.69	0.00	8.82	6.08	0.27	14.68	0.00	35.97	0.69	94.92
	6	E	0.68	14.25	13.70	0.06	8.86	6.07	0.27	14.71	0.04	35.29	0.86	94.79

Appendix 4. Continued.

BIOTITE ANALYSES

Rainier Mesa Member

Sample	Grain #	Pos.	Na_2O	Al_2O_3	MgO	CaO	K_2O	TiO_2	MnO	FeO	NiO	SiO_2	BaO	Total
R23-27	1	E	0.71	14.69	14.41	0.03	8.33	5.33	0.20	14.42	0.00	35.04	1.40	94.56
	2	E	0.82	14.80	14.78	0.02	8.17	5.55	0.17	13.53	0.00	35.30	1.70	94.84
	2	C	0.90	15.12	15.04	0.02	8.12	5.51	0.17	13.62	0.00	35.20	2.05	95.75
	3	E	0.89	15.48	15.34	0.00	8.35	5.24	0.15	13.61	0.00	36.13	1.45	96.64
	4	E	0.85	14.55	14.31	0.04	8.32	5.56	0.18	14.02	0.00	35.37	1.36	94.56
	5	E	0.79	15.16	14.55	0.05	8.22	5.73	0.19	13.88	0.00	34.47	1.52	94.56
	6	E	0.91	15.49	15.23	0.07	7.91	5.26	0.17	13.20	0.00	34.53	1.67	94.44
	7	E	1.00	15.55	15.24	0.03	8.09	5.27	0.16	13.52	0.00	35.89	1.70	96.45
	8	E	0.78	14.69	14.27	0.05	7.92	5.45	0.16	13.43	0.00	34.69	1.34	92.78
	8	C	0.74	15.10	14.61	0.03	8.24	5.61	0.21	14.20	0.00	35.26	1.34	95.34
	9	E	0.90	15.18	15.08	0.00	8.30	5.42	0.15	13.40	0.06	33.95	1.88	94.31
R21-1	1	E	0.70	14.43	13.39	0.02	6.84	5.09	0.45	14.52	0.00	34.45	0.85	90.74
	2	E	0.53	14.11	14.18	0.05	6.70	5.03	0.29	14.20	0.00	35.68	0.29	91.06
	3	E	0.60	14.34	14.26	0.03	6.60	4.92	0.28	14.18	0.00	35.52	0.75	91.48
	4	E	0.68	14.28	14.91	0.05	7.26	4.92	0.29	14.27	0.00	36.24	3.16	96.06
	5	E	0.59	14.30	13.63	0.02	6.64	5.13	0.29	14.57	0.00	35.39	1.11	91.67
	6	E	0.60	14.14	14.19	0.31	6.07	4.95	0.29	14.11	0.00	35.54	0.27	90.47
R21-5	1	E	0.66	13.62	15.22	0.00	7.07	4.11	0.37	13.46	0.00	37.36	0.00	91.87
	2	E	0.58	13.30	15.10	0.00	7.24	4.14	0.34	13.85	0.00	37.79	0.00	92.34
R21-13	1	E	0.93	14.80	14.92	0.00	6.31	4.75	0.22	13.08	0.00	35.74	1.44	92.19
	2	E	0.88	15.16	15.05	0.03	8.41	5.42	0.15	13.40	0.01	35.99	1.50	96.00
	3	E	0.91	14.69	15.11	0.03	8.00	5.34	0.10	13.14	0.03	35.83	1.72	94.90
	3	E	1.04	15.01	15.09	0.02	8.17	5.26	0.18	13.12	0.00	35.98	1.56	95.43
	4	E	0.73	14.13	15.03	0.05	9.24	5.54	0.24	14.39	0.02	38.19	0.24	97.80
	5	E	0.67	14.47	14.46	0.04	9.23	5.95	0.34	15.58	0.43	37.29	0.58	99.04
	6	E	1.10	15.63	15.43	0.04	8.17	5.45	0.18	13.10	0.02	37.12	1.91	98.15
	7	E	0.91	15.74	15.37	0.06	8.39	5.37	0.12	13.50	0.03	37.69	1.51	98.69
	8	E	0.68	14.29	14.68	0.03	9.19	6.14	0.33	14.81	0.03	37.23	0.67	98.08
	9	E	0.65	14.58	14.13	0.03	9.04	6.06	0.57	15.02	0.31	36.62	1.24	98.25
	10	E	0.88	15.37	15.51	0.03	8.63	5.56	0.12	13.83	0.00	36.19	1.65	97.77
	11	E	1.00	15.34	15.35	0.05	8.56	5.59	0.20	13.44	0.02	37.29	1.41	98.25

Appendix 4. Continued.

BIOTITE ANALYSES

Ammonia Tanks Member

Sample	Grain #	Pos.	Na_2O	Al_2O_3	MgO	CaO	K_2O	TiO_2	MnO	FeO	NiO	SiO_2	BaO	Total
A5-3	1	E	0.38	12.05	17.37	0.18	7.86	2.93	0.83	11.69	0.00	38.55	0.04	91.88
	2	E	0.33	12.05	16.40	0.16	7.84	2.94	0.71	11.82	0.00	38.47	0.00	90.72
	3	E	0.28	11.96	16.32	0.28	7.26	2.95	0.89	11.99	0.00	38.15	0.17	90.25
	4	E	0.31	11.90	16.81	0.26	6.59	2.96	0.79	11.80	0.00	38.49	0.00	89.91
	5	E	0.32	11.67	16.85	0.20	7.60	2.87	0.77	11.43	0.00	38.64	0.04	90.39
	6	E	0.41	11.90	17.00	0.17	7.19	3.02	0.78	12.68	0.00	38.10	0.04	91.29
A5-35	1	E	0.66	12.78	15.00	0.12	9.03	4.31	0.62	13.99	0.00	37.22	0.15	93.88
	2	E	0.38	12.77	14.49	0.30	6.96	3.88	0.41	13.25	0.03	39.04	0.34	91.85
	3	E	0.39	12.75	14.37	0.25	6.99	4.42	0.45	13.63	0.00	37.40	0.42	91.07
	4	E	0.34	12.45	14.64	0.33	7.49	3.96	0.44	13.87	0.00	37.95	0.14	91.61
	5	E	0.44	11.96	14.45	0.35	7.43	4.01	0.46	13.58	0.00	39.53	0.10	92.31
	6	E	0.55	12.88	15.60	0.26	7.54	4.33	0.41	14.20	0.00	38.24	0.23	94.24
A5-58	1	E	0.37	13.05	15.42	0.04	8.63	4.65	0.49	13.51	0.00	37.96	0.39	94.51
	2	E	0.51	13.58	15.08	0.11	8.55	5.06	0.59	13.79	0.00	37.53	0.25	95.05
	3	E	0.77	13.53	14.59	0.03	8.01	6.96	0.26	11.99	0.00	35.36	1.87	93.37
	4	E	0.50	13.15	15.22	0.04	8.49	5.23	0.68	14.01	0.00	37.13	0.71	95.16
A5-63	1	E	0.77	14.90	14.70	0.04	7.97	6.97	0.16	12.27	0.04	35.52	3.16	96.50
	2	E	0.86	14.98	14.42	0.04	7.76	7.05	0.21	12.43	0.00	34.61	3.10	95.46
	3	E	0.70	14.35	14.58	0.08	7.68	7.18	0.20	12.63	0.00	34.88	2.54	94.82
	4	E	0.81	14.63	14.60	0.02	7.88	7.08	0.20	12.35	0.00	34.69	2.68	94.94
	5	E	0.83	14.36	14.30	0.02	7.76	6.80	0.10	11.92	0.00	34.49	3.61	94.19
A5-69	1	E	0.89	14.89	14.76	0.02	7.86	7.07	0.20	12.23	0.00	34.69	2.77	95.38
	2	E	0.80	14.98	14.22	0.04	7.83	6.87	0.24	12.71	0.00	34.00	3.35	95.04
	3	E	0.74	14.07	13.92	0.04	7.57	6.70	0.20	11.80	0.00	32.84	2.74	90.62
	4	E	0.77	14.40	14.90	0.02	8.18	6.77	0.19	11.94	0.00	35.34	1.71	94.22

Appendix 4. Continued.

BIOTITE ANALYSES

Ammonia Tanks Member

Sample	Grain #	Pos.	Na_2O	Al_2O_3	MgO	CaO	K_2O	TiO_2	MnO	FeO	NiO	SiO_2	BaO	Total
A5-71	1	E	0.67	13.69	14.34	0.05	7.97	5.56	0.43	13.58	0.03	35.95	0.32	92.59
	2	E	0.60	13.50	14.87	0.23	7.67	5.38	0.44	13.54	0.00	36.44	0.04	92.71
	3	E	0.29	13.31	15.33	0.00	7.89	4.56	0.48	13.17	0.03	36.93	0.02	92.01
	4	E	0.63	14.05	14.31	0.00	7.66	5.30	0.48	13.60	0.02	36.28	0.10	92.43
	5	E	0.56	13.71	14.31	0.03	7.73	5.65	0.46	13.67	0.04	35.54	0.34	92.04
	6	E	0.68	14.18	14.57	0.04	8.04	5.55	0.39	13.60	0.06	34.69	0.21	92.01
	7	E	0.68	13.87	14.40	0.01	7.77	5.51	0.40	13.19	0.06	36.62	0.03	92.54
	8	E	0.74	13.64	14.10	0.02	7.65	5.84	0.43	13.25	0.04	36.20	0.31	92.22
	9	E	0.67	13.56	13.95	0.06	7.31	6.16	0.33	12.95	0.03	34.86	0.95	90.83
	10	E	0.72	14.94	14.11	0.01	6.90	6.38	0.27	13.01	0.02	35.13	2.24	93.73
A5-72	1	E	0.75	14.52	14.59	0.03	7.47	6.43	0.24	12.77	0.00	36.26	1.37	94.43
	2	E	0.72	14.90	14.55	0.06	7.43	6.61	0.23	12.98	0.00	36.16	2.21	95.85
	3	E	0.70	14.67	13.97	0.01	6.99	6.55	0.26	13.15	0.00	34.84	2.46	93.60
	4	E	0.56	14.65	13.91	0.02	6.95	6.42	0.28	13.25	0.00	33.94	1.71	91.69
	5	E	0.72	14.76	15.29	0.05	7.59	6.01	0.20	12.72	0.00	36.75	0.32	94.41
A5-75	1	E	0.95	15.20	14.80	0.00	6.67	6.52	0.10	11.95	0.00	34.34	2.79	93.32
	2	E	0.80	15.10	13.89	0.00	6.59	6.02	0.16	12.19	0.00	34.61	2.50	91.86
	3	E	1.01	15.48	15.21	0.00	6.64	6.38	0.29	12.25	0.00	35.23	2.76	95.25
	4	E	0.96	14.55	15.44	0.03	6.84	6.14	0.16	11.73	0.00	35.78	1.37	93.00
	5	E	0.80	14.80	14.95	0.00	6.48	5.94	0.14	12.00	0.00	34.56	2.40	92.07
	6	E	0.92	15.43	15.50	0.02	6.66	6.30	0.18	11.95	0.00	34.61	4.02	95.59
	7	E	0.82	15.04	14.84	0.01	6.60	6.44	0.18	12.46	0.00	35.11	2.68	94.18
A21-18	1	E	0.62	12.20	16.58	0.02	7.41	2.75	0.83	12.24	0.00	38.88	0.00	91.53
	2	E	0.61	12.54	16.65	0.00	7.78	2.75	0.90	12.48	0.00	38.68	0.00	92.39
	3	E	0.58	12.35	16.71	0.05	7.50	2.83	0.80	12.73	0.00	39.14	0.00	92.69
	4	E	0.50	13.47	15.24	0.05	7.22	2.62	0.89	11.68	0.00	38.27	0.00	89.94
	5	E	0.52	12.48	16.80	0.02	7.87	2.93	0.89	12.66	0.02	38.36	0.00	92.55

Appendix 4. Continued.

BIOTITE ANALYSES -- University of Michigan

Ammonia Tanks Member

Sample	Grain #	Pos.	Na_2O	MgO	Al_2O_3	SiO_2	K_2O	CaO	BaO	TiO_2	MnO	FeO	Total
A4-70	1	C	0.67	16.42	13.39	38.25	9.27	0.00	0.15	4.50	0.56	14.70	97.91
	2	E	0.60	16.37	13.41	38.00	9.36	0.00	0.10	4.32	0.57	14.50	97.19
	3	C	0.62	15.64	13.91	36.47	8.76	0.00	1.37	4.63	0.56	14.84	96.79
A5-9	1	C	0.49	15.38	13.47	35.30	7.40	0.23	0.53	4.35	0.49	13.14	90.78
	2	C	0.37	14.95	13.45	37.89	6.98	0.18	0.50	4.42	0.50	12.98	92.20
	3	E	0.40	15.83	12.94	37.51	6.56	0.23	0.28	4.25	0.37	11.91	90.28
	4	E	0.68	15.60	13.32	36.50	8.81	0.00	1.20	4.96	0.51	14.06	95.63
A5-29	1	C	0.65	17.06	12.97	37.82	9.11	0.00	0.23	3.20	0.97	12.85	94.85
	2	E	0.64	18.70	12.36	39.63	9.14	0.02	0.00	2.61	0.88	11.76	95.73
	3	E	0.62	16.77	13.25	37.94	9.00	0.00	0.40	3.92	0.92	12.96	95.77
	4	E	0.63	18.97	12.50	39.70	8.78	0.05	0.00	2.82	0.83	11.44	95.71
A5-30	1	E	0.58	15.18	14.51	34.44	6.88	0.16	1.92	6.48	0.35	12.39	92.89
	2	E	0.45	14.96	13.82	35.01	6.66	0.27	0.84	6.29	0.28	12.15	90.73
	3	C	0.70	14.65	14.72	35.64	8.11	0.00	1.92	6.67	0.39	13.72	96.52
A5-31	1	E	0.65	16.15	15.27	35.90	6.53	0.26	1.75	6.20	0.17	11.75	94.62
	2	E	0.71	16.24	15.13	35.68	6.85	0.21	1.96	6.04	0.14	11.10	94.05
	3	C	0.89	16.60	15.59	36.27	7.63	0.02	2.25	6.36	0.13	11.97	97.71
A5-37	1	E	0.69	17.21	13.26	38.23	8.73	0.01	0.39	3.65	0.81	12.47	95.45
	2	E	0.33	16.03	12.87	39.12	7.36	0.20	0.02	2.55	1.28	11.11	90.89
	3	E	0.40	18.23	11.75	38.69	7.84	0.15	0.00	2.66	0.73	11.05	91.50
A5-68	1	E	0.68	17.33	13.22	38.35	8.63	0.04	0.08	3.91	0.53	12.68	95.45
	2	E	0.56	16.54	12.95	37.05	7.64	0.23	0.17	4.04	0.51	13.18	92.87
	3	E	0.65	17.00	13.26	37.77	8.95	0.01	0.15	3.99	0.59	13.17	95.53
A5-79	1	E	0.62	18.61	12.34	39.95	9.05	0.00	0.00	2.79	0.90	11.97	96.22
	2	E	0.39	18.09	12.16	38.67	8.69	0.01	0.00	2.67	0.86	12.21	93.738
	3	E	0.58	17.86	11.61	38.16	9.07	0.00	0.02	2.67	0.79	12.31	93.07
	4	E	0.69	19.35	12.68	40.29	9.14	0.00	0.00	2.75	0.85	12.40	98.15

Appendix 4. Continued.

CLINOPYROXENE ANALYSES

Rainier Mesa Member

Sample	Grain #	Pos.	Na_2O	Al_2O_3	MgO	CaO	K_2O	TiO_2	MnO	FeO	NiO	SiO_2	BaO	Total
R8-25	1	E	0.55	1.30	13.50	21.47	0.01	0.26	0.98	8.44	0.00	52.19	0.14	98.84
	1	C	0.55	1.88	13.93	21.48	0.00	0.39	0.78	8.58	0.00	52.38	0.06	100.03
	2	E	0.48	0.74	14.16	20.63	0.00	0.15	1.25	8.78	0.00	52.16	0.12	98.47
	2	C	0.51	1.15	13.71	21.34	0.00	0.28	1.00	8.33	0.00	52.52	0.17	99.01
	3	E	0.47	0.81	14.30	20.70	0.02	0.15	1.18	8.62	0.00	53.80	0.10	100.15
	4	E	0.57	1.25	13.92	21.30	0.02	0.29	0.95	8.71	0.00	52.53	0.04	99.58
	4	C	0.53	0.98	14.11	20.67	0.03	0.18	1.17	8.48	0.00	52.80	0.05	99.00
	5	E	0.63	1.83	12.85	21.69	0.00	0.34	0.73	8.77	0.00	51.40	0.11	98.35
	6	E	0.69	2.27	13.15	21.18	0.00	0.44	0.84	9.23	0.00	51.21	0.18	99.19
	7	E	0.44	0.89	14.45	20.47	0.00	0.19	1.23	8.73	0.00	50.85	0.04	97.29
	8	E	0.57	1.11	13.81	21.41	0.00	0.29	1.14	8.48	0.00	51.84	0.04	98.69
	9	E	0.62	1.86	14.00	21.04	0.00	0.34	0.93	8.68	0.00	51.66	0.23	99.36
	10	E	0.66	1.60	13.94	21.14	0.00	0.37	0.84	8.24	0.00	52.05	0.00	98.84
	11	E	0.63	1.39	14.09	21.54	0.00	0.26	0.88	8.06	0.02	52.38	0.03	99.28
	12	E	0.64	1.54	14.08	21.54	0.01	0.32	0.85	8.44	0.00	52.31	0.09	99.82
	13	E	0.58	1.27	13.74	21.64	0.02	0.28	0.87	8.29	0.00	52.69	0.12	99.50
R8-44	1	E	0.59	1.84	14.32	20.77	0.00	0.43	0.82	8.47	0.00	53.19	0.00	100.43
	2	E	0.46	0.69	14.18	20.81	0.00	0.18	1.15	8.53	0.00	53.24	0.00	99.24
	2	C	0.48	0.71	14.37	21.11	0.00	0.12	1.23	8.51	0.00	53.60	0.00	100.13
	3	E	0.57	1.60	13.49	23.14	0.00	0.26	0.75	8.25	0.00	50.51	0.00	98.57
	4	E	1.04	0.76	14.36	22.29	0.00	0.19	1.29	8.12	0.00	48.48	0.00	96.53
	5	E	0.61	0.80	13.80	22.04	0.00	0.22	1.28	8.90	0.00	50.59	0.00	98.24
	6	E	0.53	2.10	13.91	21.23	0.00	0.48	0.72	9.73	0.00	52.45	0.00	101.15
	6	C	0.44	1.71	13.84	21.53	0.00	0.36	0.76	8.58	0.00	53.01	0.00	100.23
	7	E	0.54	1.42	13.73	20.98	0.00	0.24	0.89	8.48	0.00	52.99	0.00	99.27
	7	C	0.56	1.37	13.71	21.34	0.00	0.26	0.95	8.59	0.00	52.81	0.00	99.59
	8	E	1.04	0.76	14.36	22.29	0.00	0.19	1.29	8.12	0.00	48.48	0.00	96.53
	9	C	0.67	1.21	14.69	21.24	0.00	0.24	1.04	8.83	0.00	54.35	0.00	102.27

Appendix 4. Continued.

CLINOPYROXENE ANALYSES

Rainier Mesa Member

Sample	Grain #	Pos.	Na_2O	Al_2O_3	MgO	CaO	K_2O	TiO_2	MnO	FeO	NiO	SiO_2	BaO	Total
R8-45	1	E	0.64	2.13	13.79	21.43	0.00	0.39	0.79	8.77	0.00	52.63	0.00	100.57
	2	E	0.61	1.33	13.80	21.40	0.00	0.30	0.83	8.29	0.02	52.39	0.00	98.97
	2	C	0.63	1.96	13.31	21.91	0.00	0.40	0.77	8.79	0.00	51.91	0.07	99.75
	3	E	0.71	1.63	14.04	21.19	0.00	0.28	0.96	8.65	0.00	52.33	0.00	99.79
	4	E	0.61	2.00	14.29	20.73	0.00	0.47	0.71	8.13	0.00	52.12	0.00	99.06
	5	E	0.57	1.85	14.24	21.46	0.00	0.43	0.78	8.19	0.00	52.73	0.06	100.31
	6	E	0.55	1.96	13.90	22.03	0.00	0.30	0.70	8.55	0.04	51.67	0.05	99.75
	6	C	0.64	2.43	13.10	21.84	0.00	0.42	0.63	9.07	0.22	51.46	0.00	99.81
	7	E	0.61	1.62	14.09	21.64	0.00	0.32	0.84	8.33	0.03	53.07	0.00	100.55
	7	C	0.66	2.06	13.98	20.99	0.00	0.40	0.92	8.26	0.03	52.52	0.02	99.84
	8	E	0.59	1.21	14.16	21.20	0.00	0.20	0.95	8.28	0.03	53.13	1.86	101.61
	8	C	0.57	1.22	14.25	21.20	0.00	0.26	1.05	8.68	0.04	53.13	0.00	100.40
	9	E	0.66	2.05	13.99	21.50	0.00	0.46	0.87	8.83	0.03	52.50	0.00	100.89
	10	E	0.69	1.61	13.59	19.11	0.00	0.33	1.30	10.16	0.03	51.58	0.00	98.40
	11	E	0.59	1.25	13.43	21.19	0.00	0.28	1.02	8.60	0.02	52.26	0.00	98.64
R11-5	1	E	0.56	1.61	14.15	21.57	0.00	0.36	0.64	7.96	0.02	51.68	0.00	98.55
	2	E	0.57	1.80	13.72	21.86	0.00	0.41	0.52	8.09	0.00	51.72	0.00	98.69
	3	E	0.61	1.66	14.18	20.97	0.00	0.36	0.56	8.01	0.04	51.87	0.00	98.26
	4	E	0.51	1.63	13.84	21.51	0.00	0.35	0.59	7.99	0.02	52.28	0.00	98.72
	4	C	0.52	1.64	13.99	21.10	0.00	0.36	0.65	8.00	0.01	52.21	0.00	98.48
	5	E	0.60	2.14	13.45	21.10	0.00	0.48	0.58	8.23	0.00	51.16	0.00	97.74
	6	E	0.62	2.06	13.59	20.93	0.00	0.44	0.64	8.19	0.02	50.64	0.08	97.21
	6	C	0.59	1.59	14.00	21.19	0.03	0.31	0.68	7.89	0.04	50.70	0.00	97.02
	7	E	0.55	1.82	13.93	21.19	0.00	0.40	0.63	8.22	0.01	52.13	2.08	100.96
	8	E	0.55	1.69	13.85	22.16	0.00	0.42	0.60	8.07	0.00	52.14	0.00	99.48
	9	E	0.50	1.76	14.07	22.39	0.00	0.42	0.70	8.16	0.04	52.34	0.00	100.38
	10	E	0.52	1.58	14.38	21.61	0.00	0.36	0.60	8.00	0.00	52.60	0.00	99.65
	11	E	0.59	1.79	14.41	21.70	0.02	0.42	0.65	8.23	0.00	51.80	0.05	99.66

Appendix 4. Continued.

CLINOPYROXENE ANALYSES

Rainier Mesa Member

Sample	Grain #	Pos.	Na_2O	Al_2O_3	MgO	CaO	K_2O	TiO_2	MnO	FeO	NiO	SiO_2	BaO	Total
R23-13	1	E	0.62	1.06	14.23	20.75	0.00	0.20	1.10	8.44	0.03	53.63	0.00	100.06
	2	E	0.57	1.22	13.86	21.57	0.00	0.22	0.81	8.28	0.01	53.69	0.00	100.23
	2	C	0.62	0.73	13.49	21.17	0.00	0.21	1.24	9.42	0.04	53.20	0.00	100.12
	3	E	0.60	1.04	13.82	21.37	0.00	0.22	1.06	8.61	0.01	53.03	0.00	99.76
	4	E	0.56	1.00	14.36	21.18	0.00	0.18	1.18	8.66	0.02	53.43	0.00	100.57
	5	E	0.71	1.73	13.94	21.28	0.00	0.35	0.93	8.60	0.20	52.44	0.00	100.18
	6	E	0.58	1.25	13.91	21.75	0.00	0.29	1.12	8.47	0.03	53.35	0.00	100.75
	7	E	0.51	0.80	14.57	20.77	0.00	0.09	1.47	8.96	0.03	54.86	0.00	102.06
	8	E	0.55	1.11	14.19	21.34	0.00	0.27	1.00	8.77	0.06	53.94	0.00	101.23
	9	E	0.60	1.49	13.61	21.17	0.00	0.31	0.95	8.92	0.02	53.73	0.00	100.80
	9	C	0.49	1.17	14.39	21.65	0.00	0.21	0.69	8.07	0.03	53.29	0.05	100.04
	10	E	0.65	1.22	14.12	19.57	0.03	0.23	1.54	9.65	0.00	52.57	0.00	99.58
	11	E	0.59	0.92	14.30	20.89	0.03	0.21	1.15	8.16	0.71	53.46	0.00	100.42
	12	E	0.65	1.23	13.87	21.17	0.00	0.30	0.92	8.21	0.00	53.22	0.00	99.57
	13	E	0.62	1.30	13.99	20.76	0.02	0.30	0.95	8.10	0.00	52.27	0.00	98.31
	14	E	0.62	1.36	14.08	21.12	0.01	0.29	0.78	7.98	0.00	52.99	0.00	99.23
	15	E	0.55	1.42	14.05	21.16	0.03	0.25	0.95	7.93	0.00	52.93	0.00	99.27
	16	E	0.58	1.42	13.56	21.14	0.01	0.27	0.92	8.29	0.44	52.02	0.00	98.65
	17	E	0.54	1.11	13.91	21.19	0.02	0.23	1.04	8.08	0.00	51.99	0.00	98.11
	18	E	0.57	1.33	13.97	21.38	0.00	0.27	1.00	8.43	0.02	52.67	0.10	99.74
	18	C	0.56	1.05	13.61	21.41	0.00	0.25	1.16	8.37	0.06	52.98	0.10	99.55
	19	E	0.53	2.09	13.39	22.07	0.00	0.45	0.77	8.44	0.03	51.23	0.10	99.10
R23-24	1	E	0.55	1.83	14.29	20.99	0.00	0.36	0.59	7.93	0.73	51.26	0.00	98.53
	2	E	0.47	1.81	14.24	20.91	0.00	0.42	0.56	8.04	0.00	52.56	0.00	99.01
	3	E	0.51	1.53	14.49	21.88	0.02	0.36	0.83	8.03	0.00	52.29	0.06	100.00
	4	E	0.59	1.85	13.83	21.54	0.00	0.46	0.60	8.40	0.03	51.96	0.00	99.26
	4	C	0.75	2.22	13.68	21.07	0.02	0.56	0.70	8.61	0.00	50.71	0.00	98.32
	5	E	0.59	1.94	14.39	21.66	0.00	0.40	0.67	8.09	0.06	52.43	0.04	100.27
	5	C	0.63	1.64	14.08	21.37	0.01	0.42	0.67	8.05	0.00	51.90	0.12	98.89

Appendix 4. Continued.

CLINOPYROXENE ANALYSES

Rainier Mesa Member

Sample	Grain #	Pos.	Na_2O	Al_2O_3	MgO	CaO	K_2O	TiO_2	MnO	FeO	NiO	SiO_2	BaO	Total
R23-26	1	E	0.51	1.22	14.11	21.03	0.00	0.24	0.93	8.38	0.00	51.55	0.00	97.97
	2	E	0.50	1.14	13.71	21.07	0.00	0.26	1.09	8.87	0.00	52.27	0.00	98.91
	2	C	0.63	1.54	13.85	21.06	0.00	0.29	0.89	8.20	0.03	52.39	0.00	98.88
	3	E	0.62	1.88	13.64	20.87	0.00	0.36	0.84	8.27	0.00	50.56	0.00	97.04
	3	C	0.61	2.01	13.62	21.34	0.00	0.49	0.87	8.63	0.00	50.67	0.82	99.06
	4	E	0.66	1.36	14.30	21.25	0.02	0.31	0.83	8.34	0.00	52.10	0.00	99.17
	4	C	0.59	1.57	13.97	20.96	0.00	0.29	0.64	7.87	0.00	50.31	0.00	96.20
	5	E	0.48	1.23	13.83	20.90	0.00	0.26	0.71	8.51	0.00	52.08	0.00	98.00
	6	E	0.61	1.63	13.90	21.03	0.00	0.30	0.68	8.56	0.00	52.05	0.00	98.76
	7	E	0.69	1.34	13.92	21.07	0.00	0.26	1.04	8.62	0.00	52.13	0.00	99.07
	7	C	0.68	1.26	13.65	21.27	0.01	0.27	1.24	8.48	0.00	51.55	0.00	98.41
	8	E	0.54	1.53	13.11	21.59	0.00	0.28	0.96	8.50	0.00	50.32	0.00	96.83
	9	E	0.55	1.09	13.92	21.58	0.00	0.26	1.05	8.31	0.00	53.56	0.00	100.32
	10	E	0.76	1.47	13.70	20.64	0.01	0.32	1.23	9.15	0.00	52.44	0.08	99.80
	11	E	0.42	0.69	17.47	12.85	0.00	0.26	1.53	12.52	0.00	52.51	0.00	98.25
	12	E	0.57	1.24	13.56	21.31	0.00	0.27	1.01	8.68	0.00	51.99	0.00	98.63
	13	E	0.60	1.61	14.11	21.53	0.00	0.38	0.91	8.51	0.02	52.07	0.00	99.74
	14	E	0.61	1.01	14.71	20.57	0.00	0.26	1.03	8.46	0.02	52.55	0.03	99.25
	15	E	0.67	1.20	13.64	21.39	0.02	0.29	1.03	8.49	0.00	51.69	0.00	98.42
R21-1	1	E	0.65	1.57	13.75	18.20	0.00	0.25	1.00	8.42	0.00	51.06	0.00	94.90
	1	C	0.58	1.45	13.45	17.91	0.00	0.27	1.13	8.10	0.00	49.62	0.03	92.54
	2	E	0.49	1.16	13.17	18.42	0.00	0.20	0.97	8.16	0.00	49.80	0.03	92.40
	2	C	0.59	1.04	13.60	17.94	0.00	0.17	1.18	8.25	0.00	49.03	0.00	91.80
	3	E	0.57	1.35	13.72	18.33	0.01	0.22	0.79	7.96	0.00	50.74	0.04	93.73
	4	E	0.60	1.15	13.96	17.57	0.00	0.19	0.96	8.23	0.00	52.08	0.00	94.74
	4	C	0.48	1.30	14.84	15.02	0.00	0.12	1.50	10.94	0.00	50.93	0.00	95.13
	5	E	0.61	1.43	14.25	17.78	0.02	0.24	0.88	7.97	0.00	51.42	0.00	94.60
	5	C	0.61	1.71	13.68	18.16	0.00	0.30	0.80	8.04	0.18	50.77	0.00	94.25
	6	E	0.57	1.04	13.74	18.00	0.02	0.20	0.97	8.08	0.00	52.17	0.02	94.81
	7	E	0.41	0.59	14.40	17.73	0.00	0.21	0.48	8.91	0.00	51.46	0.07	94.26
	8	E	0.46	1.20	13.22	17.59	0.00	0.18	1.09	8.69	0.00	49.80	0.00	92.23
	8	C	0.57	1.40	13.78	18.12	0.00	0.29	0.99	8.42	0.00	47.80	0.00	91.37
R21-5	1	E	0.53	0.85	14.23	16.94	0.03	0.12	1.27	8.76	0.00	49.76	0.00	92.49

Appendix 4. Continued.

CLINOPYROXENE ANALYSES

Ammonia Tanks Member

Sample	Grain #	Pos.	Na_2O	Al_2O_3	MgO	CaO	K_2O	TiO_2	MnO	FeO	NiO	SiO_2	BaO	Total
A5-35	1	E	0.66	0.80	13.53	21.82	0.00	0.21	1.49	8.58	0.00	49.92	0.03	97.04
	1	C	0.59	0.71	13.36	21.58	0.00	0.15	2.16	8.35	0.00	49.47	0.00	96.37
	2	E	0.44	0.91	14.63	22.02	0.00	0.20	0.68	7.57	0.00	51.33	0.00	97.78
	2	C	0.41	1.02	14.26	20.99	0.00	0.31	1.07	8.56	0.00	50.97	2.13	99.72
	3	E	0.59	0.95	13.88	21.47	0.00	0.14	1.58	8.29	0.00	51.15	0.03	98.08
	3	C	0.67	1.07	13.41	21.83	0.02	0.32	0.99	8.02	0.00	49.93	0.06	96.32
	4	E	0.64	0.78	12.79	20.73	0.02	0.20	1.70	8.71	0.04	51.02	0.09	96.72
	5	E	0.46	0.73	13.53	21.20	0.02	0.17	1.55	8.26	0.06	50.39	0.04	96.41
	6	E	0.42	0.92	14.88	21.19	0.01	0.27	0.90	8.00	0.07	47.89	0.03	94.58
	7	E	0.53	0.87	14.33	20.31	0.00	0.20	1.47	8.25	0.03	51.35	0.00	97.34
	8	C	0.67	1.53	13.66	21.30	0.02	0.40	1.09	7.78	0.05	49.67	0.04	96.21
A5-58	1	E	0.61	0.67	12.88	21.16	0.00	0.15	1.51	8.03	0.00	50.72	0.09	95.82
	1	C	0.64	0.78	13.43	21.44	0.01	0.18	1.47	8.23	0.00	51.53	0.08	97.78
	2	E	0.63	0.98	13.73	20.81	0.00	0.30	1.58	8.05	0.04	51.76	0.02	97.89
	2	C	0.63	1.10	14.49	20.63	0.00	0.27	1.43	7.98	0.00	51.21	0.00	97.74
	3	E	0.76	1.15	13.51	21.73	0.00	0.27	1.34	8.18	0.00	52.03	0.05	99.02
	4	E	0.66	0.95	13.15	21.41	0.02	0.28	1.49	7.84	0.00	50.95	0.03	96.77
	5	E	0.66	0.76	13.59	20.89	0.00	0.17	1.67	8.12	0.02	51.04	0.02	96.94
	6	E	0.66	0.76	13.19	20.19	0.03	0.20	1.99	8.50	0.01	51.29	0.02	96.84
	7	E	0.62	0.96	12.88	21.14	0.00	0.25	1.59	8.23	0.00	49.88	0.00	95.55
	8	E	0.67	1.15	12.28	20.43	0.02	0.19	1.84	8.78	0.00	50.93	0.43	96.72
	9	E	0.47	0.84	14.47	20.54	0.02	0.24	1.01	8.25	0.00	51.09	0.00	96.93
	10	E	0.70	0.85	13.54	21.52	0.04	0.19	1.32	7.96	0.00	51.69	0.00	97.81
	10	C	0.68	0.79	13.62	21.71	0.02	0.23	1.34	8.36	0.00	51.19	0.00	97.94
	11	E	0.63	0.85	13.97	21.61	0.01	0.21	1.44	8.01	0.00	51.61	0.05	98.39
	12	E	0.43	0.71	15.03	19.72	0.00	0.15	0.91	7.58	0.00	49.51	0.00	94.04
A5-63	1	E	0.57	2.10	15.27	20.48	0.01	0.57	0.54	7.42	0.00	51.57	0.09	98.62
	1	C	0.55	2.16	15.13	20.42	0.00	0.63	0.50	7.70	0.00	51.30	0.06	98.45
	2	E	0.65	2.88	13.72	20.71	0.00	0.76	0.70	7.77	0.00	49.19	0.05	96.43
	3	E	0.58	2.02	14.57	20.69	0.00	0.53	0.74	7.81	0.00	47.34	0.15	94.43
	4	E	0.55	1.88	14.88	20.40	0.01	0.45	0.64	7.78	0.00	48.60	1.36	96.55
	5	E	0.62	1.94	15.07	20.68	0.00	0.47	0.66	7.48	0.00	48.94	0.08	95.94
	5	C	0.51	2.71	14.56	20.04	0.00	0.67	0.51	7.88	0.00	48.99	0.00	95.87
	6	E	0.56	2.10	14.61	20.41	0.02	0.56	0.67	7.87	0.00	50.44	0.83	98.07

Appendix 4. Continued.

CLINOPYROXENE ANALYSES

Ammonia Tanks Member

Sample	Grain #	Pos.	Na_2O	Al_2O_3	MgO	CaO	K_2O	TiO_2	MnO	FeO	NiO	SiO_2	BaO	Total
A5-69	1	E	0.61	2.58	14.98	20.57	0.00	0.61	0.57	7.76	0.00	50.61	0.20	98.49
	2	E	0.53	2.11	15.26	20.00	0.00	0.56	0.56	7.61	0.00	49.95	0.08	96.66
	3	E	0.57	1.91	14.95	20.33	0.00	0.43	0.61	7.42	0.00	50.81	0.16	97.19
	4	E	0.55	1.55	14.41	20.78	0.00	0.48	0.67	7.60	0.00	49.66	0.08	95.78
	5	E	0.58	1.18	14.28	21.23	0.00	0.39	1.14	7.65	0.00	50.05	0.11	96.61
	6	E	0.49	2.20	14.39	20.18	0.02	0.59	0.48	7.43	0.00	47.83	0.17	93.78
	7	E	0.66	2.31	14.84	20.25	0.02	0.59	0.72	7.79	0.00	48.77	0.08	96.03
A5-71	1	E	0.68	1.78	14.08	18.94	0.00	0.46	0.81	7.41	0.05	50.74	0.00	94.95
	1	C	0.61	1.72	14.22	19.27	0.00	0.42	0.72	7.45	0.03	51.02	0.00	95.46
	2	E	0.77	1.39	13.67	19.17	0.00	0.37	1.20	8.01	0.76	51.29	0.06	96.69
	3	E	0.68	1.45	13.74	18.79	0.00	0.42	1.23	8.02	0.00	51.33	0.00	95.66
	3	C	0.53	0.86	14.01	19.49	0.00	0.27	0.78	7.79	0.03	50.37	0.00	94.13
	4	E	0.61	1.96	14.27	19.16	0.00	0.46	0.76	7.47	0.03	50.32	0.00	95.04
	4	C	0.60	2.57	14.05	18.75	0.00	0.61	0.75	7.75	0.03	49.93	0.02	95.06
	5	E	0.73	1.24	13.52	18.85	0.00	0.33	1.24	8.20	0.02	50.66	0.00	94.79
	5	C	0.69	1.17	13.64	18.93	0.00	0.29	1.29	7.85	0.04	51.43	0.02	95.35
	6	E	0.66	1.37	13.55	18.55	0.00	0.33	1.21	7.79	0.02	51.07	0.05	94.60
	7	E	0.70	1.41	13.13	19.32	0.00	0.37	1.47	8.81	0.02	50.40	0.08	95.71
	8	E	0.63	1.11	13.38	19.03	0.00	0.32	1.63	8.65	0.03	51.03	0.07	95.88
	9	E	0.66	1.19	13.33	19.77	0.00	0.28	1.11	7.88	0.05	51.36	0.00	95.63
	10	E	0.63	0.92	13.58	18.59	0.00	0.26	1.54	8.09	0.06	52.04	0.00	95.71
	11	E	0.75	1.01	13.05	19.19	0.00	0.24	1.26	8.36	0.03	50.56	0.00	94.45
A5-72	1	E	0.62	1.66	14.52	19.67	0.00	0.41	0.74	7.68	0.00	50.48	0.00	95.78
	1	C	0.57	1.02	14.42	19.61	0.00	0.25	1.18	7.80	0.00	51.55	0.00	96.40
	2	E	0.58	1.60	14.32	20.01	0.01	0.38	0.90	7.78	0.00	49.94	0.00	95.52
	2	C	0.66	1.72	14.70	19.68	0.00	0.45	0.76	7.76	0.00	49.75	0.04	95.52
	3	E	0.57	1.62	14.25	20.02	0.03	0.43	0.78	7.72	0.00	49.20	0.00	94.62
	3	C	0.59	1.52	14.41	20.09	0.02	0.36	0.84	7.63	0.00	49.74	0.04	95.24
	4	E	0.59	1.68	14.30	18.68	0.00	0.38	0.80	7.86	0.00	48.93	0.00	93.22
	4	C	0.56	1.60	14.60	19.00	0.00	0.47	0.79	7.78	0.00	50.04	0.00	94.84
	5	E	0.57	2.32	14.93	18.04	0.00	0.50	0.89	7.62	0.00	51.72	0.03	96.62
	5	C	0.56	2.28	14.96	19.23	0.00	0.51	0.61	7.80	0.00	51.67	0.05	97.67
	6	E	0.59	1.50	13.86	18.56	0.05	0.43	0.86	7.57	0.00	49.91	0.12	93.45
	6	C	0.59	1.85	14.24	18.77	0.00	0.44	0.82	7.94	0.00	51.15	0.02	95.82
	7	E	0.53	1.95	14.19	18.40	0.01	0.42	0.76	7.66	0.02	51.41	0.00	95.35
	7	C	0.55	1.93	14.99	18.63	0.00	0.38	0.67	7.77	0.00	51.87	0.05	96.84
	8	E	0.60	1.70	13.95	19.23	0.02	0.43	0.90	7.81	0.00	51.15	0.00	95.79

Appendix 4. Continued.

CLINOPYROXENE ANALYSES

Ammonia Tanks Member

Sample	Grain #	Pos.	Na_2O	Al_2O_3	MgO	CaO	K_2O	TiO_2	MnO	FeO	NiO	SiO_2	BaO	Total
A5-75	1	E	0.68	1.86	15.00	18.61	0.00	0.45	0.64	7.58	0.18	51.10	0.02	96.12
	1	C	0.56	1.93	14.69	18.73	0.00	0.48	0.65	7.91	0.00	50.70	0.06	95.71
	2	E	0.64	2.27	15.09	21.09	0.01	0.55	0.68	8.01	0.00	51.09	0.00	99.43
	3	E	0.59	1.87	15.25	20.95	0.02	0.46	0.62	7.76	0.00	51.65	0.00	99.17
	4	E	0.75	2.35	14.11	18.83	0.13	0.51	0.54	7.88	0.00	46.90	0.11	92.11
	4	C	0.59	1.73	14.85	19.02	0.00	0.40	0.76	7.56	0.00	50.65	0.00	95.56
	5	E	0.62	2.04	15.14	19.34	0.00	0.45	0.66	7.56	0.00	49.40	0.04	95.25
	5	C	0.66	2.11	14.98	19.00	0.00	0.53	0.66	7.97	0.00	48.19	0.05	94.15
	6	E	0.59	1.77	14.25	18.65	0.00	0.36	0.59	8.24	0.00	51.19	0.02	95.66
	7	E	0.53	2.63	14.61	18.27	0.00	0.51	0.97	7.70	0.00	49.70	0.04	94.96
	7	C	0.52	2.85	14.79	18.95	0.00	0.58	0.47	7.67	0.00	50.48	0.00	96.31
	8	E	0.60	2.04	14.95	18.76	0.00	0.44	0.67	7.68	0.00	51.17	0.03	96.34
	8	C	0.63	2.03	14.67	18.63	0.00	0.41	0.69	7.50	0.00	50.40	0.10	95.06
	9	E	0.56	2.26	15.18	17.91	0.01	0.48	0.51	7.98	0.00	50.86	0.04	95.79
	9	C	0.55	2.23	14.93	17.45	0.00	0.45	0.57	7.97	0.00	50.98	0.00	95.13
	10	E	0.65	1.77	14.86	18.43	0.00	0.38	0.69	7.68	0.00	50.83	0.05	95.34
	10	C	0.63	1.46	14.88	17.73	0.00	0.35	0.83	7.71	0.00	51.48	0.06	95.13
	11	E	0.56	2.87	13.91	17.80	0.00	0.66	0.54	8.05	0.00	49.39	0.00	93.78
	11	C	0.64	1.97	14.90	18.29	0.00	0.42	0.65	7.41	0.00	50.10	0.05	94.43

Appendix 4. Continued.

CLINOPYROXENE ANALYSES -- University of Michigan

Ammonia Tanks Member

Sample	Grain #	Pos.	Na_2O	MgO	Al_2O_3	SiO_2	K_2O	CaO	BaO	TiO_2	MnO	FeO	Total
A4-70	1	E	0.46	15.48	0.95	51.89	0.00	20.56	0.02	0.29	1.09	8.43	99.16
	2	E	0.64	14.73	0.78	53.09	0.02	21.32	0.13	0.23	1.42	8.42	100.77
	3	E	0.71	14.03	1.48	52.47	0.02	21.19	0.06	0.44	1.28	9.29	100.96
A5-9	1	E	0.68	13.95	1.01	51.38	0.00	21.41	0.05	0.33	1.30	8.03	98.12
	2	E	0.71	14.43	0.94	51.72	0.01	21.04	0.04	0.29	1.65	8.09	98.93
	3	E	0.67	16.22	1.68	53.48	0.00	20.83	0.07	0.51	0.77	7.38	101.61
A5-30	1	E	0.72	15.14	1.43	51.70	0.01	20.51	0.07	0.34	1.02	7.22	98.16
	2	E	0.64	14.44	1.51	50.13	0.01	20.92	0.03	0.60	0.91	7.36	96.56
	3	E	0.64	14.98	1.08	51.83	0.02	21.07	0.02	0.28	1.14	7.64	98.70
	4	E	0.70	14.78	1.27	51.38	0.00	20.94	0.04	0.32	0.96	7.53	97.91
A5-31	1	E	0.58	16.06	2.23	50.87	0.00	20.30	0.03	0.55	0.58	6.91	98.12
	2	E	0.59	14.93	3.09	48.91	0.02	20.20	0.02	0.77	0.56	7.75	96.83
	3	E	0.59	15.05	1.60	50.98	0.00	20.70	0.00	0.51	0.72	7.46	97.60
A5-68	1	E	0.66	14.30	0.73	52.09	0.00	20.12	0.02	0.19	1.74	7.87	97.73
	2	E	0.45	15.82	0.88	52.80	0.00	20.39	0.07	0.20	0.97	7.48	99.05
	3	E	0.60	14.38	0.63	52.27	0.00	20.33	0.00	0.20	1.81	7.98	98.21

Appendix 4. Continued.

ORTHOPYROXENE ANALYSES

Rainier Mesa Member

Sample	Grain #	Pos.	Na_2O	Al_2O_3	MgO	CaO	K_2O	TiO_2	MnO	FeO	NiO	SiO_2	BaO	Total
R23-13	1	E	0.00	0.36	22.43	0.98	0.01	0.13	2.64	20.39	0.00	52.37	0.00	99.31
	1	E	0.06	0.36	22.46	0.90	0.00	0.12	2.72	20.00	0.00	51.64	0.00	98.26
	1	E	0.00	0.38	22.13	0.95	0.01	0.13	2.47	20.55	0.00	52.76	0.00	99.38
	2	E	0.09	0.35	22.26	1.06	0.02	0.10	2.66	19.58	0.00	52.93	0.05	99.10
	2	E	0.08	0.40	22.97	0.96	0.03	0.12	2.57	19.61	0.00	54.15	0.00	100.89
	3	E	0.00	0.33	22.28	0.99	0.02	0.12	2.57	19.92	0.00	53.65	0.00	99.88
	3	E	0.03	0.38	21.85	0.89	0.02	0.12	2.45	19.64	0.00	53.85	0.11	99.34
	3	E	0.00	0.39	21.86	0.94	0.01	0.09	2.48	19.91	0.00	53.37	0.02	99.07
R8-45	1	E	0.03	0.39	21.97	0.95	0.00	0.11	2.55	19.94	0.04	53.11	0.00	99.09
	1	E	0.00	0.49	22.64	0.98	0.00	0.12	2.52	20.35	0.00	53.29	0.00	100.39
	1	E	0.03	0.33	22.28	0.93	0.00	0.11	2.50	19.97	0.04	54.06	0.00	100.25
R23-26	1	E	0.09	0.31	22.68	0.99	0.00	0.14	2.52	19.63	0.00	53.97	0.00	100.33
	1	E	0.08	0.33	22.79	0.95	0.03	0.14	2.44	19.89	0.00	54.11	0.04	100.80
	1	E	0.07	0.36	22.64	0.90	0.00	0.14	2.53	19.77	0.00	54.14	0.05	100.60
	2	E	0.05	0.30	22.48	0.87	0.02	0.12	2.82	19.72	0.03	54.73	0.04	101.18
	2	E	0.06	0.46	22.78	0.87	0.02	0.16	2.68	20.02	0.04	54.34	0.00	101.43
	3	E	0.06	0.38	24.12	1.03	0.00	0.15	2.43	19.21	0.02	53.21	0.00	100.61
	4	E	0.06	0.38	22.34	0.90	0.03	0.11	2.83	20.62	0.05	52.10	0.00	99.42
	4	E	0.07	0.27	22.56	0.85	0.01	0.13	2.87	20.16	0.02	51.55	0.00	98.49
R8-44	1	E	0.03	0.30	22.32	0.96	0.00	0.11	2.91	20.43	0.00	53.05	0.00	100.11
	2	E	0.02	0.31	23.45	0.98	0.00	0.11	2.63	19.04	0.00	54.90	0.00	101.44
R21-1	1	E	0.03	0.41	23.83	0.74	0.00	0.07	2.41	18.13	0.00	52.94	0.10	98.66
	1	E	0.00	0.30	22.35	0.84	0.00	0.08	2.52	19.41	0.00	51.92	0.00	97.42
	2	E	0.00	0.32	21.20	0.81	0.00	0.09	2.51	19.89	0.00	50.89	0.00	95.71
	2	E	0.00	0.35	21.69	0.80	0.00	0.07	2.57	19.94	0.00	52.07	0.09	97.58
	3	E	0.00	0.28	21.94	0.82	0.00	0.06	2.43	19.89	0.00	51.77	0.09	97.28
R21-5	1	E	0.03	0.36	22.52	0.75	0.02	0.08	2.39	19.59	0.00	52.61	0.00	98.35
	1	C	0.00	0.33	21.95	0.72	0.02	0.09	2.38	20.18	0.00	51.38	0.00	97.05
	2	E	0.00	0.31	21.15	0.73	0.01	0.07	2.60	19.52	0.00	50.55	0.00	94.94
	2	C	0.00	0.38	21.54	0.73	0.02	0.09	2.42	20.15	0.00	51.77	0.00	97.10
	3	E	0.00	0.36	22.13	0.67	0.01	0.08	2.60	19.79	0.00	52.03	0.00	97.67
	4	E	0.00	0.31	21.45	0.71	0.02	0.05	2.83	20.35	0.00	52.00	0.00	97.72
	4	C	0.00	0.30	21.44	0.76	0.01	0.04	2.54	20.10	0.00	51.77	0.00	96.96

Appendix 4. Continued.

ORTHOPYROXENE ANALYSES

Ammonia Tanks Member

Sample	Grain #	Pos.	Na_2O	Al_2O_3	MgO	CaO	K_2O	TiO_2	MnO	FeO	NiO	SiO_2	BaO	Total
A5-58	1	E	0.00	0.37	20.76	0.94	0.01	0.13	2.26	18.59	0.05	46.04	0.02	89.17
	1	C	0.05	0.74	23.32	1.16	0.02	0.19	2.26	18.49	0.20	51.42	0.00	97.85

ORTHOPYROXENE ANALYSES -- University of Michigan

Ammonia Tanks Member

Sample	Grain #	Pos.	Na_2O	MgO	Al_2O_3	SiO_2	K_2O	CaO	BaO	TiO_2	MnO	FeO	Total
A5-30	1	E	0.03	25.75	0.49	53.25	0.00	1.08	0.04	0.13	2.07	16.48	99.31
	2	C	0.03	25.82	0.59	53.26	0.02	1.05	0.00	0.19	2.46	16.19	99.60

Appendix 4. Continued.

AMPHIBOLE ANALYSES

Rainier Mesa Member

Sample	Grain #	Pos.	Na_2O	Al_2O_3	MgO	CaO	K_2O	TiO_2	MnO	FeO	NiO	SiO_2	BaO	Total
R8-44	1	E	2.53	12.25	13.32	11.17	0.78	3.81	0.38	12.10	0.00	42.22	0.07	98.63
R8-45	1	E	2.41	12.36	13.05	10.95	0.81	3.50	0.33	12.45	0.02	41.08	0.00	96.96
	1	E	2.55	12.12	13.59	11.14	0.79	3.60	0.28	12.34	0.02	42.11	0.14	98.68
R11-5	1	E	2.34	11.79	12.26	10.99	0.97	3.47	0.38	13.16	0.00	41.21	0.08	96.65
	2	E	2.58	11.10	13.12	10.75	0.98	3.46	0.41	12.17	0.00	42.12	0.15	96.84
	3	E	2.37	10.51	12.95	10.89	0.97	3.10	0.54	12.34	0.06	42.26	0.09	96.08
	4	E	2.34	10.59	12.99	10.90	0.95	2.65	1.08	12.46	0.00	43.16	0.00	97.12
	5	E	2.49	11.66	12.21	11.82	0.99	3.67	0.42	12.57	0.00	40.57	0.00	96.40
	6	E	2.43	11.17	13.06	10.84	1.06	3.20	0.44	13.17	0.00	42.48	0.02	97.87
	7	E	2.20	10.64	13.11	10.95	0.99	2.79	0.41	12.46	0.00	42.92	0.00	96.47
R11-7	1	E	2.25	10.22	12.71	10.81	1.13	2.95	0.33	12.98	0.00	42.19	0.00	95.57
	2	E	2.33	12.55	12.48	10.40	0.79	3.46	0.38	12.47	0.00	40.03	0.00	94.89
	3	E	2.72	11.95	12.61	11.07	0.76	3.79	0.28	12.34	0.00	40.88	0.00	96.40
	4	E	2.41	12.02	12.92	10.84	0.79	3.56	0.32	12.12	0.00	40.37	0.08	95.43
	5	E	2.49	11.77	12.70	10.63	0.82	3.22	0.36	12.51	0.00	40.79	0.00	95.29
	6	E	2.58	11.91	12.50	11.07	0.89	3.59	0.44	13.55	0.00	40.82	0.00	97.35
	7	E	2.62	11.92	12.90	11.19	0.80	3.63	0.37	12.60	0.00	41.68	0.00	97.71
R21-13	1	E	2.59	12.19	12.85	8.86	0.64	3.28	0.37	12.13	0.00	40.33	0.00	93.24
	1	C	2.49	11.92	12.58	9.20	0.60	3.29	0.36	12.39	0.00	40.08	0.03	92.94
	2	E	2.60	11.91	12.77	8.93	0.70	2.92	0.35	12.12	0.00	40.56	0.00	92.86
	3	E	2.43	11.74	12.53	8.84	0.58	3.10	0.35	12.16	0.00	40.30	0.00	92.03
	4	C	2.57	12.45	13.32	9.17	0.67	3.30	0.22	11.21	0.00	40.20	0.00	93.11
	5	E	2.28	10.76	13.13	9.05	0.74	2.62	0.32	11.92	0.00	40.95	0.00	91.77
	5	C	2.48	12.19	13.13	9.27	0.61	3.09	0.28	11.83	0.00	40.90	0.00	93.78
	6	E	2.65	12.34	12.99	9.57	0.61	3.49	0.31	12.21	0.00	40.60	0.00	94.77
	7	E	2.55	12.16	12.88	9.62	0.63	3.35	0.29	11.41	0.00	40.26	0.00	93.15
	8	E	2.59	12.47	13.19	9.34	0.62	3.34	0.28	11.44	0.00	40.66	0.09	94.02
	9	E	2.62	11.91	12.68	9.30	0.68	3.01	0.40	12.81	0.00	40.51	0.00	93.92
	10	E	2.61	11.53	12.52	9.04	0.70	2.92	0.39	12.52	0.00	40.13	0.00	92.36
	11	E	2.46	12.35	12.73	8.99	0.61	3.55	0.32	11.64	0.00	39.49	2.71	94.85
	12	E	2.48	12.03	11.93	8.99	0.58	3.29	0.33	12.62	0.00	38.83	0.00	91.08

Appendix 4. Continued.

AMPHIBOLE ANALYSES

Rainier Mesa Member

Sample	Grain #	Pos.	Na_2O	Al_2O_3	MgO	CaO	K_2O	TiO_2	MnO	FeO	NiO	SiO_2	BaO	Total
R23-13	1	E	2.61	12.79	13.09	11.18	0.76	3.31	0.53	13.16	0.05	40.57	0.00	98.05
	2	E	2.47	11.69	13.08	11.13	0.98	3.25	0.46	13.02	0.02	42.47	0.00	98.57
	3	E	2.44	12.01	13.38	11.21	0.91	3.34	0.32	12.98	0.00	42.66	0.00	99.25
	3	C	2.56	12.35	13.45	11.21	0.92	3.61	0.33	12.18	0.02	42.35	0.08	99.06
	4	E	2.51	12.12	13.04	11.01	0.91	3.33	0.34	13.00	0.02	41.86	0.00	98.14
	5	E	2.59	12.11	13.12	11.18	0.84	3.83	0.31	12.57	0.03	42.64	0.06	99.28
	6	E	2.55	12.47	12.62	11.11	0.84	3.42	0.42	13.45	0.04	42.28	0.02	99.22
R23-24	1	E	2.46	11.42	13.41	10.75	0.78	3.37	0.32	11.54	0.00	41.14	0.00	95.19
	2	E	2.48	12.11	12.53	10.89	0.68	3.61	0.61	12.51	0.00	40.99	0.00	96.41
	3	E	2.56	11.74	12.87	10.58	0.82	3.31	0.36	12.08	0.00	41.21	0.01	95.54
	4	E	2.42	11.52	13.11	10.96	0.87	3.00	0.41	12.16	0.00	41.46	0.00	95.91
	5	E	2.33	10.84	13.35	11.08	1.05	3.27	0.37	12.26	0.00	42.63	0.00	97.18
	6	E	2.50	12.00	12.69	11.02	0.77	3.59	0.37	12.84	0.00	41.01	0.00	96.79
	7	E	2.35	10.92	13.53	10.82	0.91	2.82	0.42	12.14	0.00	41.99	0.00	95.90
	8	E	2.49	12.11	13.06	10.63	0.80	3.57	0.32	11.64	0.00	40.36	0.27	95.25
	9	E	2.38	11.55	13.97	10.53	0.74	3.26	0.29	11.15	0.00	41.57	0.00	95.44
R23-27	1	E	2.63	12.06	12.98	11.13	0.81	3.61	0.34	12.79	0.00	40.27	0.00	96.62
	2	E	2.68	12.83	13.01	11.10	0.85	4.02	0.31	12.53	0.00	40.40	0.03	97.76
	3	E	2.76	12.09	13.41	10.97	0.82	4.10	0.28	12.01	0.00	40.99	0.09	97.52
	4	E	2.48	12.28	13.59	11.05	0.84	3.74	0.32	11.77	0.00	41.17	0.00	97.24
	5	E	2.66	12.43	13.55	11.17	0.69	4.19	0.21	11.89	0.00	40.51	0.04	97.34
	6	E	2.66	12.35	12.58	11.18	0.83	3.66	0.37	12.97	0.00	40.30	0.11	97.01
	7	E	2.51	12.09	13.20	10.74	0.84	3.57	0.32	12.50	0.00	41.32	0.00	97.09
	7	C	2.44	12.23	13.61	10.91	0.82	3.72	0.23	11.59	0.00	42.26	0.01	97.82

AMPHIBOLE ANALYSES

Ammonia Tanks Member

Sample	Grain #	Pos.	Na_2O	Al_2O_3	MgO	CaO	K_2O	TiO_2	MnO	FeO	NiO	SiO_2	BaO	Total
A5-75	1	E	2.43	11.84	13.65	11.03	1.17	4.00	0.25	11.48	0.00	40.35	0.00	96.20
	2	E	2.57	11.47	14.08	11.38	1.18	3.90	0.35	11.41	0.00	41.36	0.04	97.74

Appendix 4. Continued.

OLIVINE ANALYSES

Ammonia Tanks Member

Sample	Grain #	Pos.	Na_2O	Al_2O_3	MgO	CaO	K_2O	TiO_2	MnO	FeO	NiO	SiO_2	BaO	Total
A5-3	1	E	0.00	0.00	0.00	0.03	0.01	0.00	21.88	46.75	0.00	30.78	0.00	99.45
	1	E	0.00	0.00	0.00	0.03	0.01	0.00	23.23	46.03	0.00	30.58	0.00	99.88
	2	E	0.13	0.04	0.00	0.04	0.02	0.00	2.10	83.62	0.03	5.88	0.02	91.88
	2	C	0.16	0.00	0.00	0.04	0.01	0.00	2.21	83.76	0.06	5.97	0.02	92.23
	3	E	0.00	0.00	0.00	0.02	0.00	0.00	19.76	48.88	0.02	30.77	0.04	99.49
	4	E	0.10	0.18	0.09	0.10	0.00	0.05	1.38	84.15	0.00	4.64	0.00	90.69
	5	E	0.03	0.04	0.00	0.10	0.01	0.10	23.48	45.20	0.01	30.47	0.03	99.47
	6	E	0.03	0.00	0.00	0.03	0.00	0.01	23.53	45.62	0.02	30.58	0.02	99.84
	7	E	0.00	0.03	0.02	0.12	0.01	0.07	21.61	46.33	0.02	30.24	0.06	98.51
	8	E	0.11	0.27	0.04	0.19	0.04	0.07	1.35	86.43	0.06	3.68	0.00	92.24
	9	E	0.00	0.01	0.00	0.06	0.00	0.00	23.25	44.72	0.02	30.20	0.00	98.26
	10	E	0.04	0.02	0.00	0.03	0.00	0.00	21.61	48.12	0.00	30.69	0.00	100.51
	11	E	0.00	0.00	0.00	0.08	0.02	0.00	20.63	47.71	0.03	29.57	0.03	98.07
	11	NE	0.00	0.00	0.02	0.06	0.00	0.00	20.40	49.02	0.43	30.83	0.02	100.78
	11	NC	0.00	0.00	0.00	0.03	0.02	0.02	20.29	49.92	0.00	30.67	0.06	101.01
	11	C	0.00	0.00	0.00	0.05	0.01	0.03	19.48	50.03	0.06	31.25	0.00	100.91
	11	NC	0.00	0.02	0.08	0.08	0.02	0.06	18.89	49.28	0.04	30.41	0.00	98.88
A21-18	1	E	0.03	0.17	0.07	0.09	0.00	0.05	20.72	43.77	0.00	32.68	0.03	97.61
	1	E	0.00	0.20	0.06	0.12	0.03	0.01	21.57	45.35	0.02	31.39	0.08	98.83
	2	E	0.12	0.07	0.06	0.03	0.00	0.03	22.60	43.38	0.00	31.48	0.00	97.77
	3	E	0.00	0.14	0.00	0.12	0.00	0.02	20.25	42.22	0.00	32.03	0.10	94.88
	3	E	0.00	0.09	0.00	0.07	0.00	0.02	20.32	39.44	0.00	33.25	0.08	93.27
	3	E	0.11	0.43	0.14	0.61	0.04	0.08	16.53	40.13	0.00	32.39	0.18	90.64
	4	E	0.00	0.05	0.00	0.13	0.00	0.00	22.94	45.67	0.01	28.62	0.17	97.59
	4	E	0.00	0.04	0.00	0.11	0.00	0.05	24.46	42.47	0.00	30.25	0.04	97.42

OLIVINE ANALYSES -- University of Michigan

Ammonia Tanks Member

Sample	Grain #	Pos.	Na_2O	MgO	Al_2O_3	SiO_2	K_2O	CaO	BaO	TiO_2	MnO	FeO	Total
A5-37	1	E	0.00	0.00	0.13	29.73	0.06	0.28	0.09	0.11	20.32	43.88	94.60
	2	E	0.00	0.00	0.00	29.98	0.02	0.11	0.10	0.11	21.20	45.35	96.87
A5-68	1	E	0.02	24.15	0.21	51.92	0.00	1.02	0.05	0.13	2.55	16.65	96.71

Appendix 4. Continued.

MAGNETITE AND ILMENITE ANALYSES

Rainier Mesa Member

Sample	Grain #	Cr_2O_3	Al_2O_3	MgO	FeO	TiO_2	MnO	Total
R8-25								
	1p1	0.02	2.21	0.63	80.58	5.30	0.40	89.14
	1p1	0.04	2.34	0.89	81.17	4.46	0.29	89.19
	2p1	0.00	1.21	3.97	40.48	40.68	2.23	88.57
	3	0.03	1.97	1.21	84.19	5.69	1.15	94.24
	3	0.04	2.02	1.01	80.52	6.44	1.12	91.15
	3	0.05	1.87	1.13	81.19	7.62	1.51	93.37
	4	0.03	2.29	0.89	81.84	6.53	1.38	92.96
	4	0.03	2.19	0.91	82.04	6.24	0.63	92.04
	5	0.04	1.95	1.04	82.99	5.31	1.11	92.44
	5	0.04	1.94	1.20	83.79	5.96	1.33	94.26
	5	0.03	1.66	1.74	78.92	12.14	1.62	96.11
	6	0.00	0.17	1.84	54.44	37.34	1.24	95.03
	6	0.00	0.39	1.91	54.52	39.00	1.42	97.24
	6	0.00	0.16	1.90	55.12	37.83	1.25	96.26
	7p2	0.04	2.07	1.12	83.16	5.56	1.34	93.29
	7p2	0.03	1.86	1.08	80.82	5.75	1.27	90.81
	7p2	0.05	2.02	1.15	82.41	5.63	1.19	92.45
	8p2	0.00	0.07	3.63	44.44	45.18	3.30	96.62
	9	0.00	0.21	1.72	55.32	38.92	1.27	97.44
	9	0.00	0.17	1.62	54.78	38.83	1.40	96.80
	9	0.00	0.17	1.68	54.78	37.06	1.28	94.97
	10	0.00	0.19	2.02	55.23	38.62	1.40	97.46
	10	0.00	0.16	1.98	53.84	38.60	1.50	96.08
	11	0.03	2.01	1.25	80.90	8.17	1.21	93.57
R8-44								
	1	0.04	1.81	1.93	79.48	8.32	1.07	92.65
	1	0.04	1.95	1.84	79.00	8.58	1.12	92.53
	2	0.00	2.35	1.52	74.47	7.95	1.17	87.46
	2	0.06	1.90	1.65	82.95	8.07	1.25	95.88
	3	0.03	1.64	1.31	80.23	7.80	1.01	92.02
	4	0.04	1.85	1.53	80.78	9.22	1.23	94.65
	4	0.06	1.89	1.62	83.28	8.33	1.23	96.41
	4	0.02	2.31	2.04	77.82	8.00	1.17	91.36
	4	0.03	1.82	1.48	81.97	7.99	1.25	94.54
	5	0.00	0.25	2.22	54.43	37.86	1.24	96.00
	5	0.00	0.28	2.24	54.87	37.60	1.12	96.11
	6	0.00	0.14	1.86	55.51	37.90	1.58	96.99
	6	0.00	0.18	1.75	54.86	39.02	1.48	97.29
	7	0.00	0.18	1.93	53.69	39.26	1.42	96.48
	7	0.00	0.17	1.94	54.00	38.51	1.59	96.21
	8	0.00	0.20	2.18	54.58	37.78	1.22	95.96

Appendix 4. Continued.

MAGNETITE AND ILMENITE ANALYSES

Rainier Mesa Member

Sample	Grain #	Cr_2O_3	Al_2O_3	MgO	FeO	TiO_2	MnO	Total
R8-44, Continued								
	8	0.02	0.22	2.08	54.66	38.36	1.25	96.59
	9	0.00	0.21	2.13	55.47	38.95	1.08	97.84
	9	0.00	0.27	2.04	55.33	37.36	1.11	96.11
	9	0.00	0.24	2.09	54.69	37.93	1.96	96.91
	10	0.00	0.16	1.85	54.39	37.19	1.31	94.90
	10	0.00	0.19	2.00	56.20	37.51	1.29	97.19
	11	0.04	1.68	1.44	81.06	7.75	1.27	93.24
	11	0.05	1.62	1.38	81.56	7.44	1.31	93.36
	12	0.00	0.16	2.03	54.25	37.78	1.45	95.67
	13	0.00	0.25	1.98	56.71	42.01	1.25	102.20
	14	0.05	1.74	1.50	84.01	7.80	1.22	96.32
	15	0.00	0.28	2.22	56.59	37.27	1.12	97.48
	15	0.00	0.29	2.13	56.31	38.42	1.15	98.30
	16	0.00	0.31	2.15	55.89	37.90	1.17	97.42
	17	0.00	0.35	0.11	86.33	0.00	0.12	86.91
	18	0.04	2.12	1.65	81.75	7.93	1.16	94.65
	18	0.06	1.98	1.65	82.91	7.76	1.30	95.66
	19	0.01	1.94	1.54	83.70	7.94	1.57	96.70
	20	0.03	2.02	1.50	84.46	7.40	1.33	96.74
	20	0.06	1.85	1.50	81.76	7.72	1.31	94.20
R8-45								
	1	0.00	1.87	1.62	82.89	8.66	1.26	96.30
	1	0.03	1.87	1.72	82.78	8.42	1.16	95.98
	2	0.00	1.87	1.60	82.92	8.09	1.20	95.68
	2	0.00	1.80	1.64	82.22	7.66	1.20	94.52
	3	0.02	1.82	1.74	82.10	7.78	1.13	94.59
	3	0.00	1.83	1.59	82.15	7.56	1.32	94.45
	4	0.00	1.84	1.61	82.96	8.90	1.14	96.45
	4	0.03	1.86	1.57	82.97	7.65	1.28	95.36
	5	0.03	1.88	1.69	83.80	8.15	1.39	96.94
	5	0.03	1.91	1.57	82.48	8.40	1.17	95.56
	6	0.00	0.23	2.14	55.49	37.50	1.16	96.52
	6	0.00	0.24	2.17	55.25	37.57	1.09	96.32
	7	0.00	0.26	2.24	55.01	37.86	1.20	96.57
	7	0.00	0.23	2.07	56.27	39.32	1.27	99.16
	8	0.00	0.22	2.10	54.64	37.69	1.49	96.14
	8	0.00	0.22	2.27	54.28	38.15	1.22	96.14
	9	0.01	1.79	1.66	81.19	7.99	1.34	93.98
	9	0.00	1.90	1.65	82.33	7.81	1.18	94.87
	10	0.00	0.23	2.23	55.45	38.02	1.08	97.01

Appendix 4. Continued.

MAGNETITE AND ILMENITE ANALYSES

Rainier Mesa Member

Sample	Grain #	Cr_2O_3	Al_2O_3	MgO	FeO	TiO_2	MnO	Total
R8-45, Continued								
	10	0.00	0.22	2.23	55.29	37.87	1.13	96.74
	11	0.00	0.24	2.20	54.60	38.39	1.10	96.53
	11	0.00	0.26	2.26	54.23	37.70	1.15	95.60
	12	0.00	0.24	2.19	55.30	38.58	1.05	97.36
	12	0.00	0.21	2.27	54.75	37.42	1.14	95.79
	13	0.03	1.90	1.62	82.06	8.11	1.25	94.97
	13	0.06	1.97	1.69	83.02	7.87	1.22	95.83
	13	0.03	2.01	1.61	84.21	8.00	1.15	97.01
	14	0.04	1.99	1.66	82.35	8.30	1.24	95.58
	14	0.04	1.94	1.65	84.13	8.14	1.13	97.03
	15	0.02	1.99	1.69	84.37	7.69	1.18	96.94
	15	0.01	2.01	1.66	84.56	8.27	1.16	97.67
	16pl	0.03	1.98	1.53	81.79	8.11	1.22	94.66
	16pl	0.03	2.05	1.50	83.37	8.12	1.21	96.28
	17pl	0.00	0.30	2.31	56.05	37.74	1.06	97.46
	17pl	0.00	0.29	2.24	55.21	39.25	1.19	98.18
R11-5								
	1	0.00	0.32	1.93	55.56	40.57	1.10	99.48
	1	0.00	0.23	1.57	55.88	37.27	1.34	96.29
	2	0.04	2.25	1.38	80.28	8.30	1.33	93.58
	2	0.01	2.18	1.37	81.19	8.33	1.44	94.52
	2	0.02	2.11	1.32	81.46	8.17	1.40	94.48
	3	0.00	0.31	2.07	55.24	36.45	0.98	95.05
	3	0.00	0.36	1.98	55.75	37.01	1.02	96.12
	4	0.03	2.23	1.53	81.31	7.74	1.18	94.02
	4	0.04	2.23	1.56	82.22	8.02	1.14	95.21
	5	0.03	2.34	1.29	80.23	8.22	1.39	93.50
	5	0.03	2.36	1.34	81.36	8.36	1.40	94.85
	6	0.00	2.30	1.60	79.77	8.33	1.25	93.25
	6	0.03	2.33	1.61	79.83	8.46	1.31	93.57
	7	0.02	0.25	1.93	55.44	36.75	1.34	95.73
	7	0.02	0.27	2.02	55.24	37.17	1.27	95.99
	8	0.00	0.27	1.93	54.79	36.80	1.31	95.10
	9	0.00	0.20	0.09	84.02	0.46	0.07	84.84
	10	0.00	2.42	1.65	78.99	8.33	1.23	92.62
	10	0.03	2.31	1.66	80.28	7.94	1.95	94.17
	11	0.02	0.30	2.02	54.37	36.72	1.33	94.76
	11	0.00	0.33	2.14	54.74	37.60	1.23	96.04
	12	0.00	0.35	2.27	55.20	36.73	1.13	95.68
	12	0.00	0.35	2.10	54.98	36.55	1.19	95.17
	13	0.00	0.31	2.09	55.19	37.44	1.09	96.12
	13	0.00	0.29	2.12	55.60	37.32	1.03	96.36

Appendix 4. Continued.

MAGNETITE AND ILMENITE ANALYSES

Rainier Mesa Member

Sample	Grain #	Cr_2O_3	Al_2O_3	MgO	FeO	TiO_2	MnO	Total
R11-7								
	1	0.00	1.16	0.61	82.93	5.54	1.94	92.18
	1	0.02	1.12	0.64	82.06	4.88	2.00	90.72
	2	0.02	1.12	0.51	83.01	4.90	1.79	91.35
	3	0.00	0.05	1.23	47.63	42.21	4.01	95.13
	3	0.00	0.02	1.22	46.57	42.63	4.04	94.48
	4	0.02	1.13	0.62	81.82	5.27	1.64	90.50
	5	0.00	1.15	1.04	81.58	4.82	1.68	90.27
	5	0.00	1.18	0.51	82.74	4.71	1.87	91.01
	6	0.00	1.19	0.52	84.46	4.91	1.93	93.01
	7	0.00	0.06	1.15	46.18	43.14	4.21	94.74
	8	0.00	1.14	0.60	83.24	4.50	1.72	91.20
	9	0.00	0.04	1.26	46.88	41.61	4.85	94.64
	10	0.00	1.19	0.55	83.24	4.73	1.95	91.66
	10	0.00	1.10	0.58	82.19	4.69	1.89	90.45
	11	0.00	0.06	1.28	47.37	42.66	3.85	95.22
	11	0.00	0.03	1.14	46.91	43.52	3.75	95.35
	12	0.00	0.04	1.19	45.55	42.83	5.67	95.28
	13	0.00	1.24	0.56	83.86	5.17	1.94	92.77
	13	0.00	1.20	0.57	83.70	5.98	1.92	93.37
	14	0.00	0.07	1.23	46.49	43.23	4.01	95.03
	15	0.00	0.06	1.16	47.31	42.89	3.94	95.36
	16	0.00	0.06	1.20	47.16	42.71	3.91	95.04
	17	0.00	0.06	1.32	45.42	43.35	6.05	96.20
	18	0.00	1.23	0.70	82.69	4.63	2.30	91.55
	18	0.00	1.14	0.58	81.30	4.35	2.19	89.56
R18-2, Run #1								
	1	0.00	0.12	1.36	49.22	44.43	2.38	97.51
	2	0.04	1.27	0.69	81.70	5.91	1.39	90.99
	3	0.00	0.13	0.70	47.23	41.60	1.46	91.12
	4	0.00	0.11	1.04	49.18	40.71	2.66	93.71
	5	0.05	1.12	0.65	82.12	5.73	1.43	91.10
	5	0.05	1.22	0.77	83.17	5.62	1.14	91.97
	6	0.05	1.44	0.53	81.64	5.15	1.63	90.44
	6	0.04	1.31	0.48	82.48	5.14	1.64	91.08
	7	0.00	0.16	1.41	48.00	41.60	1.83	93.00
	8	0.00	0.09	1.48	49.10	40.42	2.27	93.36
	8	0.00	0.14	1.52	48.50	40.25	2.47	92.88
	9	0.03	1.18	0.72	81.62	5.76	1.19	90.50
	10	0.03	1.20	0.75	81.34	5.54	1.31	90.17
	11	0.00	0.14	1.50	49.11	40.71	2.38	93.84
	12	0.00	0.13	1.45	48.88	40.79	2.49	93.74

Appendix 4. Continued.

MAGNETITE AND ILMENITE ANALYSES

Rainier Mesa Member

Sample #	Grain	Cr_2O_3	Al_2O_3	MgO	FeO	TiO_2	MnO	Total
R18-2, Run #2								
	1	0.00	1.27	0.76	82.59	6.42	1.28	92.32
	2	0.00	1.17	0.77	83.11	5.95	1.59	92.60
	2	0.00	1.12	0.73	83.87	5.73	1.72	93.18
	3	0.04	1.02	0.85	82.81	5.65	1.74	92.12
	4	0.00	0.11	1.58	51.05	41.40	2.39	96.51
	5	0.00	0.13	1.35	49.52	41.92	2.36	95.29
	6	0.00	1.22	0.74	81.91	5.10	1.33	90.30
	6	0.00	1.27	0.76	83.49	5.41	1.30	92.23
	7	0.00	0.12	1.66	50.01	41.77	2.55	96.11
	8	0.00	1.18	0.92	82.78	5.75	1.24	91.87
	9	0.00	1.21	0.81	82.66	5.17	1.42	91.28
	9	0.00	1.11	0.78	82.50	5.89	1.56	91.83
	10	0.00	0.10	1.64	50.17	42.27	2.35	96.53
	11	0.00	0.08	1.36	49.68	41.58	2.21	94.91
	12	0.00	1.23	0.75	82.26	5.87	1.52	91.62
	12	0.00	1.26	0.73	81.70	5.55	1.37	90.61
	13	0.00	0.13	1.42	49.39	40.93	2.47	94.34
	14	0.00	0.08	1.54	48.65	42.35	2.29	94.91
	15	0.00	1.33	0.83	82.29	5.45	1.53	91.44
	16	0.00	1.18	0.69	81.86	6.10	1.24	91.07
	16	0.00	1.25	0.72	83.41	5.89	1.23	92.50
	17	0.00	0.11	1.46	47.92	42.51	2.50	94.50
	17	0.00	0.11	1.61	48.99	42.27	2.70	95.68
R18-16								
	1	0.01	1.42	0.83	84.67	6.80	1.40	95.13
	2	0.00	0.10	1.60	51.80	43.56	2.15	99.21
	2	0.00	0.09	1.51	50.87	43.08	1.93	97.48
	3	0.00	0.09	1.51	51.67	43.29	1.84	98.40
	3	0.00	0.10	1.73	52.35	42.39	2.68	99.25
	4	0.01	1.42	0.75	83.55	6.05	1.26	93.04
	4	0.07	1.33	0.72	84.08	6.22	1.12	93.54
	5	0.03	1.13	1.00	86.44	5.96	1.59	96.15
	5	0.05	1.16	0.85	84.94	5.69	1.64	94.33
	6	0.00	0.08	1.70	52.21	41.67	2.30	97.96
	6	0.00	0.11	1.49	52.45	41.55	2.29	97.89
	7	0.12	1.17	1.02	84.06	5.92	1.52	93.81
	7	0.11	1.10	1.16	85.50	5.69	1.65	95.21
	8	0.00	0.07	1.67	52.17	41.41	2.19	97.51
	9	0.00	0.08	1.52	51.88	43.03	2.06	98.57
	10p1	0.01	1.31	0.29	83.42	5.71	0.29	91.03
	10p1	0.01	1.07	0.23	82.99	5.46	0.17	89.93

Appendix 4. Continued.

MAGNETITE AND ILMENITE ANALYSES

Rainier Mesa Member

Sample #	Grain	Cr_2O_3	Al_2O_3	MgO	FeO	TiO_2	MnO	Total
R18-16, Continued								
	11p1	0.00	0.16	1.78	51.10	43.39	2.21	98.64
	12	0.00	1.33	0.91	86.07	5.97	1.39	95.67
	12	0.04	1.36	0.94	85.24	6.27	1.54	95.39
	13	0.04	1.23	0.75	83.02	6.01	0.93	91.98
	13	0.00	1.12	0.25	81.76	7.21	0.50	90.84
	14	0.00	0.10	1.44	52.94	41.97	2.44	98.89
	15	0.05	1.26	0.90	85.82	6.24	1.46	95.73
	16	0.00	0.12	1.62	51.65	42.86	2.16	98.41
R21-1, Run #1								
	1	0.02	1.77	1.44	80.20	6.72	0.99	91.14
	1	0.04	1.84	1.47	81.42	5.03	1.29	91.09
	1	0.04	1.72	1.27	81.25	5.24	1.06	90.58
	2	0.07	1.70	1.40	84.88	4.93	1.08	94.06
	2	0.04	1.72	1.55	82.74	4.89	1.33	92.27
	3	0.00	0.19	2.41	53.47	26.96	1.24	84.27
	3	0.00	0.18	2.31	53.93	26.20	1.19	83.81
	4	0.00	0.16	2.18	54.78	25.64	1.15	83.91
R21-1, Run #2								
	1	0.02	1.67	1.38	80.17	9.65	1.56	94.45
	1	0.03	1.56	1.27	81.01	7.48	1.14	92.49
	1	0.00	1.66	1.48	81.51	7.60	1.33	93.58
	2	0.02	1.87	1.33	77.55	9.45	1.55	91.77
	2	0.05	1.70	1.10	78.59	9.22	1.30	91.96
	3	0.00	0.24	1.69	55.68	38.92	1.00	97.53
	4	0.04	1.57	0.49	77.14	8.55	0.69	88.48
	5	0.00	0.18	1.83	54.92	40.27	1.28	98.48
	5	0.00	0.29	2.23	54.83	38.98	1.47	97.80
	6	0.01	1.65	1.31	81.11	8.05	1.15	93.28
	7	0.00	0.23	2.11	53.12	40.02	1.26	96.74
	8	0.02	1.62	1.11	79.95	7.35	1.13	91.18
	9	0.04	1.62	1.15	77.96	7.98	1.07	89.82
	10	0.00	0.20	2.27	53.79	39.16	1.38	96.80
	10	0.00	0.18	2.16	52.09	39.35	0.70	94.48
	11	0.03	1.55	1.11	81.34	7.97	1.17	93.17
	11	0.03	1.59	1.09	81.20	8.32	1.12	93.35
	12	0.00	0.22	2.14	54.72	39.39	1.16	97.63
	12	0.00	0.23	1.44	55.47	37.55	0.98	95.67
	13	0.04	1.57	1.39	82.69	8.24	1.36	95.29
	13	0.04	1.60	1.28	84.07	6.76	1.27	95.02
	13	0.03	1.58	1.35	83.18	6.77	1.31	94.22

Appendix 4. Continued.

MAGNETITE AND ILMENITE ANALYSES

Rainier Mesa Member

Sample	Grain #	Cr_2O_3	Al_2O_3	MgO	FeO	TiO_2	MnO	Total
R21-5								
	1	0.00	1.29	1.13	82.75	7.31	1.32	93.80
	1	0.00	1.38	1.14	84.03	4.65	1.28	92.48
	2	0.00	1.29	0.39	81.31	4.31	0.53	87.83
	2	0.00	1.26	0.15	78.06	6.23	0.29	85.99
	3	0.00	1.30	1.11	84.22	4.52	1.37	92.52
	3	0.00	1.32	0.25	79.44	4.08	0.34	85.43
	3	0.00	1.46	1.17	84.37	2.81	1.24	91.05
	4	0.00	0.10	1.84	53.86	37.16	1.31	94.27
	4	0.00	0.15	1.89	54.92	37.31	1.32	95.59
	5	0.00	1.32	0.38	77.54	5.85	0.59	85.68
	5	0.01	1.34	1.19	82.49	5.65	1.17	91.85
	5	0.00	1.27	0.55	79.99	5.28	0.74	87.83
	6	0.00	0.17	1.93	53.73	38.23	1.48	95.54
	7	0.00	0.12	1.85	52.33	39.49	1.44	95.23
	7	0.00	0.14	1.17	52.21	39.23	0.85	93.60
	8	0.00	0.17	1.72	55.55	37.08	1.25	95.77
	9	0.00	0.13	1.70	52.46	39.25	1.26	94.80
	9	0.00	0.15	1.65	52.74	37.41	1.27	93.22
	10	0.00	1.19	1.25	79.89	8.72	1.49	92.54
	10	0.00	1.39	1.31	83.61	6.50	1.28	94.09
	10	0.00	1.37	1.19	82.31	5.92	1.26	92.05
	11p1	0.00	0.17	1.76	54.91	37.93	1.27	96.04
	11p1	0.00	0.18	1.88	54.90	37.87	1.38	96.21
	12p1	0.00	1.42	1.04	81.33	5.50	1.04	90.33
	12p1	0.00	1.27	1.07	81.41	6.40	1.16	91.31
R21-13								
	1	0.01	3.53	2.42	76.70	9.15	0.88	92.70
	1	0.00	2.84	1.81	78.01	9.00	0.61	92.27
	2	0.00	3.40	2.30	76.60	9.50	0.70	92.50
	2	0.00	3.22	2.09	76.06	8.75	0.54	90.67
	3	0.01	2.64	3.02	75.30	7.88	1.32	90.18
	3	0.00	2.61	1.82	76.58	8.59	0.56	90.16
	4	0.00	0.25	2.76	50.38	40.11	0.78	94.30
	4	0.00	0.39	2.15	57.17	34.06	0.42	94.20
	5	0.00	0.26	3.06	53.56	35.61	0.79	93.28
	5	0.00	0.29	2.76	50.31	40.47	0.83	94.65
	6	0.00	0.32	2.59	53.17	38.00	0.67	94.75
	6	0.00	0.38	2.93	55.70	35.20	0.71	94.92
	6	0.00	0.30	3.11	52.18	37.39	0.79	93.76

Appendix 4. Continued.

MAGNETITE AND ILMENITE ANALYSES

Rainier Mesa Member

Sample	Grain #	Cr_2O_3	Al_2O_3	MgO	FeO	TiO_2	MnO	Total
R23-13								
	1	0.00	1.40	0.99	81.35	8.64	1.32	93.70
	1	0.00	1.42	0.98	82.40	6.98	1.41	93.19
	2	0.00	2.04	1.52	79.77	10.21	0.81	94.35
	2	0.00	2.37	1.26	79.58	8.80	0.81	92.82
	3	0.00	1.75	1.07	79.65	9.48	1.03	92.98
	3	0.00	2.25	1.11	78.62	7.88	1.13	90.99
	4	0.00	1.77	1.09	80.03	8.60	1.22	92.71
	4	0.00	1.93	1.23	81.16	8.41	1.27	94.00
	4	0.00	1.94	1.00	71.83	7.78	1.36	83.91
	5	0.00	0.19	1.92	53.26	37.88	1.27	94.52
	5	0.00	0.25	1.86	53.12	39.08	1.18	95.49
	6	0.00	0.15	2.31	51.06	40.22	1.94	95.68
	7	0.00	0.20	2.11	51.10	37.97	1.34	92.72
	7	0.00	0.22	1.65	51.86	39.99	1.17	94.89
	8	0.00	0.17	1.95	54.78	35.14	1.38	93.42
	9	0.00	2.12	1.23	80.89	8.22	1.29	93.75
	10	0.00	1.81	1.15	79.93	8.89	1.21	92.99
	10	0.04	1.85	1.21	81.54	8.31	1.35	94.30
	11	0.00	0.21	1.69	50.52	39.65	2.00	94.07
	11	0.00	0.18	2.13	51.85	39.34	1.75	95.25
	12	0.00	0.26	2.31	49.31	40.54	1.46	93.88
	13	0.01	1.76	1.13	80.01	8.96	1.02	92.89
	13	0.00	1.94	1.20	78.94	8.81	1.21	92.10
	14	0.00	0.19	2.51	52.91	37.99	2.34	95.94
	15	0.04	1.91	1.61	78.05	9.64	1.14	92.39
	15	0.03	2.27	1.59	80.30	10.04	1.19	95.42
	16	0.00	0.26	2.11	51.13	39.70	1.22	94.42
	16	0.00	0.23	2.36	51.48	39.86	1.19	95.12
	17	0.02	1.76	1.48	80.52	8.56	1.17	93.51
	17	0.00	1.02	1.31	81.94	9.28	1.54	95.09
	18	0.00	0.23	1.99	55.31	38.77	1.11	97.41
	18	0.00	0.22	1.88	55.77	37.66	1.05	96.58
	19	0.01	1.84	1.47	81.39	8.46	1.36	94.53
	19	0.00	1.59	1.14	79.13	8.79	1.05	91.70
	20	0.00	0.22	2.19	52.52	41.14	1.45	97.52
	20	0.00	0.20	1.34	54.65	37.80	0.86	94.85

Appendix 4. Continued.

MAGNETITE AND ILMENITE ANALYSES

Rainier Mesa Member

Sample #	Grain	Cr_2O_3	Al_2O_3	MgO	FeO	TiO_2	MnO	Total
R23-24								
	1	0.00	3.13	1.96	74.61	10.67	0.62	90.99
	1	0.00	2.68	2.01	77.54	8.64	0.77	91.64
	2	0.02	2.74	2.35	75.05	8.78	0.91	89.85
	2	0.01	2.78	2.32	78.02	9.05	0.81	92.99
	3	0.00	3.44	2.20	76.07	9.39	0.71	91.81
	3	0.00	2.58	2.17	77.63	8.69	0.86	91.93
	4	0.04	1.85	1.61	77.91	9.04	0.87	91.32
	4	0.00	1.64	1.73	78.05	8.89	0.88	91.19
	5	0.00	2.73	2.23	77.59	9.49	0.84	92.88
	5	0.00	2.76	2.52	75.68	9.19	1.87	92.02
	6	0.00	0.43	2.50	51.18	38.32	0.52	92.95
	6	0.00	0.40	2.79	51.18	38.30	0.66	93.33
	7	0.00	1.63	1.61	78.69	9.26	0.84	92.03
	7	0.00	2.02	1.67	78.35	9.38	0.82	92.24
	8	0.00	0.32	2.38	50.23	38.61	0.63	92.17
	8	0.00	0.39	2.45	52.19	38.82	0.62	94.47
	9	0.00	0.32	2.40	52.29	38.10	0.61	93.72
	10	0.00	0.40	2.61	50.87	38.81	0.61	93.30
	10	0.00	0.33	2.73	51.77	36.90	0.60	92.33
	11	0.00	0.41	2.73	52.35	39.42	0.58	95.49
	11	0.00	0.41	2.62	51.44	39.60	0.69	94.76
	12	0.03	3.16	2.31	75.10	10.65	0.80	92.05
	12	0.00	3.09	2.16	76.52	9.49	0.69	91.95
	13	0.00	3.27	2.20	72.19	11.39	0.82	89.87
	14	0.00	3.31	2.31	76.05	9.31	0.82	91.80
	15	0.00	2.93	2.16	74.51	9.68	0.99	90.27
	15	0.00	2.75	2.06	75.82	9.06	0.95	90.64
	16	0.01	2.83	2.21	75.58	9.19	0.93	90.75
	17	0.00	0.39	2.75	52.00	38.31	0.63	94.08
	17	0.00	0.35	2.07	50.38	37.79	0.43	91.02
	18	0.00	2.56	2.27	74.51	9.41	1.03	89.78
	18	0.00	2.39	2.23	75.65	9.81	0.94	91.02
	19	0.00	0.33	2.34	51.60	38.34	0.62	93.23
	19	0.00	0.31	2.82	52.65	36.83	0.67	93.28
	20	0.00	2.42	2.11	75.82	9.38	0.83	90.56
	20	0.02	2.63	2.33	76.39	9.27	0.89	91.53
	21	0.00	0.39	2.76	51.49	38.52	0.55	93.71
	21	0.00	0.38	2.71	51.47	39.86	0.55	94.97
	22	0.00	0.27	2.94	50.49	39.37	0.73	93.80
	23	0.00	3.54	2.25	77.40	10.90	0.68	94.77
	23	0.00	2.98	1.69	79.50	9.32	0.53	94.04
	23	0.04	2.59	2.34	79.45	9.63	0.98	95.05
	24	0.00	0.44	2.71	52.70	40.39	0.65	96.89

Appendix 4. Continued.

MAGNETITE AND ILMENITE ANALYSES

Rainier Mesa Member

Sample	Grain #	Cr_2O_3	Al_2O_3	MgO	FeO	TiO_2	MnO	Total
R23-24, Continued								
	24	0.00	0.41	2.61	52.12	40.90	0.54	96.58
R23-26								
	1	0.00	0.31	1.93	55.68	40.40	1.06	99.37
	1	0.00	0.32	2.08	54.19	40.15	1.00	97.74
	2	0.04	1.77	1.47	80.22	9.78	1.01	94.28
	2	0.04	1.81	1.67	80.89	9.90	1.21	95.51
	3	0.01	2.00	1.96	79.76	8.15	1.51	93.39
	3	0.03	1.58	1.52	79.15	8.79	1.45	92.52
	4	0.03	2.35	1.72	78.84	9.06	1.31	93.31
	4	0.00	2.58	1.80	79.77	7.92	1.25	93.32
	5	0.03	2.58	1.99	77.47	8.57	1.40	92.04
	5	0.03	2.16	1.62	78.59	9.97	1.38	93.76
	6	0.00	0.25	2.38	53.41	39.77	1.42	97.22
	6	0.00	0.28	1.65	55.35	38.82	0.97	97.07
	7	0.03	1.71	2.06	80.20	9.10	1.52	94.60
	7	0.00	1.87	1.58	77.76	9.31	1.12	91.64
	8	0.00	0.19	3.16	53.22	40.26	1.60	98.43
	8	0.00	0.20	2.71	53.90	38.32	1.28	96.42
	9	0.00	0.20	2.31	55.52	38.42	1.11	97.56
	9	0.00	0.17	2.35	55.86	38.33	1.11	97.83
	10	0.03	1.27	1.41	84.01	6.34	1.03	94.08
	10	0.03	1.36	1.39	85.21	5.87	1.02	94.88
	10	0.03	1.31	1.91	81.94	8.39	1.51	95.09
R23-27								
	1	0.02	2.64	1.78	79.92	9.86	0.71	94.94
	1	0.01	2.85	2.01	80.09	9.35	0.77	95.09
	2	0.05	2.28	2.05	80.10	9.62	0.89	94.98
	2	0.02	3.07	2.26	78.73	9.51	0.87	94.45
	3	0.02	2.78	2.27	79.24	9.55	0.85	94.71
	3	0.05	2.99	2.24	79.14	10.24	0.75	95.40
	4	0.01	0.42	2.53	53.45	39.15	0.55	96.11
	4	0.00	0.32	2.54	53.86	39.43	0.66	96.80
	5	0.00	0.35	2.39	53.44	39.13	0.61	95.93
	5	0.00	0.36	2.64	54.03	39.27	0.65	96.95
	6	0.00	0.37	2.27	54.46	38.74	0.51	96.36
	6	0.00	0.36	2.52	55.40	38.76	0.89	97.94
	7	0.01	2.47	1.71	80.25	8.82	0.96	94.22
	7	0.03	2.60	2.16	79.75	9.34	0.81	94.69

Appendix 4. Continued.

MAGNETITE AND ILMENITE ANALYSES

Ammonia Tanks Member

Sample	Grain #	Cr_2O_3	Al_2O_3	MgO	FeO	TiO_2	MnO	Total
A5-3								
	1	0.02	0.65	0.68	84.82	5.44	3.03	94.64
	2	0.01	0.62	0.65	82.23	5.21	2.65	91.37
	3	0.03	0.63	0.66	84.15	4.75	2.67	92.89
	4	0.01	0.69	0.70	84.46	4.77	2.95	93.58
	5	0.05	0.22	0.38	84.16	0.23	2.45	87.49
	6	0.04	0.59	0.41	83.21	4.87	2.69	91.81
	7	0.03	0.69	0.69	83.40	4.79	2.56	92.16
	8	0.02	0.61	0.67	85.56	4.65	2.95	94.46
	9	0.02	0.66	0.77	82.35	4.83	2.92	91.55
	10	0.02	0.67	0.71	85.35	4.92	2.00	93.67
	10	0.03	0.65	0.63	84.55	5.26	2.36	93.48
	11	0.00	0.06	1.53	43.91	46.01	6.58	98.09
A5-35								
	1	0.00	0.77	0.89	83.35	6.34	1.91	93.26
	1	0.00	0.69	0.82	83.87	5.98	2.02	93.38
	2pl	0.00	0.06	1.73	49.97	41.38	3.31	96.45
	2pl	0.01	0.77	0.69	85.14	6.11	1.73	94.45
	3	0.00	0.00	1.73	50.59	42.33	3.06	97.71
	4	0.00	0.60	0.47	84.36	6.12	1.56	93.11
	5	0.00	0.66	0.79	84.52	5.76	1.98	93.71
	6	0.00	0.00	1.56	50.87	41.30	3.22	96.95
	7	0.00	0.03	1.70	49.07	41.62	4.10	96.52
	8	0.00	0.78	0.78	83.83	6.15	1.87	93.41
	9	0.00	0.77	0.62	84.13	6.28	1.48	93.28
	10	0.00	0.00	1.60	50.83	42.13	3.29	97.85
	11	0.00	0.02	1.63	50.21	42.55	3.23	97.64
	12	0.00	0.00	0.12	86.66	0.05	0.47	87.30
	13	0.00	0.06	1.71	49.64	41.59	3.16	96.16
	14	0.00	0.82	0.77	83.07	5.86	1.90	92.42
A5-58								
	1	0.00	0.10	2.60	43.62	48.58	3.41	98.31
	2	0.00	0.09	3.01	45.31	43.09	4.29	95.79
	3pl	0.03	1.27	1.12	79.54	8.39	2.08	92.43
	4pl	0.00	0.12	1.79	46.53	44.00	2.33	94.77
	3pl	0.04	1.08	1.26	79.55	7.98	2.15	92.06
	3pl	0.03	1.23	0.98	79.56	8.29	1.72	91.81
	3pl	0.06	1.03	1.20	81.70	7.64	2.09	93.72
	5	0.05	1.33	1.30	77.74	8.21	2.81	91.44
	6	0.00	0.12	2.93	43.72	43.40	4.14	94.31
	7	0.00	0.08	2.48	47.30	42.58	3.75	96.19
	8	0.00	0.09	1.94	46.24	42.79	3.13	94.19

Appendix 4. Continued.

MAGNETITE AND ILMENITE ANALYSES

Ammonia Tanks Member

Sample	Grain #	Cr_2O_3	Al_2O_3	MgO	FeO	TiO_2	MnO	Total
A5-58, Continued								
	8p2	0.00	0.10	2.61	44.77	43.74	3.45	94.67
	9p2	0.03	0.89	0.93	78.17	8.06	1.84	89.92
	9p2	0.03	1.05	1.12	79.53	8.15	2.08	91.96
	9p2	0.07	1.19	1.24	79.53	7.79	2.19	92.01
	9p2	0.06	1.22	1.33	79.25	8.26	2.28	92.40
	8p2	0.00	0.13	2.78	45.09	44.13	3.94	96.07
	10p3	0.00	0.11	1.71	47.80	42.37	2.51	94.50
	11p3	0.05	1.16	1.10	77.13	8.53	2.16	90.13
	11p3	0.06	0.85	0.76	80.41	8.04	1.61	91.73
	11p3	0.06	0.97	1.03	78.94	7.84	2.15	90.99
	11p3	0.06	0.84	0.90	79.82	7.85	2.25	91.72
	12	0.03	0.94	1.18	81.19	7.18	2.12	92.64
	12	0.05	0.94	1.05	80.21	7.97	2.27	92.49
	12	0.07	1.01	1.24	78.98	7.92	2.20	91.42
A5-71								
	1	0.01	0.18	3.46	45.62	43.96	2.91	96.14
	2	0.03	0.17	3.41	44.20	44.83	3.00	95.64
	3	0.01	0.15	2.39	44.49	43.96	2.37	93.37
	4	0.10	1.63	1.48	79.18	7.98	1.83	92.20
	4	0.06	1.51	1.83	78.34	8.12	1.73	91.59
	4	0.09	1.30	1.79	78.57	7.95	1.94	91.64
	5	0.07	2.04	2.31	75.59	11.38	1.12	92.51
	5	0.06	2.29	2.52	75.57	9.90	1.24	91.58
	6	0.04	0.25	3.12	47.56	41.97	1.58	94.52
	6	0.02	0.24	2.90	47.17	41.27	1.62	93.22
	7	0.01	0.12	3.14	45.63	42.00	3.10	94.00
	8	0.08	1.87	2.24	73.66	10.21	1.73	89.79
	8	0.09	1.66	2.21	75.43	12.10	1.76	93.25
	9	0.09	1.44	1.43	78.34	8.23	1.98	91.51
	9	0.07	1.88	1.81	79.20	8.57	2.08	93.61
	9	0.06	1.85	1.85	79.43	6.89	2.09	92.17
	10	0.01	0.09	2.07	48.33	41.28	2.15	93.93
	11	0.01	0.14	3.47	45.17	44.23	3.01	96.03
	12	0.08	1.64	1.72	74.10	11.09	2.09	90.72
	12	0.07	1.41	1.77	76.19	10.27	2.04	91.75
	12	0.07	1.58	1.64	75.17	12.09	1.77	92.32
	13	0.09	1.39	1.68	75.12	10.41	1.98	90.67
	13	0.08	1.35	1.53	73.50	14.18	1.76	92.40

Appendix 4. Continued.

MAGNETITE AND ILMENITE ANALYSES

Ammonia Tanks Member

Sample #	Grain	Cr_2O_3	Al_2O_3	MgO	FeO	TiO_2	MnO	Total
A5-72								
	1	0.06	1.94	2.25	72.61	19.58	1.28	97.72
	1	0.05	1.48	2.46	82.90	4.95	1.64	93.48
	1	0.06	2.21	2.29	74.39	13.37	1.56	93.88
	2	0.05	2.43	2.55	76.01	10.24	1.60	92.88
	2	0.08	2.27	2.58	76.32	11.78	1.57	94.60
	2	0.04	1.94	2.41	75.66	11.70	1.56	93.31
	3	0.03	2.29	2.61	76.79	11.06	1.38	94.16
	3	0.06	2.13	2.69	77.85	11.81	1.26	95.80
	4	0.03	0.29	0.07	86.06	0.00	0.42	86.87
	4	0.03	0.09	0.22	87.31	0.00	0.10	87.75
	5	0.00	0.24	3.07	49.02	41.88	1.36	95.57
	5	0.00	0.27	3.10	48.42	42.30	1.31	95.40
	6	0.01	0.34	0.16	80.05	0.59	0.69	81.84
	7	0.00	0.23	3.59	46.87	42.38	1.48	94.55
	7	0.00	0.25	3.53	47.69	42.71	1.37	95.55
	8	0.03	2.14	2.34	75.04	11.51	1.36	92.42
A5-75								
	1	0.03	4.45	3.51	77.04	7.86	0.92	93.81
	1	0.02	3.26	3.22	78.37	7.01	0.89	92.77
	1	0.00	3.72	3.31	76.11	7.59	0.93	91.66
	2	0.03	3.32	3.00	77.56	7.41	0.78	92.10
	2	0.06	3.22	3.14	77.86	7.62	0.76	92.66
	2	0.04	3.62	3.32	76.02	8.18	0.74	91.92
	3	0.04	4.01	3.17	77.84	7.55	0.65	93.26
	3	0.06	2.15	2.37	79.49	6.70	0.80	91.57
	4	0.06	2.48	2.86	81.57	5.31	0.79	93.07
	4	0.04	4.49	3.60	74.81	10.77	0.74	94.45
	4	0.05	3.76	3.62	86.22	1.27	0.85	95.77
	4	0.06	0.77	2.10	86.36	0.08	0.55	89.92
	4	0.03	1.58	2.22	81.63	3.05	1.02	89.53
	5	0.03	0.10	0.09	88.48	0.02	0.24	88.96
	5	0.02	0.00	0.08	90.53	0.63	0.20	91.46
	6	0.01	0.27	0.06	87.35	0.05	0.26	88.00
	6	0.03	0.22	0.00	88.29	0.06	0.00	88.60

Appendix 4. Continued.

MAGNETITE AND ILMENITE ANALYSES -- University of Michigan

Ammonia Tanks Member

Sample	Grain #	FeO	TiO_2	Al_2O_3	MnO	MgO	CaO	Cr_2O_3	SiO_2	Total
A4-70	1	48.068	41.159	0.091	3.380	2.122	0.041	0.000	0.000	94.861
	1	49.814	35.346	0.066	5.938	3.414	0.011	0.022	0.009	94.620
	1	47.892	42.242	0.079	2.634	1.792	0.064	0.015	0.015	94.734
	2	49.115	41.219	0.064	2.314	1.723	0.000	0.000	0.009	94.444
	2	47.044	44.812	0.064	1.486	1.101	0.020	0.000	0.000	94.527
	3	47.070	41.997	0.066	3.275	1.807	0.000	0.000	0.000	94.214
	3	47.999	42.407	0.085	2.881	1.552	0.000	0.001	0.009	94.933
	4	47.614	38.282	0.070	5.715	3.527	0.000	0.000	0.000	95.207
	4	55.189	35.343	0.094	1.988	1.036	0.000	0.009	0.002	93.662
	5	42.357	42.804	0.057	6.747	3.553	0.000	0.000	0.000	95.518
	5	43.797	43.713	0.072	4.377	2.669	0.006	0.000	0.002	94.636
	6	50.660	34.996	0.057	5.925	3.520	0.000	0.000	0.006	95.165
	7p1	39.712	43.593	0.030	7.835	3.523	0.015	0.000	0.000	94.710
	7p1	46.969	39.274	0.089	5.479	2.931	0.000	0.026	0.002	94.771
	8p1	84.189	5.051	0.773	1.641	0.746	0.018	0.020	0.028	92.466
	8p1	82.767	6.449	0.761	1.073	0.416	0.059	0.000	0.039	91.564
	9p2	39.194	48.696	0.064	5.325	3.293	0.017	0.003	0.000	96.591
	9p2	36.077	51.952	0.077	5.414	2.752	0.010	0.000	0.011	96.293
	10p2	85.718	1.718	1.221	1.961	1.098	0.021	0.022	0.071	91.829
	10p2	84.580	0.644	1.262	4.706	2.099	0.020	0.026	0.021	93.359
	11p3	46.412	41.853	0.070	4.344	2.475	0.021	0.000	0.006	95.182
	11p3	49.375	40.339	0.083	2.870	1.821	0.020	0.006	0.015	94.528
	12p3	82.548	6.761	0.671	1.513	0.668	0.011	0.000	0.009	92.181
	12p3	81.410	7.003	0.875	1.747	0.653	0.000	0.042	0.049	91.779
	13	82.211	7.675	0.675	1.169	0.507	0.014	0.029	0.049	92.329
	13	80.521	6.831	1.564	2.292	1.005	0.084	0.037	0.045	92.378

Appendix 4. Continued.

MAGNETITE AND ILMENITE ANALYSES -- University of Michigan

Ammonia Tanks Member

Sample	Grain #	FeO	TiO_2	Al_2O_3	MnO	MgO	CaO	Cr_2O_3	SiO_2	Total
A5-9	1	49.333	42.814	0.102	3.874	1.729	0.022	0.023	0.017	97.915
	1	49.545	42.859	0.085	3.954	1.779	0.000	0.001	0.000	98.223
	1	48.660	42.551	0.108	4.091	1.723	0.034	0.000	0.045	97.210
	2p1	83.395	6.912	1.094	1.424	0.812	0.085	0.000	0.053	93.777
	2p1	83.132	6.976	1.049	1.839	0.904	0.074	0.023	0.051	94.048
	3p1	49.277	42.517	0.096	3.295	1.958	0.116	0.006	0.019	97.285
	3p1	50.177	42.819	0.111	3.333	1.827	0.077	0.000	0.000	98.344
	3p1	49.370	42.706	0.108	3.259	1.791	0.000	0.015	0.015	97.263
	4p2	49.755	43.061	0.081	3.087	1.874	0.194	0.000	0.000	98.052
	4p2	49.703	42.604	0.117	3.096	2.129	0.000	0.000	0.017	97.667
	5p2	82.480	6.792	1.047	1.843	1.058	0.000	0.013	0.021	93.254
	5p2	83.137	6.667	1.083	1.872	1.013	0.024	0.004	0.036	93.837
	6p3	49.708	42.519	0.085	3.069	1.953	0.515	0.009	0.021	97.880
	6p3	49.671	42.000	0.108	3.032	1.587	0.057	0.001	0.092	96.548
	7p3	81.774	6.591	1.168	1.424	0.955	0.008	0.044	0.030	91.993
	7p3	83.971	6.779	1.113	1.392	0.940	0.042	0.020	0.034	94.292
	7p3	83.357	6.649	1.007	2.003	1.048	0.071	0.000	0.009	94.144
	8p4	50.508	42.577	0.104	3.302	2.003	0.146	0.010	0.015	98.665
	8p4	49.365	42.809	0.106	3.087	1.834	0.042	0.006	0.000	97.249
	9p4	83.270	6.996	1.043	1.804	0.812	0.021	0.007	0.047	94.000
	9p4	83.776	6.859	0.969	2.267	0.672	0.024	0.034	0.034	94.634
A5-29	1	85.206	0.000	0.045	2.346	0.194	0.041	0.019	3.673	91.524
	1	87.639	0.058	0.121	1.840	0.162	0.022	0.000	2.723	92.566
	1	82.649	5.253	1.878	3.361	0.474	0.000	0.018	0.000	93.632
	1	84.034	5.268	1.808	2.735	0.630	0.007	0.007	0.017	94.506
	1	83.081	5.349	1.778	2.532	0.501	0.000	0.000	0.000	93.241
	2	83.221	5.039	1.723	2.111	0.403	0.673	0.028	0.024	93.222
	2	83.046	5.161	1.908	2.477	0.594	0.000	0.016	0.009	93.210
	3	83.927	5.201	1.959	2.712	0.681	0.014	0.000	0.002	94.497
	3	83.538	5.233	1.886	2.821	0.625	0.006	0.000	0.009	94.117
	4	45.419	45.049	0.151	5.923	1.413	0.000	0.015	0.034	98.004
	5	45.408	45.294	0.123	5.671	1.404	0.000	0.012	0.032	97.944
	6	44.989	46.068	0.100	6.129	1.373	0.000	0.000	0.030	98.690
	7	83.841	5.061	1.986	2.861	0.685	0.000	0.034	0.056	94.523
	7	83.794	5.154	1.880	2.971	0.610	0.000	0.022	0.058	94.489

Appendix 4. Continued.

MAGNETITE AND ILMENITE ANALYSES -- University of Michigan

Ammonia Tanks Member

Sample	Grain #	FeO	TiO_2	Al_2O_3	MnO	MgO	CaO	Cr_2O_3	SiO_2	Total
A5-30	1	50.825	41.953	0.285	1.650	3.581	0.034	0.022	0.000	98.351
	1	51.071	41.757	0.302	1.663	3.480	0.032	0.013	0.024	98.342
	2p1	78.661	9.380	2.258	1.387	2.255	0.049	0.041	0.043	94.072
	2p1	78.480	9.728	2.054	1.617	2.267	0.122	0.015	0.041	94.323
	3p1	50.757	40.969	0.274	1.432	3.494	0.115	0.013	0.000	97.053
	3p1	50.171	40.892	0.278	1.540	3.706	0.147	0.051	0.002	96.788
	4p2	78.040	10.330	1.965	1.281	1.491	0.029	0.047	0.047	93.230
	4p2	79.484	8.741	2.033	1.451	2.101	0.034	0.061	0.060	93.965
	5p2	50.505	41.171	0.251	1.538	3.024	0.011	0.001	0.000	96.502
	5p2	50.171	41.118	0.249	1.507	3.348	0.000	0.042	0.026	96.461
	6p3	77.689	9.720	2.022	1.611	2.394	0.025	0.050	0.060	93.571
	6p3	78.606	9.970	1.984	1.512	2.369	0.017	0.038	0.045	94.542
	7p3	51.026	40.427	0.319	1.429	3.714	0.011	0.047	0.015	96.988
	7p3	51.055	40.691	0.316	1.466	3.649	0.059	0.013	0.006	97.255
	8	77.949	9.938	2.139	1.641	2.787	0.024	0.077	0.068	94.624
	8	78.663	10.012	2.046	1.383	2.268	0.007	0.037	0.047	94.463
A5-35	1p1	49.919	42.546	0.087	3.170	1.726	0.000	0.000	0.000	97.448
	1p1	49.482	43.041	0.085	3.077	1.743	0.000	0.004	0.000	97.432
	2p1	83.508	5.953	0.905	1.826	0.774	0.000	0.048	0.032	93.047
	2p1	83.768	5.928	0.913	1.626	0.804	0.000	0.013	0.047	93.099
	3p2	84.740	5.840	0.903	1.724	0.723	0.000	0.000	0.026	93.956
	3p2	84.738	5.741	0.886	1.757	0.822	0.003	0.020	0.026	93.994
	4p2	49.295	42.557	0.085	3.285	1.764	0.000	0.009	0.000	96.995
	4p2	49.531	42.684	0.093	3.364	1.898	0.000	0.000	0.011	97.580
	5p3	49.514	42.944	0.083	3.267	1.746	0.000	0.000	0.000	97.554
	5p3	49.878	42.908	0.104	3.127	1.743	0.000	0.023	0.002	97.785
	5p3	49.418	42.762	0.100	3.280	1.713	0.000	0.000	0.002	97.275
	6p3	84.272	6.217	0.905	1.429	0.650	0.020	0.038	0.244	93.775
	6p3	84.307	5.935	0.905	1.491	0.612	0.003	0.031	0.036	93.320
	7p4	84.375	5.922	0.905	1.463	0.794	0.000	0.037	0.013	93.508
	7p4	83.289	5.950	0.892	1.734	0.536	0.024	0.016	0.002	92.443
	8p4	49.068	42.924	0.077	3.401	1.661	0.105	0.000	0.000	97.237
	8p4	49.428	42.659	0.085	3.222	1.733	0.007	0.000	0.000	97.133

Appendix 4. Continued.

MAGNETITE AND ILMENITE ANALYSES -- University of Michigan

Ammonia Tanks Member

Sample	Grain #	FeO	TiO_2	Al_2O_3	MnO	MgO	CaO	Cr_2O_3	SiO_2	Total
A5-37	1p1	45.590	45.518	0.191	5.972	1.333	0.000	0.000	0.000	98.604
	2p1	84.136	5.086	1.818	2.850	0.635	0.013	0.019	0.017	94.573
	2p1	83.283	5.024	1.931	3.037	0.635	0.004	0.031	0.024	93.968
	3	83.778	5.088	1.793	2.939	0.635	0.001	0.000	0.017	94.251
	3	83.814	5.029	1.880	2.925	0.607	0.059	0.000	0.011	94.324
	4p2	44.638	44.334	0.134	7.826	1.030	0.029	0.000	0.002	97.993
	4p2	45.226	43.773	0.176	7.182	1.066	0.031	0.000	0.017	97.471
	5p2	88.317	0.132	0.093	1.036	0.393	0.045	0.047	2.725	92.787
	5p2	89.301	0.267	0.136	0.687	0.290	0.036	0.010	2.375	93.102
A5-63	1	77.633	9.461	3.016	1.056	3.187	0.017	0.032	0.077	94.478
	2	78.341	9.650	3.057	1.023	3.349	0.000	0.053	0.075	95.548
	3	78.341	9.728	3.051	1.047	3.218	0.000	0.047	0.083	95.517
	4	77.516	9.543	3.034	1.021	3.298	0.011	0.018	0.088	94.529
A5-68	1p1	83.949	4.999	1.638	2.083	0.864	0.000	0.018	0.011	93.561
	1p1	82.475	7.218	2.470	1.548	0.804	0.000	0.000	0.006	94.521
	1p1	87.438	2.781	1.258	1.422	0.819	0.078	0.007	0.024	93.827
	2p1	43.125	45.863	0.197	4.474	1.764	0.028	0.000	0.019	95.471
	2p1	43.062	46.063	0.223	4.260	1.857	0.050	0.000	0.135	95.651
	3p2	81.329	6.961	2.214	2.542	0.867	0.000	0.000	0.000	93.914
	3p2	82.818	6.619	2.415	2.243	0.821	0.000	0.000	0.024	94.939
	4p2	40.374	45.078	0.268	7.259	2.860	0.000	0.000	0.000	95.839
	4p2	40.653	45.448	0.656	5.666	3.054	0.015	0.000	0.304	95.796
	5p3	79.305	7.945	3.626	1.998	0.915	0.000	0.000	0.019	93.808
	6p3	45.405	44.295	0.227	4.500	2.766	0.071	0.000	0.000	97.264
	6p3	45.921	43.735	0.314	4.160	2.466	0.010	0.020	0.000	96.626
	7p4	81.605	6.360	2.462	2.035	0.751	0.011	0.000	0.026	93.250
	7p4	83.018	5.768	2.441	2.018	0.635	0.038	0.000	0.032	93.950
	8p4	47.806	44.290	0.325	2.065	1.018	0.017	0.000	0.000	95.520
	8p4	50.644	42.204	0.291	1.623	0.864	0.000	0.000	0.000	95.625
	8p4	48.028	44.470	0.297	2.957	1.436	0.001	0.000	0.000	97.189
	9p4	82.038	7.226	2.991	1.799	0.738	0.014	0.000	0.034	94.839

Appendix 4. Continued.

MAGNETITE AND ILMENITE ANALYSES -- University of Michigan

Ammonia Tanks Member

Sample	Grain #	FeO	TiO_2	Al_2O_3	MnO	MgO	CaO	Cr_2O_3	SiO_2	Total
A5-69	1	79.070	5.555	4.023	1.393	4.318	0.025	0.056	0.092	94.530
	1	76.639	9.461	2.870	1.161	3.251	0.041	0.037	0.088	93.548
	2	75.739	9.611	3.263	0.983	3.399	0.194	0.031	0.066	93.287
	3	74.746	8.812	5.060	1.068	3.747	0.236	0.038	0.079	93.787
	4	79.964	6.734	2.804	1.047	3.069	0.007	0.069	0.077	93.771
	5	75.379	10.776	6.171	0.868	2.737	0.025	0.013	0.079	96.048
	6	73.601	10.694	12.476	0.974	3.628	0.018	0.013	0.068	101.472
	7	86.607	0.894	1.780	1.245	3.442	0.024	0.038	0.066	94.096
A5-75	1	69.106	17.882	9.980	1.016	2.986	0.000	0.019	0.068	101.057
	2	76.917	13.825	1.236	0.919	2.018	0.011	0.023	0.083	95.033
A5-79	1	78.720	9.761	1.606	2.453	0.519	0.024	0.041	0.045	93.169
	1	79.547	8.232	2.216	2.171	0.617	0.034	0.045	0.077	92.938
	2	81.601	4.597	2.411	3.454	0.799	0.018	0.047	0.071	92.998
	2	84.361	2.809	2.260	3.493	0.748	0.028	0.000	0.058	93.756
	3	42.593	44.132	0.140	6.206	1.501	0.122	0.000	0.032	94.724
	3	40.300	45.226	0.147	7.940	1.782	0.155	0.000	0.028	95.579
	4	34.105	50.289	0.125	8.587	1.862	0.292	0.000	0.039	95.298
	4	36.437	45.463	0.098	11.076	2.462	0.067	0.000	0.015	95.619
	5	34.521	46.918	0.170	11.023	2.519	0.004	0.000	0.034	95.189
	5	43.176	46.370	0.166	3.868	0.894	0.032	0.016	0.028	94.550
	5	40.735	47.932	0.166	4.819	1.263	0.000	0.001	0.045	94.962

BIBLIOGRAPHY

BIBLIOGRAPHY

Andersen, D.J., and Lindsley, D.H., 1988, Internally consistent solution models for Fe-Mg-Mn-Ti oxides: Fe-Ti oxides: American Mineralogist, v. 73, p. 714-726.

Aramaki, S., and Lipman, P.W., 1965, Possible leaching of Na_2O during hydration of volcanic glasses: Japan Acadamy Proceedings, v. 41, p. 467-470.

Arth, J.G., 1976, Behavior of trace elements during magmatic processes: A summary of theoretical models and their applications: Journal of Research, U.S. Geological Survey, v. 4, p. 41-47.

Arth, J.G., and Hanson, G.N., 1975, Geochemistry and origin of the early Precambrian crust of northeastern Minnesota: Geochemica et Cosmochimica Acta, v. 39, p. 325-362.

Bacon, C.R., 1983, Eruptive history of Mount Mazama and Crater Lake caldera, Cascade Range, U.S.A.: Journal of Volcanology and Geothermal Research, v. 18, p. 57-115.

_____, 1986, Magmatic inclusions in silicic and intermediate volcanic rocks: Journal of Geophysical Research, v. 91, p. 6091-6112.

Bacon, C.R., and Druitt, T.H., 1988, Compositional evolution of the zoned calcalkaline magma chamber of Mount Mazama, Crater Lake, Oregon: Contributions to Mineralogy and Petrology, v. 98, p. 224-256.

Bacon, C.R., and Hirschmann, M.M., 1988, Mg/Mn partitioning as a test for equilibrium between coexisting Fe-Ti oxides: American Mineralogist, v. 73, p. 57-61.

Bacon, C.R., Hildreth, W., and Druitt, T.H., 1987, Partition coefficients determined from phenocryst and glass analyses of the climactic ejecta of Mount Mazama, Oregon: U.S. Geological Survey Open-File Report 87-589, 4 p.

Baker, B.H., and McBirney, A.R., 1985, Liquid fractionation. Part III: Geochemistry of zoned magmas and the compositional effects of liquid fractionation: Journal of Volcanology and Geothermal Research, v. 24, p. 55-81.

Ball, S.H., 1907, A geologic reconnaissance in southwestern Nevada and eastern California: U.S. Geological Survey Bulletin 308, 218 p.

Barth, T.F.W., 1934, Polymorphic phenomena and crystal structure: American Journal of Science, v. 5, p. 273.

_____, 1951, The feldspar geological thermometers: Neues Jahrb. Mineral. Abhandl., v. 82, p. 143-154.

Bence, A.E., and Albee, A.L., 1968, Empirical correction factors for the electron microanalysis of silicates and oxides: Journal of Geology, v. 76, p. 382-403.

Blake, S., 1981, Eruptions from zoned magma chambers: Journal Geological Society of London, v. 138, p. 281-287.

Blake, S., and Ivey, G.N., 1986, Magma-mixing and the dynamics of withdrawal from stratified reservoirs: Journal of Volcanology and Geothermal Research, v. 27, p. 153-178.

Bohlen, S.R., and Essene, E.J., 1977, Feldspar and oxide thermometry of granulites in the Adirondack Highlands: Contributions to Mineralogy and Petrology, v. 62, p. 153-169.

Bowen, N.L., 1928, The evolution of the igneous rocks: Princeton University Press, 334 p.

Brown, W.L., and Parsons, I., 1981, Towards a more practical two-feldspar geothermometer: Contributions to Mineralogy and Petrology, v. 76, p. 369-377.

Broxton, D.E., Vaniman, D., Caporuscio, F., Arney, B., and Heiken, G., 1982, Detailed petrographic descriptions and microprobe data for drill holes USW-G2 and UE25b-1H, Yucca Mountain, Nevada: Los Alamos National Laboratory Report, LA-9324-MS, 168 p.

Broxton, D.E., Byers, F.M., Jr., Warren, R.G., and Scott, R.B., 1985, Trends in phenocryst chemistry in the Timber Mountain-Oasis Valley volcanic field of southwest Nevada: Evidence for episodic injection of primitive magma into an evolving magma system: Geological Society of America Abstracts with Programs, v. 17, no. 6, p.

Broxton, D.E., Warren, R.G., Byers, F.M., Jr., and Scott, R.B., 1989, Chemical and mineralogic trends within the Timber Mountain-Oasis Valley caldera complex, Nevada: Evidence for multiple cycles of chemical evolution in a long-lived silicic magma system: Journal of Geophysical Research, v. 94, no. B5, p. 5961-5986.

Buddington, A.F., and Lindsley, D.H., 1964, Iron-titanium oxide minerals and synthetic equivalents: Journal of Petrology, v. 5, p. 310-357.

Byers, F.M., Jr., 1985, Petrochemical variation of Topopah Spring Tuff matrix with depth (stratigraphic level), drill hole USW G-4, Yucca Mountain, Nevada: Los Alamos National Laboratory Report, LA-10561-MS, 38 p.

Byers, F.M., Jr., Carr, W.J., Orkild, P.P., Quinlivan, W.D., and Sargent, K.A., 1976a, Volcanic suites and related cauldrons of Timber Mountain-Oasis Valley Caldera Complex, southern Nevada: U.S. Geological Survey Professional Paper 919, 70 p.

Byers, F.M., Jr., Carr, W.J., Christiansen, R.L., Lipman, P.W., Orkild, P.P, and Quinlivan, W.D., 1976b, Geologic map of the Timber Mountain caldera area, Nye County, Nevada: U.S. Geological Survey Miscellaneous Geologic Investigations Map I-891.

Byers, F.M., Jr., Orkild, P.P., Car, W.J., and Quinlivan, W.D., 1968, Timber Mountain Tuff, southern Nevada, and its relation to cauldron subsidence, in Nevada Test Site: Geological Society of America Memoir 110, p. 87-97.

Byers, F.M., Jr., and Moore, L.M., 1987, Petrographic variation of the Topopah Spring Tuff matrix within and between cored holes, Yucca Mountain, Nevada: Los Alamos National Laboratory Report, LA-10901-MS, 72 p.

Cameron, K.L., 1983, Bishop Tuff revisited: New rare-earth element data consistent with crystal fractionation: Science, v. 224, p. 1338-1340.

Carmichael, I.S.E., and Nicholls, J., 1967, Iron-titanium oxides and oxygen fugacities in volcanic rocks: Journal of Geophysical Research, v. 72, p. 4665-4687.

Carr, W.J., 1982, Volcano-tectonic history of Crater Flat, southwestern Nevada, as suggested by new evidence from drill hole USW VH-1: U.S. Geological Survey Open-File Report, 82-457, 23 p.

Carr, W.J., 1984, Regional structural setting of Yucca Mountain, southwestern Nevada, and late Cenozoic rates of tectonic activity in part of the southwestern Great Basin, Nevada and California, U.S. Geological Survey Open-File Report 84-854, 109 p.

Carr, W.J., Byers, F.M., Jr., and Orkild, P.P., 1986, Stratigraphic and volcano-tectonic relations of Crater Flat Tuff and some older volcanic units, Nye County, Nevada: U.S. Geological Survey Professional Paper 1323, 28 p.

Christiansen, R.L., Lipman, P.W., Orkild, P.P. and Byers, F.M., Jr., 1965, Structure of the Timber Mountain caldera, southern Nevada, and its relation to Basin-Range structure, in Geological Survey research, 1965,: U.S. Geological Survey Professional Paper 525-B, p. B43-B48.

Christiansen, R.L. and Noble, D.C., 1968, Geologic map of the Trail Ridge quadrangle, Nye County, Nevada: U.S. Geologic Survey Map, GQ-774.

Christiansen, R.L., Lipman, P.W., Carr, W.J., Byers, F.M., Jr., Orkild, P.P., and Sargent, K.A., 1977, Timber Mountain-Oasis Valley caldera complex of southern Nevada: Geological Society of America Bulletin, v. 88, p. 943-959.

Criss, J., 1980, Fundamental parameter calculations on a laboratory microcomputer. Advances in X-ray Analysis, v. 23, p. 93-97.

Cornwall, H.R., and Kleinhampl, F.J., 1964, Geology of Bullfrog quadrangle and ore depsits related to Bullfrog Hills caldera, Nye County, Nevada, and Inyo County, California: U.S. Geological Survey Professional Paper 454-J, p. J1-J25.

Cox, K.G., Bell, J.D., and Pankhurst, R.J., 1979, The interpretation of igneous rocks: George Allen and Unwin, London, 450 p.

Cross, T.A., and Pilger, R.H., Jr., 1978, Constraints on absolute motion and plate interaction inferred from Cenozoic igneous activity in the western United States: American Journal of Science, v. 278, p. 865-902.

Czamanske, G.K., Ishihara, S., and Atkin, S.A., 1981, Chemistry of rock-forming minerals of the Cretaceous-Paleocene batholith of southwestern Japan and implications for magma genesis: Journal of Geophysical Research, v. 86, p. 10431-10469.

Druitt, T.H., and Bacon, C.R., 1986, Lithic breccia and ignimbrite erupted during the collapse of Crater Lake caldera, Oregon: Journal of Volcanology and Geothermal Research, v. 29, p. 1-32.

Eaton, G.P., 1979, Regional geophysics, Cenozoic tectonics, and geological resources of the Basin and Range Province and adjoining regions, in Newman, G.W., and Goode, H.D., eds., Basin and Range symposium and Great Basin field conference: Rocky Mountain Association of Geologists and Utah Geological Association, p. 11-40.

Eaton, G.P., 1984, The Miocene Great Basin of western North America as an extending back-arc region, in Carlson, R.L., and Kobayashi, K., eds., Geodynamics of back-arc regions: Tectonophysics, v. 102, p. 275-295.

Eckel, E.B., 1968, Development of geological knowledge at Nevada Test Site, in, Nevada Test Site: Geological Society of America Memoir 110, p. 5-10.

Fisher, R.V., and Schmincke, H.-U., 1984, Pyroclastic rocks: Springer-Verlag, Berlin, 472 p.

Flood, T.P., 1987, Cyclic evolution of a magmatic system: The Paintbrush Tuff, SW Nevada Volcanic Field [Ph.D. Thesis]: East Lansing, Michigan, Michigan State University, 147 p.

Flood, T.P., Vogel, T.A., and Schuraytz, B.C., 1989a, Chemical evolution of a magmatic system: The Paintbrush Tuff: Southwest Nevada Volcanic Field: Journal of Geophysical Research, v. 94, no. B5, p. 5943-5960.

Flood, T.P., Schuraytz, B.C., and Vogel, T.A., 1989b, Magma mixing due to the disruption of a layered magma body: Journal of Volcanology and Geothermal Research, v. 36, p. 241-255.

Fridrich, C.J., and Mahood, G.A., 1987, Compositional layers in the zoned magma chamber of the Grizzly Peak Tuff: Geology, v. 15, p. 299-303.

Fuhrman, M.L., and Lindsley, D.H., 1988, Ternary-feldspar modeling and thermometry: American Mineralogist, v. 73, p. 201-215.

Gordon, G.E., Keith, R., Goles, G.G., Corliss, J.B., Beeson, M.H., and Oxley, S.S., 1968, Instrumental activation analysis of standard rocks with high-resolution gamma ray detectors: Geochimica et Cosmochimica Acta, v. 32, p. 369-396.

Green, N.L., and Usdansky, S.I., 1986, Ternary-feldspar mixing relations and thermobarometry: American Mineralogist, v. 71, p. 1100-1108.

Greenland, L.P., 1970, An equation for trace element distribution during magmatic crystallization: American Mineralogist, v. 55, p. 455-465.

Grunder, A.L., and Boden, D.R., 1987, Comment on "... Magmatic conditions of the Fish Canyon Tuff, central San Juan Volcanic Field, Colorado" by Whitney and Stormer (1985): Journal of Petrology, v. 28, p. 737-746.

Haggerty, S.E., 1976, Opaque mineral oxides in terrestrial igneous rocks, Oxide Minerals: Short Course Notes Mineralogical Society of America, v. 3, p. 101-300.

Hammarstrom, J.M., and Zen, E., 1986, Aluminum in hornblende: An empirical igneous geobarometer: American Mineralogist, v. 71, p. 1297-1313.

Hart, S.R., and C.J., Allegre, 1980, Trace-element constraints on magma genesis: in Physics of Magmatic Processes, Hargraves, R.B., ed., Princeton University Press, 585 p.

Haskin, L.A., Haskin, M.A., Frey, F.A., and Wildeman, T.R., 1968, Relative and absolute terrestrial abundances of the Rare Earths: in, Origin and Distribution of the Elements, Ahrens, L.H., ed., Pergamon Press, New York, p. 889-912.

Hay, R.L., 1959, Formation of the crystal-rich glowing avalanche deposits of St. Vincent, B.W.I.: Journal of Geology, v. 67, p. 540-562.

Henderson, P., 1982, Inorganic Geochemistry: Pergamon Press, New York, 353 p.

Hildreth, E.W., 1979, The Bishop Tuff: Evidence for the origin of compositional zonation in silicic magma chambers: Geological Society of America Special Paper 180, p. 43-75.

_____, 1981, Gradients in silicic magma chambers: Implications for lithospheric magmatism: Journal of Geophysical Research, v. 86, p. 10153-10192.

_____, 1983, The compositionally zoned eruption of 1912 in the Valley of Ten Thousand Smokes, Katmai National park, Alaska: Journal of Volcanology and Geothermal Research, v. 18, p. 1-56.

Hildreth, W., and Mahood, G., 1985, Correlation of ash-flow tuffs: Geological Society of America Bulletin, v. 96, p. 968-974.

Hollister, L.S., Grissom, G.C., Peters, E.K., Stowell, H.H., and Sisson, V.B., 1987, Confirmation of the empirical correlation of Al in hornblende with pressure of solidification of calc-alkaline plutons: American Mineralogist, v. 72, p. 231-239.

Huppert, H.E., and Sparks, R.S.J., 1984, Double-diffusive convection due to crystallization in magmas: Annual Reviews Earth and Planetary Science, v. 12, p. 11-37.

Huppert, H.E., Sparks, R.S.J., and Turner, J.S., 1984, Some effects of viscosity on the dynamics of replenished magma chambers: Journal of Geophysical Research, v. 89, p. 6857-6877.

Hyndman, D.W., 1985, Petrology of igneous and metamorphic rocks, 2nd ed.: McGraw-Hill, New York, 786 p.

Irvine, T.N., and Baragar, W.R.A., 1971, A guide to the chemical classification of the common rocks: Canadian Journal of Earth Science, v. 8, p. 523-48.

Jackson, M.L., 1979, Soil chemical analysis advanced course; 2nd ed., 11th printing, p. 34, published by author, Madison, Wisconsin.

Johnson, M.C., and Rutherford, M.J., 1989, Experimentally determined conditions in the Fish Canyon Tuff, Colorado, magma chamber: Journal of Petrology, v. 30, p. 711-737.

Katsui, Y., 1963, Evolution and magmatic history of some Krakatoan calderas in Hokkaido, Japan: Hokkaido University Faculty Science Journal, Series 4, Geology and Mineralogy, v. 11, no. 4, p. 631-650.

Le Bas, M.J., Le Maitre, R.W., Streckeisen, A., and Zanettin, B., 1986, A chemical classification of volcanic rocks based on the Total Alkali-Silica diagram: Journal of Petrology, v. 27, p. 745-750.

Leat, P.T., Macdonald, R., and Chapman, G.R., 1984, Geochemical evolution of the Menengai caldera volcano, Kenya: Journal of Geophysical Research, v. 89, no. B10, p. 8571-8592.

Lindsley, D.H., and Spencer, K.J., 1982, Fe-Ti oxide geothermometry: Reducing analyses of coexisting Ti-magnetite (Mt) and ilmenite (Ilm): EOS, Transactions, American Geophysical Union, abstract, v. 63, p. 471.

Lipman, P.W., 1965, Chemical comparison of glassy and crystalline volcanic rocks: Geological Society of America Special Paper 82, p. 260-261.

_____, 1967, Mineral and chemical variations within an ash-flow sheet from Aso caldera, southwestern Japan: Contributions to Mineralogy and Petrology, v. 16, p. 300-327.

Lipman, P.W., 1971, Iron-titanium oxide phenocrysts in compositionally zoned ash-flow sheets from southern Nevada: Journal of Geology, v. 79, p. 438-456.

Lipman, P.W., Protska, H.J., and Christiansen, R.L., 1972, Cenozoic volcanism and plate tectonic evolution of the western United States; 1. Early and middle Cenozoic: Royal Society of London Philosophical Transactions, ser. A, v. 271, p. 217-248.

Lipman, P.W., and Friedman, I., 1975, Interaction of meteoric water with magma: An oxygen-isotope study of ash-flow sheets from southern Nevada: Geological Society of America Bulletin, v. 86, p. 695-702.

Lipman, P.W., Christiansen, R.L., and O'Connor, J.T., 1966, A compositionally zoned ash-flow sheet in southern Nevada: U.S. Geological Survey Professional Paper 524-F, p. F1-F47.

Mahood, G.A., 1981, A summary of the geology and petrology of the Sierra La Primavera, Jalisco, Mexico: Journal of Geophysical Research, v. 86, p. 10137-10152.

Mahood, G.A., and Hildreth, E.W., 1983, Large partition coefficients for trace elements in high-silica rhyolites: Geochimica et Cosmochimica Acta, v. 47, p. 11-30.

McBirney, A.R., 1968, Compositional variations of the climactic eruption of Mount Mazama, in Dole, H.M., ed., Andesite Conference Guidebook: Oregon Department of Geology and Mineral Industry Bulletin, v. 62, p. 53-56.

_____, 1980, Mixing and unmixing of magmas: Journal of Volcanology and Geothermal Research, v. 7, p. 357-371.

McBirney, A.R., Baker, B.H. and Nilson, R.H., 1985, Liquid fractionation, Part I: Basic principles and experimental simulations, Journal of Volcanology and Geothermal Research, v. 24, p. 1-24.

Michael, P.J., 1983a, Chemical differentiation of the Bishop Tuff and other high-silica magmas through crystallization processes: Geology, v. 11, p. 31-34.

_____, 1983b, Comment and reply on 'Chemical differentiation of the Bishop Tuff and other high-silica magmas through crystallization processes': Geology, v. 11, p. 622-624.

_____, 1988, Partition coefficients for rare earth elements in mafic minerals of high silica rhyolites: The importance of accessory mineral inclusions: Geochimica et Cosmochimica Acta, v. 52, p. 275-282.

Mills, J.G., Jr., and Rose, T.P., 1986, Geochemistry of glassy pumices from the Timber Mountain Tuff, southwestern Nevada: EOS, Transactions, American Geophysical Union, v. 67, p. 1262.

Mills, J.G., Jr. and Vogel, T.A., 1988, Compositional interfaces in magma bodies: Geothermometry of Fe-Ti oxides in glassy pumice fragments: EOS, Transactions, American Geophysical Union, v. 69, p. 526.

Mills, J.G., Jr. and Rose, T.P., 1991, Manganoan fayalite ($(Fe,Mn)_2SiO_4$): A new occurrence in rhyolitic ash-flow tuff, southwestern Nevada, U.S.A.: American Mineralogist, (in press).

Mills, J.G., Jr., Schuraytz, B.C., Flood, T.P., Rose, T.P., and Vogel, T.A., 1987, Evolution of a zoned magmatic system in the southwestern Nevada volcanic field: Geological Society of America, Abstracts with Programs, v. 19, p. 773.

Mossman, D.J., and Pawson, D.J., 1976, X-ray and optical characterization of the forsterite-fayalite-tephroite series with comments on knebelite from Bluebell Mine, British Columbia: Canadian Mineralogist, v. 14, p. 479-486.

Nash, W.P., and Crecraft, H.R., 1985, Partition coefficents for the trace elements in silicic magmas: Geochimica et Cosmochimica Acta, v. 49, p. 2309-2322.

Newman, S., Epstein, S., and Stolper, E., 1988, Water, carbon dioxide, and hydrogen isotopes in glasses from the ca. 1340 A.D. eruption of the Mono Craters, California: Constraints on degassing phenomena and initial volatile content: Journal of Volcanology and Geothermal Research, v. 35, p. 75-96.

Nilson, R.H., McBirney, A.R., and Baker, B.H., 1985, Liquid fractionation, Part II: Fluid dynamics and quantitative implications for magmatic systems: Journal of Volcanlogy and Geothermal Research, v. 24, p. 25-54.

Noble, D.C., 1965, Gold Flat Member of the Thirsty Canyon Tuff - A pantellerite ash-flow sheet in southern Nevada; U.S. Geological Survey Professional Paper, 525-B, p. 85-90.

_____, 1967, Sodium, potassium, and ferrous iron contents of some secondarily hydrated natural silicic glasses: American Mineralogist, v. 52, p. 280-286.

Noble, D.C. and Christiansen, R.L., 1968, Geologic map of the southwest quarter of the Black Mountain quadrangle, Nye County, Nevada: U.S. Geological Survey, Miscellaneous Geological Investigations Map, I-562.

_____, 1974, Black Mountain volcanic center, Guidebook to the geology of four Tertiary volcanic centers in central Nevada: Nevada Bureau of Mines Geologic Report 19, p. 27-34.

Noble, D.C., Krushensky, R.D., McKay, E.J., and Ege, J.R., 1967, Geologic map of the Dead Horse Flat quadrangle, Nye County, Nevada: U.S. Geological Survey Geologic Quadrangle Map GQ-614.

Noble, D.C., Sargent, K.A., Mehnert, H.H., Ekren, E.B., and Byers, Jr., F.M., 1968, Silent Canyon volcanic center, Nye County, Nevada, Studies of Geology and Hydrology, Nevada Test Site: Geological Society of America, Memoir 110, p. 65-75.

Noble, D.C., Drake, J.C., Whallon, M.K., 1969, Some preliminary observations on compositional variations within the pumice- and scoria-flow deposits of Mount Mazama: Proceedings Andestie Conference, State of Oregon Department Geology and Mineral Industries, p. 157-164.

Perchuck, L.L. and Ryabchikov, I.D., 1968, Mineral equilibria in the system nepheline-alkali feldspar-plagioclase and their petrological significance: Journal of Petrology, v. 9, p. 123-167.

Phillips. W.R., and Griffen, D.T., 1981, Optical mineralogy: The nonopaque minerals: W.H. Freeman and Company, San Francisco, 677 p.

Ransome, F.L., Emmons, W.H., and Garrey, G.H., 1910, Geology and ore deposits of the Bullfrog district, Nevada: U.S. Geological Survey Bulletin 407, 130 p.

Ratte, J.C., and Steven, T.A., 1967, Ash flows and related volcanic rocks associated with the Creede caldera, San Juan Mountains, Colorado: U.S. Geological Survey Professional Paper 524-H, 58 p.

Reynolds, R.C., Jr., 1963, Matrix corrections in trace element analysis by X-ray fluorescence: Estimation of the mass absorption coeffecient by Compton scattering: American Mineralogist, v. 48, p. 1133-1143.

Reynolds, R.C., Jr., 1967, Estimation of mass absorption coefficients by Compton scattering: Improvements and extensions of the method: American Mineralogist, v. 52, p. 1493-1502.

Ross, C.S., and Smith, R.L, 1961, Ash-flow tuffs-their origin, geologic relations and identification: U.S. Geological Survey Professional Paper 366, 81 p.

Rose, T.P., 1988, A model for the origin of the chemically zoned Ammonia Tanks Member of the Timber Mountain Tuff due to crystal fractionation [M.S. Thesis]: East Lansing, Michigan, Michigan State University, 72 p.

Rumble, D., 1969, Thermodynamic analysis of phase equilibria in the system Fe_2TiO_4-Fe_3O_4-TiO_2: Carnegie Institution of Washington Yearbook, v. 69, p. 198-207.

Sawyer, D.A., and Sargent, K.A., 1989, Petrologic evolution of divergent peralkaline magmas from the Silent Canyon Calder complex, Southwestern Nevada Volcanic Field: Journal of Geophysical Research, v. 94, p. 6021-6040.

Schuratyz, B.C., 1988, Geochemical gradients in the Topopah Spring Member of the Paintbrush Tuff: Evidence for eruption across a magmatic interface [Ph.D. Thesis]: East Lansing, Michigan, Michigan State University, 148 p.

Schuraytz, B.C., Vogel, T.A., and Younker, L.W., 1986, Geochemical gradients in the Topopah Spring Member of the Paintbrush Tuff: Evidence for eruption across a magmatic interface: Lawrence Livermore National Laboratory Report UCRL-53698, 59 p.

_____, 1989, Evidence for dynamic withdrawal from a layered magma body: The Topopah Spring Tuff, sourthwestern Nevada: Journal of Geophysical Research, v. 94, no. B5, p. 5925-5942.

Scott, R.B., Byers, F.M., Jr., and Warren, R.G., 1984, Evolution of magma below clustered calderas, southwest Nevada volcanic field: EOS, Transactions, American Geophysical Union, v. 65, no. 45, p. 1126-1127.

Smith, A.L., 1970, Sphene, perovskite and co-existing Fe-Ti oxide minerals: American Mineralogist, v. 55, p. 264-269.

Smith, R.L., 1960a, Ash flows: Geological Society of America Bulletin, v. 71, p. 795-842.

_____, 1960b, Zones and zonal variations in welded ash flows: U.S. Geological Survey Professional Paper 354-F, p. 149-159.

_____, 1979, Ash-flow magmatism: Geological Society of America Special Paper 180, p. 5-27.

Snyder, W.S., Dickinson, W.R., and Silberman, M.L., 1976, Tectonic implications of space-time patterns of Cenozoic magmatism in the western United States: Earth and Planetary Science Letters, v. 32, p. 91-106.

Sparks, R.S.J., and Walker, G.P.L., 1977, The significance of vitric-enriched air-fall ashes associated with crystal-enriched ignimbrites: Journal of Volcanology and Geothermal Research, v. 2, p. 329-341.

Sparks, R.S.J., Huppert, H.E., and Turner, J.S., 1984, The fluid dynamics of evolving magma chambers: Philosophical Transactions Royal Society of London, v. A310, p. 511-534.

Spell, T.L., and Kyle, P.R., 1989, Petrogenesis of Valle Grande Member rhyolites, Vales Caldera, New Mexico: Implications for evolution of the Jemez Mountains magmatic system: Journal of Geophysical Research, v. 94, no. B8, p. 10379-10396.

Spera, F.J., Yuen, D.A., Greer, J.C., and Sewell, G., 1986, Dynamics of magma withdrawl from stratified magma chambers: Geology, v. 14, no. 9, p. 723-726.

Stormer, J.C., Jr., 1975, A practical two-feldspar geothermometer: American Mineralogist, v. 60, p. 667-674.

_____, Jr., 1983, The effects of recalculation on estimates of temperature and oxygen fugacity from analyses of multicomponent iron-titanium oxides: American Mineralogist, v. 68, p. 586-594.

Stormer, J.C., and Whitney, J.A., 1985, Two feldspar and iron-titanium oxide equilibria in silicic magmas and the depth of origin of large volume ash-flow tuffs: American Mineralogist, v. 70, p. 52-64.

Tegtmeyer, K.J., Farmer, G.L., and Broxton, D.E., 1989, Isotopic evidence for the origin of Late Tertiary metaluminous and peralkaline rhyolites from the Great Basin, western U.S.: New Mexico Bureau of Mines and Mineral Resources Bulletin 131, Continental Magmatism (abstracts), p. 266.

Thompson, R.N., Morrison, M.A., Hendry, G.L., and Parry, S.J., 1984, An assessment of the relative roles of a crust and mantle in magma genesis: an elemental approach: Philosophical Transactions of the Royal Society of London, A310, p. 549-590.

Verhoogen, J., 1962, Distribution of titanium between silicates and oxides in igneous rocks: American Journal of Science, v. 260, p. 211-220.

Vogel, T.A., Mills, J.G., Jr., Aines, R.D. and Merzbacher, C.I., 1989, Pre-eruptive volatiles in a chemically zoned magma body based on melt inclusions: Geological Society of America, Abstracts with Programs, v. 21, no. 6, p. A271.

Vogel, T.A., Noble, D.C., and Younker, L.W., 1983, Chemical evolution of a high-level magma system: The Black Mountain volcanic center, southern Nevada: Lawrence Livermore National Laboratory Report UCRL-53444, 49 p.

Vogel, T.A., Mills, J.G., Schuraytz, B.C., Flood, T.P., Rose, T.P., and Younker, L.W., 1988, Zoned magma bodies: Fractional crystallization of homogeneous magmas or melting of independant sources?: Geological Society of America, Abstracts with Programs, v. 20, no. 7, p. A313.

Walker, G.P.L, 1972, Crystal concentration in ignimbrites: Contributions to Mineralogy and Petrology, v. 36, p. 135-146.

Warren, R.G., Byers, F.M., Jr., and Caporusio, F.A., 1984, Petrography and mineral chemistry of units of the Topopah Spring, Calico Hills and Crater Flat tuffs, and older volcanic units, with emphasis on samples from drill hole USW G-1, Yucca Mountain, Nevada Test Site, Report Los Alamos National Laboratory, La-10003-MS, p. 1-78.

Warren, R.G., McDowell, F.W., Byers, F.M., Jr., Broxton, D.E., Carr, W.J., and Orkild, P.P., 1988, Episodic leaks from Timber Mountain caldera: New evidence from rhyolite lavas of Fortymile Canyon, WE Nevada volcanic field: Geological Society of America, Abstracts with Programs, v. 20, p. 241.

Warren, R.G., Byers, F.M., Jr., Broxton, D.E., Freeman, S.H., and Hagan, R.C., 1989, Phenocryst abundances and glass and phenocryst compositions as indicators of magmatic environments of larege-volume ash flow sheets in southwestern Nevada: Journal of Geophysical Research, v. 94, no. B5, p. 5987-6020.

Weiss, S.I., and Noble, D.C., 1989, Stonewall Mountain Volcanic Center, southern Nevada: Stratigraphic, structural, and facies relations of outflow sheets, near-vent tuffs, and intracaldera units: Journal of Geophysical Research, v. 94, p. 6059-6074.

Whitney, J.A. and Stormer, J.C., Jr., 1976, Geothermometry and geobarometry in epizonal granitic intrusions: A comparison of iron-titanium and coexisting feldspars: American Mineralogist, v. 61, p. 751-761.

Whitney, J.A. and Stormer, 1977, Two-feldspar geothermometry, geobarometry in mesozonal granitic intrusions: Three examples from the Piedmont of Georgia: Contributions to Mineralogy and Petrology, v. 63, p. 51-64.

Whitney, J.A., 1985, Mineralogy, petrology, and magmatic conditions form the Fish Canyon Tuff, central San Juan Volcanic Field, Colorado: Journal of Petrology, v. 26, p. 726-762.

Whitney, J.A., Dorais, M.J., Stormer, Jr., J.C., Kline, S.W., and Matty, D.J., 1988, Magmatic conditions and development of chemical zonation in the Carpenter Ridge Tuff, central San Juan Volcanic Field, Colorado: American Journal of Science, v. 288-A, p. 16-44.

Wilband, J.T., 1975, Rapid method for background corrections in trace element analysis by X-ray fluorescence: An extension of Reynolds method: American Mineralogist, v. 60 p. 320-323.

Williams, H., 1942, The geology of Crater Lake National Park, Oregon, with a reconnaissnce of the Cascade Range southward to Mount Shasta: Carnegie Institute of Washington Publication 540, 162 p.

_____, 1952, Volcanic history of the Meseta Central Occidental, Costa Rica: California University Publications, Department of Geological Science, v. 29, no. 4, p. 145-180.

Wolff, J.A., 1985, The effect of explosive eruption processes on geochemical patterns within pyroclastic deposits: Journal of Volcanology and Geothermal Research, v. 26, p. 189-201.

Wolff, J.A., and Storey, M., 1984, Zoning in highly alkaline magma bodies: Geological Magazine, v. 121, p. 563-575.

Wones, D.R., 1966, Mineralogical indicators of relative oxidation states of magmatic systems: Transactions, American Geophysical Union, v. 47, p. 216.

Yoder, H.S., Jr., Stewart, D.B., and Smith, J.R., 1957, Ternary feldspars: Carnegie Institute Washington Year Book, v. 56, p. 206-214.

Zoback, M.L., Anderson, R.E., and Thompson, G.A., 1981, Cainozoic evolution of the state of stress and style of tectonism of the Basin and Range province of the western United States: Royal Society of London Philosophical Transactions, ser. A, v. 300, p. 407-434.